BEST AVAILABLE IMAGES

Defective images within this document are accurate representations of the original documents submitted by the applicant.

Defects in the images may include (but are not limited to):

- BLACK BORDERS
- TEXT CUT OFF AT TOP, BOTTOM OR SIDES
- FADED TEXT
- ILLEGIBLE TEXT
- SKEWED/SLANTED IMAGES
- COLORED PHOTOS
- BLACK OR VERY BLACK AND WHITE DARK PHOTOS
- GRAY SCALE DOCUMENTS

IMAGES ARE BEST AVAILABLE COPY.

As rescanning documents *will not* correct images, please do not report the images to the Image Problem Mailbox.

=> d his

(FILE 'HOME' ENTERED AT 16:03:44 ON 04 MAR 2001)

FILE 'MEDLINE, EMBASE, BIOSIS, CAPLUS' ENTERED AT 16:03:54 ON 04 MAR 2001

```
L1         54535 S FIBROBLAST## GROWTH FACTOR
L2         17453 S VASCULAR ENDOTHELIAL GROWTH FACTOR
L3          4517 S VASCULAR PERMEABILITY FACTOR
L4         18645 S L2 OR L3
L5       1302140 S ANTIBOD## OR IMMUNOGEN?
L6          4686 S L5 AND (L3 OR L1)
L7       2576468 S TUMOR OR CANCER OR METASTASIS
L8          1290 S L7 AND L6
L9         48497 S ANGIOGEN?
L10          507 S L8 AND L9
L11          316 DUP REM L10 (191 DUPLICATES REMOVED)
L12       387585 S FRAGMENT
L13           21 S L12 AND L10
L14           12 DUP REM L13 (9 DUPLICATES REMOVED)
L15         1705 S HEPARIN BINDING DOMAIN
L16            5 S L15 AND L10
L17            2 DUP REM L16 (3 DUPLICATES REMOVED)
L18           14 S L14 OR L17
L19         7231 S MURAMYL
L20            0 S L19 AND L10
L21            1 S L19 AND L8
L22           39 S KEYHOLE LYMPET
L23         5936 S KLH
L24         5954 S L23 OR L22
L25            0 S L24 AND L10
L26            0 S L24 AND L8
L27            2 S L24 AND L6
L28            1 DUP REM L27 (1 DUPLICATE REMOVED)
L29         4777 S MALTOSE BINDING
L30            1 S L29 AND L10
L31            1 S L29 AND L8
L32            1 S L30 OR L31
L33        80023 S BOVINE SERUM ALBUMIN OR BSA
L34            4 S L33 AND L10
L35           20 S L33 AND L8
L36           59 S L33 AND L6
L37        34133 S OVALBUMIN
L38            2 S L37 AND L10
L39            2 S L37 AND L8
L40            5 S L37 AND L6
L41         5061 S FLAGELLIN
L42            0 S L41 AND L10
L43            1 S L41 AND L8
L44            1 S L41 AND L6
L45        22505 S THYROGLOBULIN
L46            4 S L45 AND L6
L47        29289 S GAMMA GLOBULIN
L48            0 S L47 AND L6
L49          212 S SYNGENEIC CELL
L50            0 S L49 AND L6
L51        20841 S CARRIER PROTEIN OR IMMUNOGENIC CARRIER
L52           11 S L51 AND L6
L53           92 S L52 OR L46 OR L44 OR L40 OR L36 OR L32 OR L27 OR L21
L54           50 DUP REM L53 (42 DUPLICATES REMOVED)
```

```
=> d his

     (FILE 'HOME' ENTERED AT 16:03:44 ON 04 MAR 2001)

     FILE 'MEDLINE, EMBASE, BIOSIS, CAPLUS' ENTERED AT 16:03:54 ON 04 MAR 2001
L1         54535 S FIBROBLAST## GROWTH FACTOR
L2         17453 S VASCULAR ENDOTHELIAL GROWTH FACTOR
L3          4517 S VASCULAR PERMEABILITY FACTOR
L4         18645 S L2 OR L3
L5       1302140 S ANTIBOD## OR IMMUNOGEN?
L6          4686 S L5 AND (L3 OR L1)
L7       2576468 S TUMOR OR CANCER OR METASTASIS
L8          1290 S L7 AND L6
L9         48497 S ANGIOGEN?
L10          507 S L8 AND L9
L11          316 DUP REM L10 (191 DUPLICATES REMOVED)
L12       387585 S FRAGMENT
L13           21 S L12 AND L10
L14           12 DUP REM L13 (9 DUPLICATES REMOVED)
L15         1705 S HEPARIN BINDING DOMAIN
L16            5 S L15 AND L10
L17            2 DUP REM L16 (3 DUPLICATES REMOVED)
L18           14 S L14 OR L17
L19         7231 S MURAMYL
L20            0 S L19 AND L10
L21            1 S L19 AND L8
L22           39 S KEYHOLE LYMPET
L23         5936 S KLH
L24         5954 S L23 OR L22
L25            0 S L24 AND L10
L26            0 S L24 AND L8
L27            2 S L24 AND L6
L28            1 DUP REM L27 (1 DUPLICATE REMOVED)
L29         4777 S MALTOSE BINDING
L30            1 S L29 AND L10
L31            1 S L29 AND L8
L32            1 S L30 OR L31
L33        80023 S BOVINE SERUM ALBUMIN OR BSA
L34            4 S L33 AND L10
L35           20 S L33 AND L8
L36           59 S L33 AND L6
L37        34133 S OVALBUMIN
L38            2 S L37 AND L10
L39            2 S L37 AND L8
L40            5 S L37 AND L6
L41         5061 S FLAGELLIN
L42            0 S L41 AND L10
L43            1 S L41 AND L8
L44            1 S L41 AND L6
L45        22505 S THYROGLOBULIN
L46            4 S L45 AND L6
L47        29289 S GAMMA GLOBULIN
L48            0 S L47 AND L6
L49          212 S SYNGENEIC CELL
L50            0 S L49 AND L6
L51        20841 S CARRIER PROTEIN OR IMMUNOGENIC CARRIER
L52           11 S L51 AND L6
L53           92 S L52 OR L46 OR L44 OR L40 OR L36 OR L32 OR L27 OR L21
L54           50 DUP REM L53 (42 DUPLICATES REMOVED)
```

L54 ANSWER 1 OF 50 CAPLUS COPYRIGHT 2001 ACS
ACCESSION NUMBER: 2000:900792 CAPLUS
DOCUMENT NUMBER: 134:52231
TITLE: Induction of vascular endothelial growth factor expression by serine/threonine protein kinase Akt
INVENTOR(S): Guo, Kun; Ivashchenko, Yuri; Clark, Kenneth
PATENT ASSIGNEE(S): Aventis Pharmaceuticals Products Inc., USA
SOURCE: PCT Int. Appl., 66 pp.
CODEN: PIXXD2
DOCUMENT TYPE: Patent
LANGUAGE: English
FAMILY ACC. NUM. COUNT: 1
PATENT INFORMATION:

PATENT NO.	KIND	DATE	APPLICATION NO.	DATE
WO 2000077190	A2	20001221	WO 2000-US15098	20000601

W: AE, AL, AM, AT, AU, AZ, BA, BB, BG, BR, BY, CA, CH, CN, CR, CU, CZ, DE, DK, DM, EE, ES, FI, GB, GD, GE, GH, GM, HR, HU, ID, IL, IN, IS, JP, KE, KG, KP, KR, KZ, LC, LK, LR, LS, LT, LU, LV, MA, MD, MG, MK, MN, MW, MX, NO, NZ, PL, PT, RO, RU, SD, SE, SG, SI, SK, SL, TJ, TM, TR, TT, TZ, UA, UG, US, UZ, VN, YU, ZA, ZW, AM, AZ, BY, KG, KZ, MD, RU, TJ, TM
RW: GH, GM, KE, LS, MW, MZ, SD, SL, SZ, TZ, UG, ZW, AT, BE, CH, CY, DE, DK, ES, FI, FR, GB, GR, IE, IT, LU, MC, NL, PT, SE, BF, BJ, CF, CG, CI, CM, GA, GN, GW, ML, MR, NE, SN, TD, TG

PRIORITY APPLN. INFO.: US 1999-138724 19990611
GB 1999-26058 19991103

AB The present invention relates to methods and compns. for induction of vascular endothelial growth factor (VEGF) expression by the serine/threonine protein kinase Akt. Preferably, the compns. and methods according to the invention comprise a nucleic acid encoding Akt, and administration thereof using a plasmid or viral vector. A viral vector derived from retrovirus, adenovirus, adeno-assocd. virus, herpes virus, or vaccinia virus are used. Akt1, Akt2, or Akt3 is used to induce expression of VEGF123, VEGF165, VEGF189, VEGF206, VEGF-2, VEGF-B, or VEGF-D. Administration of a transition metal ion and/or a vasodilator together with the Akt coding sequence is claimed. A sequence encoding a second ***angiogenic*** factor, such as VEGF, acidic ***fibroblast*** ***growth*** ***factor*** , basic ***fibroblast*** ***growth*** ***factor*** , endothelial cell growth factor, or angiopoietin, may also be introduced. Gene therapy for patients suffering from ischemic conditions, cerebrovascular ischemia, renal ischemia, pulmonary ischemia, limb ischemia, myocardial ischemia, or ischemic, idiopathic or hypertrophic cardiomyopathy, is claimed. A pharmaceutical compn. comprising the above described components are claimed. A method of inhibiting ***angiogenesis*** in ***tumor*** patients using Akt antisense nucleic acid, an intracellular binding protein such as a single chain Fv ***antibody*** (scFv), or nucleic acid encoding a dominant neg. form of Akt, is also claimed. Stimulation of VEGF expression in cells transfected with an adenovirus carrying a sequence encoding activated mouse Akt1, or active human Akt3, was demonstrated.

L54 ANSWER 2 OF 50 CAPLUS COPYRIGHT 2001 ACS

ACCESSION NUMBER: 2000:645881 CAPLUS
DOCUMENT NUMBER: 133:251263
TITLE: Compositions and methods for treating ***cancer*** and hyperproliferative disorders
INVENTOR(S): Holaday, John W.; Ruiz, Antonio; Madsen, John
PATENT ASSIGNEE(S): Entremed, Inc., USA
SOURCE: PCT Int. Appl., 95 pp.
CODEN: PIXXD2
DOCUMENT TYPE: Patent
LANGUAGE: English
FAMILY ACC. NUM. COUNT: 1
PATENT INFORMATION:

PATENT NO.	KIND	DATE	APPLICATION NO.	DATE
WO 2000053219	A2	20000914	WO 2000-US6320	20000310
WO 2000053219	A3	20010125		

W: AE, AL, AM, AT, AU, AZ, BA, BB, BG, BR, BY, CA, CH, CN, CR, CU, CZ, DE, DK, DM, EE, ES, FI, GB, GD, GE, GH, GM, HR, HU, ID, IL, IN, IS, JP, KE, KG, KP, KR, KZ, LC, LK, LR, LS, LT, LU, LV, MA, MD, MG, MK, MN, MW, MX, NO, NZ, PL, PT, RO, RU, SD, SE, SG, SI, SK, SL, TJ, TM, TR, TT, TZ, UA, UG, US, UZ, VN, YU, ZA, ZW, AM, AZ, BY, KG, KZ, MD, RU, TJ, TM
RW: GH, GM, KE, LS, MW, SD, SL, SZ, TZ, UG, ZW, AT, BE, CH, CY, DE, DK, ES, FI, FR, GB, GR, IE, IT, LU, MC, NL, PT, SE, BF, BJ, CF, CG, CI, CM, GA, GN, GW, ML, MR, NE, SN, TD, TG

PRIORITY APPLN. INFO.: US 1999-266543 19990311

AB Compns. and methods effective for eliciting an immune response for inhibiting abnormal or undesirable cell proliferation, particularly endothelial cell proliferation and ***angiogenesis*** related to neovascularization and ***tumor*** growth are provided. The compns. comprise a naturally occurring or synthetic protein, peptide, or protein ***fragment*** contg. all or an active portion of a growth factor in a pharmaceutically acceptable carrier. The preferred growth factors comprise basic ***fibroblast*** ***growth*** ***factor*** and vascular endothelial growth factor. The methods involve administering to a human or animal the compns. described herein in a dosage sufficient to elicit an immune response. The methods are useful for treating diseases and processes mediated by undesired and uncontrolled cell proliferation, such as ***cancer*** , particularly where uncontrolled cell proliferation is influenced by the presence of growth factors. Administration of the compn. to a human or animal having metastasized tumors is useful for preventing the growth or expansion of such tumors.

L54 ANSWER 3 OF 50 CAPLUS COPYRIGHT 2001 ACS
ACCESSION NUMBER: 2000:309145 CAPLUS
DOCUMENT NUMBER: 133:206140
TITLE: Regulation of ***angiogenesis*** in vivo by ligation of integrin .alpha.5.beta.1 with the central cell-binding domain of fibronectin
AUTHOR(S): Kim, Semi; Bell, Kelly; Mousa, Shaker A.; Varner, Judith A.
CORPORATE SOURCE: Department of Medicine/Cancer Center, Cellular and Molecular Medicine East, University of California San Diego, La Jolla, CA, 92093-0684, USA
SOURCE: Am. J. Pathol. (2000), 156(4), 1345-1362
CODEN: AJPAA4; ISSN: 0002-9440
PUBLISHER: American Society for Investigative Pathology
DOCUMENT TYPE: Journal

LANGUAGE: English

AB ***Angiogenesis*** depends on the cooperation of growth factors and cell adhesion events. Although .alpha.v integrins have been shown to play crit. roles in ***angiogenesis*** , recent studies in .alpha.v-null mice suggest that other adhesion receptors and their ligands also regulate this process. Evidence is now provided that the integrin .alpha.5.beta.1 and its ligand fibronectin are coordinately up-regulated on blood vessels in human ***tumor*** biopsies and play crit. roles in ***angiogenesis*** , resulting in ***tumor*** growth in vivo. ***Angiogenesis*** induced by multiple growth factors in chick embryos was blocked by monoclonal antibodies to the cell-binding domain of fibronectin. Furthermore, application of fibronectin or a proteolytic ***fragment*** of fibronectin contg. the central cell-binding domain to the chick chorioallantoic membrane enhanced ***angiogenesis*** in an integrin .alpha.5.beta.1-dependent manner. Importantly, ***antibody*** , peptide, and novel nonpeptide antagonists of integrin .alpha.5.beta.1 blocked ***angiogenesis*** induced by several growth factors but had little effect on ***angiogenesis*** induced by vascular endothelial growth factor (VEGF) in both chick embryo and murine models. In fact, these .alpha.5.beta.1 antagonists inhibited ***tumor*** ***angiogenesis*** , thereby causing regression of human tumors in animal models. Thus, fibronectin and integrin .alpha.5.beta.1, like integrin .alpha.v.beta.3, contribute to an ***angiogenesis*** pathway that is distinct from VEGF-mediated ***angiogenesis*** , yet important for the growth of tumors.

REFERENCE COUNT: 74

REFERENCE(S): (1) Akiyama, S; Cell Adhes Commun 1995, V3, P13 CAPLUS
(2) Anzano, M; Cancer Res 1989, V49, P2898 CAPLUS
(4) Arenberg, D; J Clin Invest 1996, V97, P2792 CAPLUS
(5) Bader, B; Cell 1998, V95, P507 CAPLUS
(6) Basilico, C; Adv Cancer Res 1992, V59, P115 CAPLUS

ALL CITATIONS AVAILABLE IN THE RE FORMAT

L54 ANSWER 4 OF 50 EMBASE COPYRIGHT 2001 ELSEVIER SCI. B.V.

ACCESSION NUMBER: 2001005447 EMBASE

TITLE: Administration of a liposomal FGF-2 peptide vaccine leads to abrogation of FGF-2-mediated ***angiogenesis*** and ***tumor*** development.

AUTHOR: Plum S.M.; Holaday J.W.; Ruiz A.; Madsen J.W.; Fogler W.E.; Fortier A.H.

CORPORATE SOURCE: S.M. Plum, EntreMed, Inc., 9640 Medical Center Drive, Rockville, MD 20850, United States. stacyp@entremed.com

SOURCE: Vaccine, (8 Dec 2000) 19/9-10 (1294-1303).
Refs: 32
ISSN: 0264-410X CODEN: VACCDE

PUBLISHER IDENT.: S 0264-410X(00)00210-3

COUNTRY: United Kingdom

DOCUMENT TYPE: Journal; Article

FILE SEGMENT: 016 Cancer
026 Immunology, Serology and Transplantation
037 Drug Literature Index

LANGUAGE: English
SUMMARY LANGUAGE: English
AB Basic ***fibroblast*** ***growth*** ***factor*** (FGF-2) is an important stimulator of ***angiogenesis*** that has been implicated in neoplastic progression. Attempts to neutralize or modulate FGF-2 have met with some success in controlling neovascularity and ***tumor*** growth. In the present study, two peptides: one corresponding to the ***heparin*** ***binding*** ***domain*** and the other to the receptor binding domain of FGF-2, exerted dose-dependent inhibition of FGF-2-stimulated human umbilical vein endothelial cell proliferation (IC(50) = 70 and 20 .mu.g/ml, respectively). The identification of these functional regions suggested that targeting these domains might be an approach for the modulation of FGF-2 function. To investigate this possibility, we vaccinated mice with either the ***heparin*** ***binding*** ***domain*** peptide or the receptor binding domain peptide of FGF-2 in a liposome/adjuvant format, and analyzed the effect of vaccination on FGF-2-driven ***angiogenesis*** , ***tumor*** development and immune status. Mice vaccinated with the ***heparin*** ***binding*** ***domain*** peptide generated a specific ***antibody*** response to FGF-2, blocked neovascularization in a gelfoam sponge model of ***angiogenesis*** , and inhibited experimental ***metastasis*** by > 90% in two ***tumor*** models: the B16BL6 melanoma and the Lewis lung carcinoma. These effects were not observed in mice treated with the receptor binding domain peptide conjugated to liposomes or liposomes lacking conjugated peptide. These data suggest that a ***heparin*** ***binding*** ***domain*** peptide of FGF-2, when presented to a host in a liposomal adjuvant formulation, can ultimately lead to inhibition of ***angiogenesis*** and ***tumor*** growth. .COPYRGT. 2000 Elsevier Science Ltd.

L54 ANSWER 5 OF 50 MEDLINE
ACCESSION NUMBER: 2000459321 MEDLINE
DOCUMENT NUMBER: 20425110
TITLE: Endostatins derived from collagens XV and XVIII differ in structural and binding properties, tissue distribution and anti- ***angiogenic*** activity.
AUTHOR: Sasaki T; Larsson H; Tisi D; Claesson-Welsh L; Hohenester E; Timpl R
CORPORATE SOURCE: Max-Planck-Institut fur Biochemie, Martinsried, D-82152, Germany.
SOURCE: JOURNAL OF MOLECULAR BIOLOGY, (2000 Sep 1) 301 (5) 1179-90.
Journal code: J6V. ISSN: 0022-2836.
PUB. COUNTRY: ENGLAND: United Kingdom
Journal; Article; (JOURNAL ARTICLE)
LANGUAGE: English
FILE SEGMENT: Priority Journals
OTHER SOURCE: PDB-1DY2
ENTRY MONTH: 200012
ENTRY WEEK: 20001201
AB Endostatin is a ***fragment*** of the C-terminal domain NC1 of collagen XVIII that inhibits ***angiogenesis*** and ***tumor*** growth. We report the characterization of a collagen XV endostatin analogue and its parent NC1 domain, obtained by recombinant expression in mammalian cells. Both NC1 domains contain a trimerization domain, a hinge

region that is more sensitive to proteolysis in collagen XVIII and the endostatin domain. Unlike endostatin-XVIII, endostatin-XV does not bind zinc or heparin, which is explained by the crystal structure of endostatin-XV. The collagen XV and XVIII fragments inhibited chorioallantoic membrane ***angiogenesis*** induced by basic ***fibroblast*** ***growth*** ***factor*** (FGF-2) or vascular endothelial growth factor (VEGF), but there are striking differences depending on which cytokine is used and whether free endostatins or NC1 domains are applied. The collagen XV and XVIII fragments showed a similar binding repertoire for extracellular matrix proteins. Differences were found in the immunohistological localization in vessel walls and basement membrane zones. Together, these data indentify endostatin-XV as an ***angiogenesis*** inhibitor, which differs from endostatin-XVIII in several important functional details. Copyright 2000 Academic Press.

L54 ANSWER 6 OF 50 EMBASE COPYRIGHT 2001 ELSEVIER SCI. B.V.
ACCESSION NUMBER: 2000341834 EMBASE
TITLE: Cilengitide. Oncolytic, angiogenesis inhibitor, integrin .alpha.v.beta.3,.alpha.v.beta.5 antagonist.
AUTHOR: Sorbera L.A.; Graul A.; Castaner J.
CORPORATE SOURCE: L.A. Sorbera, Prous Science, P.O. Box 540, 08080 Barcelona, Spain
SOURCE: Drugs of the Future, (2000) 25/7 (674-678).
Refs: 21
ISSN: 0377-8282 CODEN: DRFUD4
COUNTRY: Spain
DOCUMENT TYPE: Journal; Article
FILE SEGMENT: 016 Cancer
030 Pharmacology
037 Drug Literature Index
LANGUAGE: English

L54 ANSWER 7 OF 50 EMBASE COPYRIGHT 2001 ELSEVIER SCI. B.V.DUPLICATE 1
ACCESSION NUMBER: 2000425613 EMBASE
TITLE: Quantitation of basic ***fibroblast*** ***growth*** ***factor*** by immunoassay using BIAcore(TM) 2000.
AUTHOR: Zhu G.; Yang B.; Jennings R.N.
CORPORATE SOURCE: G. Zhu, Pharmaceutics Department, Scios Inc., 820 West Maude Avenue, Sunnyvale, CA 94086, United States
SOURCE: Journal of Pharmaceutical and Biomedical Analysis, (15 Dec 2000) 24/2 (281-290).
Refs: 16
ISSN: 0731-7085 CODEN: JPBADA
PUBLISHER IDENT.: S 0731-7085(00)00417-9
COUNTRY: Netherlands
DOCUMENT TYPE: Journal; Article
FILE SEGMENT: 029 Clinical Biochemistry
003 Endocrinology
037 Drug Literature Index
LANGUAGE: English
SUMMARY LANGUAGE: English
AB A sensitive, accurate, and efficient immunoassay using a BIAcore(TM) 2000 biosensor instrument for the quantitation of basic ***fibroblast*** ***growth*** ***factor*** (bFGF) in HEPES-buffered saline containing 100 .mu.g/ml heparin (HHBS) has been developed and validated. In this method, anti-bFGF monoclonal ***antibody*** 48.1 (MAb 48.1) was selected as a binding ligand and immobilized to the matrix surface of

Sensor Chip CM5 by amine coupling. A high immobilization level of MAb 48.1 (12643.+-.816 RU, mean.+-.S.D., n=5) was achieved with high reproducibility (i.e. coefficient of variation (CV) was 6.5%). This immobilized MAb 48.1 sensor surface was used to detect and quantify bFGF. This assay has a range of reliable BIAcore(TM) response from 5.65 to 1440 ng/ml bFGF in HHBS, which was well fitted with a sigmoidal model. The immobilized MAb 48.1 was found to be stable for at least 150 regeneration cycles and for at least 9 days at room temperature. Intra- and interassay CVs ranged from 0.9 to 5.9% and from 2.7 to 8.5%, respectively. Matrices such as serum, ***bovine*** ***serum*** ***albumin*** (***BSA***), and two pharmaceutical excipients (Pluronic.RTM. F127 surfactant and sodium carboxymethylcellulose) did not interfere with bFGF analysis over the sensor surface. Therefore, this validated assay has good precision, accuracy and specificity, and has been found useful in quantifying bFGF in several research and development studies. Copyright (C) 2000 Elsevier Science B.V.

L54 ANSWER 8 OF 50 CAPLUS COPYRIGHT 2001 ACS
ACCESSION NUMBER: 1999:795994 CAPLUS
DOCUMENT NUMBER: 132:31744
TITLE: Gene probes used for genetic profiling in healthcare screening and planning
INVENTOR(S): Roberts, Gareth Wyn
PATENT ASSIGNEE(S): Genostic Pharma Ltd., UK
SOURCE: PCT Int. Appl., 745 pp.
CODEN: PIXXD2
DOCUMENT TYPE: Patent
LANGUAGE: English
FAMILY ACC. NUM. COUNT: 2
PATENT INFORMATION:

PATENT NO.	KIND	DATE	APPLICATION NO.	DATE
WO 9964627	A2	19991216	WO 1999-GB1780	19990604

W: AE, AL, AM, AT, AU, AZ, BA, BB, BG, BR, BY, CA, CH, CN, CU, CZ, DE, DK, EE, ES, FI, GB, GD, GE, GH, GM, HR, HU, ID, IL, IN, IS, JP, KE, KG, KP, KR, KZ, LC, LK, LR, LS, LT, LU, LV, MD, MG, MK, MN, MW, MX, NO, NZ, PL, PT, RO, RU, SD, SE, SG, SI, SK, SL, TJ, TM, TR, TT, UA, UG, US, UZ, VN, YU, ZA, ZW, AM, AZ, BY, KG, KZ, MD, RU, TJ, TM

RW: GH, GM, KE, LS, MW, SD, SL, SZ, UG, ZW, AT, BE, CH, CY, DE, DK, ES, FI, FR, GB, GR, IE, IT, LU, MC, NL, PT, SE, BF, BJ, CF, CG, CI, CM, GA, GN, GW, ML, MR, NE, SN, TD, TG

PRIORITY APPLN. INFO.:	
GB 1998-12099	19980606
GB 1998-13291	19980620
GB 1998-13611	19980624
GB 1998-13835	19980627
GB 1998-14110	19980701
GB 1998-14580	19980707
GB 1998-15438	19980716
GB 1998-15574	19980718
GB 1998-15576	19980718
GB 1998-16085	19980724
GB 1998-16086	19980724
GB 1998-16921	19980805
GB 1998-17097	19980807
GB 1998-17200	19980808
GB 1998-17632	19980814

GB 1998-17943 19980819

AB There is considerable evidence that significant factor underlying the individual variability in response to disease, therapy and prognosis lies in a person's genetic make-up. There have been numerous examples relating that polymorphisms within a given gene can alter the functionality of the protein encoded by that gene thus leading to a variable physiol. response. In order to bring about the integration of genomics into medical practice and enable design and building of a technol. platform which will enable the everyday practice of mol. medicine a way must be invented for the DNA sequence data to be aligned with the identification of genes central to the induction, development, progression and outcome of disease or physiol. states of interest. According to the invention, the no. of genes and their configurations (mutations and polymorphisms) needed to be identified in order to provide crit. clin. information concerning individual prognosis is considerably less than the 100,000 thought to comprise the human genome. The identification of the identity of the core group of genes enables the invention of a design for genetic profiling technologies which comprises of the identification of the core group of genes and their sequence variants required to provide a broad base of clin. prognostic information - "genostics". The "Genostic.RTM." profiling of patients and persons will radically enhance the ability of clinicians, healthcare professionals and other parties to plan and manage healthcare provision and the targeting of appropriate healthcare resources to those deemed most in need. The use of this invention could also lead to a host of new applications for such profiling technologies, such as identification of persons with particular work or environment related risk, selection of applicants for employment, training or specific opportunities or for the enhancing of the planning and organization of health services, education services and social services.

L54 ANSWER 9 OF 50 CAPLUS COPYRIGHT 2001 ACS
ACCESSION NUMBER: 1999:795993 CAPLUS
DOCUMENT NUMBER: 132:31743
TITLE: Gene probes used for genetic profiling in healthcare screening and planning
INVENTOR(S): Roberts, Gareth Wyn
PATENT ASSIGNEE(S): Genostic Pharma Limited, UK
SOURCE: PCT Int. Appl., 149 pp.
CODEN: PIXXD2
DOCUMENT TYPE: Patent
LANGUAGE: English
FAMILY ACC. NUM. COUNT: 2
PATENT INFORMATION:

PATENT NO.	KIND	DATE	APPLICATION NO.	DATE
WO 9964626	A2	19991216	WO 1999-GB1779	19990604

W: AE, AL, AM, AT, AU, AZ, BA, BB, BG, BR, BY, CA, CH, CN, CU, CZ, DE, DK, EE, ES, FI, GB, GD, GE, GH, GM, HR, HU, ID, IL, IN, IS, JP, KE, KG, KP, KR, KZ, LC, LK, LR, LS, LT, LU, LV, MD, MG, MK, MN, MW, MX, NO, NZ, PL, PT, RO, RU, SD, SE, SG, SI, SK, SL, TJ, TM, TR, TT, UA, UG, US, UZ, VN, YU, ZA, ZW, AM, AZ, BY, KG, KZ, MD, RU, TJ, TM

RW: GH, GM, KE, LS, MW, SD, SL, SZ, UG, ZW, AT, BE, CH, CY, DE, DK, ES, FI, FR, GB, GR, IE, IT, LU, MC, NL, PT, SE, BF, BJ, CF, CG, CI, CM, GA, GN, GW, ML, MR, NE, SN, TD, TG

AU 9941586	A1	19991230	AU 1999-41586	19990604
AU 9941587	A1	19991230	AU 1999-41587	19990604
GB 2339200	A1	20000119	GB 1999-12914	19990604
PRIORITY APPLN. INFO.:			GB 1998-12098	19980606
			GB 1998-28289	19981223
			GB 1998-16086	19980724
			GB 1998-16921	19980805
			GB 1998-17097	19980807
			GB 1998-17200	19980808
			GB 1998-17632	19980814
			GB 1998-17943	19980819
			WO 1999-GB1779	19990604

AB There is considerable evidence that significant factor underlying the individual variability in response to disease, therapy and prognosis lies in a person's genetic make-up. There have been numerous examples relating that polymorphisms within a given gene can alter the functionality of the protein encoded by that gene thus leading to a variable physiol. response.

In order to bring about the integration of genomics into medical practice and enable design and building of a technol. platform which will enable the everyday practice of mol. medicine a way must be invented for the DNA sequence data to be aligned with the identification of genes central to the induction, development, progression and outcome of disease or physiol. states of interest. According to the invention, the no. of genes and their configurations (mutations and polymorphisms) needed to be identified in order to provide crit. clin. information concerning individual prognosis is considerably less than the 100,000 thought to comprise the human genome. The identification of the identity of the core group of genes enables the invention of a design for genetic profiling technologies.

L54 ANSWER 10 OF 50 MEDLINE

ACCESSION NUMBER:	2000093838 MEDLINE
DOCUMENT NUMBER:	20093838
TITLE:	Different antitumor activities of anti-bFGF neutralizing antibodies: ***heparin*** - ***binding*** ***domain*** provides an inefficient epitope for neutralization in vivo.
AUTHOR:	Aonuma M; Yoshitake Y; Nishikawa K; Tanaka N G
CORPORATE SOURCE:	New Product Research Laboratories IV, Daiichi Pharmaceutical Co., Ltd., Tokyo, Japan.
SOURCE:	ANTICANCER RESEARCH, (1999 Sep-Oct) 19 (5B) 4039-44. Journal code: 59L. ISSN: 0250-7005.
PUB. COUNTRY:	Greece
	Journal; Article; (JOURNAL ARTICLE)
LANGUAGE:	English
FILE SEGMENT:	Priority Journals; Cancer Journals
ENTRY MONTH:	200004
ENTRY WEEK:	20000404

AB Basic ***fibroblast*** ***growth*** ***factor*** (bFGF) plays an important role in ***tumor*** growth and ***angiogenesis*** . To elucidate the efficient recognition sites by anti-bFGF neutralizing antibodies, we generated two anti-bFGF neutralizing monoclonal IgG1

antibodies (mAbs), 2G11 and 1E6, recognizing different sites, and estimated as binding to the heparin-binding and the receptor-binding regions of bFGF, respectively, both of which have been shown to be important for its receptor interaction. Despite their high in vitro anti-bFGF activity in the absence of heparin, 2G11, with in vitro activity in competition with heparin, failed to inhibit the in vivo ***tumor*** growth of bFGF-producing RPMI4788 cells, though 1E6, showing non-competition with heparin, exhibited a significant antitumor effect. These results show that the ***heparin*** - ***binding*** ***domain*** of bFGF provides an inefficient epitope for in vivo neutralization of anti-bFGF mAb, and anti-bFGF neutralizing mAbs without competition against heparin have the potential to show in vivo antitumor effects.

L54 ANSWER 11 OF 50 MEDLINE
ACCESSION NUMBER: 1999293019 MEDLINE
DOCUMENT NUMBER: 99293019
TITLE: Role and localization of urokinase receptor in the formation of new microvascular structures in fibrin matrices.
AUTHOR: Kroon M E; Koolwijk P; van Goor H; Weidle U H; Collen A; van der Pluijm G; van Hinsbergh V W
CORPORATE SOURCE: Gaubius Laboratory, Leiden University Hospital, Groningen Leiden The Netherlands.
SOURCE: AMERICAN JOURNAL OF PATHOLOGY, (1999 Jun) 154 (6) 1731-42. Journal code: 3RS. ISSN: 0002-9440.
PUB. COUNTRY: United States
Journal; Article; (JOURNAL ARTICLE)
LANGUAGE: English
FILE SEGMENT: Abridged Index Medicus Journals; Priority Journals; Cancer Journals
ENTRY MONTH: 199909
AB Fibrin or a fibrinous exudate can facilitate ***angiogenesis*** in many pathological conditions. In vitro, the outgrowth of capillary-like structures in fibrin can be mimicked by exposing human microvascular endothelial cells (hMVECs) to an ***angiogenic*** growth factor and ***tumor*** necrosis factor (TNF)-alpha. Urokinase-type plasminogen activator (u-PA) and plasmin activities are required for this ***angiogenic*** process. This study focuses on the role and localization of the u-PA receptor (u-PAR) in newly formed microvascular structures. The u-PAR-blocking monoclonal ***antibody*** (MAb) H-2 completely inhibited the formation of capillary-like tubular structures induced by exposure of hMVECs to basic ***fibroblast*** ***growth*** ***factor*** and TNF-alpha. This was accompanied by a several-fold increase in u-PA accumulation in the conditioned medium. The effect of MAb H-2 was not caused by blocking cellular activation by u-PA/u-PAR interaction, as the amino-terminal ***fragment*** (ATF) of u-PA, which also activates u-PAR, prevented tube formation. In addition, the inhibition by MAb H-2 was not due to an effect of the ***antibody*** on u-PAR-vitronectin binding. These data show that inhibition of tube formation can be caused not only by inhibition of u-PA or plasmin activities but also by unavailability of the u-PAR for cell-bound proteolysis. Immunohistochemical analysis showed that in in vitro ***angiogenesis*** u-PAR and u-PA were localized on the invading, tube-forming hMVECs and not on the endothelial cells that are located on top of the fibrin matrix. u-PAR and u-PA were also prominently expressed

on endothelial cells of neovessels present in an atherosclerotic plaque. These data may give more insight into the role of u-PAR in repair-associated ***angiogenesis*** .

L54 ANSWER 12 OF 50 MEDLINE DUPLICATE 2
ACCESSION NUMBER: 1999115214 MEDLINE
DOCUMENT NUMBER: 99115214
TITLE: Progesterone maintains large rat granulosa cell viability indirectly by stimulating small granulosa cells to synthesize basic ***fibroblast*** ***growth*** ***factor*** .
AUTHOR: Peluso J J; Pappalardo A
CORPORATE SOURCE: Department of Obstetrics and Gynecology, University of Connecticut Health Center, Farmington, Connecticut 06030, USA.. peluso@nso2.uchc.edu
CONTRACT NUMBER: RO1-HD 33467-01A2 (NICHD)
SOURCE: BIOLOGY OF REPRODUCTION, (1999 Feb) 60 (2) 290-6. Journal code: A3W. ISSN: 0006-3363.
PUB. COUNTRY: United States
Journal; Article; (JOURNAL ARTICLE)
LANGUAGE: English
FILE SEGMENT: Priority Journals
ENTRY MONTH: 199906
ENTRY WEEK: 19990603
AB Ovarian follicles are composed of small and large granulosa cells (GCs). Since progesterone (P4) inhibits large GCs from undergoing apoptosis, studies were designed to determine whether both sizes of GCs bind P4. These studies revealed that fluorescein isothiocyanate- ***BSA*** -P4 bound only to the surface membranes of small GCs. This binding was steroid-specific and inhibited by an ***antibody*** directed against the ligand-binding domain of the nuclear P4 receptor (PR). In addition, a cell-impermeable derivative of P4, ***BSA*** -conjugated P4, was as effective as P4 in preventing apoptosis. Quantitative in situ hybridization studies showed that P4 increased the relative amount of basic ***fibroblast*** ***growth*** ***factor*** (bFGF) mRNA expressed per cell as well as the percentage of small GCs that expressed bFGF. To determine whether the anti-apoptotic action of P4 was mediated by bFGF, GCs were cultured in control medium supplemented with either P4, a neutralizing ***antibody*** to bFGF, or both P4 and the bFGF ***antibody*** . The results from this study demonstrated that P4 suppressed apoptosis and that this effect was attenuated in presence of the bFGF ***antibody*** . Basic FGF also prevented GC apoptosis, and its action was not influenced by either the PR antagonist (RU-486), an inhibitor of P4 synthesis (aminoglutethimide), or a PR ***antibody*** .

Finally, FGF receptors were detected on both small and large GCs. Collectively, these data support the hypothesis that P4 acts through a putative membrane receptor on small GCs to stimulate the synthesis of bFGF. Basic FGF then activates its receptors within large GCs, and this initiates a signal transduction pathway that maintains large GC viability.

L54 ANSWER 13 OF 50 MEDLINE
ACCESSION NUMBER: 1999107224 MEDLINE
DOCUMENT NUMBER: 99107224
TITLE: Endostatin: yeast production, mutants, and antitumor effect in renal cell carcinoma.
AUTHOR: Dhanabal M; Ramchandran R; Volk R; Stillman I E; Lombardo

M; Iruela-Arispe M L; Simons M; Sukhatme V P
CORPORATE SOURCE: Renal Division, Beth Israel Deaconess Medical Center and Harvard Medical School, Boston, Massachusetts 02215, USA.
SOURCE: CANCER RESEARCH, (1999 Jan 1) 59 (1) 189-97.
Journal code: CNF. ISSN: 0008-5472.
PUB. COUNTRY: United States
Journal; Article; (JOURNAL ARTICLE)
LANGUAGE: English
FILE SEGMENT: Priority Journals; Cancer Journals
ENTRY MONTH: 199904
ENTRY WEEK: 19990401

AB Endostatin is a Mr 20,000 COOH-terminal ***fragment*** of collagen XVIII that inhibits the growth of several primary tumors. We report here the cloning and expression of mouse endostatin in both prokaryotic and eukaryotic expression systems. Soluble recombinant protein expressed in yeast (15-20 mg/L) inhibited the proliferation and migration of endothelial cells in response to stimulation by basic ***fibroblast*** ***growth*** ***factor*** . A rabbit polyclonal ***antibody*** was raised that showed positive immunoreactivity to the recombinant protein expressed from both systems. Importantly, the biological activity of the mouse recombinant protein could be neutralized by this antiserum in both endothelial proliferation and chorioallantoic membrane assays. Systemic administration of endostatin at 10 mg/kg suppressed the growth of renal cell ***cancer*** in a nude mouse model. The inhibition of ***tumor*** growth with soluble yeast-produced protein was comparable to that obtained with non-refolded precipitated protein expressed from bacteria. In addition, two closely related COOH-terminal deletion mutants of endostatin were also tested and showed strikingly differing activity. Collectively, these findings demonstrate the expression of a biologically active form of mouse endostatin in yeast, define a role for the molecule in inhibiting endothelial cell migration, extend its antitumor effects to renal cell carcinoma, and provide a formal proof (via the neutralizing antiserum experiments and the mutant data) that endostatin (and not a possible contaminant) acts as an antiangiogenic agent. Finally, the high level expression of mouse endostatin in yeast serves as an endotoxin free, soluble source of protein for fundamental studies on the mechanisms of ***tumor*** growth suppression by ***angiogenesis*** inhibitors.

L54 ANSWER 14 OF 50 CAPLUS COPYRIGHT 2001 ACS
ACCESSION NUMBER: 1998:621330 CAPLUS
DOCUMENT NUMBER: 129:240871
TITLE: Adenoviral vectors with modified tropism for gene therapy
INVENTOR(S): Sosnowski, Barbara A.; Baird, Andrew; Pierce, Glenn F.; Curiel, David T.; Douglas, Joanne T.; Rogers, Buck E.
PATENT ASSIGNEE(S): USA
SOURCE: PCT Int. Appl., 205 pp.
CODEN: PIXXD2
DOCUMENT TYPE: Patent
LANGUAGE: English
FAMILY ACC. NUM. COUNT: 1
PATENT INFORMATION:

PATENT NO.	KIND	DATE	APPLICATION NO.	DATE

WO 9840508		A1	19980917	WO 1998-US4964	19980313
	W:	AL, AM, AT, AU, BA, BB, BG, BR, BY, CA, CH, CN, CU, CZ, DE, DK, EE, ES, FI, GB, GE, GH, GM, GW, HU, ID, IL, IS, JP, KE, KG, KP, KR, KZ, LC, LK, LR, LS, LT, LU, LV, MD, MG, MK, MN, MW, MX, NO, NZ, PL, PT, RO, RU, SD, SE, SG, SI, SK, SL, TJ, TM, TR, TT, UA, UG, UZ, VN, YU, ZW, AM, AZ, BY, KG, KZ, MD, RU, TJ, TM			
	RW:	GH, GM, KE, LS, MW, SD, SZ, UG, ZW, AT, BE, CH, DE, DK, ES, FI, FR, GB, GR, IE, IT, LU, MC, NL, PT, SE, BF, BJ, CF, CG, CI, CM, GA, GN, ML, MR, NE, SN, TD, TG			
AU 9864629		A1	19980929	AU 1998-64629	19980313
EP 973926		A1	20000126	EP 1998-910375	19980313
	R:	AT, BE, CH, DE, DK, ES, FR, GB, GR, IT, LI, LU, NL, SE, MC, PT, IE, FI			
PRIORITY APPLN. INFO.:				US 1997-40782	19970314
				US 1997-65265	19971110
				WO 1998-US4964	19980313

AB The present invention relates to gene therapy. In particular, therapeutic agents, therapeutic gene products, and compns. are disclosed. Various systems and methods useful in targeting and delivering non-native nucleotide sequences to specific cells are disclosed, wherein virus-***antibody*** -ligand conjugates are used to facilitate targeting and delivery. Thus, FAB- ***fibroblast*** ***growth*** ***factor*** 2 conjugates are constructed by linking modified recombinant ***fibroblast*** ***growth*** ***factor*** (FGF) with the FAB ***fragment*** from a blocking monoclonal ***antibody*** , 1D6.14, which was generated against adenovirus type 5 knob region. FGF2 retargeting of an adenovirus (i.e., altering the tropism of an adenovirus using a ***fibroblast*** ***growth*** ***factor***) significant enhances targeting efficiency and nuclear trafficking of the adenovirus vector well above that seen when the vector retains its native adenoviral tropism. In addn., FGF retargeting increases the infectability of adenovirus in various cells (e.g., cells expressing Kaposi's sarcoma) compared to the use of native adenovirus tropism alone, even in cell lines hat are resistant to adenovirus infection. The use of FGF retargeting vectors enhances potency; FGF-retargeted vectors deliver and promote the expression of a therapeutic gene to more target cells and in each cell so targeted. The vectors of the present invention are also significantly less toxic to the liver and are less ***immunogenic*** than are other adenovirus vectors. Finally, retargeting the viral vector retarged with FGF induces cytotoxicity to specific cell types when therapeutic gene sequences (e.g., cytotoxic sequences, such as herpes simplex virus thymidine kinase) are delivered. FGF retargeted vectors are thus able to transduce cells which are normally insensitive to adenovirus infection.

L54 ANSWER 15 OF 50 CAPLUS COPYRIGHT 2001 ACS

ACCESSION NUMBER:	1998:612020 CAPLUS
DOCUMENT NUMBER:	129:225720
TITLE:	Concurrent in-vivo immunoconjugate binding to multiple epitopes of ***vascular*** ***permeability*** ***factor*** on tumor-associated blood vessels
INVENTOR(S):	Senger, Donald R.; Dvorak, Harold F.
PATENT ASSIGNEE(S):	Beth Israel Deaconess Medical Center, USA
SOURCE:	PCT Int. Appl., 70 pp. CODEN: PIXXD2
DOCUMENT TYPE:	Patent

LANGUAGE: English
FAMILY ACC. NUM. COUNT: 3
PATENT INFORMATION:

PATENT NO.	KIND	DATE	APPLICATION NO.	DATE
WO 9839037	A1	19980911	WO 1998-US3765	19980226
W: AU, CA, JP				
RW: AT, BE, CH, DE, DK, ES, FI, FR, GB, GR, IE, IT, LU, MC, NL, PT, SE				
US 6022541	A	20000208	US 1997-807992	19970303
AU 9867570	A1	19980922	AU 1998-67570	19980226
AU 722722	B2	20000810		
EP 968002	A1	20000105	EP 1998-912888	19980226
R: AT, BE, CH, DE, DK, ES, FR, GB, GR, IT, LI, NL, SE, PT, IE, FI				

PRIORITY APPLN. INFO.: US 1997-807992 19970303
US 1991-779384 19911018
US 1994-327709 19941024
WO 1998-US3765 19980226

AB An immunol. prepn. is provided which comprises not less than two types of conjugate mols. in admixt. for concurrent specific binding to a spatially exposed region of ***vascular*** ***permeability*** ***factor*** (VPF) bound in-vivo to a tumor-assocd. blood vessel. Each conjugate mol. type comprises at least a binding portion of an ***antibody*** specific for an epitope present within a spatially exposed region of bound VPF; and an effector moiety covalently bound to the specific binding portion. The immunol. prepn. has wide uses and applications including anal. studies, in-vivo diagnostic testing, and in-vivo therapeutic treatments. The effector mol. may be a radionuclide, antimetabolite, bacterial exotoxin, etc.

L54 ANSWER 16 OF 50 MEDLINE
ACCESSION NUMBER: 1998428671 MEDLINE
DOCUMENT NUMBER: 98428671
TITLE: VEGF and the Fab ***fragment*** of a humanized neutralizing ***antibody*** : crystal structure of the complex at 2.4 A resolution and mutational analysis of the interface.
AUTHOR: Muller Y A; Chen Y; Christinger H W; Li B; Cunningham B C; Lowman H B; de Vos A M
CORPORATE SOURCE: Department of Protein Engineering Genentech, Inc. 1 DNA Way, South San Francisco, CA 94080, USA.
SOURCE: STRUCTURE, (1998 Sep 15) 6 (9) 1153-67.
Journal code: B31. ISSN: 0969-2126.
PUB. COUNTRY: ENGLAND: United Kingdom
Journal; Article; (JOURNAL ARTICLE)
LANGUAGE: English
FILE SEGMENT: Priority Journals
OTHER SOURCE: PDB-1BJ1; PDB-1BJSF
ENTRY MONTH: 199902
ENTRY WEEK: 19990204

AB BACKGROUND: Vascular endothelial growth factor (VEGF) is a highly specific ***angiogenic*** growth factor; anti- ***angiogenic*** treatment through inhibition of receptor activation by VEGF might have important therapeutic applications in diseases such as diabetic retinopathy and ***cancer*** . A neutralizing anti-VEGF ***antibody*** shown to suppress ***tumor*** growth in an in vivo murine model has been used

as the basis for production of a humanized version. RESULTS: We present the crystal structure of the complex between VEGF and the Fab ***fragment*** of this humanized ***antibody*** , as well as a comprehensive alanine-scanning analysis of the contact residues on both sides of the interface. Although the VEGF residues critical for ***antibody*** binding are distinct from those important for high-affinity receptor binding, they occupy a common region on VEGF, demonstrating that the neutralizing effect of ***antibody*** binding results from steric blocking of VEGF-receptor interactions. Of the residues buried in the VEGF-Fab interface, only a small number are critical for high-affinity binding; the essential VEGF residues interact with those of the Fab ***fragment*** , generating a remarkable functional complementarity at the interface. CONCLUSIONS: Our findings suggest that the character of antigen- ***antibody*** interfaces is similar to that of other protein-protein interfaces, such as ligand-receptor interactions; in the case of VEGF, the principal difference is that the residues essential for binding to the Fab ***fragment*** are concentrated in one continuous segment of polypeptide chain, whereas those essential for binding to the receptor are distributed over four different segments and span across the dimer interface.

L54 ANSWER 17 OF 50 MEDLINE DUPLICATE 3
ACCESSION NUMBER: 1998435605 MEDLINE
DOCUMENT NUMBER: 98435605
TITLE: Autocrine self-elimination of cultured ovarian cancer cells by tumour necrosis factor alpha (TNF-alpha).
AUTHOR: Simonitsch I; Krupitza G
CORPORATE SOURCE: Institute of Clinical Pathology, University of Vienna, Austria.
SOURCE: BRITISH JOURNAL OF CANCER, (1998 Oct) 78 (7) 862-70. Journal code: AV4. ISSN: 0007-0920.
PUB. COUNTRY: SCOTLAND: United Kingdom
Journal; Article; (JOURNAL ARTICLE)
LANGUAGE: English
FILE SEGMENT: Priority Journals; Cancer Journals
ENTRY MONTH: 199812
AB Human ovarian adenocarcinoma cells N.1 secrete an autocrine activity that stimulates active cell death under serum-reduced conditions. To substitute the autocrine activity by a single physiological component, 28 cytokines, growth factors and biomodulators were tested [interleukin 1alpha (IL-1alpha), IL-1beta, IL-2, IL-3, IL-4, IL-6, IL-10, IL-11, stem cell factor (SCF), platelet-derived growth factor (PDGF), acid ***fibroblast*** ***growth*** ***factor*** (aFGF), basic ***fibroblast*** ***growth*** ***factor*** (bFGF), insulin-like growth factor (IGF-1), IGF-2, insulin, macrophage colony-stimulating factor (M-CSF), granulocyte colony-stimulating factor (G-CSF), granulocyte-macrophage colony-stimulating factor (GM-CSF), oncostatin, RANTES (regulated on activation normal T cell expressed and secreted), angiogenin, leukaemia inhibitory factor (LIF), erythropoietin (EPO), interferon alpha (INF-alpha), INF-gamma, transferrin, tumour necrosis factor alpha (TNF-alpha, TNF-beta and ***bovine*** ***serum*** ***albumin*** for control reasons]. In these experiments, only TNF-alpha and TNF-beta rapidly induced apoptosis. TNF-alpha and TNF-receptor 1 were expressed by N.1 cells, and the secretion of TNF-alpha was verified by

enzyme-linked immunosorbent assay (ELISA). Autocrine factor-triggered apoptosis was inhibited when conditioned supernatant was preincubated with anti-TNF-alpha ***antibody*** . These findings suggested that the apoptosis-inducing component of the N.1 autocrine activity was TNF-alpha. In the presence of antisense c-myc oligonucleotides, induction of cell death by autocrine factor was partly inhibited. Autocrine factor and TNF-alpha stimulated transcription of the invasiveness-related protease plasminogen activator/urokinase mRNA (upa) with similar kinetics. When N.1 cells were exposed to purified plasminogen activator/urokinase protein (uPA), cell matrix contact was disrupted. Thus, uPA might serve a physiological role during TNF-induced apoptosis by affecting the interactions between cells and the basal membrane, thereby facilitating anoikis. This mechanistic study, which was restricted to a single human ovarian carcinoma model cell line (N.1), provides evidence that N.1 maintains the capacity to undergo c-myc-dependent apoptosis by the TNF-TNF-receptor pathway, and no additional pharmacological stimuli for induction of apoptosis are required.

L54 ANSWER 18 OF 50 EMBASE COPYRIGHT 2001 ELSEVIER SCI. B.V.
ACCESSION NUMBER: 1998140290 EMBASE
TITLE: Protein release from alginate matrices.
AUTHOR: Gombotz W.R.; Siong Fong Wee
CORPORATE SOURCE: W.R. Gombotz, Analytical Chem./Formulation Dept., Immunex Corporation, 51 University Street, Seattle, WA 98101, United States
SOURCE: Advanced Drug Delivery Reviews, (4 May 1998) 31/3 (267-285).
Refs: 129
ISSN: 0169-409X CODEN: ADDREP
PUBLISHER IDENT.: S 0169-409X(97)00124-5
COUNTRY: Netherlands
DOCUMENT TYPE: Journal; Article
FILE SEGMENT: 037 Drug Literature Index
039 Pharmacy
LANGUAGE: English
SUMMARY LANGUAGE: English
AB There are a variety of both natural and synthetic polymeric systems that have been investigated for the controlled release of proteins. Many of the procedures employed to incorporate proteins into a polymeric matrix can be harsh and often cause denaturation of the active agent. Alginate, a naturally occurring biopolymer extracted from brown algae (kelp), has several unique properties that have enabled it to be used as a matrix for the entrapment and/or delivery of a variety of biological agents. Alginate polymers are a family of linear unbranched polysaccharides which contain varying amounts of 1,4'-linked .beta.-D-mannuronic acid and .alpha.-L-guluronic acid residues. The residues may vary widely in composition and sequence and are arranged in a pattern of blocks along the chain. Alginate can be ionically crosslinked by the addition of divalent cations in aqueous solution. The relatively mild gelation process has enabled not only proteins, but cells and DNA to be incorporated into alginate matrices with retention of full biological activity. Furthermore, by selection of the type of alginate and coating agent, the pore size, degradation rate, and ultimately release kinetics can be controlled. Gels

of different morphologies can be prepared including large block matrices, large beads (>1 mm in diameter) and microbeads (<0.2 mm in diameter). In situ gelling systems have also been made by the application of alginate to the cornea, or on the surfaces of wounds. Alginate is a bioadhesive polymer which can be advantageous for the site specific delivery to mucosal tissues. All of these properties, in addition to the nonimmunogenicity of alginate, have led to an increased use of this polymer as a protein delivery system. This review will discuss the chemistry of alginate, its gelation mechanisms, and the physical properties of alginate gels. Emphasis will be placed on applications in which biomolecules have been incorporated into and released from alginate systems.

L54 ANSWER 19 OF 50 MEDLINE DUPLICATE 4
ACCESSION NUMBER: 1998288750 MEDLINE
DOCUMENT NUMBER: 98288750
TITLE: Efficient purification of mouse anti-FGF receptor IgM monoclonal ***antibody*** by magnetic beads.
AUTHOR: Quitadamo I J; Schelling M E
CORPORATE SOURCE: Department of Genetics and Cell Biology, Washington State University, Pullman 99164-4234, USA.
SOURCE: HYBRIDOMA, (1998 Apr) 17 (2) 199-207.
Journal code: GFS. ISSN: 0272-457X.
PUB. COUNTRY: United States
Journal; Article; (JOURNAL ARTICLE)
LANGUAGE: English
FILE SEGMENT: Priority Journals
ENTRY MONTH: 199810
ENTRY WEEK: 19981004
AB Affinity chromatography has been widely used for the purification of monoclonal antibodies (MAb). Traditionally, activated agarose beads conjugated with specific antisera have been used as a solid support in chromatographic protein purification. Magnetic beads conjugated with various antibodies have recently become an alternative method for the isolation of diverse proteins, nucleic acids, and cell types. In this study, murine anti- ***fibroblast*** ***growth*** ***factor*** receptor 1 (FGFR1) immunoglobulin M (IgM) was isolated from protein solutions to compare immunoaffinity column chromatography and magnetic bead IgM purification methods. Using immobilized rat anti-mouse IgM MAb, an UltraLink 1-ethyl-3-(3-dimethylaminopropyl)carboiimide (EDC)/diaminodipropylamine (DADPA) immunoaffinity column and polystyrene-coated magnetic beads were used for the purification of mouse IgM from ***bovine*** ***serum*** ***albumin*** /phosphate-buffered saline (***BSA*** /PBS) as well as from crude ascites. Protein quantitation and percent IgM yield were determined by reducing SDS-PAGE electrophoresis followed by silver staining, then IgM and protein contaminants were quantitated using densitometry analysis. IgM anti-FGFR1 binding specificity and immunologic activity were determined by enzyme-linked immunosorbant assay (ELISA). This study demonstrates that magnetic bead isolation of IgM from ascites is more effective than traditional affinity chromatography purification as determined by greater IgM yield, purity, and immunologic activity.

L54 ANSWER 20 OF 50 MEDLINE
ACCESSION NUMBER: 97236834 MEDLINE
DOCUMENT NUMBER: 97236834
TITLE: Advanced glycation end products-driven angiogenesis in

vitro. Induction of the growth and tube formation of human microvascular endothelial cells through autocrine vascular endothelial growth factor.

AUTHOR: Yamagishi Si; Yonekura H; Yamamoto Y; Katsuno K; Sato F; Mita I; Ooka H; Satozawa N; Kawakami T; Nomura M; Yamamoto H

CORPORATE SOURCE: Department of Biochemistry, Kanazawa University School of Medicine, Kanazawa 920, Japan.

SOURCE: JOURNAL OF BIOLOGICAL CHEMISTRY, (1997 Mar 28) 272 (13) 8723-30.
Journal code: HIV. ISSN: 0021-9258.

PUB. COUNTRY: United States
Journal; Article; (JOURNAL ARTICLE)

LANGUAGE: English

FILE SEGMENT: Priority Journals; Cancer Journals

ENTRY MONTH: 199707

AB This study was undertaken to determine whether and how advanced glycation end products (AGE), senescent macroproteins accumulated in various tissues under hyperglycemic states, cause angiogenesis, the principal vascular derangement in diabetic microangiopathy. We first prepared AGE- ***bovine*** ***serum*** ***albumin*** (***BSA***) and anti-AGE antiserum using AGE-RNase A. Then AGE- ***BSA*** was administered to human skin microvascular endothelial cells in culture, and their growth was examined. The AGE- ***BSA*** , but not nonglycated ***BSA*** , was found to induce a statistically significant increase in the number of viable endothelial cells as well as their synthesis of DNA. The increase in DNA synthesis by AGE- ***BSA*** was abolished by anti-AGE antibodies. AGE- ***BSA*** also stimulated the tube formation of endothelial cells on Matrigel. We obtained the following evidence that it is vascular endothelial growth factor (VEGF) that mainly mediates the angiogenic activities of AGE. (1) Quantitative reverse transcription-polymerase chain reaction analysis of poly(A)+ RNA from microvascular endothelial cells revealed that AGE- ***BSA*** up-regulated the levels of mRNAs for the secretory forms of VEGF in time- and dose-dependent manners, while endothelial cell expression of the genes encoding the two VEGF receptors, kinase insert domain-containing receptor and fms-like tyrosine kinase 1, remained unchanged by the AGE treatment. Immunoprecipitation analysis revealed that AGE- ***BSA*** did increase de novo synthesis of VEGF. (2) Monoclonal ***antibody*** against human VEGF completely neutralized both the AGE-induced DNA synthesis and tube formation of the endothelial cells. The results suggest that AGE can elicit angiogenesis through the induction of autocrine vascular VEGF, thereby playing an active part in the development and progression of diabetic microangiopathies.

L54 ANSWER 21 OF 50 MEDLINE

ACCESSION NUMBER: 97270470 MEDLINE

DOCUMENT NUMBER: 97270470

TITLE: A monoclonal ***antibody*** to Borrelia burgdorferi ***flagellin*** modifies neuroblastoma cell neuritogenesis in vitro: a possible role for autoimmunity in the neuropathy of Lyme disease.

AUTHOR: Sigal L H; Williams S

CORPORATE SOURCE: Department of Medicine, University of Medicine and Dentistry of New Jersey-Robert Wood Johnson Medical

School,
New Brunswick 08903, USA.
SOURCE: INFECTION AND IMMUNITY, (1997 May) 65 (5) 1722-8.
Journal code: GO7. ISSN: 0019-9567.
PUB. COUNTRY: United States
Journal; Article; (JOURNAL ARTICLE)
LANGUAGE: English
FILE SEGMENT: Priority Journals; Cancer Journals
ENTRY MONTH: 199707
ENTRY WEEK: 19970703
AB Although Borrelia burgdorferi is found at the site of many manifestations of Lyme disease, local infection may not explain all features of the disease. Previous work has demonstrated that the organism's ***flagellin*** cross-reacts with a component of human peripheral nerve axon, heat shock protein 60. The cross-reacting epitope is identified by a single anti-B. burgdorferi ***flagellin*** monoclonal ***antibody*** , H9724. We now report that the spontaneous and peptide growth factor-stimulated in vitro neuritogenesis of SK-N-SH neuroblastoma cells and other neural tumor cell lines is suppressed by H9724. In contrast, changes induced by exposure of these cells to optimal and suboptimal concentrations of cyclic AMP, phorbol ester, or retinoic acid are not affected by H9724. H9724 does not decrease cell viability or the ability of the cells to anchor to the culture plate or extracellular matrix and does not block nerve growth factor binding to the cells. These findings are compatible with the premise that antiaxonal antibodies formed during the immune response to B. burgdorferi ***flagellin*** might modify axonal function in vivo and play a role in the pathogenesis of neurologic features of Lyme disease. A humoral immune response predicated on molecular mimicry could explain persistent or ongoing neurologic dysfunction occurring after elimination of the organism by appropriate antibiotic therapy.

L54 ANSWER 22 OF 50 EMBASE COPYRIGHT 2001 ELSEVIER SCI. B.V.
ACCESSION NUMBER: 97169882 EMBASE
DOCUMENT NUMBER: 1997169882
TITLE: TGF-.beta. in kidney fibrosis: A target for gene therapy.
AUTHOR: Border W.A.; Noble N.A.
CORPORATE SOURCE: Dr. W.A. Border, Division of Nephrology, Univ. of Utah Sch.
of Med., 50 North Medical Drive, Salt Lake City, UT 84132, United States
SOURCE: Kidney International, (1997) 51/5 (1388-1396).
Refs: 40
ISSN: 0085-2538 CODEN: KDYIA5
COUNTRY: United States
DOCUMENT TYPE: Journal; General Review
FILE SEGMENT: 005 General Pathology and Pathological Anatomy
028 Urology and Nephrology
029 Clinical Biochemistry
037 Drug Literature Index
038 Adverse Reactions Titles
LANGUAGE: English

L54 ANSWER 23 OF 50 EMBASE COPYRIGHT 2001 ELSEVIER SCI. B.V.DUPLICATE 5
ACCESSION NUMBER: 97140306 EMBASE
DOCUMENT NUMBER: 1997140306
TITLE: Effect of growth factors and antigen on hybridoma cell

culture dynamics.
AUTHOR: Dandulakis G.; Herr J.C.; Kirwan D.J.
CORPORATE SOURCE: G. Dandulakis, Department of Chemical Engineering, Center for Bioprocess Development, University of Virginia, Charlottesville, VA 22903-2442, United States.
gd8f@virginia.edu
SOURCE: Biotechnology and Bioengineering, (1997) 54/4 (357-364).
Refs: 21
ISSN: 0006-3592 CODEN: BIBIAU
COUNTRY: United States
DOCUMENT TYPE: Journal; Article
FILE SEGMENT: 029 Clinical Biochemistry
LANGUAGE: English
SUMMARY LANGUAGE: English
AB The cell growth and monoclonal ***antibody*** production kinetics of hybridoma cell cultures continuously exposed to growth factors and the cognate antigen were investigated. The growth factors were the epidermal growth factor, ***fibroblast*** ***growth*** ***factor*** , and interleukin-2, whereas the antigen was the trinitrophenyl group conjugated to a ***carrier*** ***protein*** . The cultures were carried out in a protein-free medium in batch operation. During the entire cultivation period there was continuously available free, ***antibody*** -unbound antigen to interact with the cells. The produced ***antibody*** was measured with an ELISA after it was released from the antigen-protein conjugate by competitive elution with non-protein-conjugated antigen. Cultures with growth factors and without antigen increased the total ***antibody*** produced by up to 30%, whereas cell growth remained unaffected. Soluble antigen-protein conjugates had no effect on the hybridoma cultures. In contrast, immobilized antigen-protein on sepharose beads in cultures with growth factors induced significant changes. Total ***antibody*** produced was higher by up to 40%. More importantly, the specific ***antibody*** production shifted from a growth-phase-independent to a growth-phase-dependent pro-file, with approximately twice as much specific ***antibody*** production during the late growth-early stationary phase relative to constant specific ***antibody*** production in the antigen-free, factor-free culture. The culture changes induced by the presence of immobilized antigen and growth factors were reversed when the antigen and the growth factors were removed from the cells' environment.

L54 ANSWER 24 OF 50 BIOSIS COPYRIGHT 2001 BIOSIS
ACCESSION NUMBER: 1997:250406 BIOSIS
DOCUMENT NUMBER: PREV199799549609
TITLE: Effect of growth factors and antigen on hybridoma cell culture dynamics.
AUTHOR(S): Dandulakis, Gregory (1); Herr, John C.; Kirwan, Donald J.
CORPORATE SOURCE: (1) Cent. Bioprocess Development, Dep. Chemical Engineering, Univ. Virginia, Charlottesville, VA 22903-2442
USA
SOURCE: Biotechnology and Bioengineering, (1997) Vol. 54, No. 4, pp. 356-364.
ISSN: 0006-3592.

DOCUMENT TYPE: Article
LANGUAGE: English
AB The cell growth and monoclonal ***antibody*** production kinetics of hybridoma cell cultures continuously exposed to growth factors and the cognate antigen were investigated. The growth factors were the epidermal growth factor, ***fibroblast*** ***growth*** ***factor*** , and interleukin-2, whereas the antigen was the trinitrophenyl group conjugated to a ***carrier*** ***protein*** . The cultures were carried out in a protein-free medium in batch operation. During the entire cultivation period there was continuously available free, ***antibody*** -unbound antigen to interact with the cells. The produced ***antibody*** was measured with an ELISA after it was released from the antigen-protein conjugate by competitive elution with non-protein conjugated antigen. Cultures with growth factors and without antigen increased the total ***antibody*** produced by up to 30%, whereas cell growth remained unaffected. Soluble antigen-protein conjugates had no effect on the hybridoma cultures. In contrast, immobilized antigen protein on sepharose beads in cultures with growth factors induced significant changes. Total ***antibody*** produced was higher by up to 40%. More importantly, the specific ***antibody*** production shifted from a growth phase-independent to a growth-phase-dependent profile, with approximately twice as much specific ***antibody*** production during the late growth-early stationary phase relative to constant specific ***antibody*** production in the antigen-free, factor-free culture. The culture changes induced by the presence of immobilized antigen and growth factors were reversed when the antigen and the growth factors were removed from the cells' environment.

L54 ANSWER 25 OF 50 MEDLINE
ACCESSION NUMBER: 96215296 MEDLINE
DOCUMENT NUMBER: 96215296
TITLE: The degradation of human endothelial cell-derived perlecan and release of bound basic ***fibroblast*** ***growth*** ***factor*** by stromelysin, collagenase, plasmin, and heparanases.
AUTHOR: Whitelock J M; Murdoch A D; Iozzo R V; Underwood P A
CORPORATE SOURCE: Commonwealth Scientific and Industrial Research Organization, Division of Biomolecular Engineering, P.O. Box 184, North Ryde, Sydney, New South Wales 2114, Australia.
CONTRACT NUMBER: RO1 CA-39481 (NCI)
RO1 CA-47282 (NCI)
SOURCE: JOURNAL OF BIOLOGICAL CHEMISTRY, (1996 Apr 26) 271 (17) 10079-86.
Journal code: HIV. ISSN: 0021-9258.
PUB. COUNTRY: United States
Journal; Article; (JOURNAL ARTICLE)
LANGUAGE: English
FILE SEGMENT: Priority Journals; Cancer Journals
ENTRY MONTH: 199608
AB Perlecan is a modular heparan sulfate proteoglycan that is localized to cell surfaces and within basement membranes. Its ability to interact with basic ***fibroblast*** ***growth*** ***factor*** (bFGF) suggests a central role in ***angiogenesis*** during development,

wound healing, and ***tumor*** invasion. In the present study we investigated, using domain specific anti-perlecan monoclonal antibodies, the binding site of bFGF on human endothelial perlecan and its cleavage by proteolytic and glycolytic enzymes. The heparan sulfate was removed from perlecan by heparitinase treatment, and the approximately 450-kDa protein core was digested with various proteases. Plasmin digestion resulted in a large ***fragment*** of approximately 300 kDa, whereas stromelysin and rat collagenase cleaved the protein core into smaller fragments. All three proteases removed immunoreactivity toward the anti-domain I ***antibody*** . We showed also that perlecan bound bFGF specifically by the heparan sulfate chains located on the amino-terminal domain I. Once bound, the growth factor was released very efficiently by stromelysin, rat collagenase, plasmin, heparitinase I, platelet extract, and heparin. Interestingly, heparinase I, an enzyme with a substrate specificity for regions of heparan sulfate similar to those that bind bFGF, released only small amounts of bFGF. Our findings provide direct evidence that bFGF binds to heparan sulfate sequences attached to domain I and support the hypothesis that perlecan represents a major storage site for this growth factor in the blood vessel wall. Moreover, the concerted action of proteases that degrade the protein core and heparanases that remove the heparan sulfate may modulate the bioavailability of the growth factor.

L54 ANSWER 26 OF 50 EMBASE COPYRIGHT 2001 ELSEVIER SCI. B.V.
ACCESSION NUMBER: 96107804 EMBASE
DOCUMENT NUMBER: 1996107804
TITLE: Cooperative effect of TNF.alpha., bFGF, and VEGF on the formation of tubular structures of human microvascular endothelial cells in a fibrin matrix. Role of urokinase activity.
AUTHOR: Koolwijk P.; Van Erck M.G.M.; De Vree W.J.A.; Vermeer A.; Weich H.A.; Hanemaaijer R.; Van Hinsbergh V.W.M.
CORPORATE SOURCE: Gaubius Laboratory TNO-PG, P.O. Box 2215,2301 CE Leiden, Netherlands
SOURCE: Journal of Cell Biology, (1996) 132/6 (1177-1188). ISSN: 0021-9525 CODEN: JCLBA3
COUNTRY: United States
DOCUMENT TYPE: Journal; Article
FILE SEGMENT: 029 Clinical Biochemistry
LANGUAGE: English
SUMMARY LANGUAGE: English
AB In ***angiogenesis*** associated with tissue repair and disease, fibrin and inflammatory mediators are often involved. We have used three-dimensional fibrin matrices to investigate the humoral requirements of human microvascular endothelial cells (hMVEC) to form capillary-like tubular structures. bFGF and VEGF165 were unable to induce tubular structures by themselves. Simultaneous addition of one or both of these factors with TNF.alpha. induced outgrowth of tubules, the effect being the strongest when bFGF, VEGF165, and TNF.alpha. were added simultaneously. Exogenously added u-PA, but not its nonproteolytic amino-terminal ***fragment*** , could replace TNF.alpha., suggesting that TNF.alpha.-induced u-PA synthesis was involved. Soluble u-PA receptor (u-PAR) or antibodies that inhibited u-PA activity prevented the formation of tubular structures by 59-99%. .epsilon.-ACA and trasylol which inhibit

the formation and activity of plasmin reduced file extent of tube formation by 71-95%. TNF.alpha. or u-PA did not induce tubular structures without additional growth factors. bFGF and VEGF165 enhanced of the u-PAR by 72 and 46%, but TNF.alpha. itself also increased u-PAR in hMVEC by 30%.

Induction of mitogenesis was not the major contribution of bFGF and VEGF165 because the cell number did not change significantly in the presence of TNF.alpha., and tyrphostin A47, which inhibited mitosis completely, reduced the formation of tubular structures only by 28-36%.

These data show that induction of cell-bound u-PA activity by the cytokine TNF.alpha. is required in addition to the ***angiogenic*** factors VEGF165 and/or bFGF to induce in vitro formation of capillary- like structures by hMVEC in fibrin matrices. These data may provide insight in the mechanism of ***angiogenesis*** as occurs in pathological conditions.

L54 ANSWER 27 OF 50 MEDLINE DUPLICATE 6
ACCESSION NUMBER: 96183755 MEDLINE
DOCUMENT NUMBER: 96183755
TITLE: Interaction with fibronectin regulates cytokine gene expression in human melanoma cells.
AUTHOR: Lupetti R; Mortarini R; Panceri P; Sensi M; Anichini A
CORPORATE SOURCE: Division of Experimental Oncology D, Istituto Nazionale Tumori, Milan, Italy.
SOURCE: INTERNATIONAL JOURNAL OF CANCER, (1996 Mar 28) 66 (1) 110-6.
Journal code: GQU. ISSN: 0020-7136.
PUB. COUNTRY: United States
Journal; Article; (JOURNAL ARTICLE)
LANGUAGE: English
FILE SEGMENT: Priority Journals; Cancer Journals
ENTRY MONTH: 199608

AB Our study was aimed at investigating whether interaction of human melanoma cells with the extracellular matrix (ECM) protein fibronectin (FN) could regulate lymphokine gene expression. Serum-deprived cells (quiescent condition) of a metastatic melanoma cloned line were cultured either on uncoated or on FN- or ***BSA*** -coated surfaces. By means of reverse transcriptase- polymerase chain reaction (RT-PCR), we analyzed mRNA expression of 4 cytokines interleukin (IL)-1alpha, IL, 1beta, IL-6 and IL-8-and 9 growth factors-endothelial cell growth factor (ECGF), basic ***fibroblast*** ***growth*** ***factor*** (bFGF), ***fibroblast*** ***growth*** ***factor*** (FGF)-5, HST, keratinocyte growth factor (KGF), transforming growth factor (TGF)-alpha TGF-beta1, TGF-beta2 and TGF-beta3. When cultured on FN, melanoma cells expressed IL-1beta and IL-6 transcripts in addition to IL-1beta, IL-8, ECGF, TGF-beta1, TGF-beta2 and TGF-beta3, already present in quiescent cells. Amplification parameters to achieve semi-quantitative RT-PCR were then determined for each detectable factor, thus allowing us to measure a selective enhancement of mRNA levels for IL-1alpha, IL-6, IL-8 and TGF-beta2 upon interaction with FN by quiescent melanoma cells. This augmented expression was inhibited by an anti-integrin beta1 chain monoclonal ***antibody*** (MAb). Moreover, the amounts of IL-6, IL-8 and IL-beta produced in the supernatants, as assessed by ELISA, correlated with the corresponding mRNA expression. Extension of this analysis to the other 5 human primary and metastatic melanoma lines confirmed the ability of FN to selectively up-regulate only IL-6 and IL-8 secretion. Our data indicate that FN is able to modulate expression and secretion of a

defined
subset of lymphokines in human melanoma.

L54 ANSWER 28 OF 50 EMBASE COPYRIGHT 2001 ELSEVIER SCI. B.V.
ACCESSION NUMBER: 95176214 EMBASE
DOCUMENT NUMBER: 1995176214
TITLE: Oncology and hematology.
AUTHOR: Burtness B.A.
CORPORATE SOURCE: Yale University School of Medicine,New Haven, CT, United States
SOURCE: Journal of the American Medical Association, (1995) 273/21 (1702-1703).
ISSN: 0098-7484 CODEN: JAMAAP
COUNTRY: United States
DOCUMENT TYPE: Journal; General Review
FILE SEGMENT: 016 Cancer
022 Human Genetics
026 Immunology, Serology and Transplantation
029 Clinical Biochemistry
037 Drug Literature Index
LANGUAGE: English
SUMMARY LANGUAGE: English
AB The isolation of the BRCA1 gene marks the beginning of translating this knowledge into useful information for patients. - The increase in our understanding of polypeptide growth factors and their receptors has led to
trials of therapies that specifically target these regulatory processes.

L54 ANSWER 29 OF 50 CAPLUS COPYRIGHT 2001 ACS
ACCESSION NUMBER: 1995:341048 CAPLUS
DOCUMENT NUMBER: 122:114888
TITLE: Compositions and methods for treating ***cancer*** and hyperproliferative disorders
INVENTOR(S): Nacy, Carol A.; Holaday, John W.
PATENT ASSIGNEE(S): Entremed, Inc., USA
SOURCE: PCT Int. Appl., 23 pp.
CODEN: PIXXD2
DOCUMENT TYPE: Patent
LANGUAGE: English
FAMILY ACC. NUM. COUNT: 1
PATENT INFORMATION:

PATENT NO.	KIND	DATE	APPLICATION NO.	DATE
WO 9427635	A1	19941208	WO 1994-US5927	19940526
W: AT, AU, BB, BG, BR, BY, CA, CH, CN, CZ, DE, DK, ES, FI, GB, HU, JP, KP, KR, KZ, LK, LU, LV, MG, MN, MW, NL, NO, NZ, PL, PT, RO, RU, SD, SE, SI, SK, TT, UA, UZ, VN				
RW: AT, BE, CH, DE, DK, ES, FR, GB, GR, IE, IT, LU, MC, NL, PT, SE, BF, BJ, CF, CG, CI, CM, GA, GN, ML, MR, NE, SN, TD, TG				
CA 2163652	AA	19941208	CA 1994-2163652	19940526
AU 9469890	A1	19941220	AU 1994-69890	19940526
EP 702563	A1	19960327	EP 1994-918667	19940526
R: AT, BE, CH, DE, DK, ES, FR, GB, GR, IE, IT, LI, LU, MC, NL, PT, SE				
JP 08510751	T2	19961112	JP 1994-500957	19940526
US 5919459	A	19990706	US 1995-467101	19950606
PRIORITY APPLN. INFO.:			US 1993-68717	19930527
			WO 1994-US5927	19940526
			US 1994-271557	19940707

AB The present invention encompasses methods for reducing or inhibiting growth factor in ***cancer*** cells and tissues. More particularly ***immunogenic*** growth factor-contg. compns. are administered to a human or animal with a ***cancer*** or ***tumor*** . The ***immunogenic*** compns. elicit the prodn. of antibodies specific for growth factor which reduce the level or circulating growth factor, thus reducing or eliminating the proliferation of ***cancer*** . The present invention encompasses growth factor-contg. liposomes and vesicles having portions of growth factor externally presented on their surfaces. The present invention also includes antibodies specific for growth factor.

Thus, according to the present invention, growth factor levels are reduced either by active immunization of an individual using ***immunogenic*** growth factor-contg. compns. or by passive immunization via administering to the individual an ***antibody*** or a group of antibodies specific for growth factor.

L54 ANSWER 30 OF 50 EMBASE COPYRIGHT 2001 ELSEVIER SCI. B.V.
ACCESSION NUMBER: 94334569 EMBASE
DOCUMENT NUMBER: 1994334569
TITLE: Proliferation and differentiation of fetal human oligodendrocytes in culture.
AUTHOR: Satoh J.; Kim S.U.
CORPORATE SOURCE: Division of Neurology, Department of Medicine, University Hospital-UBC Site,Vancouver, BC V6T 2B5, Canada
SOURCE: Journal of Neuroscience Research, (1994) 39/3 (260-272). ISSN: 0360-4012 CODEN: JNREDK
COUNTRY: United States
DOCUMENT TYPE: Journal; Article
FILE SEGMENT: 002 Physiology
008 Neurology and Neurosurgery
LANGUAGE: English
SUMMARY LANGUAGE: English

AB Phenotypic expression and proliferative capacity of the cells of oligodendrocyte lineage were investigated in primary cultures isolated from fetal human brains of 12-15 weeks' gestation using double immunolabeling with Ranscht-monoclonal ***antibody*** (R-mAb) or O4 and antibromodeoxyuridine (BrdU) ***antibody*** . Cultured cells of oligodendrocyte lineage consisted of a major population of R-mAb+O4- cells and minor populations of R-mAb-O4+ and R- mAb+O4+ cells. Most of the R-mAb+O4- cells exhibited a uni-, bi-, or tripolar immature morphology, while the majority of the R-mAb+O4+ cells exhibited a multipolar mature morphology. R-mAb-O4+ cells contained a mixture of immature and mature cell types. When incubated in serum-free culture medium containing BrdU for 4 days, 42% of total oligodendrocytes expressed nuclear BrdU immunolabeling. R-mAb+ cells exhibited a higher degree of BrdU immunolabeling, indicating that they have greater capacities for proliferation than O4+ cells. The large majority of BrdU+ cells exhibited an immature morphology. Inclusion of insulin, insulin-like growth factor (IGF)-I, basic ***fibroblast*** ***growth*** ***factor*** (bFGF), or fetal bovine serum in culture medium did not stimulate proliferation of oligodendrocytes, while platelet-derived growth factor (PDGF) or PDGF plus bFGF increased the number of R-mAb+BrdU+ and O4+BrdU+ cells over control, even though the results were not statistically significant. In addition, insulin and IGF-I induced a 3-fold increase in the number of R-mAb+O4+ cells, indicating that they promoted differentiation of oligodendrocytes. The present study indicates that

fetal human oligodendrocytes in culture exhibit a considerable degree of proliferative capacity without requirement of exogenous growth factors and that both insulin and IGF-I promote their differentiation.

L54 ANSWER 31 OF 50 MEDLINE DUPLICATE 7
ACCESSION NUMBER: 94329309 MEDLINE
DOCUMENT NUMBER: 94329309
TITLE: Immunohistochemical localization in the rat brain of an epitope corresponding to the ***fibroblast*** ***growth*** ***factor*** receptor-1.
AUTHOR: Matsuo A; Tooyama I; Isobe S; Oomura Y; Akiguchi I; Hanai K; Kimura J; Kimura H
CORPORATE SOURCE: Department of Neurology, Kyoto University, Japan..
SOURCE: NEUROSCIENCE, (1994 May) 60 (1) 49-66.
Journal code: NZR. ISSN: 0306-4522.
PUB. COUNTRY: ENGLAND: United Kingdom
Journal; Article; (JOURNAL ARTICLE)
LANGUAGE: English
FILE SEGMENT: Priority Journals
ENTRY MONTH: 199411
AB The localization of ***fibroblast*** ***growth*** ***factor*** receptor-1 was investigated in rat brain by immunohistochemistry using a polyclonal ***antibody*** against an acidic peptide sequence of chicken ***fibroblast*** ***growth*** ***factor*** receptor-1.

For raising the antisera in rabbits, we synthesized the oligopeptide EDDDDEDDSSSEEKEAD which is a highly acidic region of chicken ***fibroblast*** ***growth*** ***factor*** receptor-1. The oligopeptide was used as a haptenic antigen by conjugating with poly-L-glutamate as a ***carrier*** ***protein*** . On immunospot assay, the best antiserum was capable of detecting 15.7 pmols of both the chicken and its analogous human oligopeptides but failed to react even with up to 1 nmol of poly-L-glutamate. When rat brain homogenate was examined by Western blots, the antiserum revealed two bands with molecular weights of 145,000 and 75,000 corresponding to known sizes of the membrane-bound and secreted forms of the rat receptor, respectively. Immunohistochemistry in rat brain demonstrated that putative ***fibroblast*** ***growth*** ***factor*** receptor-1 immunoreactivity sites were present mainly in neurons but also in tanycytes and ependymal cells. Positive neurons were distributed widely in various brain regions, but were particularly abundant in such regions as the lateral hypothalamus, substantia nigra, locus coeruleus and raphe nuclei. The present study suggests that ***fibroblast*** ***growth*** ***factor*** receptor-1 is expressed preferentially in certain neuronal systems that appear to be under the influence of fibroblast growth factors in the normal brain. The result should facilitate study of the functional significance of fibroblast growth factors in these brain neurons.

L54 ANSWER 32 OF 50 EMBASE COPYRIGHT 2001 ELSEVIER SCI. B.V.
ACCESSION NUMBER: 93306601 EMBASE
DOCUMENT NUMBER: 1993306601
TITLE: Tumour ***angiogenesis*** .
AUTHOR: Le Querrec A.; Duval D.; Tobelem G.
CORPORATE SOURCE: Biology Dept, Laboratoire d'Hematologie, CHU, Avenue de la

Cote de Nacre,14000 Caen, France
SOURCE: Bailliere's Clinical Haematology, (1993) 6/3 (711-730).
ISSN: 0950-3536 CODEN: BCHAEW
COUNTRY: United Kingdom
DOCUMENT TYPE: Journal; General Review
FILE SEGMENT: 005 General Pathology and Pathological Anatomy
016 Cancer
025 Hematology
037 Drug Literature Index
LANGUAGE: English
SUMMARY LANGUAGE: English

AB The progressive emergence of a close relationship between the formation of blood vessels in the vicinity of tumour cells and the development and spreading of tumours, strongly suggests that ***angiogenesis*** might be a prerequisite for tumour development. ***Angiogenesis*** starts and develops in response to two sets of extracellular signals: soluble ***angiogenic*** factors and extracellular matrix. Different experimental models have been used to study ***angiogenesis*** in vivo, but they have numerous limitations. Three-dimensional culture systems reconstitute normal interactions between endothelial cells and the surrounding extracellular matrix. Numerous parameters including ***angiogenic*** growth factors and cytokines, cell-to-cell interactions and cell-to-extracellular matrix adhesion influence the growth and differentiation of endothelial cells in vitro as well as in vivo. ***Angiogenesis*** plays a major role not only in tumour growth but also in ***metastasis*** development. Mechanisms of switching to ***angiogenic*** phenotype have been recently described and onset of ***angiogenic*** activity is now recognized as another discrete step in tumorigenesis. Tumour cells can induce b-FGF expression and exportation, VEGF and VEGF receptor expression and inactivation of the ***cancer*** suppressor gene encoding for a ***fragment*** of thrombospondin. A controlled net proteolytic balance produced by tumour cells or endothelial cells is required to favour migration and invasion of endothelial cells and ***angiogenesis*** . The hypothesis that assessment of tumour ***angiogenesis*** might predict tumour aggressiveness in human ***cancer*** has recently gained support from several clinical studies. This has been shown for cutaneous melanoma, breast carcinoma, and non-small-cell lung ***cancer*** by quantitation of microvessels in human biopsies using von Willebrand factor or CD 3 antigen labelling with specific antibodies. However, more specific and sensitive markers are needed to improve this approach for predicting tumour aggressiveness. Folkman proposed twenty years ago that inhibition of ***angiogenesis*** might represent a suitable complementary strategy for the treatment of various forms of ***cancer*** . Since then numerous angiostatic compounds have been identified but very few of them fit the required criteria of a potential drug. Fumagillin and particularly its synthetic analogue AGM 1470 might be developed for use in humans in the near future.

L54 ANSWER 33 OF 50 CAPLUS COPYRIGHT 2001 ACS
ACCESSION NUMBER: 1991:651669 CAPLUS
DOCUMENT NUMBER: 115:251669
TITLE: A method for the stepwise, controlled synthesis of

chemical species, particularly peptides, on protein substrates, coupled products obtained by the method, and the use of these coupled products, e.g. as vaccines

INVENTOR(S): Houen, Gunnar; Holm, Arne
PATENT ASSIGNEE(S): Den.
SOURCE: PCT Int. Appl., 106 pp.
CODEN: PIXXD2
DOCUMENT TYPE: Patent
LANGUAGE: English
FAMILY ACC. NUM. COUNT: 1
PATENT INFORMATION:

PATENT NO.	KIND	DATE	APPLICATION NO.	DATE
WO 9108220	A1	19910613	WO 1990-DK311	19901130
W: AT, AU, BB, BG, BR, CA, CH, DE, DK, ES, FI, GB, GR, HU, JP, KP, KR, LK, LU, MC, MG, MW, NL, NO, RO, SD, SE, SU, US				
RW: AT, BE, BF, BJ, CF, CG, CH, CM, DE, DK, ES, FR, GA, GB, GR, IT, LU, ML, MR, NL, SE, SN, TD, TG				
AU 9168929	A1	19910626	AU 1991-68929	19901130
PRIORITY APPLN. INFO.:			DK 1989-6085	19891201
			WO 1990-DK311	19901130

AB Chem. species, esp. peptides, are synthesizied by a stepwise, controlled process using a proteinaceous substances as the synthesis substrate. The coupled products obtained by the process can be used, e.g., as vaccines, matrix materials, or carrier mols. The products, including peptides and peptide derivs., prepd. by the method are also claimed. ***Bovine*** ***serum*** ***albumin*** (***BSA***) was placed in a silylated reaction vessel and the CO2H groups were diethylamidated before coupling glutamic acid as the Fmoc (9-fluorenylmethyloxycarbonyl) and tert-Bu protected Dhbt (3-hydroxy-3,4-dihydrobenzotriazin-4-one ester, blocking remaining amino groups with acetic anhydride, and sequentially coupling Fmoc- and side chain-protected Dhbt esters of lysine, serine, threonine, aspartic acid, methionine, and serine. Piperidine was used to remove the Fmoc protecting group between couplings. Side chain protection groups were removed in CH2Cl2/F3CCO2H (1:1 vol./vol.) at 0.degree.. The product had an av. of 35 synthesized peptide chains per ***BSA*** mol. The coupled product was used to raise antibodies to Ser-Met-Asp-Thr-Ser-Lys-Glu in rabbits.

L54 ANSWER 34 OF 50 MEDLINE DUPLICATE 8
ACCESSION NUMBER: 91249356 MEDLINE
DOCUMENT NUMBER: 91249356
TITLE: Regulation of growth by a nerve growth factor-like protein which modulates paracrine interactions between a neoplastic epithelial cell line and stromal cells of the human prostate.
AUTHOR: Djakiew D; Delsite R; Pflug B; Wrathall J; Lynch J H; Onoda M
CORPORATE SOURCE: Department of Anatomy and Cell Biology, Georgetown University School of Medicine, Washington, DC 20007..
CONTRACT NUMBER: CA50229 (NCI)
N01-NS7-2310 (NINDS)
P01-NS28130 (NINDS)
SOURCE: CANCER RESEARCH, (1991 Jun 15) 51 (12) 3304-10.
Journal code: CNF. ISSN: 0008-5472.

PUB. COUNTRY: United States
Journal; Article; (JOURNAL ARTICLE)
LANGUAGE: English
FILE SEGMENT: Priority Journals; Cancer Journals
ENTRY MONTH: 199109

AB Nerve growth factor-like substance(s) were identified in both conditioned media of a human prostatic tumor epithelial cell line (TSU-pr1) and a human prostatic stromal cell line (HPS) by Western blot analysis and bioassay of neurite outgrowth of PC12 cells. Nerve growth factor-beta (NGF) immunofluorescence was also localized to secretory vesicles in the cytoplasm of both the TSU-pr1 and HPS cells. Western blot of the TSU-pr1 and HPS cell-secreted protein identified an Mr 65,000 major protein which immunoreacted with murine NGF ***antibody*** . NGF Western blot of HPS cell-secreted protein also identified an Mr 42,000 minor band under reduced and nonreduced conditions and an Mr 61,000 minor band under reduced conditions. The secreted protein from the TSU-pr1 cells (50 micrograms/ml) and HPS (50 micrograms/ml), as well as murine NGF (50 ng/ml) or human recombinant NGF (50 ng/ml), stimulated neurite outgrowth from PC12 cells. This neurite outgrowth activity was partially inhibited by treatment with NGF ***antibody*** . Neither the serum containing growth medium nor ***bovine*** ***serum*** ***albumin*** (50 micrograms/ml) stimulated neurite outgrowth. The NGF-like secretory protein appeared to play a role in the paracrine regulation of prostatic growth between TSU-pr1 cells and HPS cells. The relative growth of TSU-pr1 cells, as indicated by [3H]thymidine incorporation, in response to HPS secretory protein was stimulated 2.8-fold in a dose-dependent manner. In the converse interaction, the relative growth of HPS cells in response to TSU-pr1 secretory protein was stimulated 1.8-fold in a dose-dependent manner. Immunoneutralization of TSU-pr1 and HPS secretory protein was performed with ***antibody*** against NGF, acidic ***fibroblast*** ***growth*** ***factor*** , and basic ***fibroblast*** ***growth*** ***factor*** . Removal of the NGF-like protein from the maximal stimulatory dose of TSU-pr1 secretory protein (100 micrograms/ml) with NGF ***antibody*** reduced HPS proliferation to 52% of maximal levels, and immunoneutralization of the NGF-like protein in the maximal stimulatory dose of HPS secretory protein (20 micrograms/ml) also reduced TSU-pr1 proliferation to 16% of maximal levels. Addition of normal rabbit serum or prior immunoprecipitation of either TSU-pr1 or HPS secretory protein with ***antibody*** against acidic ***fibroblast*** ***growth*** ***factor*** and basic ***fibroblast*** ***growth*** ***factor*** did not inhibit the proliferation of either cell type. These results suggest that TSU-pr1 tumor cells and HPS cells secrete NGF-like protein(s) which modulate their paracrine interactive growth in vitro.

L54 ANSWER 35 OF 50 MEDLINE DUPLICATE 9
ACCESSION NUMBER: 91235209 MEDLINE
DOCUMENT NUMBER: 91235209
TITLE: Proliferation of Shionogi carcinoma 115 cells by glucocorticoid-induced autocrine heparin-binding growth factor(s) in serum-free medium.
AUTHOR: Yamanishi H; Nonomura N; Tanaka A; Nishizawa Y; Terada N; Matsumoto K; Sato B
CORPORATE SOURCE: Department of Pathology, Osaka University Medical School, Japan.
SOURCE: CANCER RESEARCH, (1991 Jun 1) 51 (11) 3006-10.
Journal code: CNF. ISSN: 0008-5472.
PUB. COUNTRY: United States

Journal; Article; (JOURNAL ARTICLE)
LANGUAGE: English
FILE SEGMENT: Priority Journals; Cancer Journals
ENTRY MONTH: 199108
AB Shionogi carcinoma 115 (SC115) has been accepted for 20 years as an androgen-responsive mouse mammary tumor. Recently, the growth of the tumor was also found to be stimulated by pharmacological, but not physiological, doses of glucocorticoid. In a serum-free culture system [Ham's F-12:Eagle's minimal essential medium (1:1, v/v) containing 0.1% ***bovine*** ***serum*** ***albumin***], we have established that 10(-8) M testosterone, or 10(-6) M dexamethasone significantly stimulates the growth of SC-3 cells (a cloned cell line from a SC115 tumor) via androgen and glucocorticoid receptors, respectively. Recently, we demonstrated that the testosterone-induced growth of SC-3 cells is mediated through autocrine ***fibroblast*** ***growth*** ***factor*** (FGF)-like peptide(s). In the present study, mechanisms of glucocorticoid-induced growth of SC-3 cells were investigated. Serum-free conditioned medium obtained from 10(-6) M dexamethasone-stimulated SC-3 cells was fractionated by heparin-Sepharose affinity chromatography; one sharp peak of growth-stimulatory activity for SC-3 cells, eluted at 1.3 M NaCl, was identified. When the peak fraction was added to serum-free medium, the shape of SC-3 cells changed from an epithelial to a fibroblast-like appearance, similar to that induced with testosterone or basic (b)FGF. Furthermore, the growth-stimulatory activity induced with the peak fraction as well as testosterone or bFGF was markedly inhibited by anti-bFGF ***antibody*** immunoglobulin G (75 to 90% inhibition was obtained), and the specific binding of 125I-bFGF on SC-3 cells was significantly inhibited by the peak fraction. These results suggest that the glucocorticoid-induced growth of SC-3 cells is also mediated through FGF-like peptide(s) in an autocrine mechanism, which is very similar to that induced by testosterone, if not identical.

L54 ANSWER 36 OF 50 MEDLINE DUPLICATE 10
ACCESSION NUMBER: 92078304 MEDLINE
DOCUMENT NUMBER: 92078304
TITLE: Germ cell mitogenic activity is associated with nerve growth factor-like protein(s).
AUTHOR: Onoda M; Pflug B; Djakiew D
CORPORATE SOURCE: Department of Anatomy and Cell Biology, Georgetown University School of Medicine, Washington, D.C. 20007.
SOURCE: JOURNAL OF CELLULAR PHYSIOLOGY, (1991 Dec) 149 (3) 536-43. Journal code: HNB. ISSN: 0021-9541.
PUB. COUNTRY: United States
Journal; Article; (JOURNAL ARTICLE)
LANGUAGE: English
FILE SEGMENT: Priority Journals; Cancer Journals
ENTRY MONTH: 199203
AB The mitogenicity of germ cell proteins released from round spermatids (RS) and pachytene spermatocytes (PS) was investigated. Germ cells were isolated by centrifugal elutriation from 90-day-old rat testes and incubated in a supplement enriched culture media that lacked exogenous proteins. The conditioned culture media of RS and PS were dialysed/concentrated and lyophilized to prepare RS protein (RSP) and PS protein (PSP). Mitogenic activity of RSP and PSP was determined by 3H-thymidine incorporation into Swiss 3T3 fibroblasts. RSP and PSP

stimulated 3H-thymidine incorporation by fibroblasts in a dose-dependent manner. At a higher concentration of RSP (300 micrograms/ml), fibroblast proliferation was stimulated from 6- to 20-fold of control cultures, whereas PSP (300 micrograms/ml) stimulated fibroblast proliferation 2.5-fold of control cultures. Since RSP exhibited substantially greater mitogenic activity than PSP we further investigated the RSP mitogenic substance(s) by immunoneutralization with antibodies against several growth factors. The mitogenic activity of RSP was significantly reduced by treatment with nerve growth factor (NGF) ***antibody*** , while neither the treatment of RSP with acidic ***fibroblast*** ***growth*** ***factor*** (aFGF) ***antibody*** , nor basic ***fibroblast*** ***growth*** ***factor*** (bFGF) ***antibody*** significantly modified the mitogenic activity of RSP. Interestingly, murine NGF-beta, recombinant human NGF-beta, and ***bovine*** ***serum*** ***albumin*** (***BSA***) did not exhibit mitogenic activity on 3T3 fibroblasts. Nevertheless, the presence of a NGF-like protein in RS and PS was confirmed by indirect immunofluorescence staining with a murine NGF ***antibody*** . Subsequently, a Western blot analysis with the NGF ***antibody*** identified two immunoreactive bands of 41 +/- 2 kDa and 51 +/- 1 kDa in both RSP and PSP under reduced conditions. These germ cell NGF-like proteins were apparently different from similarly prepared murine and human NGFs (13 kDa) in their molecular weight. Furthermore, neurite outgrowth from pheochromocytoma cells (PC-12), a functional bioassay for NGF-like activity, was stimulated by addition of RSP and PSP to the culture media of the PC-12 cells. These results demonstrate mitogenic activity in germ cell proteins (RSP and PSP) and identify a NGF-like protein(s) which is associated with most of this activity.

L54 ANSWER 37 OF 50 MEDLINE DUPLICATE 11
ACCESSION NUMBER: 91217146 MEDLINE
DOCUMENT NUMBER: 91217146
TITLE: Transforming growth factor-beta and platelet-derived growth factor synergistically stimulate contraction by testicular peritubular cells in culture in serum-free medium.
AUTHOR: Tung P S; Fritz I B
CORPORATE SOURCE: Banting and Best Department of Medical Research, University of Toronto, Ontario, Canada..
SOURCE: JOURNAL OF CELLULAR PHYSIOLOGY, (1991 Mar) 146 (3) 386-93. Journal code: HNB. ISSN: 0021-9541.
PUB. COUNTRY: United States
Journal; Article; (JOURNAL ARTICLE)
LANGUAGE: English
FILE SEGMENT: Priority Journals; Cancer Journals
ENTRY MONTH: 199108
AB We report investigations on factors influencing contractility by testicular peritubular cells (PC) maintained in culture in a three-dimensional collagen gel system, and the behavior of PC in culture on a two-dimensional system. At low and moderate cell densities, PC embedded in collagen gels in serum-free Eagle's minimal essential medium (MEM) have a lesser degree of contractility than PC in culture in MEM containing calf serum. The contractility by PC, measured by determining

changes in diameter of the collagen gel, was increased by addition of transforming growth factor-beta (TGF-beta) to serum-free MEM, and this was further enhanced by supplementing the medium with platelet-derived growth factor (PDGF). In the absence of TGF-beta, however, PDGF had no detectable effects on PC contractility. Other growth factors examined (epidermal growth factor, insulin, and ***fibroblast*** ***growth*** ***factor***) did not influence the degree of contractility of PC in serum-free MEM in the presence or absence of TGF-beta. PC maintained in MEM supplemented with platelet-poor serum (PPS) have a lesser degree of contractility than their counterparts in MEM containing 2.5% calf serum. The addition of TGF-beta and PDGF to PPS-supplemented MEM restored contractility by PC to a level comparable to that observed by PC in MEM containing complete serum. The addition of nonpurified ***bovine*** ***serum*** ***albumin*** (***BSA***) to MEM greatly increased PC contractility. By contrast, highly purified ***BSA*** had no such effect, suggesting that one or more components adsorbed to the impure ***BSA*** was implicated. Polyclonal ***antibody*** against fibronectin did not influence the contractility of PC in collagen gels in the presence or absence of serum. Antiserum against TGF-beta partially blocked the enhancement of contractility of PC in MEM containing non-purified ***BSA*** . In PC plated on top of a collagen gel lattice, the attachment, spreading, and cell shape were greatly influenced by the presence of TGF-beta and PDGF, both singly and together. Data presented are interpreted to indicate that effects elicited by serum on the properties of PC in culture, and on the contractility of PC, can be attributed in part to the combined influences of TGF-beta and PDGF in serum.

L54 ANSWER 38 OF 50 MEDLINE DUPLICATE 12
ACCESSION NUMBER: 90307556 MEDLINE
DOCUMENT NUMBER: 90307556
TITLE: Production of basic ***fibroblast*** ***growth*** ***factor*** -like factor by cultured human cholangiocellular carcinoma cells [published erratum appears in Jpn J Cancer Res 1990 Oct;81(10):1076].
AUTHOR: Matsuzaki K; Yoshitake Y; Miyagiwa M; Minemura M; Tanaka M; Sasaki H; Nishikawa K
CORPORATE SOURCE: Third Department of Internal Medicine, Toyama Medical and Pharmaceutical University.
SOURCE: JAPANESE JOURNAL OF CANCER RESEARCH, (1990 Apr) 81 (4) 345-54.
Journal code: HBA. ISSN: 0910-5050.
PUB. COUNTRY: Japan
Journal; Article; (JOURNAL ARTICLE)
LANGUAGE: English
FILE SEGMENT: Priority Journals; Cancer Journals
ENTRY MONTH: 199010
AB An extract of cultured human cholangiocellular carcinoma cells (HuCC-T1) was found to contain high mitogenic activity for BALB/c3T3 cells. The growth factor eliciting most of the mitogenic activity was purified and concluded to be identical with basic ***fibroblast*** ***growth*** ***factor*** (bFGF)-like factor on the basis of its molecular weight and heparin-Sepharose elution profile, and the results of immunoblotting and radioimmunoassay. HuCC-T1 cells also secreted bFGF-like factor into

serum-free medium. A combination of insulin and transferrin or ***bovine*** ***serum*** ***albumin*** stimulated the growth of HuCC-T1 cells in serum-free medium. However, bFGF did not stimulate their growth in the presence and absence of these supplements. Neutralizing monoclonal ***antibody*** against bFGF did not inhibit growth. These results indicate that bFGF-like factor is not a growth factor for this cell line.

L54 ANSWER 39 OF 50 MEDLINE DUPLICATE 13
ACCESSION NUMBER: 91197545 MEDLINE
DOCUMENT NUMBER: 91197545
TITLE: Characterization of two preparations of antibodies to basic ***fibroblast*** ***growth*** ***factor*** which exhibit distinct patterns of immunolocalization.
AUTHOR: Kardami E; Murphy L J; Liu L; Padua R R; Fandrich R R
CORPORATE SOURCE: St Boniface General Hospital Research Centre, University of Manitoba, Winnipeg, Canada..
SOURCE: GROWTH FACTORS, (1990) 4 (1) 69-80.
Journal code: AOI. ISSN: 0897-7194.
PUB. COUNTRY: Switzerland
Journal; Article; (JOURNAL ARTICLE)
LANGUAGE: English
FILE SEGMENT: Priority Journals
ENTRY MONTH: 199107
AB Immunoglobulins reactive against basic ***fibroblast*** ***growth*** ***factor*** (bFGF) were obtained from the serum of a single rabbit immunized against residues [1-24] of bFGF conjugated to keyhole limpet hemocyanin (***KLH***). Pure immunoglobulin preparations no. 1 and no. 2 were prepared using different affinity chromatography columns and preabsorption to ***KLH*** -coupled Sepharose for preparation no. 1. Both preparations no. 1 and no. 2 were specific for bFGF in in vitro assays. Competition with synthetic peptides suggests that preparations no. 1 and no. 2 recognize predominantly epitope(s) within residues [16-24]bFGF or residues [1-10]bFGF, respectively, in situ. Furthermore, no. 2 (but not no. 1) antibodies can react with tissue-(heparin-)-bound antigen. When used in indirect immunofluorescence for bFGF in frozen heart sections, preparation no. 1 stained predominantly muscle intercalated discs (IcDs); muscle nuclei were also stained, in an overall punctate fashion. Preparation no. 2 stained muscle nuclei strongly, in association with the nuclear envelope; it also stained basement-membrane associated bFGF. Differences in immunostaining were also observed in uterine smooth muscle and kidney sections but not in skeletal muscle. It is plausible that accessibility of various epitopes within the amino-terminal region depends strongly on the local interactions of bFGF. Our data illustrate the importance of using several different antibodies to localize bFGF in a tissue.

L54 ANSWER 40 OF 50 MEDLINE DUPLICATE 14
ACCESSION NUMBER: 91054992 MEDLINE
DOCUMENT NUMBER: 91054992
TITLE: Growth stimulation by androgens, glucocorticoids or

fibroblast growth factors and the blocking of the stimulated growth by ***antibody*** against basic ***fibroblast*** ***growth*** ***factor*** in protein-free culture of Shionogi carcinoma 115 cells.

AUTHOR: Tanaka A; Matsumoto K; Nishizawa Y; Lu J; Yamanishi H; Maeyama M; Nonomura N; Uchida N; Sato B

CORPORATE SOURCE: Department of Pathology, Osaka University Medical School, Japan.

SOURCE: JOURNAL OF STEROID BIOCHEMISTRY AND MOLECULAR BIOLOGY, (1990 Sep) 37 (1) 23-9.
Journal code: AX4. ISSN: 0960-0760.

PUB. COUNTRY: ENGLAND: United Kingdom
Journal; Article; (JOURNAL ARTICLE)

LANGUAGE: English

FILE SEGMENT: Priority Journals; Cancer Journals

ENTRY MONTH: 199103

AB Shionogi carcinoma 115 (SC115) has been accepted for 20 years as an androgen-responsive mouse mammary tumor. We have established an androgen-dependent cloned cell line (SC-3) from a SC115 tumor. In a serum-free medium, testosterone (T) or fibroblast growth factors (FGFs) markedly stimulate the growth of SC-3 cells, and the T-induced growth was shown to be mediated through FGF-like peptide(s) in an autocrine mechanism. Since we used the serum-free culture including 0.1% ***bovine*** ***serum*** ***albumin*** (***BSA***), a partially serum-containing condition, putative roles of ***BSA*** - or serum-borne growth factors in growth stimulation of autocrine production of FGF-like peptide(s) could not be excluded. This paper reports findings performed in a protein-free medium including plating [Ham's F-12:MEM (1:1; v/v)]. In the protein-free culture, the growth of SC-3 cells was significantly stimulated by the addition of greater than or equal to 10(-10) M T (up to 20-fold), greater than or equal to 10(-7) M dexamethasone (Dex; up to 7-fold) or greater than or equal to 1 ng/ml basic (b) or acidic FGF (up to 10-fold); other various growth factors had no such effects. Furthermore, DNA synthesis of SC-3 cells induced by T, Dex or bFGF was similarly and markedly inhibited by bFGF neutralizing ***antibody*** IgG. Therefore, the present findings seem to demonstrate that androgens or high levels of glucocorticoids induce the production and secretion of FGF-like peptide(s) from SC-3 cells for their growth even in the absence of additional support by other factors.

L54 ANSWER 41 OF 50 MEDLINE DUPLICATE 15

ACCESSION NUMBER: 89354258 MEDLINE

DOCUMENT NUMBER: 89354258

TITLE: Inhibitory effect of ***antibody*** against basic ***fibroblast*** ***growth*** ***factor*** on androgen- or glucocorticoid-induced growth of Shionogi carcinoma 115 cells in serum-free culture.

AUTHOR: Lu J; Nishizawa Y; Tanaka A; Nonomura N; Yamanishi H; Uchida N; Sato B; Matsumoto K

CORPORATE SOURCE: Department of Pathology, Osaka University Medical School, Japan.

SOURCE: CANCER RESEARCH, (1989 Sep 15) 49 (18) 4963-7.
Journal code: CNF. ISSN: 0008-5472.

PUB. COUNTRY: United States
Journal; Article; (JOURNAL ARTICLE)

LANGUAGE: English

FILE SEGMENT: Priority Journals; Cancer Journals

ENTRY MONTH: 198912

AB Shionogi carcinoma 115 (SC115) has been accepted for 20 years as an androgen-responsive mouse mammary tumor. However, we and others recently found that the growth of SC115 cells is also stimulated by high doses of glucocorticoids. We already reported the following findings. In a serum-free medium [Ham's F-12: Eagle's minimum essential medium (1:1, v/v) containing 0.1% ***bovine*** ***serum*** ***albumin***], greater than or equal to 10(-9) M testosterone and greater than or equal to 10(-8) M dexamethasone significantly stimulated the growth of SC-3 cells (a cloned cell line from a SC115 tumor) through androgen and glucocorticoid receptors, respectively. In the present study, we have demonstrated that higher concentrations (10(-7)-10(-6) M) of weak androgens such as 4-androstene-3,17-dione or weak glucocorticoids such as corticosterone also significantly stimulate the growth of SC-3 cells and that their relative potency is found to be in parallel with their binding affinity for their receptors, respectively. Furthermore, DNA synthesis of SC-3 cells induced by 0.1 ng/ml basic ***fibroblast*** ***growth*** ***factor*** (FGF), 10(-8) M testosterone, 10(-6) M 4-androstene-3,17-dione, 10(-7) M dexamethasone, or 10(-6) M corticosterone was found to be similarly and significantly inhibited by the addition of basic FGF neutralizing ***antibody*** IgG in the present study; approximately 70% inhibition of the basic FGF, androgen, or glucocorticoid effects was attained. We already reported findings which suggest that SC-3 cells produce FGF-like peptide for their testosterone-induced growth. Therefore, the present study presents new additive information to demonstrate that the growth-stimulatory activity of various androgens or possibly glucocorticoids on SC-3 cells is mediated through a FGF-like peptide in an autocrine mechanism.

L54 ANSWER 42 OF 50 EMBASE COPYRIGHT 2001 ELSEVIER SCI. B.V.DUPLICATE 16

ACCESSION NUMBER: 89061225 EMBASE
DOCUMENT NUMBER: 1989061225
TITLE: Characterization of polyclonal antibodies that distinguish acidic and basic fibroblast growth factors by using Western immunoblotting and enzyme-linked immunosorbent assays.
AUTHOR: Riss T.L.; Sirbasku D.A.
CORPORATE SOURCE: Department of Biochemistry and Molecular Biology, University of Texas Medical School, Houston, TX 77225, United States
SOURCE: Journal of Cellular Physiology, (1989) 138/2 (405-414). ISSN: 0021-9541 CODEN: JCLLAX
COUNTRY: United States
DOCUMENT TYPE: Journal
FILE SEGMENT: 029 Clinical Biochemistry
037 Drug Literature Index
LANGUAGE: English
SUMMARY LANGUAGE: English

AB Rabbit polyclonal antibodies were raised against ***ovalbumin*** conjugates of purified bovine brain acidic ***fibroblast*** ***growth*** ***factor*** (aFGF) and a synthetic peptide containing the N(.alpha.)-terminal 1-24 amino acid sequence of bovine basic ***fibroblast*** ***growth*** ***factor*** (bFGF). These antibodies were used to specifically detect 1-ng quantities of aFGF and bFGF by using enzyme-linked immunosorbent assay (ELISA) and Western

immunoblot procedures. Antibodies raised against aFGF recognized bovine brain aFGF and bovine recombinant aFGF but very porly recognized recombinant bFGF or purified porcine or bovine pituitary bFGF with ELISA and Western immunoblot procedures. Antibodies raised against bFGF (1-24) recognized purified bovine, porcine, and recombinant human bFGF but only very poorly recognized aFGF with ELISA and Western immunoblot procedures. In vitro addition of anti-bFGF antibodies was able to partially neutralize bFGF-stimulated 3H-thymidine incorporation by COMMA-D mouse mammary epithelial cells while having no effect on aFGF or epidermal growth factor (EGF) stimulation. In vitro addition of anti-aFGF antibodies had no effect on bFGF- or EGF-stimulated 3H-thymidine incorporation, but surprisingly, had a potentiating effect on aFGF stimulation. Antibodies against aFGF immobilized on protein A-Sepharose were able to specifically and completely remove mitogenic activity from solutions containing aFGF but had no effect on removal of mitogenic activity from control solutions containing bFGF or EGF. Similarly, immobilized anti-bFGF antibodies completely removed mitogenic activity from solutions of bFGF, but not aFGF or EGF controls. These antibodies have been useful for the identification and characterization of growth factors from tissue and recombinant sources.

L54 ANSWER 43 OF 50 MEDLINE
ACCESSION NUMBER: 89306122 MEDLINE
DOCUMENT NUMBER: 89306122
TITLE: ***Thyroglobulin*** gene expression as a differentiation marker in primary cultures of calf thyroid cells.
AUTHOR: Gerard C M; Roger P P; Dumont J E
CORPORATE SOURCE: Institute of Interdisciplinary Research, Free University of Brussels, School of Medicine, Belgium.
SOURCE: MOLECULAR AND CELLULAR ENDOCRINOLOGY, (1989 Jan) 61 (1) 23-35.
Journal code: E69. ISSN: 0303-7207.
PUB. COUNTRY: Netherlands
Journal; Article; (JOURNAL ARTICLE)
LANGUAGE: English
FILE SEGMENT: Priority Journals
ENTRY MONTH: 198910
AB A system of calf thyroid follicular cells in primary cultures has been developed to investigate the control of ***thyroglobulin*** gene expression in normal cells in vitro. In low (0.1%) serum conditions, the cells remained quiescent and formed dense aggregates surrounded by slowly spreading cells. High expression of thyroid-specific differentiation markers such as ***thyroglobulin*** (Tg) mRNA accumulation and iodide transport required the continuous exposure of cells to thyrotropin (TSH) or other adenylate cyclase activators (cholera toxin and forskolin). In the absence of TSH, Tg mRNA decreased to low but still detectable levels. Addition of TSH, forskolin or cholera toxin restored high Tg gene expression. Hydrocortisone moderately stimulated basal Tg mRNA accumulation and strongly potentiated the effect of TSH. Growth promoters including serum (1-10%), epidermal growth factor (EGF), ***fibroblast*** ***growth*** ***factor*** (FGF) and 12-O-tetradecanoylphorbol 13-acetate (TPA) induced calf thyroid cells to develop as a monolayer and inhibited both basal and TSH-stimulated expression of specialized

functions. Moreover, only a partial restoration of this expression was achieved after addition of TSH or forskolin to well spread-out cells that had proliferated in response to EGF or serum. The results show that in calf thyroid cells, iodide transport and Tg gene expression are regulated by TSH through cyclic AMP; hydrocortisone potentiates this effect on Tg gene expression, while all growth promoting factors inhibit the expression of these differentiated functions.

L54 ANSWER 44 OF 50 BIOSIS COPYRIGHT 2001 BIOSIS
ACCESSION NUMBER: 1989:180482 BIOSIS
DOCUMENT NUMBER: BA87:91748
TITLE: CHARACTERIZATION OF POLYCLONAL ANTIBODIES THAT DISTINGUISH ACIDIC AND BASIC FIBROBLAST GROWTH FACTORS BY USING WESTERN IMMUNOBLOTTING AND ELISA.
AUTHOR(S): RISS T L; SIRBASKU D A
CORPORATE SOURCE: SCHERING-PLOUGH CORP., BIOTECHNOL. CELL CULTURE, 60 ORANGE ST., BLOOMFIELD, N.J. 07003.
SOURCE: J CELL PHYSIOL, (1988) 138 (2), 405-414.
CODEN: JCLLAX. ISSN: 0021-9541.
FILE SEGMENT: BA; OLD
LANGUAGE: English
AB Rabbit polyclonal antibodies were raised against ***ovalbumin*** conjugates of purified bovine brain acidic ***fibroblast*** ***growth*** ***factor*** (aFGF) and a synthetic peptide containing the N.alpha.-terminal 1-24 amino acid sequence of bovine basic ***fibroblast*** ***growth*** ***factor*** (bFGF). These antibodies were used to specifically detect 1-ng quantities of aFGF and bFGF by using enzyme-linked immunosorbent assay (ELISA) and Western immunoblot procedures. Antibodies raised against aFGF recognized bovine brain aFGF and bovine recombinant aFGF but very poorly recognized recombinant bFGF or purified porcine or bovine pituitary bFGF with ELISA and Western immunoblot procedures. Antibodies raised against bFGF (1-24) recognized purified bovine, porcine, and recombinant human bFGF but only very poorly recognized aFGF with ELISA and Western immunoblot procedures. In vitro addition of anti-bFGF antibodies was able to partially neutralize bFGF-stimulated 3H-thymidine incorporation by COMMA-D mouse mammary epithelial cells while having no effect on aFGF or epidermal growth factor (EGF) stimulation. In vitro addition of anti-aFGF antibodies had no effect on bFGF- or EGF-stimulated 3H-thymidine incorporation, but surprisingly, had a potentiating effect on aFGF stimulation. Antibodies against aFGF immobilized on protein A-Sepharose were able to specifically and completely remove mitogenic activity from solutions containing aFGF but had no effect on removal of mitogenic activity from control solutions containing bFGF or EGF. Similarly, immobilized anti-bFGF antibodies completely removed mitogenic activity from solutions of bFGF, but not aFGF or EGF controls. These antibodies have been useful for the identification and characterization of growth factors from tissue and recombinant sources.

L54 ANSWER 45 OF 50 MEDLINE DUPLICATE 17
ACCESSION NUMBER: 88244427 MEDLINE
DOCUMENT NUMBER: 88244427
TITLE: The development of a quantitative RIA for basic ***fibroblast*** ***growth*** ***factor*** using

polyclonal antibodies against the 157 amino acid form of human bFGF. The identification of bFGF in adherent elicited murine peritoneal macrophages.

AUTHOR: Joseph-Silverstein J; Moscatelli D; Rifkin D B

CORPORATE SOURCE: Department of Cell Biology, New York University Medical Center 10016..

SOURCE: JOURNAL OF IMMUNOLOGICAL METHODS, (1988 Jun 13) 110 (2) 183-92.
Journal code: IFE. ISSN: 0022-1759.

PUB. COUNTRY: Netherlands
Journal; Article; (JOURNAL ARTICLE)

LANGUAGE: English

FILE SEGMENT: Priority Journals; Cancer Journals

ENTRY MONTH: 198809

AB Polyclonal antibodies which have the capacity to neutralize the biological activity of basic fibriblast growth factor (bFGF) in vitro, have been raised in rabbits against the 157 amino acid form of bFGF purified from human placenta. In a dot blot assay the anti-bFGF antibodies do not recognize the acidic form of FGF (aFGF) with which the basic form shares significant amino acid sequence homology. As determined by immunoblotting, bFGF antibodies recognized only bFGF in a mixture of placentally derived heparin-binding proteins, demonstrating the specificity of these antibodies. Using the anti-human bFGF antibodies, we have developed a solid-phase competitive radioimmunoassay sensitive to 7.8 ng/ml (0.4 pmol/ml) for bFGF. aFGF does not compete with bFGF for binding to the antibodies in the radioimmunoassay even at 2.04 micrograms/ml. The specificity of the assay was further demonstrated by a lack of competition of cytochrome C, myoglobin, epidermal growth factor or ***bovine*** ***serum*** ***albumin*** with bFGF for binding to the antibodies.

We have identified bFGF in extracts of adherent thioglycollate-stimulated mouse peritoneal macrophages by immunological criteria including the ability of the extract to compete with 125I-bFGF for binding to affinity-purified anti-human bFGF antibodies in the RIA and the ability of these antibodies in inhibit the bFGF-like biological activity of the macrophage extract.

L54 ANSWER 46 OF 50 MEDLINE DUPLICATE 18

ACCESSION NUMBER: 85251723 MEDLINE

DOCUMENT NUMBER: 85251723

TITLE: Preparation and characterization of antibodies with specificity for the amino-terminal tetrapeptide sequence of the platelet-derived connective tissue activating peptide-III.

AUTHOR: Davis L E; Castor C W; Tinney F J; Anderson B

SOURCE: BIOCHEMISTRY INTERNATIONAL, (1985 Mar) 10 (3) 395-404.
Journal code: 9Y9. ISSN: 0158-5231.

PUB. COUNTRY: Australia
Journal; Article; (JOURNAL ARTICLE)

LANGUAGE: English

FILE SEGMENT: Priority Journals

ENTRY MONTH: 198510

AB Antisera selectively reactive with the N-terminal tetrapeptide sequence of

the platelet-derived connective tissue activating peptide-III mitogen were prepared and characterized. Solid phase synthesized Z-Asn-Leu-Ala-Lys(Z)-OH tetrapeptide representing the N-terminus of the mitogen was used as an ***immunogen*** after carbodiimide mediated coupling to methylated ***bovine*** ***serum*** ***albumin*** carrier and subsequent removal of Z groups. Anti-tetrapeptide sera demonstrated cross-reactivity to the mitogen but not beta-thromboglobulin, ***fibroblast*** ***growth*** ***factor*** , or epidermal growth factor, and a limited cross-reactivity to parathyroid hormone. The studies indicate that the N-terminal sequence of the mitogen is accessible for binding with ***antibody*** and the antitetrapeptide sera provide a reagent for the selective measurement of biologically active mitogen in the presence of structurally similar beta-thrombo-globulin. In addition, computer analysis of amino acid sequences revealed that few proteins contain the Asn-Leu-Ala-Lys sequence and of those that do, many are retroviral proteins or transforming polyproteins.

L54 ANSWER 47 OF 50 MEDLINE
ACCESSION NUMBER: 85051644 MEDLINE
DOCUMENT NUMBER: 85051644
TITLE: Cell multiplication and type II collagen production by rabbit articular chondrocytes cultivated in a defined medium.
AUTHOR: Adolphe M; Froger B; Ronot X; Corvol M T; Forest N
SOURCE: EXPERIMENTAL CELL RESEARCH, (1984 Dec) 155 (2) 527-36. Journal code: EPB. ISSN: 0014-4827.
PUB. COUNTRY: United States
Journal; Article; (JOURNAL ARTICLE)
LANGUAGE: English
FILE SEGMENT: Priority Journals; Cancer Journals
ENTRY MONTH: 198503
AB The complexity and the variations in the efficiency of different batches of serum stimulated the preparation of a serum-free medium which could promote not only growth, but also the differentiation properties of rabbit articular chondrocytes in culture. The serum-free medium (SFM) developed in this study contained insulin, transferrin, Na-selenite, human fibronectin ***bovine*** ***serum*** ***albumin*** (***BSA***), brain growth factor (BGF) or ***fibroblast*** ***growth*** ***factor*** (FGF), hydrocortisone and multiplication stimulating activity (MSA). Primary or secondary cultures of chondrocytes in such a medium attained a proliferation rate equal to 70-80% of that obtained with chondrocytes grown in a serum control medium. The deletion of various factors from SFM indicates that BGF or FGF are the most stimulating of growth factors. Insulin was beneficial when used individually; when combined with BGF or FGF, they had a synergistic effect on cell proliferation. MSA seemed not to play any role in chondrocyte growth in culture. The SFM medium did not modify either the morphology or the progression of cells into the cell cycle. It moreover allowed the maintenance of the specific function of chondrocytes to synthesize type II collagen.

L54 ANSWER 48 OF 50 CAPLUS COPYRIGHT 2001 ACS

ACCESSION NUMBER: 1970:41032 CAPLUS
DOCUMENT NUMBER: 72:41032
TITLE: Small molecular weight permeability factor in guinea pig serum: adsorption to antigen- ***antibody*** aggregates
AUTHOR(S): Movat, Henry Z.; Treloar, Mary P.; Takeuchi, Yuko
CORPORATE SOURCE: Univ. Toronto, Toronoto, Ont., Can.
SOURCE: J. Immunol. (1969), 103(4), 875-8
CODEN: JOIMA3
DOCUMENT TYPE: Journal
LANGUAGE: English
AB Immune ppts. of ***bovine*** ***serum*** ***albumin*** (I) and rabbit anti-I were incubated in siliconized test tubes with guinea pig serum which had not contacted glass at 37.degree. for 10 min. The ppts. were drained, then extd. with 0.5M NaCl at pH 8. The ext. contained a vascular permeability enhancing factor which had a mol. wt., as detd. by d. gradient centrifugation and Sephadex chromatog. about equal to that of egg albumin, and a higher mol. wt. component which enhanced clot formation and may have been Hageman's factor.

L54 ANSWER 49 OF 50 CAPLUS COPYRIGHT 2001 ACS
ACCESSION NUMBER: 1968:465633 CAPLUS
DOCUMENT NUMBER: 69:65633
TITLE: Activation of the plasma kinin system by antigen-***antibody*** aggregates. I. Generation of permeability factor in guinea pig serum
AUTHOR(S): Movat, Henry Z.; DiLorenzo, Nancy L.
CORPORATE SOURCE: Univ. Toronto, Toronto, Can.
SOURCE: Lab. Invest. (1968), 19(2), 187-200
CODEN: LAINAW
DOCUMENT TYPE: Journal
LANGUAGE: English
AB After non-glass-contacted serum from guinea pigs or rabbits was incubated with washed antigen- ***antibody*** ppt. (formed from ***bovine*** ***serum*** ***albumin*** and anti- ***bovine*** ***serum*** ***albumin***), the serum increased vascular permeability upon intradermal injection into guinea pigs or rabbits. Part of this property of activated serum was due to activation of the kinin system. The increased permeability was more pronounced when the incubation was conducted in the presence of Na diethyldithiocarbamate and less pronounced when 5-mg./kg. i.v. or i.p. doses of mepyramine maleate were given to the test animals before injection of the activated serum. The presence of hexadimethrine bromide (Polybrene), protamine sulfate, EDTA, diiso-Pr phosphorofluoridate, or salicylaldoxime in the incubation medium decreased the permeability-increasing activity of the activated serum. The addn. of Trasylol (a kallikrein inhibitor), soybean trypsin inhibitor, or .epsilon.-aminocaproic acid to the serum after incubation decreased its permeability-increasing activity in the test animals. The activated serum accelerated the clotting of plasma, caused contraction of guinea pig ileum and rat uterus, and decreased the blood pressure in rabbits. Antigen-***antibody*** aggregates adsorbed permeability-increasing and clot-promoting activity when added to normal, but not to Factor XII-deficient, human serum. The increases in blood vessel permeability

were confined mostly to the dermal venules.

L54 ANSWER 50 OF 50 CAPLUS COPYRIGHT 2001 ACS
ACCESSION NUMBER: 1969:85746 CAPLUS
DOCUMENT NUMBER: 70:85746
TITLE: Antigen- ***antibody*** activation of macrophage enzymes
AUTHOR(S): Hayashi, Hideo
CORPORATE SOURCE: Med. Sch., Kumamoto Univ., Kumamoto, Japan
SOURCE: Biochem. Acute Allerg. React., Symp. (1968), Meeting Date 1967, 141-52. Editor(s): Austen, K. Frank. F. A. Davis Co.: Philadelphia, Pa.
CODEN: 20TVAM
DOCUMENT TYPE: Conference
LANGUAGE: English
AB Omentum cells or peritoneal macrophages cultivated from the omentum or the sediment of peritoneal fluid of ***bovine*** ***serum*** ***albumin*** (***BSA***)-sensitized rabbits were used as the purest model for the study of an acute allergic reaction. The cells growing in culture were those of the histiocytic series and seemed to arise from the omentum. They contained antibodies to ***BSA*** of the 7 S and 19 S classes; it is as yet unknown whether the antibodies were produced by these cells or their precursor cells. The early phase of antigen- ***antibody*** reaction was characterized by the activation and release of the SH-dependent protease (Arthus protease) which occurred simultaneously with morphological changes in the cell membrane and ground cytoplasm of the cells. The delayed phase was characterized by the formation and release of the polypeptide inhibitor of the Arthus protease which occurred with morphological changes in the mitochondria, Golgi bodies, and nuclei of the cells. The anaphylactic release of histamine and immediate ***vascular*** ***permeability*** ***factor*** seemed assocd. with the activation of the Arthus protease, and their release was suppressed by the polypeptide inhibitor. The Arthus protease may play an integral part in the cellular mechanism or acute allergic reaction.

QR189.V82

STIC-ILL

335307

From: Holleran, Anne
Sent: Sunday, March 04, 2001 5:30 PM
To: STIC-ILL
Subject: refs. for 09/266,543

2380492

Examiner: Anne Holleran
Art Unit: 1642; Rm 8E03
Phone: 308-8892
Date needed by: ASAP

Please send me copies of the following :

1. Plum, S.M. et al. Vaccine, (2000) 19/9-10, 1294-1303
2. Aonuma, M. et al. Anticancer Res. (1999, Oct) 19(5B): 4039-4044
3. Muller, Y.A. et al. Structure (1998) 6(9): 1153-1167
4. Yamagishi, S. et al. J. Biol. Chem. (1997) 272(13): 8723-8730
5. Koolwijk, P. et al. J. Cell Biology (1996) 132(6): 1177-1188
6. Matsuo, A. et al. Neuroscience (1994) 60(1): 49-66
7. Djakiew, D. et al. Cancer Research (1991) 51(12): 3304-3310
8. Yamanishi, H. et al. Cancer Research (1991) 51(11): 3006-3010
9. Matsuzaki, K. et al. Japanese J. Cancer Research (1990) 81(4): 345-354
10. Kardami, E. et al. Growth Factors (1990) 4(1): 69-80
11. Riss, T.L. et al. J. Cellular Physiology (1989) 138(2): 405-414

112,1

ELSEVIER

Vaccine 19 (2001) 1294–1303

Vaccine

www.elsevier.com/locate/vaccine

Administration of a liposomal FGF-2 peptide vaccine leads to abrogation of FGF-2-mediated angiogenesis and tumor development

Stacy M. Plum *, John W. Holaday, Antonio Ruiz, John W. Madsen, William E. Fogler, Anne H. Fortier

EntreMed, Inc., 9640 Medical Center Drive, Rockville, MD 20850, USA

Received 26 January 2000; received in revised form 1 June 2000; accepted 1 June 2000

Abstract

Basic fibroblast growth factor (FGF-2) is an important stimulator of angiogenesis that has been implicated in neoplastic progression. Attempts to neutralize or modulate FGF-2 have met with some success in controlling neovascularity and tumor growth. In the present study, two peptides: one corresponding to the heparin binding domain and the other to the receptor binding domain of FGF-2, exerted dose-dependent inhibition of FGF-2-stimulated human umbilical vein endothelial cell proliferation ($IC_{50} = 70$ and 20 μg/ml, respectively). The identification of these functional regions suggested that targeting these domains might be an approach for the modulation of FGF-2 function. To investigate this possibility, we vaccinated mice with either the heparin binding domain peptide or the receptor binding domain peptide of FGF-2 in a liposome/adjuvant format, and analyzed the effect of vaccination on FGF-2-driven angiogenesis, tumor development and immune status. Mice vaccinated with the heparin binding domain peptide generated a specific antibody response to FGF-2, blocked neovascularization in a gelfoam sponge model of angiogenesis, and inhibited experimental metastasis by > 90% in two tumor models: the B16BL6 melanoma and the Lewis lung carcinoma. These effects were not observed in mice treated with the receptor binding domain peptide conjugated to liposomes or liposomes lacking conjugated peptide. These data suggest that a heparin binding domain peptide of FGF-2, when presented to a host in a liposomal adjuvant formulation, can ultimately lead to inhibition of angiogenesis and tumor growth.

Keywords: Vaccine; Heparin binding domain peptide; Anti-FGF-2

1. Introduction

Recent research in the field of angiogenesis has led to a current paradigm suggesting that phenotypic changes accompanying tumor-associated angiogenesis are mediated by an angiogenic switch [1]. In the homeostatic state, a balance between inhibitors and stimulators of angiogenesis is maintained. In contrast, during neoplasia, there is a shift in this balance toward the angiogenic phenotype. This switch can be mediated by either an upregulation of endogenous angiogenic stimulators, such as FGF-2, vascular endothelial growth factor (VEGF), or interleukin-8 [2–4] or the downregulation of angiogenic inhibitors, such as Angiostatin and Endostatin proteins [5–7]. This paradigm further suggests that modulation of angiogenic stimulators to homeostatic levels during tumor progression could arrest tumor growth.

FGF-2 is a single-chain polypeptide that plays an important role in embryonic development, angiogenesis, wound healing and many pathologic processes. FGF-2 is mitogenic to a number of cells including fibroblasts and endothelial cells. Through utilization of a dual receptor system, FGF-2 can induce proliferation and migration of these cells. The two-component receptor system consists of a transmembrane protein tyrosine kinase FGF receptor and heparin sulfate proteoglycan at the cell surface [2]. Alterations of either the receptor

* Corresponding author. Tel.: +1-301-5173345; fax: +1-301-2179594.

E-mail address: stacyp@entremed.com (S.M. Plum).

0264-410X/00/$ - see front matter
PII: S0264-410X(00)00210-3

binding domain or the heparin binding domain of FGF-2 may abrogate FGF-2 activity.

Evidence that FGF-2 plays an important role in angiogenesis has been shown in a number of experiments. FGF-2-induced stimulation of angiogenesis in vivo has been demonstrated in the corneal eye pocket [8,9], the gelatin sponge [10], and the matrigel plug assays [11]. Furthermore, a renal carcinoma cell line with low metastatic potential transfected with the FGF-2 gene was found to express FGF-2, and demonstrated increased neovascularization and metastatic potential in vivo [12]. Moreover, monoclonal antibodies generated against FGF-2 blocked FGF-2-stimulated angiogenesis and subcutaneous primary tumor growth [13].

With the increasing recognition that the progressive growth and development of a primary tumor and metastatic lesions is dependent on angiogenesis, considerable effort has focused on the potential therapeutic manipulation of the angiogenic compartment of a tumor. In this regard, a rationale for targeting a specific immune response to appropriate epitopes on the FGF-2 molecule for the endogenous control of tumor growth was developed. Peptides derived from the functional domains of FGF-2 were screened for the ability to competitively inhibit FGF-2-stimulated proliferation of endothelial cells. Peptides that blocked endothelial cell proliferation, but not tumor cell proliferation in vitro, were selected as target antigens, covalently linked to lipid vesicles containing lipid A as an adjuvant, and used to vaccinate mice in an attempt to generate a specific immune response directed toward the angiogenic stimulator, FGF-2. Employing this liposome technology, we demonstrate that vaccination of mice with the heparin binding domain, but not the receptor binding domain, resulted in inhibition of angiogenesis in vivo and a marked decrease in the growth and development of two murine tumors in experimental metastasis models. Therefore, a reversal of the angiogenic phenotype in malignant cancers might be achieved through the inhibition of positive regulators of vascular development.

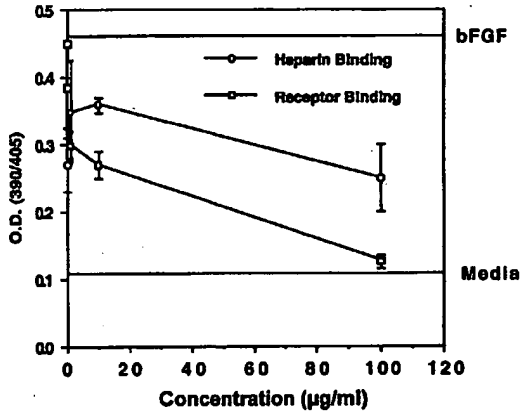

Fig. 1. Inhibition of human umbilical vein endothelial cell proliferation by FGF-2 peptides. Peptides corresponding to the heparin binding domain or the receptor binding domain of FGF-2 were applied to HUVECs in the presence of 5 ng/ml FGF-2 in a 72 h proliferation assay. Both the heparin binding (○) and the receptor binding (□) domain peptides inhibited HUVEC proliferation in a dose-dependent manner. Each point represents the mean ± one standard deviation. This figure is representative of the results obtained in three separate experiments.

Table 1
Sera from mice vaccinated with either L(HBD), L(RBD), L(LA) or PBS were assessed for immunoreactivity to the native FGF-2 molecule, the heparin binding domain peptide, the receptor binding domain peptide, or VEGF by ELISA[a]

Vaccination formulation	Antibody titer			
	FGF-2	HBD	RBD	VEGF
L(HBD)	1:5000	1:10 000	<1:100	<1:100
L(RBD)	<1:100	<1:100	<1:100	<1:100
L(LA)	<1:100	<1:100	<1:100	<1:100
PBS	<1:100	<1:100	<1:100	<1:100

[a] Responses are expressed as the reciprocal of the highest dilution that gave areading two standard deviations above the mean O.D. for normal mouse serum.

2. Materials and methods

2.1. Peptides

A 44 amino acid peptide corresponding to the heparin binding domain of FGF-2 (YCKNGGFFLRIHPDGRVDGVREKSDPHIKLQQAEEGVVSIKGV) and a 22 residue peptide corresponding to the receptor binding domain of FGF-2 (SNNYNTYRSRKYSSWYVALKR) were synthesized by Infinity Technology Inc. (Upland, PA). Peptides were hydrated in 10 mM acetic acid to a concentration of 10 mg/ml for use in proliferation assays and liposome formulations. Both peptides were analyzed by high-performance liquid chromatography for purity. The purity of the heparin binding domain (HBD) and the receptor binding domain (RBD) peptides was 90%.

2.2. Cell lines

Human umbilical vein endothelial cells (HUVECs, Clonetics, Walkersville, MD) were maintained in endothelial cell growth medium (EGM-2; Clonetics), supplemented with 1% L-glutamine (BioWhittaker, Walkersville, MD) and bovine brain extract in 75 cm^2 cell-culture flasks at 37°C, in moist air, 10% CO_2.

The B16BL6 variant line of the B16-F10 melanoma was obtained from the National Cancer Institute Cen-

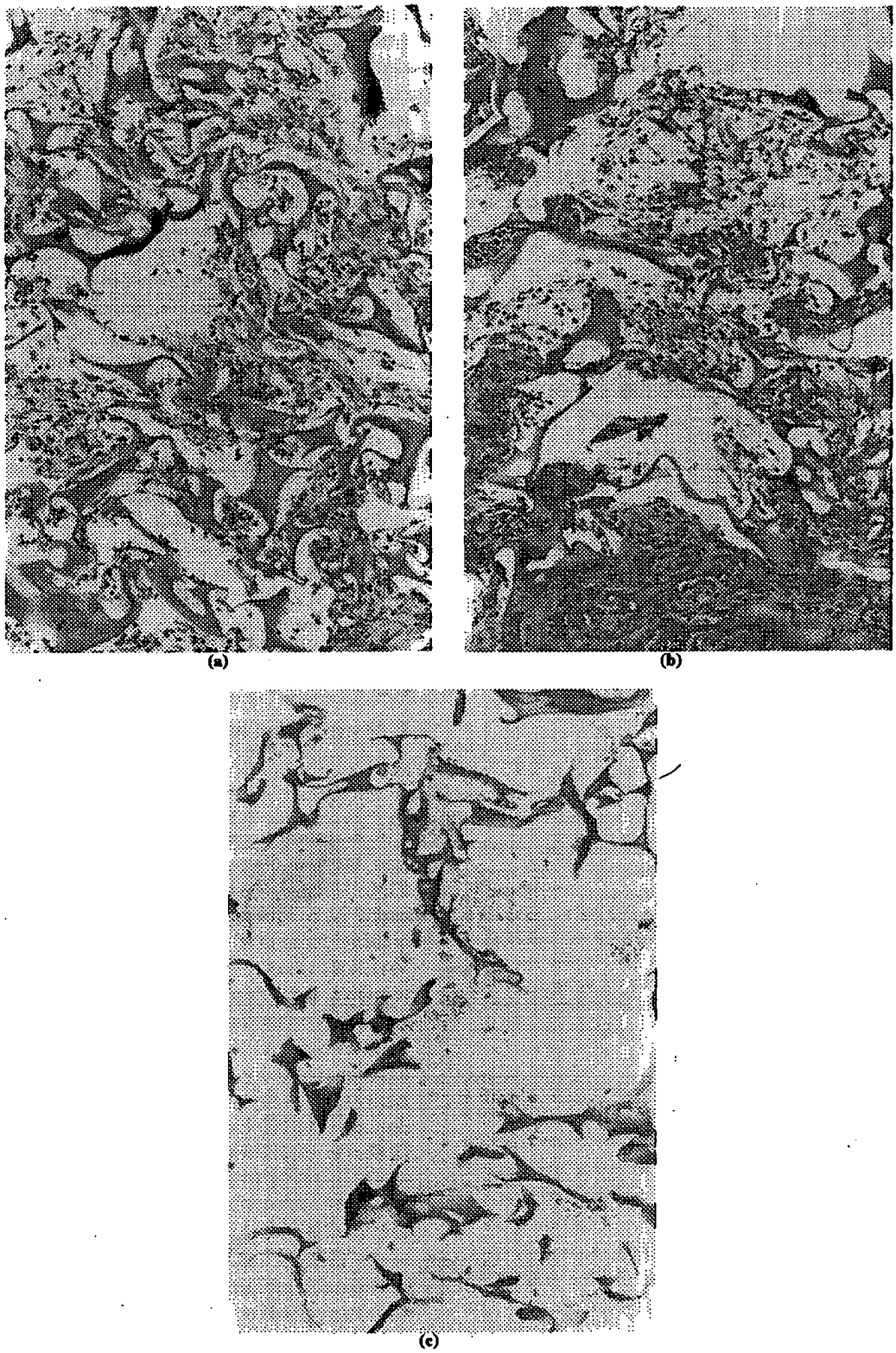

Fig. 2. Inhibition of FGF-2-induced angiogenesis. Gelatin sponges containing FGF-2 were implanted onto the livers of mice (five mice per group) pretreated with the L(HBD), L(RBD), or L(LA). Fourteen days following implantation, sponges were removed and sectioned for histology. Hematoxylin and eosin (H&E) staining of sponges from mice treated with L(LA) (a) or L(RBD) (b) revealed cellular infiltration and neovascularization. H&E staining of sponges from mice treated with L(HBD) (c) revealed a marked decrease in cellular infiltration and neovascularization. This figure is representative of the results obtained in two separate experiments.

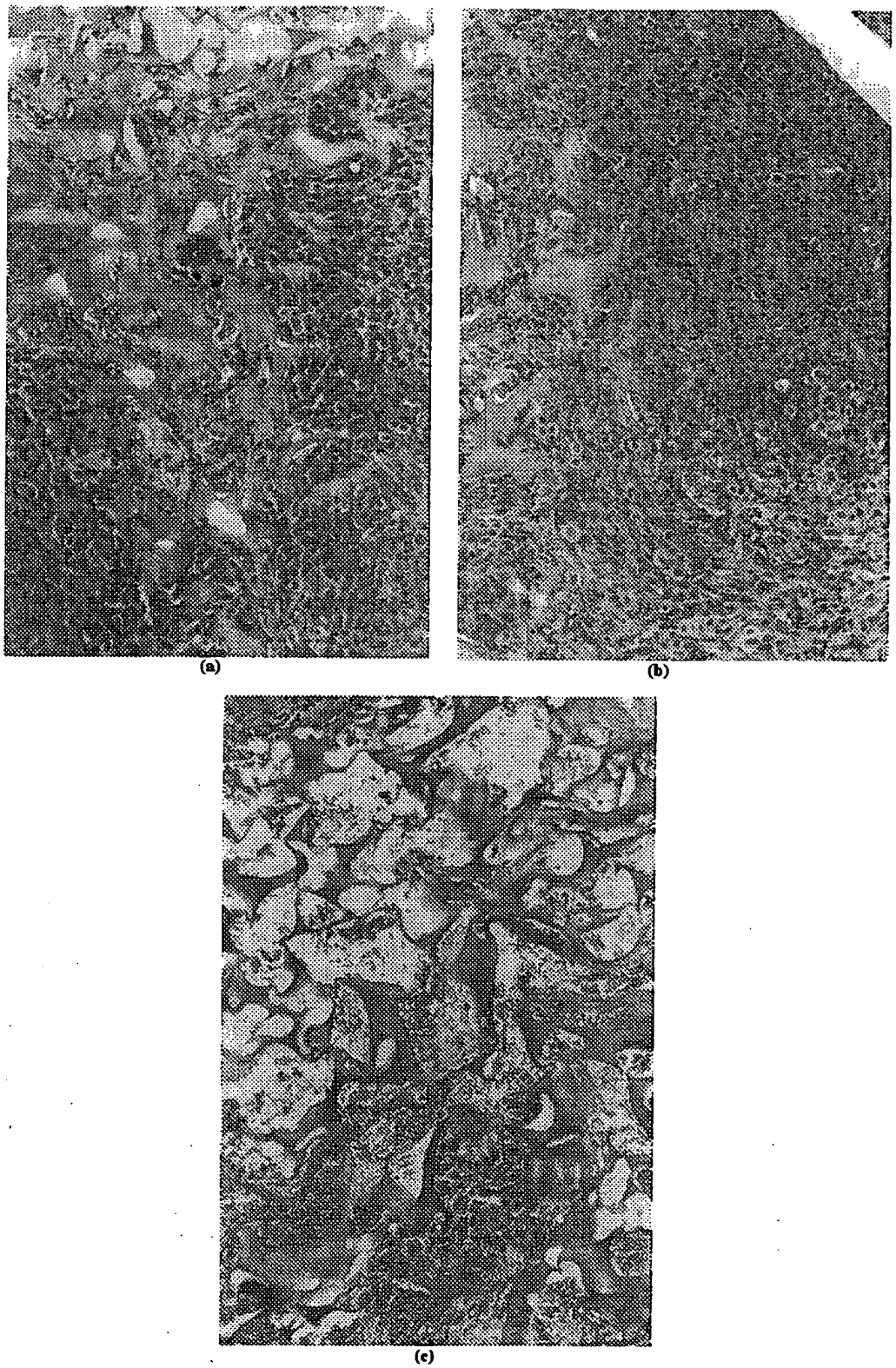

Fig. 3. Inhibition of B16BL6 tumor growth and angiogenesis in hepatic sponge implants. Gelatin sponges containing 5×10^4 B16BL6 tumor cells were implanted onto the liver of mice (five mice per group) pretreated with L(HBD), L(RBD), or L(LA). Fourteen days following implantation, sponges were removed and sectioned for histology. H&E staining of sponges removed from mice treated with L(LA) (a) or L(RBD) (b) revealed B16BL6 tumor growth and neovascularization, while sponges removed from mice treated with L(HBD) (c) contained an abundance of red blood cells lacking defined structures surrounding them. This figure is representative of the results obtained in two separate experiments.

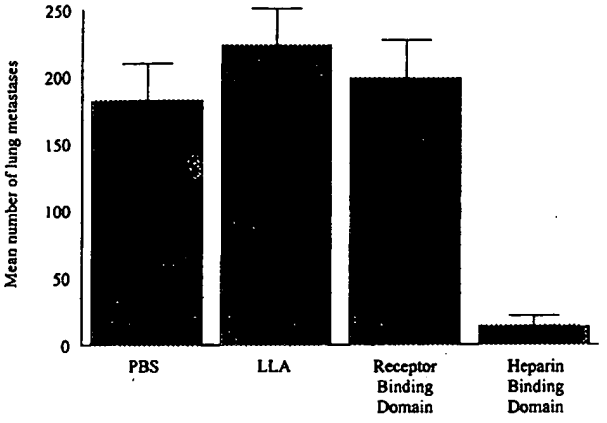

Fig. 4. Inhibition of the growth of experimental lung metastases. Mice (ten mice per group) pretreated with either L(HBD), L(RBD), L(LA) or PBS were challenged with 5×10^5 B16BL6 tumor cells intravenously. Fourteen days following inoculation, mice were sacrificed, lungs removed and surface pulmonary metastases counted using a dissecting microscope. Tumor growth was evident in all groups assayed. Mice treated with L(HBD) demonstrated 96% inhibition of surface pulmonary metastases. This figure is representative of the results obtained in five separate experiments.

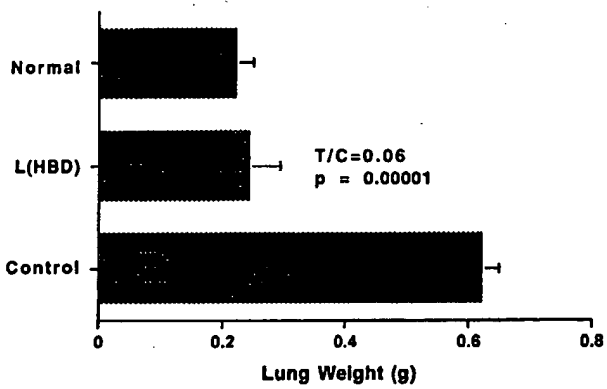

Fig. 5. Inhibition of LLC-LM experimental metastases. Mice (five mice per group) pretreated with the L(HBD) or L(LA) control were challenged with 5×10^5 LLC-LM tumor cells intravenously. Seventeen days following inoculation, mice were sacrificed, lungs removed and lung weight assessed. Mice treated with L(HBD) inhibited the development of pulmonary metastases by 95%. For comparison, lung weight from an unchallenged (normal) group of mice is included. This figure is representative of the results obtained in two separate experiments.

tral Repository (Frederick, MD). Tumor cells were grown in Dubecco's Modified Eagle's Medium (DMEM) (BioWhittaker), supplemented with 5% heat-inactivated fetal bovine serum and L-glutamine (BioWhittaker), as monolayer cultures at 37°C in a humidified atmosphere of 5% CO_2/95% air. The cells were passaged at 80% confluency and used between passages 6 and 18. The B16BL6 were certified free of mycoplasma and the following pathogenic murine viruses reovirus type 3, pneumonia virus of mice, K virus, Theiler's encephalitis virus, Sendai virus, minute virus of mice, mouse adenovirus, mouse hepatitis virus, lymphocytic choriomenengitis virus, ectromelia virus, and lactate dehydrogenase virus.

The Lewis lung carcinoma–low metastatic (LLC-LM) cell line was a kind gift from Dr Judah Folkman (Children's Hospital, Boston, MA) and was certified free of the same mycoplasma and pathogenic murine viruses already mentioned. LLC-LM was maintained in DMEM supplemented with 10% heat-inactivated fetal bovine serum and 1% L-glutamine.

2.3. Proliferation assays

HUVECs at passages two to five were washed with phosphate-buffered saline (PBS) and trypsinized with a 0.05% solution of trypsin-versene mixture (BioWhittaker). Cells were suspended in endothelial cell basal medium, (EBM-2; Clonetics) supplemented with 2% heat-inactivated fetal bovine serum (Hyclone, Logan, UT) and 2 mM L-glutamine at a concentration of 2.5×10^4 cells/ml, plated in 96-well (100 μl/well) culture plates (Costar, Cambridge, MA) and incubated for 24 h at 37°C in 5% CO_2. Cells were incubated with either the FGF-2 peptides or a 22 amino acid control peptide at 1, 10, and 100 μg/ml, or media alone for 20 min. The cells were then stimulated with 10 ng/ml human recombinant FGF-2 (R&D Systems, Minneapolis, MN) or media alone for 72 h. Cell proliferation was measured by BrdU incorporation using an enzyme linked immunosorbent assay (ELISA) (Boehringer Mannheim, Indianapolis, IN) according to the manufacturer's instructions.

2.4. Incorporation of FGF-2 peptides to liposomes

Multilamelar liposomes were made as previously described [14]. Briefly, liposomes consisting of dimyristoyl-glycero-3-[phospho-rac-(1-glycerol)], dimyristoyl-glycero-3-phosphocholine, cholesterol (Avanti Polar Lipids, Alabaster, AL), pyridyl dithio-cholesterol (PDS-Chol), and lipid A (List Biological Laboratories, Inc. Campbell, CA) were prepared in a molar ratio of 1:9:7.5:1, containing 1 mg/ml Lipid A. Lipids were mixed in a round bottom flask and solvent was removed by rotary evaporation. Multilamellar vesicles were prepared by hydrating the dried lipids in 6.4 ml sterile water (BioWhittaker) containing 2 mg of either the heparin binding domain peptide or the receptor binding domain peptide of FGF-2. This step allows the peptides to be covalently linked to the PDS-chol found in the liposome shell. Liposome formulations were incubated overnight at room temperature (RT) with gentle orbital shaking, lyophilized and resuspended in 2.135 ml of 0.1 M citrate phosphate buffer (pH 5.6). Two hundred microliters of respective peptides were added to each liposome preparation, followed by incubation for 16 h at RT on the orbital

shaker. Liposomes were centrifuged at 15 000 rpm for 30 min at 4°C. The resulting liposome formulation therefore contained peptide within the aqueous interior, as well as covalently attached to the phospholipid membrane. Quantitation of peptide associated with the liposome was assessed by amino acid analysis utilizing Edman degradation (MA BioServices, Rockville, MD). Total peptide associated with the liposomes was determined to be between 75 and 80% incorporation in all batches of liposomes.

2.5. Treatment of mice with liposomes

Specific pathogen free 5- to 7-week-old C57BL/6J male mice were purchased from The Jackson Laboratory (Bar Harbor, ME). Mice were housed in a specific pathogen free facility. In conducting the research in this report, the investigators adhered to the Guide for Laboratory Animals and Care of the Institute of Laboratory Animal Resources, National Academy of Sciences, National Research Council. Cohorts of mice (five to ten mice per group) were treated three times at 2-week intervals with liposomes containing either the heparin binding domain peptide (L(HBD)) or the receptor binding domain peptide (L(RBD)) (0.1 ml, intramuscular). The intramuscular route of administration was chosen based on previous work that demonstrated induction of both a cytotoxic T lymphocyte (CTL) as well as a humoral immune response [31]. For injection, liposomes were resuspended to a final volume of 5 ml with nonpyrogenic Mg^{2+}- and Ca^{2+}-free PBS. The pH of the final liposome preparation that was administered to animals was 7.0. Each liposome injection delivered 1 μmol phospholipid, 100 μg Lipid A, and 30 μg peptide. Control groups include mice treated with liposomes lacking conjugated peptide (L(LA)) or mice treated with PBS. Thirteen days following the last injection, mice were bled from the lateral tail vein and serum was collected for analysis of antibody. The following day, mice were either challenged with tumor cells intravenously, or challenged with FGF-2 or B16BL6 impregnated sponges (liver implant).

2.6. Determination of antibody titer and specificity

Pooled serum was obtained from mice treated with either L(HBD), L(RBD), L(LA), or PBS. Anti-FGF-2-specific antibodies were measured by ELISA. Briefly, 96-well immulon 4 plates (Dynatech, Chantilly, VA) were coated with either recombinant FGF-2, the heparin binding domain peptide of FGF-2, the receptor binding domain peptide of FGF-2, or VEGF (50 μl; 2 μg/ml in 0.2 M carbonate buffer, pH 6.9), incubated overnight at 4°C, and blocked with 3% nonfat dry milk (Giant Food, Inc.) and 0.05% Tween 20 in PBS (PBS/Tween 20). Plates were washed three times with PBS/Tween 20, and incubated with serial dilutions of anti-sera from vaccinated animals in PBS/Tween 20 for 1 h. Two negative controls were used in this ELISA: naïve mouse serum, or sera from mice vaccinated with liposomal lipid A. In addition, each plate contained a series of wells that were not coated with antigen, that were subsequently treated with serum and secondary antibody. Reactivity of naïve mouse sera as well as anti-sera from mice vaccinated with liposomal lipid A was equivalent to values obtained in wells without antigen. Plates were washed and incubated with peroxidase-labeled goat anti-mouse immunoglobin (Ig)G and IgM (Kirkegard & Perry, Gaithersburg, MD) for 1 h at RT. Following washing, wells were incubated with ABTS peroxidase substrate system (K&P). Optical density was read at 405 nm. Antibody titer was defined as the reciprocal of the serum dilution giving an O.D. reading of two standard deviations above the mean O.D. for normal mouse serum [15].

2.7. Gelfoam sponge model of angiogenesis

As previously described [10], gelfoam sponges (Upjohn, Kalamazoo, MI) were dissected into 5 mm^3 squares and hydrated in PBS for 24 h at room temperature. Following hydration, sponges were blotted dry on sterile gauze and rehydrated in 80 μl solution containing FGF-2 (8 ng/ml) and heparin (10 U/ml). Gelfoam sponges were incubated for 1 h at 37°C prior to implantation onto the livers of mice.

Mice were anesthetized with metafane and a small incision was made on the ventral region of the mouse to expose the liver. Gelfoam sponges were fixed onto the left lobe of the liver with cyanoacrylate adhesive and wounds were closed with surgical staples. Fourteen days following implantation, mice were sacrificed, sponges were removed from the liver, and fixed in 10% buffered formalin for histologic analysis.

2.8. Experimental pulmonary metastasis models

B16BL6 tumor cells in exponential growth phase were harvested by a short trypsinization (0.25% DIFCO trypsin and 0.02% ethylenediamine tetraacetic acid for 1 min at 37°C), washed and resuspended to 2.5×10^5 cells/ml in Ca^{2+}-, Mg^{2+}-free PBS. Mice were injected with 0.2 ml cell suspension (5×10^4 tumor cells/mouse) via the lateral tail vein with a 27-gauge needle. Fourteen days following inoculation, mice were sacrificed and lungs were removed and fixed in formalin. Surface pulmonary metastases were counted with a dissecting microscope (Olympus, 3X).

LLC-LM tumor cells in exponential growth phase were harvested using a cell scraper, washed and resuspended to 1×10^6 cells/ml in Ca^{2+}-, Mg^{2+}-free PBS. Mice were injected with 0.2 ml cell suspension via the

lateral tail vein with a 27-gauge needle. Seventeen days following inoculation, mice were sacrificed and lungs were removed, weighed, and fixed in 10% buffered formalin.

2.9. Histological analysis

Lungs and gelfoam sponges were fixed in 10% buffered formalin. Tissues were embedded in paraffin by routine methods, sectioned at 6 μm, and stained with hematoxylin and eosin (H&E) by Molecular Histology Labs, Inc. (Gaithersburg, MD). Photomicrographs were obtained using an Olympus IX70 microscope.

2.10. Statistical analysis

Results were analyzed for statistical significance using the two-tailed Students' *t*-test.

3. Results

3.1. Inhibition of endothelial cell proliferation

Previous studies demonstrated that peptides derived from the heparin binding domain of FGF-2 were able to specifically inhibit FGF-2-induced proliferation of 3T3 fibroblasts as well as vascular and capillary endothelial cells [16]. To further assess the inhibitory activity of a 42 amino acid peptide that corresponds to the heparin binding domain of FGF-2 (HBD) and to analyze an additional functional domain of FGF-2, the RBD, these peptides at concentrations of 1, 10, or 100 μg/ml were coincubated with 5 ng/ml FGF-2 in a HUVEC proliferation assay. Addition of FGF-2 alone stimulates proliferation of HUVECs in comparison with cells incubated without the growth factor. Both the HBD and the RBD peptides inhibited FGF-2-induced proliferation of HUVECs in a dose-dependent fashion with inhibitory concentrations (IC_{50}) of 70 and 20 μg/ml, respectively (Fig. 1). A 22 amino acid control peptide corresponding to a defined region of human angiostatin had no inhibitory effect on FGF-2-induced proliferation of HUVECs.

3.2. Delivery of the HBD and the RBD in liposome vesicles: induction of an antibody response

The peptides from the two functional domains of FGF-2, the HBD and the RBD, were covalently conjugated to and encapsulated in liposome vesicles containing the potent adjuvant Lipid A, and used to treat mice every 2 weeks for 6 weeks. Each inoculation delivered 1 μmol phospholipid, 100 μg Lipid A, and 30 μg peptide. Following treatment, mice were bled and sera were pooled for analysis of serum immunoreactivity to native FGF-2, the HBD peptide, and the RBD peptide in an ELISA format. Individual antibody titers were also assessed (data not shown). The individual titers were not different from pooled titers. Therefore, pooled titers were used. Immunoreactivity was measured in mice treated with the liposomal formulation containing the HBD peptide (L(HBD)) of FGF-2. This antibody reacted against both the HBD peptide and the parent FGF-2 molecule, with endpoint titers of 1:10 000 and 1:5 000, respectively (Table 1). The major subclass of antibody is IgG (data not shown). In contrast, sera collected from mice treated with the RBD peptide conjugated to liposomes (L(RBD)) or from mice treated with liposomes lacking a conjugated peptide (L(LA)) did not show immunoreactivity to the receptor binding domain peptide, the heparin binding domain peptide or the intact FGF-2 molecule. As expected, all mice treated with a liposome preparation containing the lipid A adjuvant, developed an antibody titer to lipid A (endpoint dilution of serum, 1:30 000) (data not shown).

To assess the specificity of the antibody generated in response to inoculation of L(HBD), sera from treated animals were assayed for immunoreactivity to another heparin binding molecule: VEGF. When assayed in an ELISA format, serum from L(HBD) treated mice did not bind VEGF (Table 1).

3.3. Inhibition of FGF-2-induced angiogenesis in hepatic sponge implants

Since mice vaccinated with L(HBD) showed immunoreactivity to FGF-2, we assessed whether we could effect a functional attribute of exogenous FGF-2. FGF-2-impregnated sponges implanted on the liver of mice stimulate neovascularization that is readily visualized after 14 days by histologic analysis. Mice treated with the L(HBD) were assessed for anti-angiogenic activity using gelatin sponge model of neovascularization [10]. Gelatin sponges containing recombinant human FGF-2 were implanted onto the left lobe of the liver of mice treated with L(LA), L(HBD), L(RBD) or PBS. Fourteen days following implantation, sponges were removed, and vascularity and leukocyte infiltration were assessed histologically (Fig. 2a–c). Well-defined blood vessels containing red blood cells were evident in sponges removed from mice treated with L(LA) or L(RBD) (Fig. 2a,b, respectively). Moreover, there was an abundant cellular infiltration, consisting of white blood cells and fibroblasts, into these sponges. In contrast, histologic analysis of sponges removed from mice treated with the L(HBD) revealed a decreased cellular infiltration and a lack of neovascularization induced by FGF-2 (Fig. 2c). While red blood cells were present in the histologic sections of the sponges taken

from mice treated with L(HBD), there was a lack of well-defined capillary structures and a marked paucity of endothelial cells.

3.4. Inhibition of B16BL6-induced angiogenesis and tumor growth in hepatic sponge implants

The gelatin sponge model of angiogenesis can also be used to evaluate angiogenesis induced by a tumor. Gelatin sponges containing 5×10^4 B16BL6 melanoma cells were implanted onto the livers of mice vaccinated with L(LA), L(HBD), L(RBD) or PBS. Fourteen days following implantation, the sponges were removed and examined histologically. Sponges removed from mice treated with L(LA), L(RBD) and PBS contained B16BL6 tumor cells (Fig. 3a–c). Neovascularization into these sponges was abundant as evidenced by endothelial cells forming defined capillary structures containing red blood cells. In contrast, sponges from mice treated with L(HBD) had no evidence of neovascularization and B16BL6 tumor growth was inhibited as well. Again, while red blood cells were observed, there were no vascular or endothelial structures surrounding them.

3.5. Inhibition of progression of experimental metastasis

To assess the ability of vaccinated mice to inhibit the development of tumors in an experimental model of metastasis in the lung, we challenged treated mice with B16BL6. Fourteen days after intravenous challenge with B16BL6, mice were sacrificed, lungs removed and surface metastases counted (Fig. 4). Treatment with L(HBD) resulted in 96% inhibition of macroscopic B16BL6 metastases in the lungs when compared with lungs of mice treated with L(LA), L(RBD), or PBS. Mice treated with either L(LA), L(RBD), or PBS had large melanotic lesions that encompassed the entire surface of the lungs. Histologic analysis of lung tissue from L(HBD) treated mice revealed few tumors that were less than ten cell layers thick. Lungs removed from control groups (L(LA) or PBS) contained numerous melanotic foci greater than ten cell layers thick.

Confirmation of the anti-tumor effects was achieved with a second model of experimental metastatic disease. Seventeen days following intravenous challenge with LLC-LM, two mice in the control groups succumbed to progressive tumor burden, while the remaining control mice exhibited labored breathing and decreased mobility. All groups were sacrificed on day 17, lungs were removed and tumor burden was assessed by measuring lung weights. Mice that received L(LA) had a considerable tumor burden confined to the lungs, whereas mice treated with L(HBD) exhibited a significant decrease in tumor burden ($P < 10^{-5}$) (Fig. 5).

4. Discussi n

In this report, a 42-mer peptide corresponding to the heparin binding domain of murine FGF-2 was synthesized and shown to block FGF-2-induced endothelial cell proliferation. Treatment of mice with this inhibitory peptide conjugated to liposomes with lipid A induced an immune response against FGF-2 and blocked the induction of neovascularization by FGF-2 in a sponge implant model of angiogenesis. Furthermore, mice vaccinated with L(HBD) and subsequently challenged with either a murine melanoma or lewis lung carcinoma inhibited tumor growth and development in the lung.

It is now well established that, for progressive tumor growth, a shift in the homeostatic balance toward an angiogenic phenotype must occur [1]. This switch entails both an upregulation of endogenous angiogenic stimulators, such as the family of fibroblast and vascular endothelial growth factors, and a downregulation of angiogenic inhibitors that include Angiostatin and Endostatin proteins. This suggests that a reversal of the angiogenic phenotype in malignant cancers and cessation of tumor growth might be achieved through the restoration of the negative regulators of vascular development [17–20]. Such is the rationale behind a number of therapeutic approaches currently under evaluation. An alternate treatment strategy can be achieved by either inhibiting or neutralizing the angiogenic stimulators. This approach has been validated by work carried out with receptor antagonists and monoclonal Ab therapies[13].

A considerable body of evidence exists in support of FGF-2 as a key mediator in the development of the angiogenic phenotype. First, levels of FGF-2 in the serum of patients with histologic specific cancer have been shown to inversely correlate with survival [21–28]. Second, transfection of a low metastatic renal carcinoma cell line with the FGF-2 gene resulted in an increase in metastatic potential, as compared with mock transfectant [12]. Finally, differences in site dependent angiogenesis and growth of renal carcinoma cells is due to the expression of FGF-2. When human renal carcinoma cells are implanted subcutaneously into nude mice, they produce slow-growing, nonmetastatic tumors that are not vascularized. In contrast, the implantation of the same cells into the kidney of mice yields rapidly growing, vascularized tumors. The kidney tumors expressed high levels of FGF-2 mRNA and protein compared with the renal carcinoma cells growing subcutaneously [29,30].

Our successful attempts to generate an immune response to FGF-2, an endogenous angiogenic stimulatory protein, was the first step toward using this treatment strategy to block pathologic angiogenesis. Mice vaccinated with the L(HBD) generated a specific

antibody response measurable by reactivity to both the homologous peptide and the native FGF-2 molecule (Table 1). The pronounced biological effects observed in mice vaccinated with L(HBD) necessitates the examination of potential mechanisms of action. In this regard, the generation of Ab in L(HBD)-treated mice could target a key mediator of pathologic angiogenesis, soluble FGF-2, and subsequently control tumor growth through restoration of the homeostatic balance. However, adoptive transfer of antisera generated in mice vaccinated with the L(HBD) was unable to confer protection against challenge with B16BL6 (data not shown). The role of antibody in mediating the observed anti-angiogenic and antimetastatic effects is currently under investigation. Additionally, previous studies employing an identical liposome vesicle conjugated to peptide report the induction of a cytotoxic T lymphocyte response [31,32]. Generation of CTL could result in the inhibition of angiogenesis, as well as tumor development, by targeting cells that respond to FGF-2. The role of cell-mediated immunity in protection against tumor challenge is currently being investigated.

The results presented in this report suggest that active immunization to an angiogenic cytokine is a valid alternative for cancer therapy that merits further investigation. The homology between murine and human FGF-2 is high (95% homologous). Moreover, the HBD peptide used in the present investigation is completely homologous to both murine and human FGF-2. Based on this information, the clinical use of this vaccine may result in similar anti-angiogenic and anti-tumor effects in humans as those observed in preclinical murine models. We do retain caution concerning the long-term effects of an immune response to a biologically important molecule. As a result, we are investigating the effects of vaccination on normal wound healing responses and reproductive capacity in female mice.

In summary, strategies aimed at restoring the angiogenic balance of a progressively growing tumor have concentrated on either an upregulation of negative mediators or passive administration of neutralizing antibody to growth factors. The results reported in this manuscript offer a novel third approach to the development of a therapy that effectively blocks tumor progression and angiogenesis.

Acknowledgements

The authors thank Dr Carl Alving for his insightful comments regarding this paper.

References

[1] Liotta LA, Steeg PS, Stetler-Stevenson WG. Cancer metastases and angiogenesis: an imbalance of positive and negative regulation. Cell 1991;64:327–36.

[2] Burgess WH, Winkles JA. The fibroblast growth factor family: multifunctional regulators of cell proliferation. In: Regulation of the Proliferation of Neoplastic Cells. Oxford: Oxford University Press, 1994:155–218.

[3] Klagsbrun M, Soker S. VEGF/VPF: the angiogenesis factor found? Curr Biol 1993;3:699–702.

[4] Streiter RM, Kunkel SL, Elner VM, Martonyl CL, Koch AE, Polverini PJ, Elner SG. Interleukin-8: a corneal factor that induces neovascularization. Am J Pathol 1992;141:1279–84.

[5] O'Reilly MS, Holmgren L, Shing Y, Chen C, Rosenthal RA, Moses M, Lane WS, Cao Y, Sage EH, Folkman J. Angiostatin: a novel angiogenesis inhibitor that mediates the suppression of metastases by a Lewis lung carcinoma. Cell 1994;79:315–28.

[6] O'Reilly MS, Boehm T, Shing Y, Fukai N, Vasios G, Lane WS, Flynn E, Birkhead JR, Olsen BR, Folkman J. Endostatin: an endogenous inhibitor of angiogenesis and tumor growth. Cell 1997;88:1–20.

[7] Voest EE, Kenyon BM, O'Reilly MS, Truitt G, D'Amato RJ, Folkman J. Inhibition of angiogenesis in vivo by IL-12. J Natl Cancer Inst 1995;87:581–6.

[8] Gaudric A, N'guyen T, Moenner M, Glacet-Bernard A, Barritault D. Quantification of angiogenesis due to basic fibroblast growth factor in a modified rabbit corneal model. Ophthalmic Res 1992;24(3):181–8.

[9] Wilting J, Christ B. A morphological study of the rabbit corneal assay. Anat Anz 1992;174:549–56.

[10] Watanabe M, McCormick KL, Volker K, Ortaldo JR, Wigginton JM, Brunda MJ, Wiltrout RH, Fogler WE. Regulation of local host mediated anti-tumor mechanisms by cytokines: direct and indirect effects on leukocyte recruitment and angiogenesis. Am J Pathol 1869;150:1880.

[11] Kibbey MC, Grant DS, Kleinman HK. Role of the SIKVAV site of laminin in promotion of angiogenesis and tumor growth: an in vivo matrigel model. JNCI 1992;84:1633–8.

[12] Miyake H, Hara I, Yoshimura K, Eto H, Arakawa S, Wada S, Chihara K, Kamidono S. Introduction of basic fibroblast growth factor gene into mouse renal cell carcinoma cell line enhances its metastatic potential. Cancer Res 1996;56:2440–5.

[13] Coppola G, Atlas-White M, Katsahambas S, Bertolini J, Hearn MT, Underwood JR. Effect of intraperitoneally, intravenously, and intralesionally administered monoclonal anti-beta-FGF antibodies on rat chondrosarcoma tumor vascularization and growth. Anticancer Res 1997;17:2033–9.

[14] Koning AWT. Lipid peroxidation in liposomes. In: Gregoriadis G, editor. Preparation of Liposomes. In: Liposomes Technology, vol. Vol. I. Boca Raton, FL: CRC Press, 1984:139–59.

[15] Frey A, Mantis N, Kozlowski PA, Quayle AJ, Bajardi A, Perdomo JJ, Robey FA, Neutra MR. Immunization of mice with peptomers covalently coupled to aluminum oxide particles. Vaccine 1999;17:3007–19.

[16] Baird A, Schubert D, Ling N, Guillemin R. Receptor- and heparin-binding domain of basic fibroblast growth factor. Proc Natl Acad Sci USA 1988;85:2324–8.

[17] O'Reilly MS, Holmgren L, Chen C, Folkman J. Angiostatin induces and sustains dormancy of human primary tumors in mice. Nat Med 1998;2:37–48.

[18] Pluda JM. Tumor-associated angiogenesis: mechanisms, clinical implications, and therapeutic strategies. Semin Oncol 1997;24:203–18.

[19] Harris AL. Antiangiogenesis for cancer therapy. Lancet 1997;349:13 -5.

[20] Folkman J. Antiangiogenic therapy. In: VT De Vita Jr, S Hellman, SA Rosenberg, editors. Cancer: Principles and Practice of Oncology. Philadelphia, PA: Lippincott, 1997. pp. 3075–3085.

[21] Duensing S, Grosse J, Atzpodien J. Increased serum levels of basic fibroblast growth factor (bFGF) are associated with progressive lung metastases in advanced renal cell carcinoma patients. Anticancer Res 1995;15:2331–3.
[22] Sluitz G, Tempfer C, Obermair A, Dadak C, Kainz C. Serum evaluation of basic FGF in breast cancer patients. Anticancer Res 1995;15:2675–7.
[23] Chopra V, Dinh TV, Hannigan EV. Serum levels of interleukins, growth factors and angiogenin in patients with endometrial cancer. J Cancer Res Clin Oncol 1997;123:167–72.
[24] Cronauer MV, Hittmair A, Eder IE, Hobisch A, Culig Z, Ramoner R, Zhang J, Bartsch G, Reissigl A, Radmayr C, Thurnher M, Klocker H. Basic fibroblast growth factor levels in cancer cells and in sera of patients suffering from proliferative disorders of the prostate. Prostate 1997;31:223–33.
[25] Landriscina M, Cassano A, Ratto C, Longo R, Ippoliti M, Palazzotti B, Crucitti F, Barone C. Quantitative analysis of basic fibroblast growth factor and vascular endothelial growth factor in human colorectal cancer. Br J Cancer 1998;78:765–70.
[26] Dosquet C, Coudert MC, Lepage E, Cabane J, Richard F. Are angiogenic factors, cytokines, and soluble adhesion molecules prognostic factors in patients with renal cell carcinoma? Clin Cancer Res 1997;3:2451–8.
[27] Dirix LY, Vermeulen PB, Pawinski A, Prove A, Benoy I, De Pooter C, Martin M, Van Oosterom AT. Elevated levels of the angiogenic cytokines basic fibroblast growth factor and vascular endothelial growth factor in sera of cancer patients. Br J Cancer 1997;76:238–43.
[28] Nanus DM, Schmitz-Drager BJ, Motzer RJ, Lee AC, Vlamis V, Cordon-Cardo C, Albino AP, Reuter VE. Expression of basic fibroblast growth factor in primary human renal tumors: correlation with poor survival. J Natl Cancer Inst 1994;85:1597–9.
[29] Singh RK, Bucana CD, Gutman M, Sanchez R, Llansa N, Fidler IJ. Organ site dependent expression of basic fibroblast growth factor in human renal cell carcinoma cells. Am J Pathol 1994;145:365–7.
[30] Naito S, von Eschenbach AC, Giavazzi R, Fidler IJ. Growth and metastasis of tumor cells isolated from a human renal cell carcinoma implanted into different organs of nude mice. Cancer Res 1986;46:4109–15.
[31] White WI, Cassatt DR, Madsen J, Burke SJ, Woods RM, Wassef NM, Alving CR. Antibody and cytotoxic T-lymphocyte responses to a single liposome-associated peptide antigen. Vaccine 1995;13:1111–22.
[32] Yasutomi Y, Koenig S, Woods RM, Madsen J, Wassef NM, Alving CR, Klein HJ, Nolan TE, Boots LJ, Kessler JA. A vaccine-elicited, single viral epitope-specific cytotoxic T lymphocyte response does not protect against intravenous, cell-free simian immunodefiency virus challenge. J Virol 1995;69:2279–84.

STIC-ILL

RC261. A1 A68

NO 5

335308

2380485

From: Holleran, Anne
Sent: Sunday, March 04, 2001 5:30 PM
To: STIC-ILL
Subject: refs. for 09/266,543

Examiner: Anne Holleran
Art Unit: 1642; Rm 8E03
Phone: 308-8892
Date needed by: ASAP

Please send me copies of the following :

10628351

1. Plum, S.M. et al. Vaccine, (2000) 19/9-10, 1294-1303
2. Aonuma, M. et al. Anticancer Res. (1999, Oct) 19(5B): 4039-4044
3. Muller, Y.A. et al. Structure (1998) 6(9): 1153-1167
4. Yamagishi, S. et al. J. Biol. Chem. (1997) 272(13): 8723-8730
5. Koolwijk, P. et al. J. Cell Biology (1996) 132(6): 1177-1188
6. Matsuo, A. et al. Neuroscience (1994) 60(1): 49-66
7. Djakiew, D. et al. Cancer Research (1991) 51(12): 3304-3310
8. Yamanishi, H. et al. Cancer Research (1991) 51(11): 3006-3010
9. Matsuzaki, K. et al. Japanese J. Cancer Research (1990) 81(4): 345-354
10. Kardami, E. et al. Growth Factors (1990) 4(1): 69-80
11. Riss, T.L. et al. J. Cellular Physiology (1989) 138(2): 405-414

112, 1

heparin binding domain

ANTICANCER RESEARCH *19*: 4039-4044 (1999)

Different Antitumor Activities of Anti-bFGF Neutralizing Antibodies: Heparin-Binding Domain Provides an Inefficient Epitope for Neutralization *in Vivo*

MASASHI AONUMA[1], YOSHINO YOSHITAKE[2], KATSUZO NISHIKAWA[2] and NORIKO G. TANAKA[1]

[1]New Product Research Laboratories IV, Daiichi Pharmaceutical Co., Ltd., 16-13, Kita-Kasai 1-Chome, Edogawa-ku, Tokyo 134; [2]Department of Biochemistry, Kanazawa Medical University, Uchinada, Ishikawa 920-02 Japan

Abstract. *Basic fibroblast growth factor (bFGF) plays an important role in tumor growth and angiogenesis. To elucidate the efficient recognition sites by anti-bFGF neutralizing antibodies, we generated two anti-bFGF neutralizing monoclonal IgG1 antibodies (mAbs), 2G11 and 1E6, recognizing different sites, and estimated as binding to the heparin-binding and the receptor-binding regions of bFGF, respectively, both of which have been shown to be important for its receptor interaction. Despite their high in vitro anti-bFGF activity in the absence of heparin, 2G11, with in vitro activity in competition with heparin, failed to inhibit the in vivo tumor growth of bFGF-producing RPMI4788 cells, though 1E6, showing non-competition with heparin, exhibited a significant antitumor effect. These results show that the heparin-binding domain of bFGF provides an inefficient epitope for in vivo neutralization of anti-bFGF mAb, and anti-bFGF neutralizing mAbs without competition against heparin have the potential to show in vivo antitumor effects.*

Basic fibroblast growth factor (bFGF) is one of a family of nine FGFs showing a wide spectrum of biological activities that include regulation of proliferation, migration and differentiation of a variety of cell types (1-3). All the family members are characterized by their high affinity for heparin and are functional ligands for FGF receptors which have intrinsic tyrosine kinase activity (2). It was shown that bFGF is isolated from a variety of tissues and cell lines including tumor cells (4) and exerts an angiogenic activity in different experimental models *in vitro* and *in vivo* (5). Therefore, bFGF is thought to play roles in the growth and angiogensis of solid tumors. Supporting this, we previously found that the tumorigenic and angiogenic potentials of various tumor cell lines correlated with the endothelial cell growth-stimulating activity due to bFGF, as well as to vascular endothelial growth factor (VEGF), all of which were produced by tumor cells (6). Even though bFGF lacks a leader sequence for secretion (7), the data suggest that bFGF is secreted from bFGF-producing cells by an alternative secretion pathway and acts through its binding to FGF receptors in both an autocrine and paracrine manner (8, 9). Several studies have indicated that the binding of bFGF to heparan sulfate proteoglycans on the cell surface should be important for its binding to FGF receptors (10-14) and that the heparin-binding domain of the FGF receptor and associated heparan sulfate proteoglycans are also essential for the binding of FGFs (15).

In several previous studies, monoclonal antibodies and polyclonal antibodies to bFGF inhibited *in vivo* solid tumor growth under defined experimental conditions (16-18). On the other hand, Dennis and Rifkin (19) reported that anti-bFGF rabbit polyclonal antibodies did not affect the in vivo solid tumor growth. To increase our understanding of the in vitro and in vivo biological action of bFGF, and to evaluate the efficient domain for the inhibition of bFGF action, we developed two anti-bFGF neutralizing mAbs, 2G11 and 1E6, that showed different anti-bFGF activity in the presence of heparin *in vitro*. The solid tumor growth of bFGF-producing human colorectal cancer cell line RPMI4788 cells implanted s.c. into nude mice has been reported to be inhibited by treatment with anti-bFGF neutralizing mAb designated bFM-1 (20). Using this solid tumor growth model, we identified different in vivo neutralizing activities of these mAbs, which may be associated with their different properties in competition with heparin.

Materials and Methods

Materials. Recombinant human bFGF and aFGF were purchased from

Correspondence to: Dr. Noriko Tanaka, New Product Research Laboratories IV, Daiichi Pharmaceutical Co., Ltd., 1-16-13, Kita-Kasai, Edogawa-ku, Tokyo 134, Japan. Tel: (81) 03-3680-0151, Fax: (81) 03-5696-4264, e-male: tanakatx@daiichipharm.co.jp.

Key Words: bFGF, neutralizing antibody, tumor angiogenesis, antitumor effect

0250-7005/99 $2.00+.40

UBI (Lake Placid, NY) and R & D Systems (Minneapolis, MN), respectively. The conditioned medium of the transformed clone, TC-1 cells, established by transfection of human hst-1 cDNA into BALB/c 3T3 cells (21) was used as a sample having endothelial cell growth-stimulating activity of recombinant human HST-1. Anti-bFGF neutralizing monoclonal antibody, 3H3 was purchased from Wako Junyaku (Osaka, Japan). Rabbit neutralizing polyclonal antibodies to bovine bFGF were purchased from R & D Systems: the antibodies cross-reacted with human bFGF. Heparin was from Daiichi Pure Chemicals Co., Ltd. (Tokyo, Japan), and Microwell ELISAmate was from KPL, Inc.(ML).

Animals. Female BALB/c mice and male athymic BALB/c nude mice were purchased from the Charles River Breeding Labs.(Tokyo, Japan) and the Shizuoka Laboratory Animal Center (Hamamatsu, Japan), respectively.

Cells and culture. Human colon cancer cell line, RPMI4788 (22, 23), was a generous gift from Dr. Akio Hizuta (First Department of Surgery, Okayama University Medical School, Okayama, Japan) and was maintained in RPMI1640 Medium supplemented with 10% fetal calf serum (FCS). To identify the growth factor activity derived from RPMI4788 cells, the medium was conditioned from confluent cultured cells for 3 days, and the cell extracts from 5 x 10^6 cells/ml were prepared by sonication. The mouse myeloma P3X63-Ag8.653 cells (American Type Culture Collection, Rockville, MO) were maintained in RPMI1640 medium supplemented with 10% FCS and 50 μM 2-mercaptoethanol. Human umbilical vein endothelial cells (HUVE cells) were purchased from Morinaga Institute of Biological Science (Kanagawa, Japan) and were cultured in 5% FCS-containing MCDB104 medium (Nissui Pharmaceutical Co., Ltd., Tokyo) with addition of 1% endothelial cell growth supplement solution (Nissui Pharmaceutical Co., Ltd.).

Generation of mAbs against bFGF. Female BALB/c mice were injected in the hind footpads with 40 μg of bFGF in Freund's complete adjuvant and boosted three times at 1-wk intervals by injection into the hind footpads with 10 μg of bFGF in saline. Three days after the final booster injection, the popliteal lymphocytes were fused with P3X63-Ag8.653 cells using 45% polyethylene glycol 1500. After selection in medium containing hypoxanthine, aminopterin and thymidine (HAT), culture supernatants of hybridomas were screened for anti-bFGF antibody activity by investigating the effect on the bFGF-induced HUVE cell proliferation, as described in the cell proliferation assay, and by an enzyme-linked immunosorbent assay (ELISA). Positive hybridomas were cloned by limiting dilution. These cell lines were implanted i.p. into male BALB/c nude mice and anti-bFGF mAbs were purified from ascites fluid by caprylic acid and ammonium sulfate precipitation (24).

Cell proliferation assay. HUVE cells and RPMI4788 cells (1000 cells/well) were plated on 96-well flat-bottomed microplates in each culture medium. After adhesion of the cells to the plates, various assay specimens were added into the culture simultaneously. After 4 days of the incubation, the growth of RPMI4788 cells was determined by counting the cells with a Coulter counter after trypsinization, and the growth of HUVE cells was measured by [3-(4,5-dimethylthiazol-2-yl)-2,5-diphenyl tetrazolium bromide] (MTT) assay (25). The absorbance at 540 nm determined by MTT assay was in good agreement with the HUVE cell growth and viability. The neutralizing activities of mAbs were expressed as the concentration causing a 50% inhibition of the growth of HUVE cells induced by bFGF (GI50).

ELISA. Nunc 96-well immunoplates (Nunc, Denmark) were coated with bFGF (100 ng/well) overnight at 4 °C. The plates were incubated with culture supernatants of hybridomas or various doses of purified mAbs, and the anti-bFGF antibody-binding to bFGF was detected using horse radish peroxidase (HRP)-conjugated goat anti-mouse IgG (KPL). The HRP reaction was measured by the increase in absorbance at 415 nm.

The effect of heparin on the binding of mAbs to bFGF was determined by sandwich ELISA. Briefly, the plates were coated with mAbs (2 μg/well) by incubating them overnight at 4°C. Then, the plates were incubated with 50 μl of 10 ng/ml of bFGF in the presence of various doses of heparin for 2 h at 25 °C. The amounts of bFGF bound to solid-phase mAbs were detected by rabbit polyclonal antibodies against bFGF, followed by the addition of HRP-conjugated goat anti-rabbit IgG (KPL). The bound HRP activity was measured as described above.

Treatment for tumor-bearing mice. RPMI4788 cells cultured in vitro (1 x 10^6 cells each) were implanted s.c. into groups of 12 nude mice on day 0. Appropriate mAbs were i.p. injected at a dose of 800 μg/0.2 ml/head, 1 day before implantation of the cells and on day 1, 5, 8, 11, 15, 18, 21 and 25. Tumor volume and body weight were measured twice a week for 29 days. The tumor volume was calculated using $L \times W^2/2$, where L and W respectively represent the length and the width of the tumor mass, measured with a caliper.

Results

Characterization of anti-bFGF mAbs. Two anti-bFGF immunoneutralizing mAbs, designated 2G11 and 1E6, and one nonneutralizing mAb, 2C2, were selected by ELISA and bioassay using HUVE cells from an original pool of hybridoma cultures. All of these mAbs belonged to IgG1 isotype and showed almost the same binding abilities to bFGF on ELISA (Figure 1A). 2G11 and 1E6 inhibited the bFGF-induced HUVE cell proliferation in the same dose-dependent manner, giving GI50 values of about 0.5 μg/ml, whereas 2C2 showed no effect even at a concentration of 100 μg/ml (Figure 1B). These mAbs had no inhibitory effects on the HUVE cell proliferation induced by aFGF or HST-1, both of which belong to the FGF family. When 2G11 and 1E6 were added together to HUVE cells, the neutralizing activity was synergistically enhanced with GI50 values of 0.04 μg/ml (Figure 1B).

Effects of heparin on the neutralizing and binding abilities of anti-bFGF mAbs. To assess whether these mAbs recognize the heparin-binding domain of bFGF, the effects of heparin on their neutralizing activity were examined. The bFGF-induced HUVE cell proliferation was not affected by the addition of 10 μg/ml of heparin, while heparin inhibited the proliferation at the GI50 values of 76 μg/ml. Ten μg/ml of heparin reduced the neutralizing activity of 2G11, giving more than 10-fold increase in GI50 values (Figure 2, Table I). The combination inhibitory effect of 2G11 and 1E6 on bFGF-induced HUVE cell proliferation was also reduced by heparin (Figure 2). On the contrary, the neutralizing activity of 1E6 was enhanced approximately 3-fold in the presence of 10 μg/ml of heparin (Figure 2, Table I).

The effect of heparin on the ability of these mAbs to bind to bFGF was then examined by sandwich ELISA. Heparin reduced the binding ability of solid-phase 2G11 to bFGF dose-dependently from concentrations as low as 2 μg/ml but did not affect that of 1E6 even at a concentration of 500 μg/ml (Figure 3).

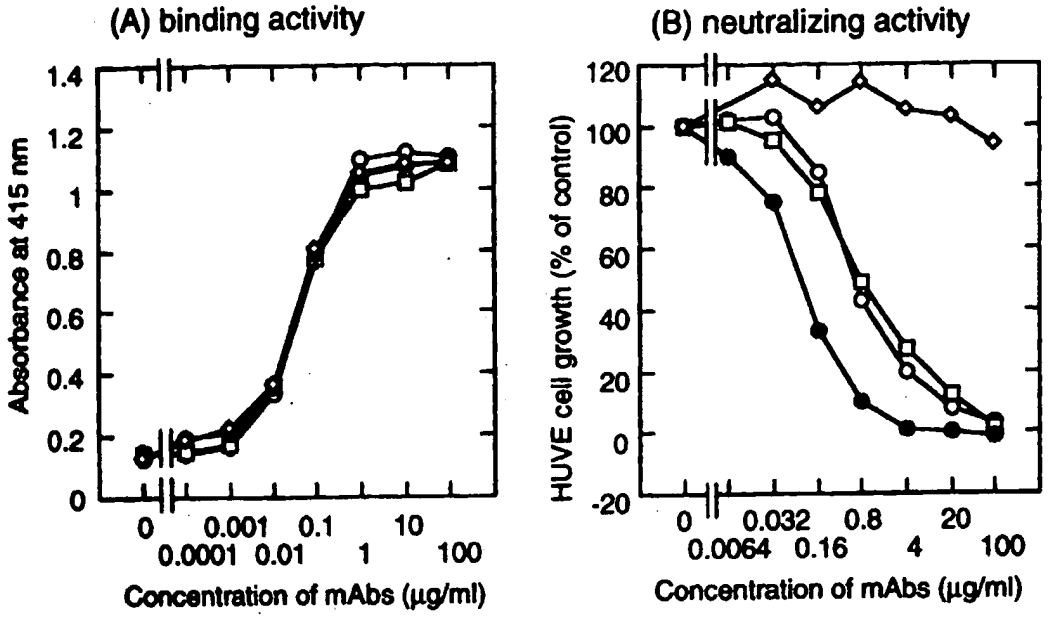

Figure 1. *Binding activity (A) and neutralizing activity (B) of anti-bFGF mAbs toward bFGF. (A) Each mAb was serially diluted and bound to solid-phase bFGF. The HRP reaction measured at 415 nm qualified the binding ability to bFGF of mAbs. (B) HUVE cells were incubated with 1 ng/ml of bFGF in the presence of various concentrations of mAbs for 4 days, and the HUVE cell growth was measured by MTT assay. The results are presented as percentages of the growth induced by bFGF in the absence of mAbs. Anti-bFGF mAb: 2G11 (○); 1E6 (□); 2G11/1E6 (1:1 mixture of 2G11 and 1E6) (●); and 2C2 (◇).*

In vitro effects of anti-bFGF mAbs against RPMI4788. The cell extract of RPMI4788 cells (5 x 10^6 cells/ml) stimulated the growth of HUVE cells in a dose-dependent manner, reaching saturation around 10% of the cell extract, but the conditioned medium did not (Figure 4A). The apparent reduction of growth factor activity for HUVE cells was observed in the presence of 20% of the cell extract (Figure 4A). The sandwich ELISA for bFGF demonstrated that about 15 ng/5 x 10^6 cells/ml of bFGF was contained in the cell extracts, but less than 0.04 ng/ml of bFGF was found in the conditioned medium. Both 2G11 and 1E6 prevented the HUVE cell proliferation induced by 10% RPMI4788 cell extract with complete inhibition at 1 μg/ml of each anti-bFGF mAb, and a synergistic inhibitory effect of the combination of these mAbs was also observed (Figure 4B). On the other hand, the in vitro growth rate of RPMI4788 cells was not affected by the exogenous addition of bFGF (data not shown), and these mAbs did not inhibit the RPMI4788 cell growth even at a concentration of 100 μg/ml (Figure 4C).

In vivo antitumor effects of anti-bFGF mAbs against RPMI4788. The administrations of 1E6 significantly ($p<0.001$) inhibited the *in vivo* solid tumor growth of RPMI4788 cells implanted s.c. into nude mice (Figure 5). In contrast, the same treatment with 2G11 had almost no antitumor effect, similar to that of nonneutralizing anti-bFGF mAb, 2C2 (Figure 5). The antitumor effect of the 2G11 and 1E6 combination was almost similar to that of 1E6 alone (Figure 5). The body weight of the mice was not affected by the administrations of these mAbs.

Discussion

Our two generated IgG1 isotype mAbs, 2G11 and 1E6, showed similar high neutralizing activity toward bFGF-induced HUVE cell proliferation in the absence of heparin. These mAbs did not affect the HUVE cell proliferation induced by the other two FGF family proteins, aFGF and HST-1, both of which have highly conserved homologous amino acid sequences with bFGF (1). Therefore, the effect of these mAbs is to block specifically the biological activity of bFGF. The combination of these mAbs exhibited a synergistic inhibitory effect on the bFGF-induced HUVE cell proliferation, suggesting that they recognize different sites essential for the receptor-binding of bFGF. In the presence of heparin, these mAbs had different neutralizing and binding properties toward bFGF: the addition of heparin reduced the activity of 2G11 but not 1E6. The recognition site of 2G11 might be the same or adjacent to the heparin-binding site of bFGF, and heparin should act as a competitor for the binding of 2G11 to bFGF. In contrast, the recognition site of 1E6

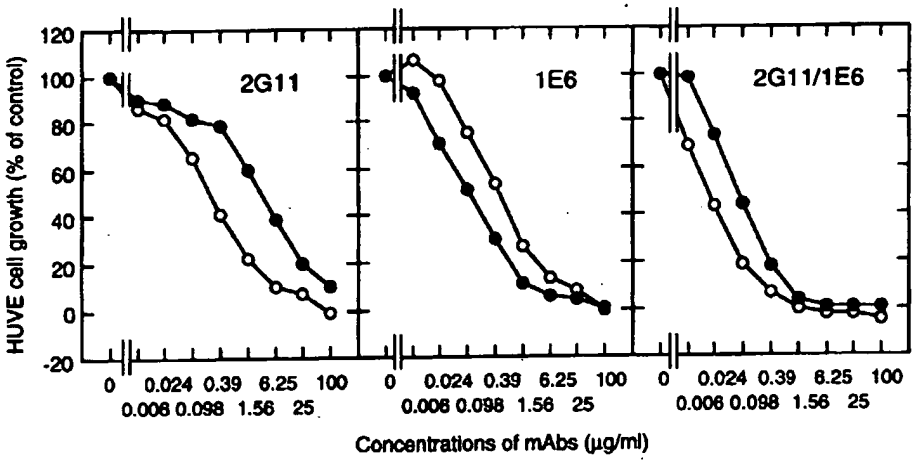

Figure 2. *Effects of heparin on neutralizing activities of anti-bFGF mAbs. HUVE cells were incubated with 1 ng/ml of bFGF and various concentrations of mAbs in the absence (○) or presence (●) of 10 μg/ml heparin for 4 days, and then the HUVE cell growth was measured by MTT assay. The results are presented as percentages of the growth induced by bFGF in the absence of mAbs, and each point is the mean of triplicate wells (SE < 5%).*

Table I. *Characteristics of anti-bFGF neutralizing mAbs.*

mAbs	Neutralizing activity[a] in vitro, GI50 (μg/ml)		Reduction of binding of[b] mAbs to bFGF by	Anti-tumor activity[c] in vivo
	heparin(-)	heparin(+)	heparin	
2G11	0.30	3.53	+	−
1E6	0.37	0.14	−	+
bFM-1	0.03	0.02	−	+
3H3	0.11	0.06	−	+

[a] The concentration of a mAb required to inhibit half the growth of HUVE cells induced by bFGF in the absence (-) or presence (+) of 10 μg/m heparin: GI50 values for 2G11 and 1E6 are mean values of two independent experiments.

[b] Effects of heparin on binding of mAbs to bFGF, determined by sandwich ELISA as shown in Figure 3: +, reduced by heparin; −, not reduced by heparin.

[c] Effects of mAbs on sold tumor growth in vivo: +, significant inhibitory effects present; −, inhibitory effects not present.

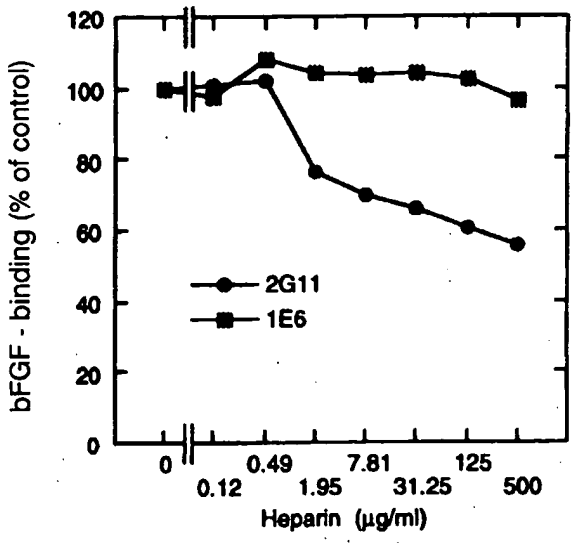

Figure 3. *Effect of heparin on the binding of anti-bFGF mAbs to bFGF. The binding of solid-phase anti-bFGF mAbs to bFGF (10 ng/ml), in the presence of serially diluted heparin, was determined by sandwich ELISA. The results are presented as percentages of the binding of mAbs to bFGF in the absence of heparin.*

might be present within the receptor-binding site of bFGF, where heparin does not compete. For efficient interaction between bFGF and its receptor, heparan sulfate proteoglycans on the cell surface have been shown to be essential, and it has been reported that the FGF receptor should be a ternary complex of heparan sulfate proteoglycan, tyrosine kinase transmembrane glycoprotein, and ligand (10-12, 14, 15). Therefore, both the heparin-binding domain and the receptor-binding domain of bFGF must be important for its binding to FGF receptors. The synergistic inhibitory effect of the combination of 2G11 and 1E6 might be due to their different recognition sites, the heparin-binding region and the receptor-binding region, respectively.

In spite of the same high neutralizing activity of 2G11 and

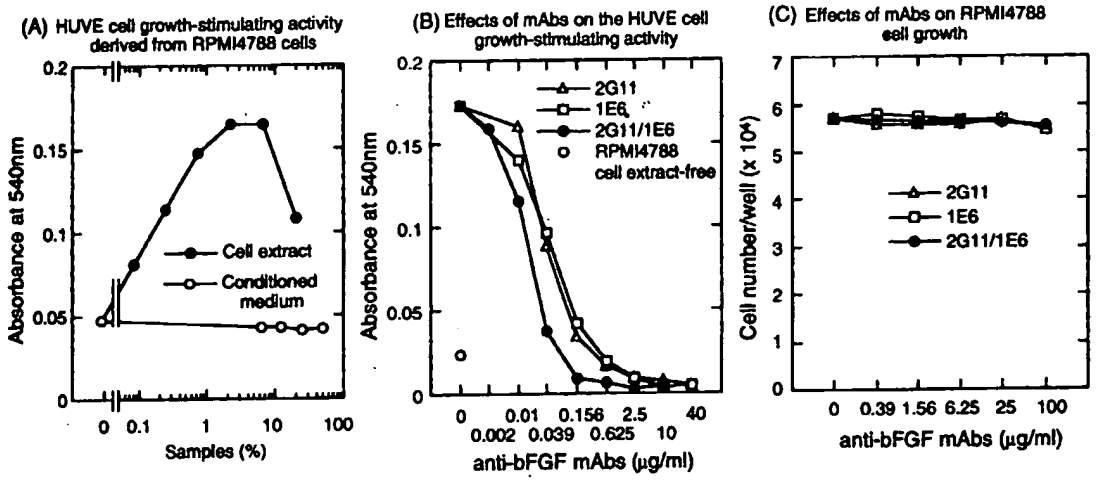

Figure 4. *HUVE cell-growth stimulating activity derived from RPMI4788 cells (A), and effects of anti-bFGF mAbs on the HUVE cell growth induced by RPMI4788 cell extract (B) and on the growth of RPMI4788 cells (C). (A, B) HUVE cell growth induced by cell extract or conditioned medium from RPMI4788 cells, in the absence or presence of mAbs, was measured by MTT assay. (C) RPMI4788 cell growth in the presence of mAbs was determined by counting the cell number with a Coulter counter.*

1E6 toward bFGF derived from RPMI4788 cells *in vitro*, the *in vivo* effects of these mAbs on the growth of RPMI4788 cells were extremely different. The administrations of 2G11 could not inhibit the solid tumor growth of RPMI4788 cells, though the same treatment of 1E6 showed a significant antitumor effect. It is considered that the anti-bFGF mAb recognizing heparin-binding region, such as 2G11, might compete in its binding to bFGF with heparan sulfate and heparin existing abundantly *in vivo*, which should cause a decrease in its neutralizing activity *in vivo*, as observed in the *in vitro* assays for 2G11. Therefore, it is possible that the *in vivo* neutralizing activity of anti-bFGF mAbs is dependent on their recognition sites on bFGF, characterized by their different responses to heparin. In support of this, we found that bFM-1 (20) and 3H3 (18), both of which have been reported to inhibit *in vivo* tumor growth under defined experimental conditions, also did not compete with heparin in the *in vitro* assays, as observed for 1E6 (Table I). These results suggest that anti-bFGF neutralizing mAbs, recognizing a heparin-non-competing region, are able to exert their neutralizing activity efficiently in vivo as well as *in vitro*.

Dennis and Rifkin (19) reported that their anti-bFGF rabbit polyclonal antibodies failed to inhibit *in vivo* tumor growth even in the experiment using the same tumor cells as those used by Baird *et al* (16). The discrepancy between those results might be caused by the difference in recognition sites of the antibodies used in each experiment: anti-bFGF polyclonal antibodies, the majority of which recognize the heparin-binding region on bFGF, might have no *in vivo* antitumor effect, as observed for 2G11 in our study.

We found that the neutralization by 1E6 of bFGF activity

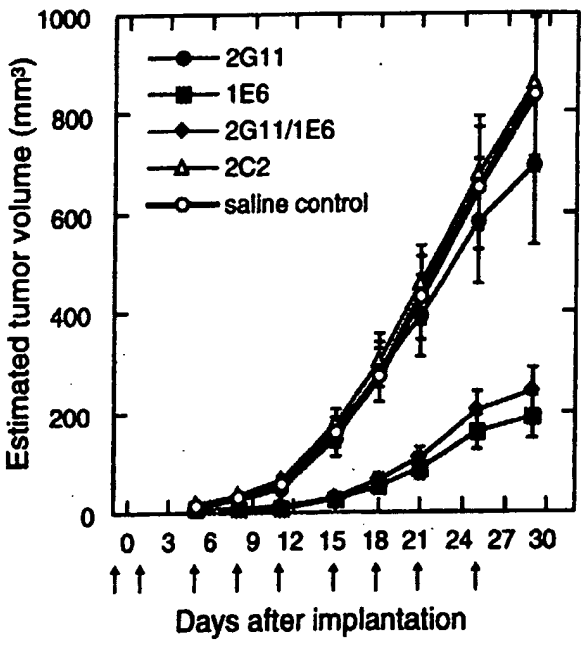

Figure 5. *Effects of anti-bFGF mAbs on the tumor growth of RPMI4788 cells implanted s.c. into nude mice. RPMI4788 cells (1x10⁶ cells each), cultured in vitro, were implanted s.c. into groups of 12 nude mice on day 0. Either of each mAb, a mixture of 2G11 and 1E6 (2G11/1E6) or saline was injected into the mice i.p., beginning 1 day before implantation of the cells, and on days 1, 5, 8, 11, 15, 18, 21 and 25 (800 μg/mouse/day). The tumor size was measured with calipers on the indicated days. The points are the mean ± SE of 12 mice.*

derived from RPMI4788 cells resulted in the inhibition of their solid tumor growth, consistent with the results obtained in the study using the other anti-bFGF mAb, bFM-1 (20), which also did not compete with heparin. RPMI4788 cells produced bFGF, but did not efficiently secrete it from the cells, supported by the observation that bFGF lacks a classical signal sequence for secretion (7). Even though the mechanism of bFGF release is unclear, the inhibition of the solid tumor growth of RPMI4788 cells by treatment with these mAbs supports the hypothesis that bFGF is released in vivo and plays an important role in solid tumor growth. Because 1E6 did not show a direct inhibitory effect on *in vitro* RPMI4788 cell growth, bFGF produced by them may contribute to the induction of angiogenesis *in vivo* in a paracrine manner, which is essential for solid tumor growth (26).

These two anti-bFGF neutralizing mAbs, 2G11 and 1E6, recognizing different sites, heparin and receptor-binding sites, respectively, should be potential tools to understand the structural and functional relationship of bFGF with its receptor and heparan sulfate proteoglycan. Furthermore, 1E6 which shows neutralizing activity *in vitro* and *in vivo* should be valuable in determining the role of bFGF in solid tumor progression, and may be useful in the therapy of angiogenic solid tumors for which bFGF is the major angiogenic mediator. In addition, this study also suggests that the receptor-binding site of bFGF where heparin does not compete may be an effective target of a bFGF inhibitor for the prevention of bFGF action *in vivo*.

Acknowledgements

We thank Dr. Y. Iigo, Ms. C. Hattori and Ms. T. Higashida for advice and technical support in the generation of mAbs against bFGF.

References

1 Basilico C and Moscatelli D: The FGF family of growth factors and oncogenes. Adv Cancer Res *59:* 115-165, 1992.

2 Hughes SE and Hall PA: The fibroblast growth factor and receptor multigene families. J Pathol *170:* 219-221, 1993.

3 Rifkin DB and Moscatelli D: Recent developments in the cell biology of basic fibroblast growth factor. J Cell Biol *109:* 1-6, 1989.

4 Gospodarowicz D, Ferrara N, Schweigerer L and Neufeld G: Structural characterization and biological functions of fibroblast growth factor. Endocrine Rev *8:* 95-114, 1987.

5 Folkman J and Shing Y: Angiogenesis. J Biol Chem *267:* 10931-34, 1992.

6 Aonuma M, Iwahana M, Nakayama Y, Hirotani K, Hattori C, Murakami K, Shibuya M and Tanaka NG: Tumorigenicity depends on angiogenic potential of tumor cells: dominant role of vascular endothelial growth factor and/or fibroblast growth factors produced by tumor cells. Angiogenesis *2:* 57-66, 1998.

7 Abraham JA, Mergia A, Whang JL, Tumolo A, Friedman J, Hjerrild KA, Gospodarowicz D and Fiddes JC: Nucleotide sequence of a bovine clone encoding the angiogenic protein, basic fibroblast growth factor. Science *233:* 545-8, 1986.

8 Coltrini D, Gualandris A, Nelli EE, Parolini S, Molinari-Tosatti MP, Quarto N, Ziche M, Giavazzi R and Presta M: Growth advantage and vascularization induced by basic fibroblast growth factor over-expression in endometrial HEC-1-B cells: an export-dependent mechanism of action. Cancer Res *55:* 4729-38, 1995.

9 Mignatti P, Morimoto T and Rifkin DB: Basic fibroblast growth factor released by single, isolated cells stimulates their migration in an autocrine manner. Proc Natl Acad Sci USA *88:* 11007-11011, 1991.

10 Mansukhani A, Dell'era P, Moscatelli D, Kornbluth S, Hanafusa H and Basilico C: Characterization of the murine BEK fibroblast growth factor (FGF) receptor: activation by three members of the FGF family and requirement for heparin. Proc Natl Acad Sci USA *89:* 3305-3309, 1992.

11 Ornitz DM, Yayon A, Flanagan JG, Svahn CM, Levi E and Leder P: Heparin is required for cell-free binding of basic fibroblast growth factor to a soluble receptor and for mitogenesis in whole cells. Mol Cell Biol *12:* 240-247, 1992.

12 Rapraeger A, Krufka A and Olwin BB: Requirement of heparan sulfate for bFGF-mediated fibroblast growth and myoblast differentiation. Science *252:* 1705-1708, 1991.

13 Savona C, Chambaz EM and Feige JJ: Proteoheparan sulfates contribute to the binding of basic FGF to its high affinity receptors on bovine adrenocortical cells. Growth Factors *5:* 273-82, 1991.

14 Yayon A, Klagsbrun M, Esko JD, Leder P and Ornitz DM: Cell surface heparin-like molecules are required for binding of basic fibroblast growth factor to its high affinity receptor. Cell *64:* 841-848, 1991.

15 Kan M, Wang F, Xu J, Crabb JW, Hou J and McKeehan WL: An essential heparin-binding domain in the fibroblast growth factor receptor kinase. Science *259:* 1918-1921, 1993.

16 Baird A, Mormede P and Bohlen P: Immunoreactive fibroblast growth factor (FGF) in a transplantable chondrosarcoma: inhibition of tumor growth by antibodies to FGF. J Cell Biochem *30:* 79-85, 1986.

17 Gross JL, Herblin WF, Dusak BA, Czerniak P, Diamond MD, Sun T, Eidsvoog K, Dexter DL and Yayon A: Effects of modulation of basic fibroblast growth factor on tumor growth in vivo. J Natl Cancer Inst *85:* 121-31, 1993.

18 Hori A, Sasada R, Matsutani E, Naito K, Sakura Y, Fujita T and Kozai Y: Suppression of solid tumor growth by immunoneutralizing monoclonal antibody against human basic fibroblast growth factor. Cancer Res *51:* 6180-4, 1991.

19 Dennis PA and Rifkin DB: Studies on the role of basic fibroblast growth factor *in vivo*: inability of neutralizing antibodies to block tumor growth. J Cell Physiol *144:* 84-98, 1990.

20 Nishikawa K and Yoshitake Y: submitted.

21 Aonuma M, Murakami K, Hirotani K, Horiuchi T, Sakamoto H, Terada M and Tanaka NG: *In vivo* malignant phenotype of hst-1-transfected cells regulated by paracrine endothelial cell growth stimulation by HST-1. Angiogenesis 2: 143-152, 1998.

22 Moore GE and Koike A: Growth of human tumor cells in vitro and in vivo. Cancer *17:* 11-20, 1964.

23 Naomoto Y, Kondo H, Tanaka N and Orita K: Novel experimental models of human cancer metastasis in nude mice: lung metastasis, intraabdominal carcinomatosis with ascites, and liver metastasis. J Cancer Res Clin Oncol *113:* 544-549, 1987.

24 Russo C, Callegaro L, Lanza E and Ferrone S: Purification of IgG monoclonal antibody by caprylic acid precipitation. J Immunol Methods *65:* 269-271, 1983.

25 Mitsui I, Kumazawa E, Hirota Y, Aonuma M, Sugimori M, Ohsuki S, Uoto K, Ejima A, Terasawa H and Sato K: A new water-soluble camptothecin derivative, DX-8951f, exhibit potent antitumor activity against human tumors *in vitro* and *in vivo*. Jpn J Cancer Res *86:* 776-782, 1995.

26 Folkman J: What is the evidence that tumors are angiogenesis dependent? J Natl Cancer Inst *82:* 4-6, 1990.

Received February 15, 1999
Accepted May 10, 1999

STIC-ILL

RC261.A1 J36

335309

2380483

From: Holleran, Anne
Sent: Sunday, March 04, 2001 5:30 PM
To: STIC-ILL
Subject: refs. for 09/266,543

Examiner: Anne Holleran
Art Unit: 1642; Rm 8E03
Phone: 308-8892
Date needed by: ASAP

Please send me copies of the following :

1. Plum, S.M. et al. Vaccine, (2000) 19/9-10, 1294-1303
2. Aonuma, M. et al. Anticancer Res. (1999, Oct) 19(5B): 4039-4044
3. Muller, Y.A. et al. Structure (1998) 6(9): 1153-1167
4. Yamagishi, S. et al. J. Biol. Chem. (1997) 272(13): 8723-8730
5. Koolwijk, P. et al. J. Cell Biology (1996) 132(6): 1177-1188
6. Matsuo, A. et al. Neuroscience (1994) 60(1): 49-66
7. Djakiew, D. et al. Cancer Research (1991) 51(12): 3304-3310
8. Yamanishi, H. et al. Cancer Research (1991) 51(11): 3006-3010
9. Matsuzaki, K. et al. Japanese J. Cancer Research (1990) 81(4): 345-354
10. Kardami, E. et al. Growth Factors (1990) 4(1): 69-80
11. Riss, T.L. et al. J. Cellular Physiology (1989) 138(2): 405-414

112, 1
unpredictability

Jpn. J. Cancer Res. 81, 345–354, April 1990

Production of Basic Fibroblast Growth Factor-like Factor by Cultured Human Cholangiocellular Carcinoma Cells

Kouichi Matsuzaki,[1] Yoshino Yoshitake,[2] Miki Miyagiwa,[1] Masami Minemura,[1] Michio Tanaka,[1] Hiroshi Sasaki[1] and Katsuzo Nishikawa[2,3]

[1]*Third Department of Internal Medicine, Toyama Medical and Pharmaceutical University, 2630 Sugitani, Toyama 930-01 and* [2]*Department of Biochemistry, Kanazawa Medical University, Uchinada, Ishikawa 920-02*

An extract of cultured human cholangiocellular carcinoma cells (HuCC-T1) was found to contain high mitogenic activity for BALB/c3T3 cells. The growth factor eliciting most of the mitogenic activity was purified and concluded to be identical with basic fibroblast growth factor (bFGF)-like factor on the basis of its molecular weight and heparin-Sepharose elution profile, and the results of immunoblotting and radioimmunoassay. HuCC-T1 cells also secreted bFGF-like factor into serum-free medium. A combination of insulin and transferrin or bovine serum albumin stimulated the growth of HuCC-T1 cells in serum-free medium. However, bFGF did not stimulate their growth in the presence and absence of these supplements. Neutralizing monoclonal antibody against bFGF did not inhibit growth. These results indicate that bFGF-like factor is not a growth factor for this cell line.

Key words: Basic fibroblast growth factor — Human cholangiocellular carcinoma

The development of new capillaries is important in the growth of solid tumors.[1] One growth factor stimulating tumor angiogenesis is thought to be FGF,[4] which is produced by tumor cells.[2,3] The FGF family are potent mitogens for a wide variety of mesoderm- and neuroectoderm-derived cells including endothelial cells and have been isolated from a variety of tissue and cell sources including tumor cells.[4,5] These factors can be grouped into two closely related classes, bFGF and aFGF. FGF exerts its biological response *in vitro* through high-affinity cell surface receptors.[5]

Transformed cells in culture acquire the ability to proliferate with little or no exogenous growth factor(s).[6] This phenomenon has been explained by the "autocrine hypothesis," which proposes that growth factors produced by the transformed cells act on their own cells via external receptors.[7,8] In support of this hypothesis, there are some reports that transformed cells secrete growth factors stimulating their own growth[9–11] and that specific antibodies against these growth factors or growth factor receptors inhibit growth of transformed cells.[12–14]

A serum-free culture system is useful in studies on the mechanisms controlling cell growth and the effects of growth factors.[15] We established a human cholangiocellular carcinoma cell line (HuCC-T1) that can grow in serum-free medium.[16] The present paper reports that a bFGF-like factor is present in HuCC-T1 cells and is also secreted from the cells, but that this factor, or neutralizing monoclonal antibody against bFGF that blocks its biological activity, does not affect the growth of these cells. On the other hand, a combination of insulin and transferrin or bovine serum albumin (BSA) stimulated the growth of these cells in serum-free medium.

MATERIALS AND METHODS

Cells and culture A human cholangiocellular carcinoma cell line (HuCC-T1) was established as described previously.[16] The stock culture was maintained in Coon's modified Ham's F12 medium (C-F12) supplemented with 15 m*M* HEPES (pH 7.3), 100 units/ml penicillin, 100 μg/ml streptomycin and 3% calf serum (CS). The BALB/c3T3-3K cell line[17] was used for assay of the activity of bFGF stimulating DNA synthesis. The cells were cultured in Dulbecco's modified Eagle's medium (DME) containing 10% CS and all the other supplements described above. Bovine capillary endothelial (BCE) cells were isolated from bovine brain cortex and maintained as described by Goetz *et al.*[18] with slight modifications. The cells were cultured in RPMI 1640 medium supplemented with 10% fetal calf serum (FCS), 1 ng/ml bFGF and all the other supplements described above in dishes that had been coated with type-IV collagen (Sigma, St. Louis, MO), and were used for growth experiments at passages 5–9. All these cells were cultured at 37°C in a humidified atmosphere of 5% CO_2 in air.

[3] To whom correspondence and requests for reprints should be addressed.

[4] Abbreviations used: FGF, fibroblast growth factor; bFGF, basic fibroblast growth factor; aFGF, acidic fibroblast growth factor; MAb, monoclonal antibody; BCE cells, bovine capillary endothelial cells; BSA, bovine serum albumin; PBS, phosphate-buffered saline.

Assay of DNA synthesis The activity of bFGF to stimulate DNA synthesis of cultured BALB/c3T3-3K cells was assayed as described previously.[17, 19] One unit of activity was defined as the amount equivalent to 1 mg of CS proteins in stimulating the incorporation of [^{3}H]-thymidine into DNA.

Growth experiments BCE cells were plated at a density of 2×10^4 in 5 ml of serum-free C-F12 medium in 60-mm Falcon dishes that had been coated with type-IV collagen. bFGF or test samples were added at the time of inoculation and on day 3. After 5 days, the cells were harvested by trypsinization and counted in a Coulter counter. HuCC-T1 cells were plated at a density of 2×10^4 in 5 ml of serum-free C-F12 medium in 60-mm Falcon dishes that had been coated with poly-D-lysine. Test samples were added only at the time of inoculation of the cells. After 5 days, cells were harvested by trypsinization and counted in a Coulter counter. Values are given as averages for duplicate experiments.

Purifications of bFGF and aFGF bFGF and aFGF were purified from bovine brain by the method of Gospodarowicz *et al.*[20] involving ammonium sulfate precipitation, and chromatographies on carboxymethyl (CM)-Sephadex and heparin-Sepharose. aFGF was further purified by cation-exchange HPLC on a Protein Pak G-SP column (8.2×75 mm) (Nihon Waters, Tokyo). The fractions eluted from the column with 0.35 *M* NaCl/50 m*M* sodium phosphate buffer (pH 6.8)/0.1% 3-[(3-cholamidopropyl)dimethylammonio]-1-propane sulfonate (CHAPS),[21, 22] which gave a single protein peak with DNA synthesis-stimulating activity, were collected. Protein concentrations of FGFs were determined with a Bicinchoninic Acid (BCA) kit (Pierce, Rockford, IL) with BSA as a standard.

Analysis of DNA synthesis-stimulating activities in cell extract (HuCC-T1-CE) and conditioned medium (HuCC-T1-CM) of HuCC-T1 cells For analysis of the mitogenic activities in HuCC-T1-CE and HuCC-T1-CM, their elution profiles on heparin affinity chromatography were examined.[21, 23] Confluent HuCC-T1 cells in 150-mm dishes were washed with protein-free C-F12 medium for 1 day and maintained in 20 ml of the medium for 4 days, and then the conditioned medium and cells were collected. The viability of the cells was more than 99%, as assessed by the trypan blue exclusion test. A crude extract of 10^7 HuCC-T1 cells in 2 ml of 10 m*M* Tris-HCl buffer (pH 7.5) and 15 ml of conditioned medium were applied to TSK Heparin-5PW HPLC columns (7.5×75 mm), which had previously been equilibrated with 10 m*M* Tris-HCl (pH 7.5) containing 0.5 *M* NaCl and 0.1% CHAPS. The columns were washed with 20 ml of the buffer and developed with a linear gradient of 0.5–2.0 *M* NaCl in the same buffer for 1 h at a flow rate of 0.8 ml/min. Fractions of 1.6 ml were collected and aliquots were assayed for stimulation of DNA synthesis in BALB/c3T3 cells as described above.

Purification of bFGF-like factor from cell extract (HuCC-T1-CE) and conditioned medium (HuCC-T1-CM) of HuCC-T1 cells A bFGF-like factor from HuCC-T1-CE was prepared by the methods of Schweigerer *et al.*[3] and Klagsbrun *et al.*[24] with some modifications. Briefly, 10^9 HuCC-T1 cells were harvested from monolayer cultures by trypsinization. The cells were suspended in 100 ml of 2 *M* NaCl/10 m*M* Tris-HCl (pH 7.5) containing 1 μg/ml leupeptin, 400 μ*M* pepstatin (both from The Peptide Institute Inc., Osaka), 1 m*M* phenylmethylsulfonyl fluoride (Sigma), 1 m*M* N-ethylmaleimide and 5 m*M* EDTA (both from Wako, Osaka). The cells were homogenized in a Potter-Elvehjem homogenizer for 3 min. The homogenate was centrifuged at 27,000*g* for 20 min, and the supernatant was dialyzed overnight against water to lower the concentration of NaCl to below 0.15 *M*. The dialyzed HuCC-T1-CE was adjusted to pH 6.0 and applied to a CM-Sephadex C-50 column (5×5 cm) (Pharmacia, Uppsala) that had been equilibrated with 0.1 *M* sodium phosphate buffer (pH 6.0). Material was then eluted stepwise with 0.1 *M* sodium phosphate buffer containing 0.15 *M* and 0.65 *M* NaCl. The material eluted with 0.65 *M* NaCl was applied to a heparin-Sepharose column (1.4×5 cm) (Pharmacia) that had been equilibrated with 0.65 *M* NaCl/10 m*M* Tris-HCl (pH 7.5)/0.1% CHAPS. The column was washed with about 5 column volumes of the same solution, and adsorbed material was then eluted with 500 ml of a linear gradient of 0.65–2.0 *M* NaCl in 10 m*M* Tris-HCl (pH 7.5)/0.1% CHAPS at a flow rate of 30 ml/h. Fractions of 10 ml were collected and tested for DNA synthesis-stimulating activity. The active fractions were combined, dialyzed against water and lyophilized. The powder was dissolved in 0.1% BSA/PBS and used for assays of biological activities and for immunological analyses. All operations were performed at about 4°C.

A bFGF-like factor from HuCC-T1-CM was prepared by the method of Schweigerer *et al.*[3] with some modifications. Briefly, HuCC-T1 cells were cultured in 850-cm^2 Falcon roller bottles with 100 ml of C-F12 containing 3% CS. After the cells had reached confluency (10^8 cells/bottle), they were washed with 100 ml of protein-free C-F12 for 1 day, and then the medium was replaced by 100 ml of fresh protein-free medium every 3 days for 2 weeks. The conditioned medium was clarified by centrifugation at 27,000*g* for 20 min and the resulting supernatant was stored at −20°C until use. Two liters of the conditioned medium was thawed, adjusted to pH 4.5 and stirred for 1 h at 4°C. Then it was centrifuged at 27,000*g* for 20 min, and the supernatant was adjusted to pH 6.0 and dialyzed overnight against water. After centrifugation at 27,000*g* for 20 min, the conditioned

medium was mixed with 300 ml of a packed suspension of CM-Sephadex C-50 in 0.1 *M* sodium phosphate buffer (pH 6.0). The suspension was stirred for 24 h and then poured into a column. The applied material was eluted from CM-Sephadex and purified by heparin-Sepharose chromatography as described for bFGF from the cell extract.

SDS-PAGE SDS-PAGE was performed by the method of Laemmli[25] in 19.5% polyacrylamide slab gel and protein bands were located with silver stain.

Immunoblots Proteins were separated by electrophoresis on SDS-12.5% polyacrylamide gel and then transferred electrophoretically to a nitrocellulose sheet. The nitrocellulose sheet was incubated first in blocking buffer (5% BSA/PBS) and then for 30 min with MAb against bFGF (bFM-2; 10 μg/ml)[26] diluted with washing buffer (0.1% Tween 20/PBS). The sheet was washed 4 times for 4 min each time with washing buffer and incubated with 500 ng/ml of biotinylated rabbit anti-mouse IgG (Vector Laboratories, Inc. Burlingame, CA) in PBS for 30 min. It was then washed again with washing buffer and incubated with horseradish peroxidase-avidin conjugate according to the manufacturer's instructions (Vector Laboratories, Inc.). The sheet was then washed extensively with washing buffer and the peroxidase activity was located with diaminobenzidine tetrahydrochloride.

Radioimmunoassay (RIA) Purified bovine bFGF was labeled with ^{125}I by the chloramine-T method and purified by heparin-Sepharose affinity chromatography.[26] The reaction mixture for RIA (0.5 ml) in a tube (Eiken, Tokyo) consisted of 0.35 ml of 0.1 *M* sodium phosphate buffer (pH 7.4)/0.02% NaN_3, 0.05 ml of 4 ng/ml ^{125}I-bFGF (8,000–15,000 cpm) in 0.1% BSA/PBS/0.02% NaN_3, 0.05 ml of unlabeled sample at an appropriate concentration in 0.1% BSA/PBS/0.02% NaN_3, and 0.05 ml of MAb against bFGF (bFM-1; 0.12 μg/ml)[26] in 0.1% BSA/PBS/0.02% NaN_3. After incubation overnight at 4°C, 0.1 ml of 1% normal mouse serum in PBS/0.02% NaN_3 and 0.1 ml of 0.77 mg/ml goat anti-mouse immunoglobulins (Dako, Glostrup) were added, and the incubation was continued for 4 h at 4°C. After addition of 1 ml of 0.2% PEG 6,000 (Nakarai Chemicals, Kyoto) the radioactivity bound to the antibody was precipitated by centrifugation and counted in an Aloka auto-well gamma system (ARC-300).

Other materials MAbs against bFGF[26] (bFM-1 and bFM-2) and hEGF (HA)[27] were obtained as described previously. Media and sera were products of Flow Lab. Inc., North Ryde, CA. Na^{125}I was obtained from the Radiochemical Centre, Amersham. Poly-D-lysine, human transferrin, defatted BSA and bovine insulin were obtained from Sigma.

RESULTS

Isolation of bFGF-like factor from HuCC-T1-CE and -CM We examined the activities to stimulate DNA synthesis in BALB/c3T3 cells of extracts of various cultured human tumor cell lines established from tumors of digestive organs, including hepatocellular carcinoma, pancreatic cancer and cholangiocellular carcinoma. HuCC-T1 cells, originating from a cholangiocellular carcinoma, had 3 to 60 times higher activity than the other cell lines examined (unpublished result). We then attempted to identify the growth factor showing this activity in an extract of the HuCC-T1 cells and also in conditioned medium obtained by culture of the cells in protein-free medium. The conditioned medium collected after maintaining 10^7 cells for 4 days in a 150-mm dish showed the activity stimulating DNA synthesis in BALB/c3T3-3K cells, when 10 μl of the conditioned medium was added to the medium for the assay. Its activity corresponded to 80 units/ml or 1.6 ng of bovine bFGF/ml when calculated on the basis of specific activity of purified bovine bFGF (5×10^7 units/mg protein). To analyze these activities, we subjected the cell extract and the conditioned medium to heparin-5PW HPLC column chromatography. As summarized in Table I, the

Table I. Distribution of Activities to Stimulate DNA Synthesis in BALB/c3T3 Cells in an Extract and Conditioned Medium of HuCC-T1 Cells[a]

	Activity (unit)/10^7 cells	Distribution on heparin-HPLC (%)[b]			Yield (%)
		non-FGF[c]	aFGF[d]	bFGF[e]	
Conditioned medium	1,600/4 days	0	0	100	43
Cell extract	4,500	1	0	99	64

a) Experimental conditions were as described in the text.
b) The total activity of all fractions was taken as 100%.
c) Activity in unadsorbed fractions and fractions eluted with a concentration of NaCl of less than 0.5 *M*.
d) Activity in fractions eluted with 0.9–1.1 *M* NaCl.
e) Activity in fractions eluted with 1.3–1.5 *M* NaCl.

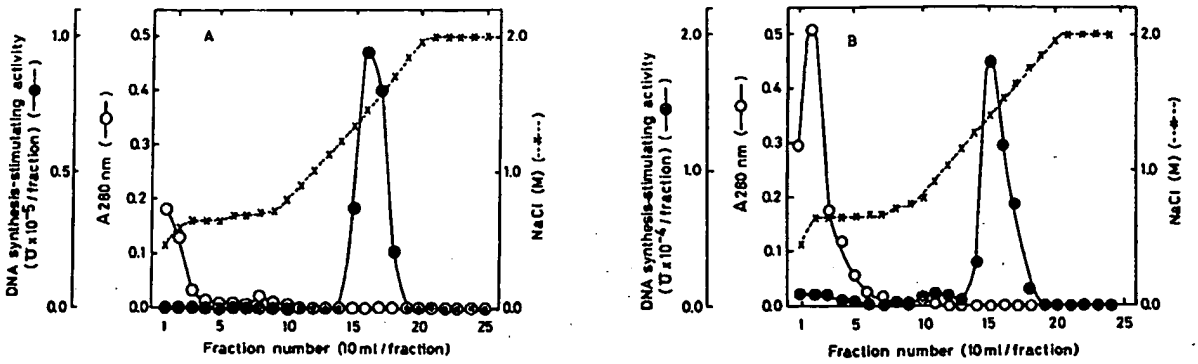

Fig. 1. Heparin-Sepharose affinity chromatography of the growth factor from an extract (A) and conditioned medium (B) of HuCC-T1 cells. Experimental conditions were as described in the text. The elution profile after washing the column with 0.65 *M* NaCl is shown.

activity in the cell extract was about 3 times that in the conditioned medium obtained by culture of confluent cells in protein-free medium for 4 days. Almost all the activity of both the extract and the conditioned medium bound to the heparin column and was eluted with 1.3–1.5 *M* NaCl, indicating that the activity was due to a bFGF-like factor.[23] The viability of the cells after collection of the medium was 99%, as assessed by the trypan blue exclusion test, and lysis and detachment of the cells were hardly observed during the culture period, indicating that the activity in the conditioned medium was not released from dead cells but secreted from live cells.

We purified these growth factors to confirm their identity with bFGF. When the cell extract was applied to a CM-Sephadex column, most of the activity was adsorbed on the column, and was eluted with 0.65 *M* NaCl (data not shown). The major active fractions were combined and applied to a heparin-Sepharose column (Fig. 1A). One peak of activity was eluted with 1.4–1.6 *M* NaCl. By these steps, 14 μg of bFGF-like factor was purified from 10^9 HuCC-T1 cells with about 30% recovery.

To purify the FGF-like factor in HuCC-T1-CM, we collected the conditioned medium from roller bottles on which HuCC-T1 cells were grown to confluency. The activity accumulated in the medium in a 4-day period varied from 60 to 80 units/ml. The activity was adsorbed on CM-Sephadex and eluted from the column with 0.65 *M* NaCl. The major active fractions were combined and applied to a heparin-Sepharose column, and one peak of the activity, like that from HuCC-T1-CE, was eluted with 1.4–1.6 *M* NaCl (Fig. 1B). By these steps, 1.5 μg of bFGF-like factor was purified from 2 liters of conditioned medium with about 20% recovery.

Characterization of bFGF-like factors We obtained two MAbs[26] against bovine bFGF, designated as bFM-1 and bFM-2, which blocked its biological activity. These MAbs were highly specific for bFGF from bovine, human and mouse sources, and did not cross-react with bovine aFGF. Moreover, we showed that bFM-1 recognized the conformation of the bFGF molecule necessary for its biological activity, whereas bFM-2 recognized the denatured bFGF. The concentration of bFGF for half-maximal displacement in RIA with bFM-1 was about one-tenth of that with bFM-2. Therefore, we assayed the bFGF-like factors using bFM-1. Fig. 2A shows that the proteins from HuCC-T1-CE and -CM both competed with radiolabeled bovine bFGF for binding to bFM-1 in a dose-dependent manner and that the displacement curves with the two bFGF-like factors were almost identical to that with purified bovine bFGF, when the doses were expressed as activity units. These results indicate that the specific activities of these growth factors were almost the same. The specific activity of purified bovine bFGF was $2.5–5 \times 10^7$ unit/mg protein, and those of the two purified bFGF-like factors were estimated to be about the same by determination of the protein concentrations of the samples, although these determinations were not accurate because the concentrations of the proteins were low. For immunoblot analysis of the bFGF-like factors, bFM-2 was used as a probe, because bFM-1 did not recognize denatured bFGF transferred to a nitrocellulose sheet. The cross-reactivities of the proteins with bFM-2 were almost the same as that of bovine bFGF, but aFGF did not cross-react with the antibody (Fig. 2B). The bFGF-like factor from the cell extract migrated as a doublet with apparent *Mr*s of 19,000 and 20,000. The factor from the conditioned medium also

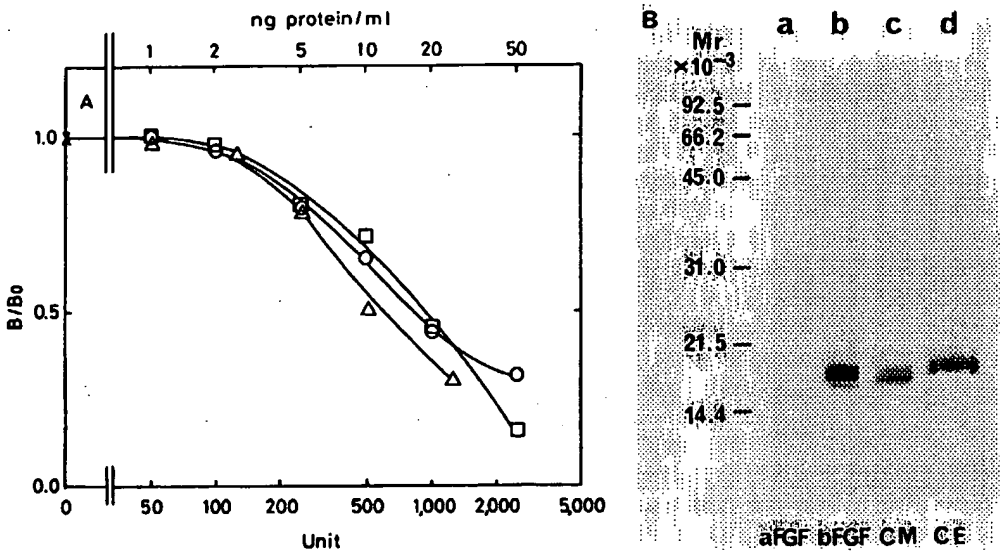

Fig. 2. (A) Cross-reactivities of bFGF (HuCC-T1-CE) and bFGF (HuCC-T1-CM) in RIA with MAb against bFGF (bFM-1). RIA was carried out as described in the text. Values of B (specific binding of ^{125}I-labeled bFGF in the presence of various concentrations of antigens) divided by B_0 (specific binding in the absence of unlabeled antigen) are plotted. The amount of bFM-1 added to the reaction mixture (0.5 ml) was 6 ng. The values of B_0 were 56% of the total tracer added. ○, bFGF (bovine); △, bFGF (HuCC-T1-CE); □, bFGF (HuCC-T1-CM). Units were determined by assay of DNA synthesis-stimulating activity as described in the text. (B) Immunoblot analyses of bFGF (HuCC-T1-CE) and bFGF (HuCC-T1-CM) using MAb against bFGF (bFM-2). Experimental conditions were as described in the text. Lane a, bovine aFGF (1 μg); lane b, bovine bFGF (1 μg); lane c, bFGF (HuCC-T1-CM) (0.5 μg); lane d, bFGF (HuCC-T1-CE) (0.5 μg). The following *Mr* markers from Bio-Rad (Richmond, CA) were used: phosphorylase B (*Mr*, 92,500), BSA (*Mr*, 66,200), ovalbumin (*Mr*, 45,000), carbonic anhydrase (*Mr*, 31,000), soybean trypsin inhibitor (*Mr*, 21,500), and lysozyme (*Mr*, 14,400).

gave two bands with apparent *Mr*s of 18,000 (major component) and 19,000 (minor component). We also examined the bFGF-like factors by means of SDS-PAGE and silver staining (Fig. 3). The proteins showed similar migration patterns to those seen on immuno-staining, although the sample of bFGF-like factor from conditioned medium gave some additional minor protein bands. bFGF was first reported to be a single-chain polypeptide composed of 146 amino acids,[28] but later some other forms that were truncated (131 or 135 amino acids)[24, 29] or extended (154 or 157 amino acids)[30, 31] at the amino terminus were also reported. It has been

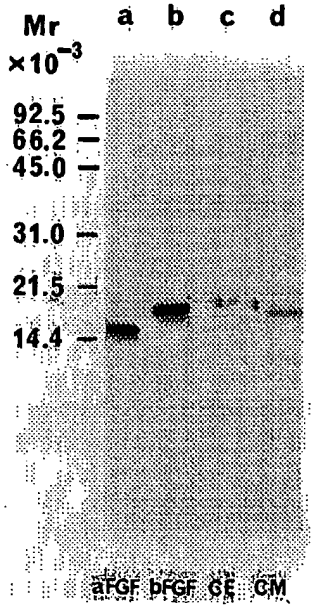

Fig. 3. SDS-PAGE of bFGF-like factors from an extract and conditioned medium of HuCC-T1 cells. Experimental conditions were as described in the text. Proteins were located with silver stain. Lane a, bovine aFGF (1 μg); lane b, bovine bFGF (1 μg); lane c, bFGF (HuCC-T1-CE) (0.5 μg); lane d, bFGF (HuCC-T1-CM) (0.5 μg). The *Mr* markers used were the same as for Fig. 2.

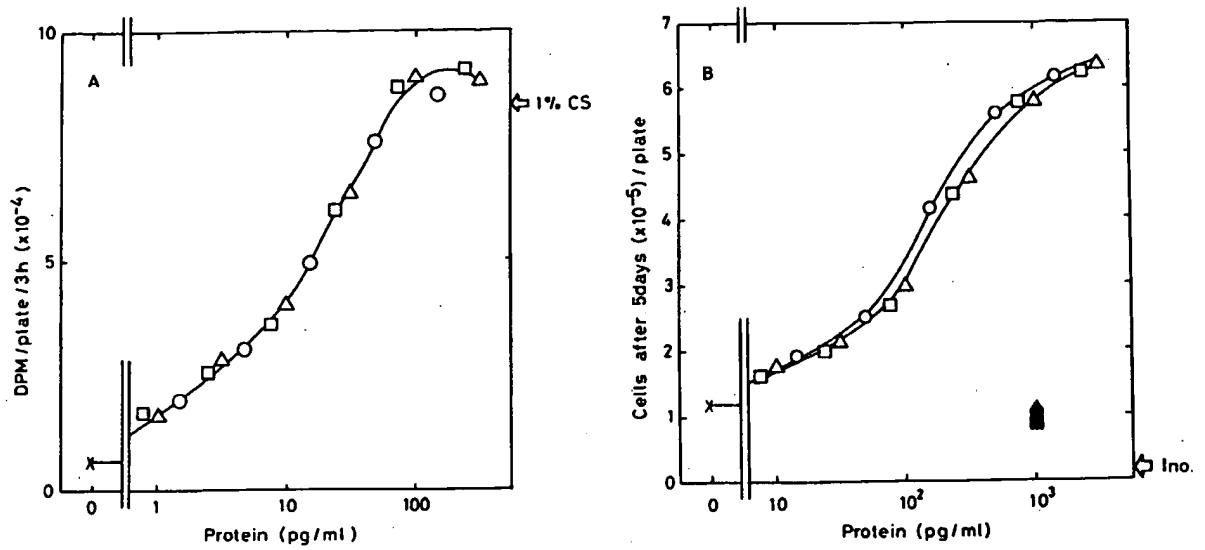

Fig. 4. Effects of bFGF-like factors from an extract and conditioned medium of HuCC-T1 cells in stimulating DNA synthesis in BALB/c3T3-3K cells (A) and growth of BCE cells (B). Experimental conditions were as described in the text. The protein concentration of bovine bFGF was determined with a BCA kit (Pierce, Illinois) with BSA as a standard, while those of bFGF (HuCC-T1-CE) and bFGF (HuCC-T1-CM) were estimated from the results of RIA. ○, bFGF (bovine); △, bFGF (HuCC-T1-CE); □, bFGF (HuCC-T1-CM); ●, bFGF+MAb (bFM-1) (10 μg/ml); ▲, bFGF (HuCC-T1-CE)+MAb (bFM-1) (10 μg/ml); ■, bFGF (HuCC-T1-CM) + MAb (bFM-1) (10 μg/ml); ×, No addition. The thick arrow in (A) indicates the activity in the presence of the optimal concentration (1%) of CS. The thick arrow in (B) (Ino.) indicates the number of cells inoculated.

suggested that the amino-terminal sequence of bFGF is apt to be cleaved by protease and that this sequence is not necessary for its biological activity. bFGF-like factor from the cell extract was purified in the presence of several protease inhibitors, but the factor from the conditioned medium was purified after being incubated in the medium probably containing proteolytic activity for a few days at 37°C. Therefore, the lower *Mr* of the factor from the conditioned medium than that from the cell extract may be due to proteolytic cleavage.

Biological activities of bFGF-like factors As described above, the bFGF-like factors purified from HuCC-T1-CE and -CM were potent mitogens for BALB/c3T3 cells. The dose-response curves of the activities to stimulate DNA synthesis in BALB/c3T3 cells of the bFGF-like factors are shown in comparison with that of bovine bFGF in Fig. 4A. The three curves were indistinguishable and indicated half-maximal and maximal effects at about 15 pg/ml and about 100 pg/ml, respectively. To determine whether these factors had similar mitogenic effects on BCE cells, we tested the effects of increasing concentrations of these factors and bovine bFGF on growth of BCE cells (Fig. 4B). Similar dose-response curves were again obtained and indicated half-maximal and maximal effects at about 200 pg/ml and 2 ng/ml, respectively. These results also support the conclusion that the bFGF-like factors from HuCC-T1-CE and -CM are indistinguishable from bFGF. MAb against bFGF (bFM-1) inhibited the growth of BCE cells stimulated by bFGF or bFGF-like factors from HuCC-T1-CE or -CM.

Effects of bFGF-like factors on growth of HuCC-T1 cells As reviewed by Barnes and Sato,[15] many kinds of cells can grow in serum-free medium supplemented with hormones, growth factors, and other defined materials. We studied the dose-dependences of the effects of some of these essential factors on growth of HuCC-T1 cells in serum-free C-F12 medium in poly-D-lysine-coated dishes. Poly-D-lysine-coated dishes were used extensively and growth was faster in these dishes than in uncoated dishes (data not shown), as in the case of A431 cells.[32] Table II summarizes results on the cell numbers after growth with optimal concentrations of these factors for 5 days. No growth stimulation was observed when bFGF or transferrin was added alone. Addition of insulin or BSA alone resulted in slight stimulation of cell growth. A combination of insulin and transferrin or BSA stimulated growth to nearly that in the presence of an optimal concentration (1%) of CS. No growth stimulation was

Table II. Effects of Various Additions on Growth of HuCC-T1 Cells in Serum-free C-F12 Medium[a]

Addition (μg/ml)	% of control cell number
None[b]	(100)
bFGF (0.003)	100
T (10)	100
I (10)	182
BSA (100)	155
T+I (10, 10)	556
T+BSA (10, 100)	185
I+BSA (10, 100)	686
I+BSA (1, 10)	441
I + BSA + bFGF (1, 10, 0.003)	433
T+I+BSA (10, 10, 100)	614
1% CS	581

a) Experimental conditions were as described in the text.
b) The cells were plated at a density of 2×10^4/dish. The cell number after 5 days in the control culture ($3.1–6.0\times10^4$ cells/dish) without any additions was taken as 100%. T=transferrin. I=insulin.

Table III. Effects of Various Additions on Growth of HuCC-T1 Cells in Serum-free C-F12 Medium Supplemented with Insulin and BSA[a]

Addition (μg/ml)	% of control cell number
None[b]	(100)
Bovine bFGF (0.003)	84
bFGF from HuCC-T1-CE (0.003)	108
bFGF from HuCC-T1-CM (0.003)	100
hEGF (0.1)	103
MAb (bFGF) (10)	161
MAb (hEGF) (10)	132

a) Experimental conditions were as described in the text.
b) The cells were plated at a density of 2×10^4/dish. The cell number after 5 days in the control culture ($2.1–3.6\times10^5$ cells/dish) with 10 μg/ml of insulin and 100 μg/ml of BSA in serum-free C-F12 medium was taken as 100%.

again observed when bFGF was added with sub-optimal concentrations of insulin (1 μg/ml) and BSA (10 μg/ml) which resulted in sub-optimal growth stimulation. Addition of higher concentrations of bFGF (up to 30 ng/ml) did not have any effect (data not shown). Transferrin and BSA with and without insulin did not have additive effects.

To determine whether the bFGF-like factors produced by HuCC-T1 cells act as an auto-stimulatory factor, we examined the effects of these factors and of MAb against bFGF (bFM-1) on growth of HuCC-T1 cells in the presence of insulin and BSA. Table III summarizes the cell numbers at the highest concentrations of these additives determined from dose-response curves. The bFGFs from bovine brain, HuCC-T1-CE and -CM did not stimulate growth, even at concentrations that caused maximal growth stimulation of BCE cells as described above. We looked for FGF receptor[5] in HuCC-T1 cells with ^{125}I-labeled bFGF and aFGF, but it could not be detected even after washing these cells with suramin or sodium acetate buffer (pH 4.0) containing 2 *M* NaCl. This result seems to be consistent with the lack of effect of bFGF on growth of these cells (Table II and Table III). hEGF also had no stimulatory effect. Moreover, although the MAb, bFM-1, completely inhibited growth of BCE cells at 10 μg/ml in the presence and absence of bFGF,[26] it did not inhibit, but slightly stimulated the growth of HuCC-T1 cells. MAb against hEGF at 10 μg/ml also slightly stimulated the growth of HuCC-T1 cells. The reason for the stimulatory effects of these IgG_1 preparations is unknown. These results indicate that the bFGF-like factor, at least the one that is secreted by HuCC-T1 cells, does not act as an autocrine growth factor.

DISCUSSION

In the present study, we showed that cultured human cholangiocellular carcinoma cells, HuCC-T1, produced a bFGF-like factor that was immunologically indistinguishable from bovine bFGF. We further found that this factor was not only associated with the cells, but also was secreted into the medium. There is no leader peptide region, which facilitates secretion, in the amino acid sequence of bFGF deduced from its cDNA nucleotide sequence.[33] Therefore, leaderless bFGF is probably produced inside the cells, carried to the cell surface with glycosaminoglycan as shown by several reports[34–36] and then released from the extracellular matrix by lysis with heparinase-like enzyme produced by the cells,[37] or by some unknown mechanism. Neither bFGF nor neutralizing MAb against bFGF affected the growth of HuCC-T1 cells in serum-free medium, suggesting that this factor in the conditioned medium does not act as autocrine growth factor. bFGF secreted from the tumor cells may function in inducing hyperplasia of adjacent normal tissue and angiogenesis and contribute to the development of solid tumors.

Recent studies have shown that three different oncogenes, int-2, hst/KS3 and FGF-5, encode FGF-homologous proteins.[38–41] These three proteins and bFGF share considerable amino acid sequence homol-

ogy, ranging from 35 to 55% identity in commonly aligned regions. However, these oncogene products have been found in only certain kinds of tumor cells. On the contrary, bFGF has been found in almost all cell lines derived from solid tumors examined.[42] The possibility of an autocrine role of bFGF in the growth of tumor cells has been suggested from studies on a human embryonal rhabdomyosarcoma cell line[3] and rat primary fibrosarcoma cells[43]: these cells produce bFGF that stimulates their own growth. In addition, transformation of cells without a requirement of bFGF for their growth has been achieved by introduction of bFGF cDNA into NIH 3T3 cells,[44] baby hamster kidney-derived (BHK) cells[45] and BALB/c 3T3 cells.[46] The conditioned media of these transformed cell lines producing bFGF was shown to contain a growth factor,[3,45,46] but the factor was not identified[46] or not quantitated.[3,45] Moreover, neutralizing polyclonal antibody against bFGF was found to inhibit growth of one of these transformed cell lines,[46] but not to inhibit growth of other two.[3,45] Therefore, it seems uncertain whether bFGF acts as an autocrine factor for bFGF-producing tumor cells. Recently, Masuda *et al.*[32,47] showed that human epidermoid carcinoma cells, A431 cells, secreted a bFGF-like factor into protein-free medium, in which the cells grew as well as in medium containing serum. They also showed that exogenous addition of this bFGF-like factor did not affect cell growth.

The present results also suggest that bFGF-like factor produced by human cancer cells, HuCC-T1, is irrelevant to the growth of these cells.

ACKNOWLEDGMENTS

This work was supported in part by a Grant-in-Aid for Cancer Research from the Ministry of Education, Science and Culture of Japan.

(Received October 5, 1989/Accepted February 21, 1990)

REFERENCES

1) Folkman, J. Tumor angiogenesis. *Adv. Cancer Res.*, **19**, 331–358 (1974).
2) Klagsbrun, M., Sasse, J., Sullivan, R. and Smith, J. A. Human tumor cells synthesize an endothelial cell growth factor that is structurally related to basic fibroblast growth factor. *Proc. Natl. Acad. Sci. USA*, **83**, 2448–2452 (1986).
3) Schweigerer, L., Neufeld, G., Mergia, A., Abraham, J. A., Fiddes, J. C. and Gospodarowicz, D. Basic fibroblast growth factor in human rhabdomyosarcoma cells: implications for the proliferation and neovascularization of myoblast-derived tumors. *Proc. Natl. Acad. Sci. USA*, **84**, 842–846 (1987).
4) Thomas, K. A. and Gimenez-Gallego, G. Fibroblast growth factors: broad spectrum mitogens with potent angiogenic activity. *Trends Biochem. Sci.*, **11**, 81–84 (1986).
5) Gospodarowicz, D., Neufeld, G. and Schweigerer, L. Fibroblast growth factor: structural and biological properties. *J. Cell. Physiol. (Suppl.)*, **5**, 15–26 (1987).
6) Heldin, C-H. and Westermark, B. Growth factors: mechanism of action and relation to oncogenes. *Cell*, **37**, 9–20 (1984).
7) Sporn, M. B. and Todaro, G. J. Autocrine secretion and malignant transformation of cells. *N. Engl. J. Med.*, **301**, 878–880 (1980).
8) Sporn, M. B. and Roberts, A. B. Autocrine growth factor and cancer. *Nature*, **313**, 745–747 (1985).
9) Kaplan, P. L., Anderson, M. and Ozanne, B. Transforming growth factor(s) production enables cells to grow in the absence of serum: an autocrine system. *Proc. Natl. Acad. Sci. USA*, **79**, 485–489 (1982).
10) Richmond, A., Lawson, D. H., Nixon, D. W. and Chawla, R. K. Characterization of autostimulatory and transforming growth factors from human melanoma cells. *Cancer Res.*, **45**, 6390–6394 (1985).
11) Hoshi, H. and McKeehan, W. L. Production of an autostimulatory growth factor by human hepatoma cells abrogates requirement for a brain-derived factor. *In Vitro Cell. Dev. Biol.*, **21**, 125–128 (1985).
12) Cuttitta, F., Carney, D. N., Mulshine, J., Moody, T. W., Fedorko, J., Fischer, A. and Minna, J. D. Bombesin-like peptides can function as autocrine growth factors in human small-cell lung cancer. *Nature*, **316**, 823–826 (1985).
13) Johnsson, A., Betsholtz, C., Heldin, C-H. and Westermark, B. Antibodies against platelet-derived growth factor inhibit acute transformation by simian sarcoma virus. *Nature*, **317**, 438–440 (1985).
14) Duprez, V., Lenoir, G. and Dautry-Varsat, A. Autocrine growth stimulation of a human T-cell lymphoma line by interleukin 2. *Proc. Natl. Acad. Sci. USA*, **82**, 6932–6936 (1985).
15) Barnes, D. and Sato, G. Serum-free cell culture: a unifying approach. *Cell*, **22**, 649–655 (1980).
16) Miyagiwa, M., Ichida, T., Tokiwa, T., Sato, J. and Sasaki, H. A new human cholangiocellular carcinoma cell line (HuCC-T1) producing carbohydrate antigen 19/9 in serum-free medium. *In Vitro Cell. Dev. Biol.*, **25**, 503–510 (1989).
17) Yoshitake, Y., Nishikawa, K. and Adachi, K. DNA synthesis-stimulating activities for BALB/3T3 cells present in histone and nonhistone protein fractions from rat

Rhodamine fibrosarcoma. *Cell Struct. Funct.*, **7**, 229–243 (1982).
18) Goetz, I. E., Warren, J., Estrada, C., Roberts, E. and Krause, D. Long-term serial cultivation of arterial and capillary endothelium from adult bovine brain. *In Vitro Cell. Dev. Biol.*, **21**, 172–180 (1985).
19) Nishikawa, K., Yoshitake, Y. and Ikuta, S. Derivation of monoclonal antibody to human epidermal growth factor. *Methods Enzymol.*, **146**, 11–22 (1987).
20) Gospodarowicz, D., Cheng, J., Lui, G-M., Baird, A. and Böhlen, P. Isolation of brain fibroblast growth factor by heparin-Sepharose affinity chromatography: identity with pituitary fibroblast growth factor. *Proc. Natl. Acad. Sci. USA*, **81**, 6963–6967 (1984).
21) Matuo, Y., Nishi, N., Muguruma, Y., Yoshitake, Y., Masuda, Y., Nishikawa, K. and Wada, F. The usefulness of CHAPS as a non-cytotoxic stabilizing agent in purification of growth factors. *Cytotechnology*, **1**, 309–318 (1988).
22) Matuo, Y., Nishi, N., Muguruma, Y., Yoshitake, Y., Masuda, Y., Nishikawa, K. and Wada, F. Stabilization of fibroblast growth factors by a non-cytotoxic zwitterionic detergent, 3-[(3-cholamidopropyl)dimethylammonio]-1-propane sulfonate (CHAPS). *In Vitro Cell. Dev. Biol.*, **24**, 477–480 (1988).
23) Shing, Y., Folkman, J., Sullivan, R., Butterfield, C., Murray, J. and Klagsbrun, M. Heparin affinity: purification of a tumor-derived capillary endothelial cell growth factor. *Science*, **223**, 1296–1299 (1984).
24) Klagsbrun, M., Smith, S., Sullivan, R., Shing, Y., Davidson, S., Smith, J. A. and Sasse, J. Multiple forms of basic fibroblast growth factor: amino-terminal cleavages by tumor cell- and brain cell-derived acid proteinases. *Proc. Natl. Acad. Sci. USA*, **84**, 1839–1843 (1987).
25) Laemmli, U. K. Cleavage of structural proteins during the assembly of the head of bacteriophage T4. *Nature*, **277**, 680–685 (1970).
26) Matsuzaki, K., Yoshitake, Y., Matuo, Y., Sasaki, H. and Nishikawa, K. Monoclonal antibodies against heparin binding growth factor II (HBGF-II)/basic fibroblast growth factor (bFGF) that block its biological activity: invalidity of the antibodies for tumor angiogenesis. *Proc. Natl. Acad. Sci. USA*, **86**, 9911–9915 (1989).
27) Yoshitake, Y. and Nishikawa, K. Production of monoclonal antibodies with specificity for different epitopes on the human epidermal growth factor molecule. *Arch. Biochem. Biophys.*, **263**, 437–446 (1988).
28) Esch, F., Baird, A., Ling, N., Ueno, N., Hill, F., Denoroy, L., Klepper, R., Gospodarowicz, D., Böhlen, P. and Guillemin, R. Primary structure of bovine pituitary basic fibroblast growth factor (FGF) and comparison with the amino-terminal sequence of bovine brain acidic FGF. *Proc. Natl. Acad. Sci. USA*, **82**, 6507–6511 (1985).
29) Gospodarowicz, D., Baird, A., Cheng, J., Lui, G. M., Esch, F. and Böhlen, P. Isolation of fibroblast growth factor from bovine adrenal gland: physicochemical and biological characterization. *Endocrinology*, **118**, 82–90 (1986).
30) Ueno, N., Baird, A., Esch, F., Ling, N. and Guillemin, R. Isolation of an amino terminal extended form of basic fibroblast growth factor. *Biochem. Biophys. Res. Commun.*, **138**, 580–588 (1986).
31) Sommer, A., Brewer, M. T., Thompson, R. C., Moscatelli, D., Presta, M. and Rifkin, D. B. A form of human basic fibroblast growth factor with extended amino terminus. *Biochem. Biophys. Res. Commun.*, **144**, 543–550 (1987).
32) Masuda, Y., Yoshitake, Y. and Nishikawa, K. Growth control of A431 cells in protein-free medium: secretory products do not affect cell growth. *In Vitro Cell. Dev. Biol.*, **2**, 893–899 (1988).
33) Abraham, J. A., Mergia, A., Whang, J. L., Tumolo, A., Friedman, J., Hjerrild, K. A., Gospodarowicz, D. and Fiddes, J. C. Nucleotide sequence of a bovine clone encoding the angiogenic protein, basic fibroblast growth factor. *Science*, **233**, 545–548 (1986).
34) Baird, A. and Ling, N. Fibroblast growth factors are present in the extracellular matrix produced by endothelial cells *in vitro*: implications for a role of heparinase-like enzymes in the neovascular response. *Biochem. Biophys. Res. Commun.*, **142**, 428–435 (1987).
35) Saksela, O., Moscatelli, D., Sommer, A. and Rifkin, D. B. Endothelial cell-derived heparan sulfate binds basic fibroblast growth factor and protects it from proteolytic degradation. *J. Cell Biol.*, **107**, 743–751 (1988).
36) Bashkin, P., Doctrow, S., Klagsbrun, M., Svahn, C. M., Folkman, J. and Vlodavsky, I. Basic fibroblast growth factor binds to subendothelial extracellular matrix and is released by heparitinase and heparin-like molecules. *Biochemistry*, **28**, 1737–1743 (1989).
37) Presta, M., Maier, J. A. M., Rusnati, M. and Ragnotti, G. Basic fibroblast growth factor is released from endothelial extracellular matrix in a biologically active form. *J. Cell. Physiol.*, **140**, 68–74 (1989).
38) Moore, R., Casey, G., Brookes, S., Dixon, M., Peters, G. and Dickson, C. Sequence, topography and protein coding potential of mouse int-2: a putative oncogene activated by mouse mammary tumor virus. *EMBO J.*, **5**, 919–924 (1986).
39) Yoshida, T., Miyagawa, K., Odagiri, H., Sakamoto, H., Little, P. F. R., Terada, M. and Sugimura, T. Genomic sequence of hst, a transforming gene encoding a protein homologous to fibroblast growth factors and the int-2-encoded protein. *Proc. Natl. Acad. Sci. USA*, **84**, 7305–7309 (1987).
40) Delli Bovi, P., Curatola, A. M., Kern, F. G., Greco, A., Ittmann, M. and Basilico, C. An oncogene isolated by transfection of Kaposi's sarcoma DNA encodes a growth factor that is a member of the FGF family. *Cell*, **50**, 729–737 (1987).
41) Zhan, X., Bates, B., Hu, X. and Goldfarb, M. The human FGF-5 oncogene encodes a novel protein related to fibroblast growth factors. *Mol. Cell. Biol.*, **8**, 3487–3495 (1988).

42) Lobb, R., Sasse, J., Sullivan, R., Shing, Y., D'Amore, P. A., Jacobs, J. and Klagsbrun, M. Purification and characterization of heparin-binding endothelial cell growth factors. *J. Biol. Chem.*, **261**, 1924–1928 (1986).

43) Nagao, Y. and Nishikawa, K. Basic fibroblast growth factor, albumin and transferrin purified from rat Rhodamine fibrosarcoma tissue are all essential for growth of primary tumor cells from the same tissue in serum-free medium. *In Vitro Cell. Dev. Biol.*, **25**, 873–880 (1989).

44) Rogelj, S., Weinberg, R. A., Fanning, P. and Klagsbrun, M. Basic fibroblast growth factor fused to a signal peptide transforms cells. *Nature*, **331**, 173–175 (1988).

45) Neufeld, G., Mitchell, R., Ponte, P. and Gospodarowicz, D. Expression of human basic fibroblast growth factor cDNA in baby hamster kidney-derived cells results in autonomous cell growth. *J. Cell Biol.*, **106**, 1385–1394 (1988).

46) Sasada, R., Kurokawa, T., Iwane, M. and Igarashi, K. Transformation of mouse BALB/c3T3 cells with human basic fibroblast growth factor cDNA. *Mol. Cell. Biol.*, **8**, 588–594 (1988).

47) Masuda, Y., Yoshitake, Y. and Nishikawa, K. Secretion of DNA synthesis factor (DSF) by A431 cells that can grow in protein-free medium. *Cell Biol. Int. Rep.*, **11**, 359–365 (1987).

STIC-ILL

From: Holleran, Anne
Sent: Sunday, March 04, 2001 5:30 PM
To: STIC-ILL
Subject: refs. for 09/266,543

Examiner: Anne Holleran
Art Unit: 1642; Rm 8E03
Phone: 308-8892
Date needed by: ASAP

Please send me copies of the following :

1. Plum, S.M. et al. Vaccine, (2000) 19/9-10, 1294-1303
2. Aonuma, M. et al. Anticancer Res. (1999, Oct) 19(5B): 4039-4044
3. Muller, Y.A. et al. Structure (1998) 6(9): 1153-1167
4. Yamagishi, S. et al. J. Biol. Chem. (1997) 272(13): 8723-8730
5. Koolwijk, P. et al. J. Cell Biology (1996) 132(6): 1177-1188
6. Matsuo, A. et al. Neuroscience (1994) 60(1): 49-66
7. Djakiew, D. et al. Cancer Research (1991) 51(12): 3304-3310
8. Yamanishi, H. et al. Cancer Research (1991) 51(11): 3006-3010
9. Matsuzaki; K. et al. Japanese J. Cancer Research (1990) 81(4): 345-354
10. Kardami, E. et al. Growth Factors (1990) 4(1): 69-80
11. Riss, T.L. et al. J. Cellular Physiology (1989) 138(2): 405-414

THE JOURNAL OF BIOLOGICAL CHEMISTRY

Vol. 272, No. 13, Issue of March 28, pp. 8723–8730, 1997
Printed in U.S.A.

Advanced Glycation End Products-driven Angi genesis *in Vitro*

INDUCTION OF THE GROWTH AND TUBE FORMATION OF HUMAN MICROVASCULAR ENDOTHELIAL CELLS THROUGH AUTOCRINE VASCULAR ENDOTHELIAL GROWTH FACTOR*

(Received for publication, August 29, 1996, and in revised form, December 23, 1996)

Sho-ichi Yamagishi‡, Hideto Yonekura‡, Yasuhiko Yamamoto‡, Kenji Katsuno§, Fumiyasu Sato§, Izumi Mita¶, Hisayoshi Ooka¶, Noboru Satozawa‖, Takuhisa Kawakami‡, Motohiro Nomura‡, and Hiroshi Yamamoto‡**

From the ‡Department of Biochemistry, Kanazawa University School of Medicine, Kanazawa 920, Japan, the §Discovery Research Laboratory 3, Kissei Pharmaceutical Co. Ltd., Hotaka 399-83, Japan, the ¶Institute of Biological Science, Mitsui Pharmaceuticals Inc., Mobara 297, Japan, and the ‖Life Science Laboratory, Mitsui Toatsu Chemicals Inc., Mobara 297, Japan

This study was undertaken to determine whether and how advanced glycation end products (AGE), senescent macroproteins accumulated in various tissues under hyperglycemic states, cause angiogenesis, the principal vascular derangement in diabetic microangiopathy. We first prepared AGE-bovine serum albumin (BSA) and anti-AGE antiserum using AGE-RNase A. Then AGE-BSA was administered to human skin microvascular endothelial cells in culture, and their growth was examined. The AGE-BSA, but not nonglycated BSA, was found to induce a statistically significant increase in the number of viable endothelial cells as well as their synthesis of DNA. The increase in DNA synthesis by AGE-BSA was abolished by anti-AGE antibodies. AGE-BSA also stimulated the tube formation of endothelial cells on Matrigel. We obtained the following evidence that it is vascular endothelial growth factor (VEGF) that mainly mediates the angiogenic activities of AGE. (1) Quantitative reverse transcription-polymerase chain reaction analysis of poly(A)$^+$ RNA from microvascular endothelial cells revealed that AGE-BSA up-regulated the levels of mRNAs for the secretory forms of VEGF in time- and dose-dependent manners, while endothelial cell expression of the genes encoding the two VEGF receptors, kinase insert domain-containing receptor and *fms*-like tyrosine kinase 1, remained unchanged by the AGE treatment. Immunoprecipitation analysis revealed that AGE-BSA did increase *de novo* synthesis of VEGF. (2) Monoclonal antibody against human VEGF completely neutralized both the AGE-induced DNA synthesis and tube formation of the endothelial cells. The results suggest that AGE can elicit angiogenesis through the induction of autocrine vascular VEGF, thereby playing an active part in the development and progression of diabetic microangiopathies.

Glucose and other reducing sugars can react nonenzymatically with the amino groups of proteins to form reversible Schiff bases and, then, Amadori products. These early glycation products undergo further complex reactions such as rearrangement, dehydration, and condensation to become irreversibly cross-linked, heterogeneous fluorescent derivatives termed advanced glycation end products (AGE)[1] (1). The formation and accumulation of AGE in various tissues have been known to progress during normal aging and at an extremely accelerated rate in diabetes mellitus. This has been implicated in the development of diabetic micro- and macro-vascular complications (1), which may account for the disabilities and high mortality rate in patients with this disease (2).

Microvessels are composed of only two types of cells, endothelial cells and pericytes, and have been known to show both functional and structural abnormalities during prolonged diabetic exposure, resulting in the deleterious effects on the organs that they supply (3–5). Using pericyte-endothelial cell co-culture systems, we have shown previously that pericytes can not only regulate the growth but also preserve the prostacyclin-producing ability and protect against lipid peroxide-induced injury of endothelial cells (6). This has provided a basis for understanding how diabetic retinopathy develops consequent to "pericyte loss," the earliest histopathological hallmark in diabetic retinopathy (5, 7).

Recently, we have found that AGE exert a growth inhibitory effect and a cell type-specific immediate toxicity on pericytes through interactions with their receptor for AGE (RAGE), a cell surface receptor belonging to the immunoglobulin superfamily (8), and have proposed a novel mechanism for pericyte loss (9). The AGE-induced, RAGE-mediated decrease in pericyte number would then indirectly cause angiogenesis (6, 9).

In the present study, we investigated the effects of AGE on the growth and tube formation of human skin microvascular endothelial cells, the key steps of angiogenesis. We demonstrate that AGE exert angiogenic activities directly on microvascular endothelial cells and that autocrine vascular endothelial growth factor (VEGF) is the major mediator of the AGE-driven angiogenesis.

EXPERIMENTAL PROCEDURES

Materials—Bovine serum albumin (BSA) was purchased from Boehringer Mannheim GmbH (Mannheim, Germany). Bovine pancreatic RNase A, bovine hemoglobin (Hb), N^{α}-tosyl-lysine methyl ester and phenylmethylsulfonyl fluoride were from Sigma. Heparin-Sepharose

* This work was supported in part by Grants-in-aid from the Ministry of Education, Science, Sports and Culture, Japan, the Sagawa Foundation for Promotion of Cancer Research, Japan, and the Japan Diabetes Foundation. The costs of publication of this article were defrayed in part by the payment of page charges. This article must therefore be hereby marked "*advertisement*" in accordance with 18 U.S.C. Section 1734 solely to indicate this fact.

** To whom correspondence and requests for reprints should be addressed. Tel.: 81-76-265-2180; Fax: 81-76-234-4226).

[1] The abbreviations used are: AGE, advanced glycation end products; RAGE, receptor for AGE; VEGF, vascular endothelial growth factor; BSA, bovine serum albumin; Hb, hemoglobin; HRP, horseradish peroxidase; CM-TsLME, N^{α}-tosyl-N^{ϵ}-carboxymethyllysine methyl ester; CM-BSA, *N*-carboxymethylated BSA; ELISA, enzyme-linked immunosorbent assay; RT-PCR, reverse transcription-polymerase chain reaction; Flt 1, *fms*-like tyrosine kinase 1; KDR, kinase insert domain-containing receptor; MoAb, monoclonal antibody; bp, base pairs.

CL-4B was from Pharmacia LKB (Uppsala, Sweden). Horseradish peroxidase (HRP)-conjugated goat anti-rabbit IgG was from BioMakor (Rehovot, Israel). [^{3}H]Thymidine and [γ-^{32}P]ATP were from DuPont NEN. Reverse transcriptase and T4 polynucleotide kinase were from Takara (Kyoto, Japan). Hybond-N$^+$ nylon membrane was from Amersham Corp. (Buckinghamshire, United Kingdom). Matrigel was from Collaborative Research (Bedford, MA).

Preparation of AGE-Proteins and Amadori Compounds – BSA (fraction V, fatty acid-free, free endotoxin) was incubated with 0.5 M glucose at 37 °C for 6 weeks under sterile conditions in the presence of 1.5 mM phenylmethylsulfonyl fluoride, 0.5 mM EDTA, 100 units/ml penicillin, and 40 μg/ml gentamycin (9–11). After unincorporated sugars were removed by dialysis against phosphate-buffered saline, glucose-modified high molecular weight materials were purified by heparin-Sepharose CL-4B column chromatography and used as AGE-BSA. Control nonglycated BSA was incubated in the same conditions except for the absence of glucose. The concentration of AGE-BSA was determined by the method of Bradford (12). AGE-RNase A and AGE-Hb were prepared according to the method of Makita *et al.* (13). For reducing AGE-Hb, $NaBH_4$ was employed as described by Horiuchi *et al.* (14). 1-Deoxy-1-propylamino-D-fructose, an Amadori compound, was synthesized by the method of Micheel and Hagemann (15). N^{α}-Tosyl-N^{ϵ}-carboxymethyllysine methyl ester (CM-TsLME) was synthesized from N^{α}-tosyl-lysine methyl ester by the method of Ahmed *et al.* (16) with minor modifications. *N*-Carboxymethylated BSA (CM-BSA) was prepared according to the method of Reddy *et al.* (17).

Preparation of Anti-AGE-RNase A Antiserum – 1 mg of AGE-RNase A was emulsified in 50% Freund complete adjuvant and injected intradermally into rabbits. Two weeks later, a booster with the same amount of AGE-RNase A was administered, followed by nine additional booster injections, with one given every 2–3 weeks. Ten days after the final injection, the antiserum was obtained.

Enzyme-linked Immunosorbent Assay (ELISA) – In the noncompetitive ELISA system, wells of 96-well microtiter plates were coated with increasing amounts of Hb, AGE-Hb, and reduced AGE-Hb. After washing and blocking, the wells were incubated with 100 μl of anti-AGE antiserum (1:4000) for 2 h and then with 100 μl of HRP-conjugated goat anti-rabbit IgG (1:2000) for 30 min. Finally, 100 μl of substrate tetramethylbenzidine solution was added into each well. After 10–15 min, the absorbance at 450 nm was measured. In the competitive ELISA system, procedures similar to the noncompetitive ELISA were used except for the following two points. Wells were first coated with reduced 100 ng/ml AGE-Hb solution as absorbent antigens, and then 50 μl of test samples were added as a competitor together with 50 μl of anti-AGE antiserum (1:2000) into each well.

Cells – Endothelial cells from human skin microvessels were maintained in E-BM medium supplemented with 5% fetal bovine serum, 0.4% bovine brain extracts, 10 ng/ml human epidermal growth factor, and 1 μg/ml hydrocortisone according to the supplier instructions (Clonetics Corp., San Diego, CA). Cells at 5–10 passages were used for the experiments. AGE treatment was carried out in a medium lacking epidermal growth factor and hydrocortisone.

Measurement of Cell Growth – Endothelial cells cultured for various time periods in the presence or absence of AGE-BSA were dislodged with trypsin, and counted by the dye exclusion method (18). [^{3}H]Thymidine incorporation was determined as described previously (19). For determining the effects of anti-AGE antiserum on endothelial cell growth, the antiserum was added to the medium at 1% (v/v) together with or without 50 μg/ml AGE-BSA, after which cells were incubated for 24 h and [^{3}H]thymidine incorporation was measured.

Primers and Probes – Oligonucleotide primers and probes for quantitative reverse transcription-polymerase chain reactions (RT-PCR) were synthesized by a Perkin-Elmer 392 DNA synthesizer (Foster City, CA) and purified as described previously (20). Primer sequences and internal oligonucleotide probes for detecting VEGF, *fms*-like tyrosine kinase 1 (*flt 1*), kinase insert domain-containing receptor (*kdr*), and β-actin mRNA were the same as described in Ref. 20.

Quantitative RT-PCR – Poly(A)$^+$ RNAs were isolated (21) from cells treated with or without AGE-BSA for the various time periods and analyzed by RT-PCR as described previously (22). 6-μl aliquots of each RT-PCR reaction mixture were electrophoresed on a 2% agarose gel and transferred to a Hybond-N$^+$ nylon membrane, and the membrane was hybridized with the respective ^{32}P-end-labeled probes (20). The amounts of poly(A)$^+$ RNA templates (30 ng) and cycle numbers (30 cycles) for amplification were chosen in quantitative ranges where reactions proceeded linearly, which had been determined by plotting signal intensities as functions of the template amounts and cycle numbers (20). Signal intensities of hybridized bands were measured by a Fujix BAS 1000 Image analyzer (Fuji Photo Film Co. Ltd., Hamamatsu, Japan).

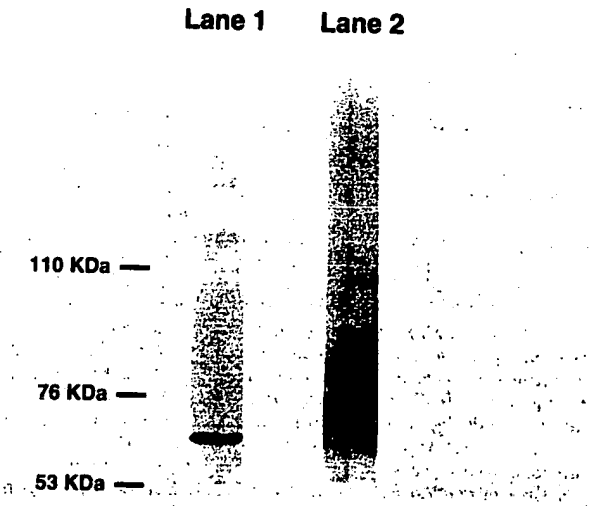

FIG. 1. **SDS-PAGE of AGE-BSA.** 10 μg of nonglycated native BSA (*lane 1*) and AGE-BSA (*lane 2*) were loaded on a 10% polyacrylamide gel with a stacking gel of 5% polyacrylamide. Staining of the gel was performed with Coomassie Brilliant Blue. Size markers (kDa) are shown on the *left*.

Metabolic Labeling and Immunoprecipitation of VEGF – Subconfluent cultures of endothelial cells were incubated in the presence or absence of 50 μg/ml AGE-BSA for 2 h and further incubated for 6 h at 37 °C in methionine-free RPMI 1640 medium/complete RPMI 1640 medium (9:1) containing 0.2 mCi/ml [^{35}S]methionine with or without AGE-BSA. Immunoprecipitation was carried out as described previously (20). The samples were analyzed on a 15% SDS-polyacrylamide gel under reducing conditions.

Preparation of Monoclonal Antibody (MoAb) against Human VEGF – Peripheral blood lymphocytes from healthy volunteers were immortalized by Epstein-Barr virus, and the resultant Epstein-Barr virus-transformants were screened (23) for their ability to produce antibody molecules that bind to recombinant human $VEGF_{165}$ (Peprotech, Rocky Hill, NJ). The candidate cells were then fused with SHM-D33 human myeloma cells (American Type Culture Collection, Rockville, MD). A cell line that consistently produced an IgM-MoAb reactive to VEGF was cloned and designated BL-2. Then the BL-2 MoAb was purified from the serum-free supernatant by 50% ammonium sulfate precipitation and by Sephadex G-200 gel chromatography. The specific binding of MoAb BL-2 to VEGF was confirmed by immunoblotting.[2]

Tube Formation in Vitro – Wells of 24-well culture cluster dishes (Coster 3524, Cambridge, MA) were coated with Matrigel solution (250 μl/well) and then allowed to solidify for at least 1 h at 37 °C (24, 25). Endothelial cells (4×10^4 cells/well) were then seeded on Matrigel with or without 10 μg/ml MoAb BL-2. After 30 min, the cells were treated with or without 50 μg/ml AGE-BSA for 6 h, 4 microscopic fields selected at random were photographed, and the lengths of tube-like structures were measured with microcomputer-assisted NIH Image (Version 1.56).

RESULTS

Characterization of AGE-BSA – AGE-BSA was prepared by incubating BSA with glucose and then purified by heparin-Sepharose CL-4B column chromatography. Fig. 1 shows its electrophoretic profile on reducing SDS-polyacrylamide gel electrophoresis. Control nonglycated BSA migrated to the position at 68 kDa. On the other hand, the purified materials migrated much more slowly, yielding a broad band larger than 68 kDa. This indicated that covalently linked adducts were formed nonenzymatically on BSA without discernible degrada-

[2] The monoclonal antibody did not cross-react with basic fibroblast growth factor or platelet-derived growth factor. Its binding to VEGF-B (49) and -C (50), recently described members of the VEGF family, was undetectable and about 1/1000 of that to VEGF, respectively. VEGF-B and -C proteins were donated from the Ludwig Institute for Cancer Research and University of Helsinki.

tion. As shown in Table I, the purified materials also exhibited spectrophotometric features characteristic to AGE (26, 27). The peak fluorescence was noted at 440 nm with excitation at 370 nm, and its intensity was increased 10-fold in comparison with nonglycated BSA. Chromogen products also appeared in the purified materials, whereas they were barely detectable in nonglycated BSA. Based on these observations, the purified materials were used as AGE-BSA.

Characterization of Anti-AGE Antiserum – As a tool to evaluate AGE and their biological effects, an antiserum was raised against AGE-RNase A. The reactivity of this antiserum to several AGE-modified proteins, Amadori compounds, and carboxymethyllysine derivatives was examined. Since it was possible that AGE-modified proteins might contain early glycation products, the immunoreactivity of the antiserum to reduced AGE-Hb was also tested because the early glycation products are known to be converted to glucitol-lysine by reduction with $NaBH_4$ (14, 28). As shown in Fig. 2*A*, there was no difference in the immunoreactivity in the noncompetitive ELISA between AGE-Hb and reduced AGE-Hb. Further, as shown in Fig. 2*B*, the antiserum binding to AGE-Hb was not competed for by 1-deoxy-1-propylamino-D-fructose in the competitive ELISA, indicating that the antiserum does not recognize Amadori compounds. We next tested whether the antiserum reacted to CM-TsLME and CM-BSA in the competitive ELISA. As shown in Fig. 2, *B* and *C*, these glycoxidative products were found to partially inhibit the antiserum binding to reduced AGE-Hb, whereas AGE-Hb and AGE-RNase A fully inhibited its binding (Fig. 2*D*). Further, the antiserum reactivity to AGE-BSA was dependent on the duration of incubation of BSA with glucose (Fig. 2*E*). These results suggested that the antiserum could recongnize AGE structures common to various AGE preparations.

TABLE I
Characterization of AGE-BSA

Data represent the mean ± S.E. of three replicate experiments. All the samples were adjusted to a protein concentration of 1.0 mg/ml.

	Fluorescence[a]	Chromogen products[b]
	arbitrary units	
BSA	1.0 ± 0.0	0.0 ± 0.0
AGE-BSA	9.9 ± 0.1	0.11 ± 0.0

[a] An arbitrary value of 1 was assigned to fluorescence of control BSA. Fluorescence was measured at excitation of 370 nm and emission of 440 nm.

[b] Measured as absorbance at 350 nm/absorbance at 280 nm.

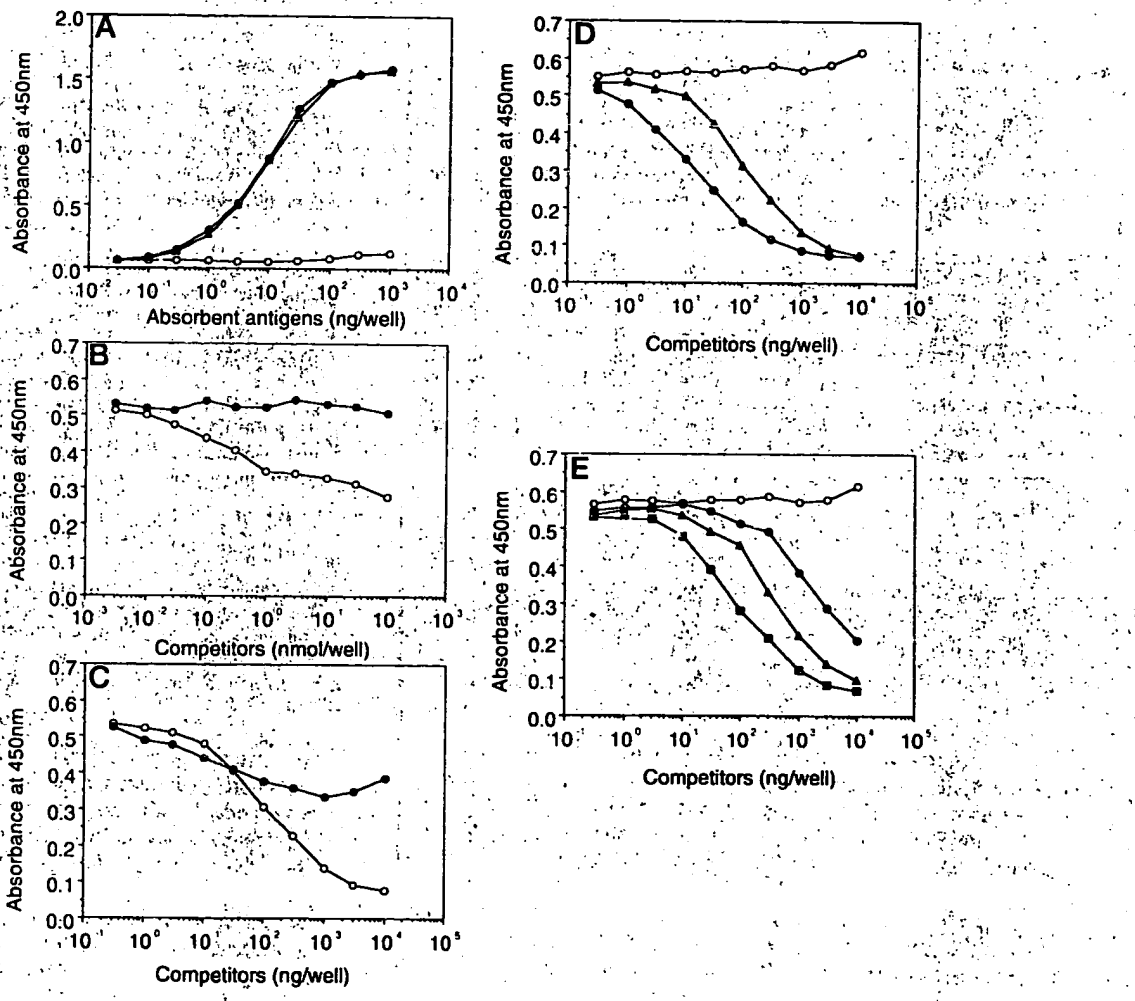

FIG. 2. **Characterization of anti-AGE antiserum.** *A*, antiserum was titered in noncompetitive ELISA using Hb (○), AGE-Hb (●), and reduced AGE-Hb (▲) as absorbent antigens, as described under "Experimental Procedures." The amounts of the antigens are indicated on the *abscissa*, and absorbance at 450 nm is on the *ordinate*. *B-D*, antiserum was titered in competitive ELISA. Wells were coated with reduced AGE-Hb and then various test samples as competitor, and anti-AGE antiserum were added. *B*, 1-deoxy-1-propylamino-D-fructose (●); CM-TsLME (○). *C*, CM-BSA ( ); 8-week incubated AGE-BSA (○). *D*, Hb (○); 8-week incubated AGE-Hb (●); 8-week incubated AGE-RNase A (▲). *E*, BSA (○); 4-week incubated AGE-BSA ( ); 8-week incubated AGE-BSA (▲); 12-week incubated AGE-BSA (■). The amounts of the competitors are indicated on the *abscissa*, and absorbance at 450 nm is on the *ordinate*. Similar results were obtained in two independent experiments.

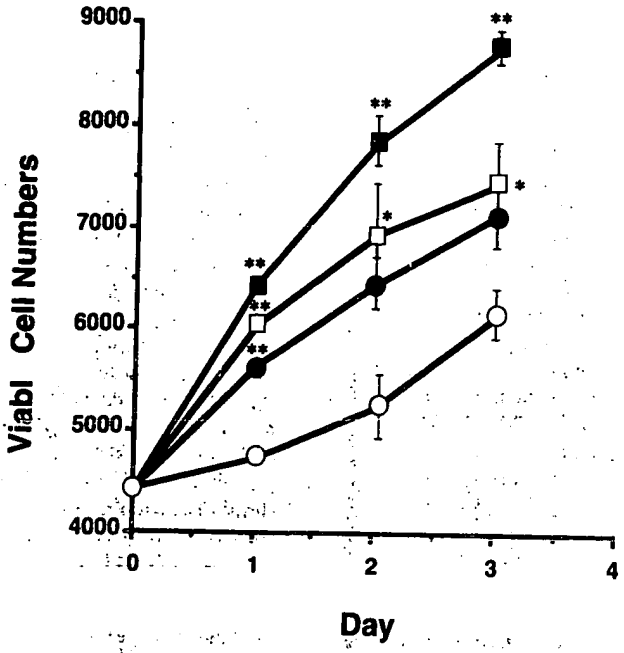

FIG. 3. **Effects of AGE-BSA on viable cell number of human skin microvascular endothelial cells.** 1×10^4 endothelial cells were seeded per well and grown in the presence of 1 (●), 10 (□), or 50 (■) μg/ml AGE-BSA or in the absence of AGE-BSA (○). The culture period after the addition of AGE-BSA is indicated on the *abscissa*, and the viable cell number is on the *ordinate*. Each *point* represents the mean ± S.E. of three replicate experiments. *, $p < 0.05$; **, $p < 0.01$, compared with the control value without additives (Student's *t* test).

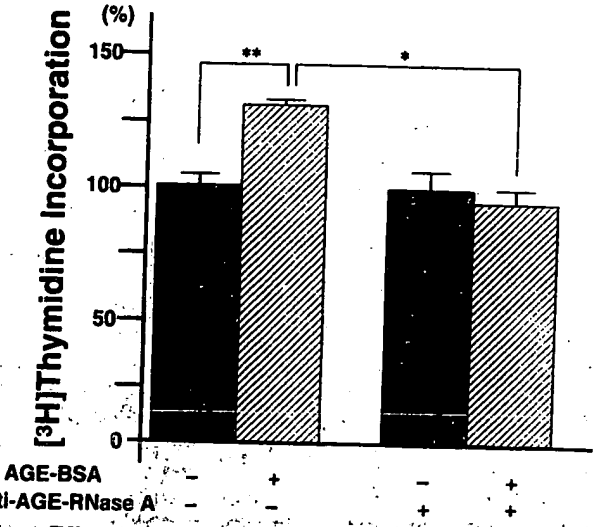

FIG. 4. **Effects of antiserum against AGE-RNase A on the AGE-induced DNA synthesis in human skin microvascular endothelial cells.** Endothelial cells were treated with antiserum against AGE-RNase A in the presence or absence of 50 μg/ml AGE-BSA. After incubation for 24 h, [³H]thymidine was added, and then its incorporation into the cells was assayed. The percentage of [³H]thymidine incorporation is indicated on the *ordinate* and related to the value for the control with no additives. Each *column* represents the mean ± S.E. of four replicate experiments. *, $p < 0.05$; **, $p < 0.01$, compared with the value with 50 μg/ml AGE-BSA alone (Student's *t* test).

Stimulation of the Growth of Microvascular Endothelial Cells by AGE—Endothelial cells obtained from human skin microvessels were cultured in the presence or absence of AGE-BSA, and the viable cell number was determined at days 1, 2, and 3 after the AGE addition. As shown in Fig. 3, AGE-BSA was found to increase the viable microvascular endothelial cell number in a dose-dependent manner; at 50 μg/ml AGE, there was about a 40% increase in viable cell number. Moreover, AGE-BSA significantly increased DNA synthesis in microvascular endothelial cells to 130% ($p < 0.01$, Fig. 4). However, nonglycated BSA induced no change in either the cell number or DNA synthesis.

Neutralization of the AGE-induced DNA Synthesis by Anti-AGE Antibody—To evaluate the specificity of the AGE-BSA effect on endothelial cell growth, we examined the effects of the antiserum against AGE-RNase A on AGE-induced DNA synthesis. As shown in Fig. 4, the anti-AGE-RNase A antiserum was found to completely neutralize the AGE-induced synthesis of endothelial cell DNA at 1%, while the same concentration of the antiserum did not affect DNA synthesis in endothelial cells not exposed to AGE-BSA.

Microvascular Endothelial Cells Express mRNA for Secretory Forms of VEGF in Response to AGE—Poly(A)$^+$ RNAs were isolated from microvascular endothelial cells treated with various concentrations of AGE-BSA for various time periods, and analyzed by a quantitative RT-PCR technique to determine the effects of AGE on the expression of the VEGF gene. It has been reported that there are four alternatively spliced products from the single VEGF gene, $VEGF_{121}$, $VEGF_{165}$, $VEGF_{189}$, and $VEGF_{206}$ (29, 30). Since Northern blot analysis cannot clearly discriminate the four mRNA species, we employed a more sensitive RT-PCR technique as described previously (20). In this experiment, 486- and 618-base pairs (bp)-long cDNA products would be amplified from mRNAs for $VEGF_{121}$ and $VEGF_{165}$, respectively (20).

As shown in Fig. 5, *A* and *B*, microvascular endothelial cells were expressing mRNAs for $VEGF_{121}$ and $VEGF_{165}$, the secretory forms of VEGF. When the endothelial cells were exposed to AGE-BSA, the level of VEGF mRNAs was found to be significantly increased in a time- and dose-dependent manner. The VEGF mRNA level began to increase at 2 h, and reached a maximum at 4 h in the presence of 50 μg/ml AGE-BSA; the peak value was 3-fold higher than the basal level when standardized with the signal intensities of β-actin mRNA as an internal control. Maximal stimulation was achieved at 50–100 μg/ml AGE. However, the larger alternatively spliced products coding for $VEGF_{189}$ and $VEGF_{206}$ were not detected in microvascular endothelial cells regardless of the presence or absence of AGE-BSA.

To confirm whether AGE-BSA increased the synthesis of VEGF proteins, we performed immunoprecipitation using the anti-VEGF monoclonal antibody (20) from lysates of the cells that had been treated with or without AGE-BSA. As shown in Fig. 5*C*, ^{35}S-labeled proteins that migrated to the positions of 18 and 22 kDa, corresponding to $VEGF_{121}$ and $VEGF_{165}$, respectively, were immunoprecipitated, and the amounts of these proteins were found to be increased to about 2.5-fold by the AGE treatment.

VEGF Receptor Expressions in Microvascular Endothelial Cells—VEGF exerts its biological actions through its specific receptors, KDR and Flt 1 (31, 32). We then determined the types of VEGF receptors expressed in microvascular endothelial cells and whether their expressions could be altered by AGE-BSA. As shown in Fig. 5*B*, both *kdr* and *flt 1* mRNA were detected in microvascular endothelial cells, and the content of *kdr* mRNA was more abundant than that of *flt 1* mRNA. In contrast to VEGF mRNAs, the levels of the two types of receptors were essentially unchanged by the exposure to AGE-BSA.

Neutralization of the AGE-Induced DNA Synthesis of Microvascular Endothelial Cells by MoAb against Human VEGF—We next investigated whether vascular VEGF may have a functional role in the AGE action on endothelial cells. Microvascular endothelial cells were preincubated with various

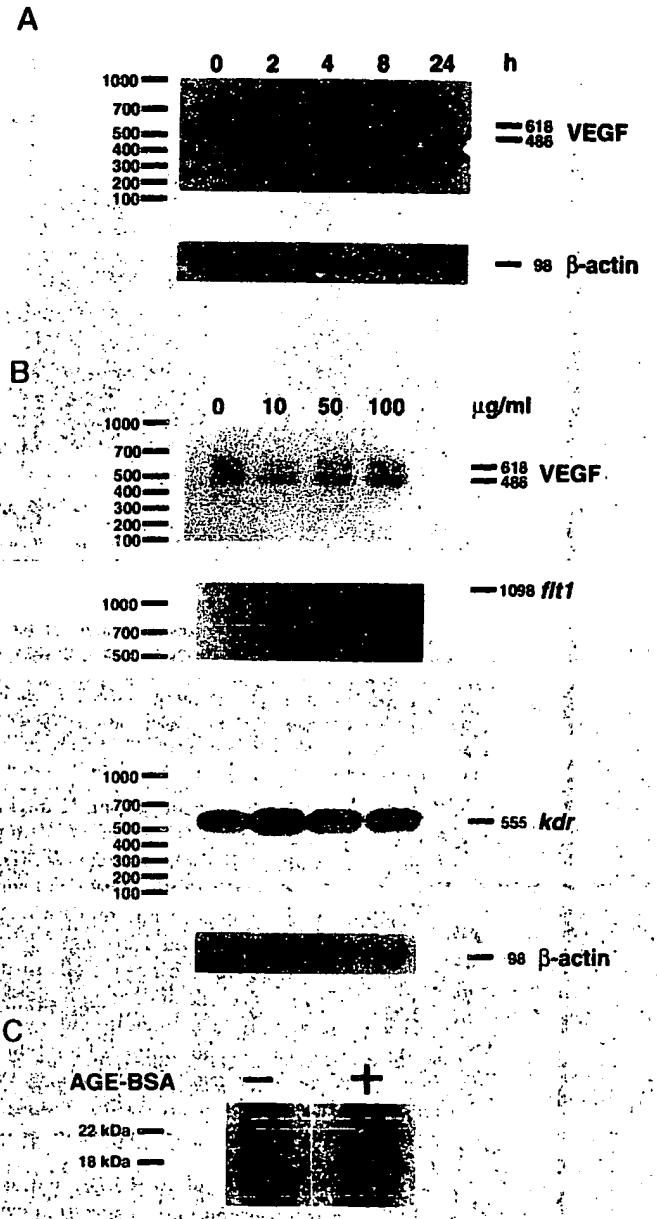

FIG. 5. **Expression of VEGF and its receptor genes in microvascular endothelial cells.** *A*, time course of VEGF mRNA induction by AGE. Endothelial cells were treated with 50 μg/ml AGE, and then 30 ng of poly(A)$^+$ RNAs were transcribed and amplified by PCR at the indicated times. *B*, dose-response of VEGF mRNA induction by AGE. Endothelial cells were incubated for 4 h with the indicated concentrations of AGE, and then 30 ng of poly(A)$^+$ RNAs were amplified by RT-PCR. *Lower panels* show expression of VEGF receptor genes. 30 ng of poly(A)$^+$ RNAs from endothelial cells treated with the various concentrations of AGE were reverse transcribed, and PCR was performed for 25 cycles. The PCR products were electrophoresed on 2% agarose gel, transferred onto nylon membranes, and hybridized with ^{32}P-end-labeled probes. PCR amplification for β-actin mRNA was performed for 20 cycles. Size markers (*bp*) are shown on the *left*. *C*, VEGF synthesis in AGE-treated and untreated endothelial cells. Immunoprecipitation was carried out as described under "Experimental Procedures." Immunoreacted materials that had been prepared from 8.0×10^6 dpm of lysates were electrophoresed on a 15% SDS-polyacrylamide gel under reducing conditions. The gel was dried and autoradiographed. The radioactivities of the bands were measured with a Fujix BAS 1000 BioImage analyzer. Specific immunoprecipitates were marked at 22 and 18 kDa. Similar results were obtained in two independent experiments.

concentrations of MoAb BL-2 for 30 min, then exposed to 50 μg/ml AGE-BSA for 24 h in the presence of the antibody, and assayed for [^{3}H]thymidine incorporation. As shown in Fig. 6,

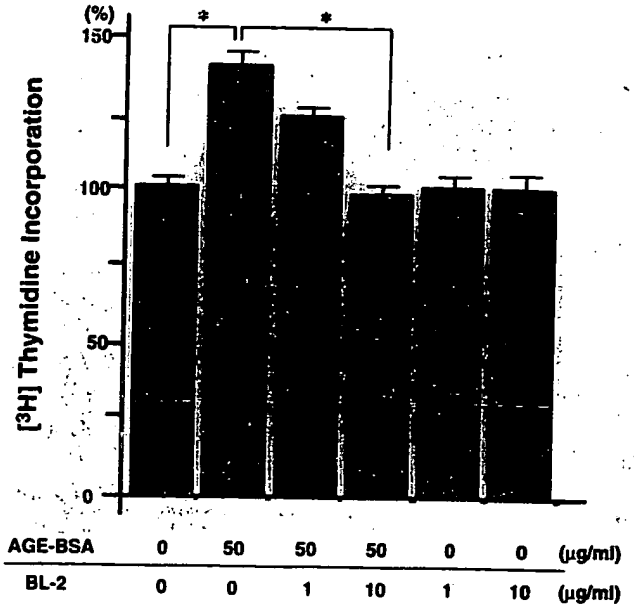

FIG. 6. **Effects of antibody against VEGF (BL-2) on the AGE-induced DNA synthesis.** Endothelial cells were preincubated with the various concentrations of BL-2 for 30 min and then treated with or without 50 μg/ml AGE for 24 h. The percentage of [^{3}H]thymidine incorporation is indicated on the *ordinate*. Each *column* represents the mean values of four replicate experiments. *Bars* show S.E. *; $p < 0.05$, compared with the values obtained in the presence of AGE alone (Student's *t* test).

MoAb BL-2 was found to significantly diminish the AGE-induced increase in DNA synthesis in a dose-dependent manner; at 10 μg/ml, a complete reversal was obtained. The MoAb alone did not affect DNA synthesis in endothelial cells not exposed to AGE.

AGE Induction of Tube Formation of Microvascular Endothelial Cells and Its Inhibition by Anti-VEGF MoAb—The process of angiogenesis has been assumed to be completed by the formation of microvascular tubes (19). *In vitro* assays for tube formation of endothelial cells have been developed and used to study this crucial step of angiogenesis. Accordingly, we examined whether AGE affect *in vitro* tube formation of microvascular endothelial cells. For this, we employed an on-gel assay system using Matrigel, in which endothelial cells take only several hours to associate with each together and form microtubes. Microvascular endothelial cells were seeded on Matrigel with or without AGE-BSA, and tube formations were judged after 6 h. As shown in Fig. 7*A*, AGE-BSA was found to double the length of the tubes of endothelial cells formed on Matrigel, and, the AGE-induced tube formation was inhibited by BL-2 MoAb as was the AGE-induced DNA synthesis of endothelial cells. The MoAb *per se* did not affect the tube formation. Fig. 7*B* shows typical micrographs; with 10 μg/ml BL-2 MoAb, AGE-induced tube formation was markedly inhibited.

DISCUSSION

In the present study, we have demonstrated for the first time that AGE, nonenzymatically glycated protein derivatives formed under hyperglycemia, stimulate the growth and tube formation of human microvascular endothelial cells, the key steps of angiogenesis which take place in this very cell type (33, 34). The present findings have extended our preliminary work employing endothelial cells from a larger vessel, *i.e.* the umbilical vein. Though modestly, AGE-BSA caused a consistent increase in cell number and in DNA synthesis of both umbilical and microvasular endothelial cells, the same AGE-BSA concentration (50 μg/ml) giving the maximal effect in both cases (35).

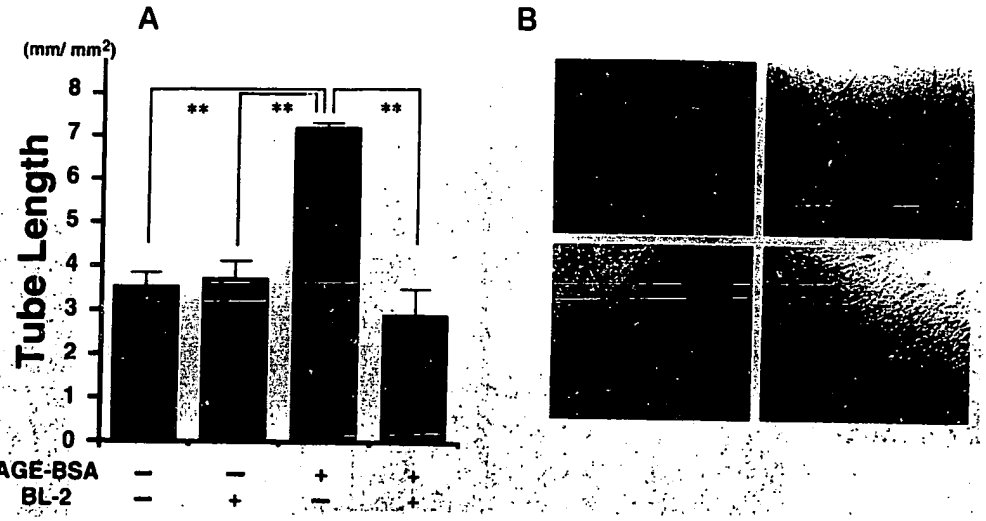

FIG. 7. **Effects of antibody against VEGF (BL-2) on the AGE-induced tube formation in endothelial cells.** *A*, endothelial cells were treated with or without 10 μg/ml antibody and then incubated in the presence or absence of 50 μg/ml AGE for 6 h. Each four fields selected at random were photographed, and the lengths of tube-like structures were quantitatively measured with microcomputer-assisted NIH Image. Each *column* represents the mean values of four replicate experiments. *Bars* show S.E. **, $p < 0.01$, compared with the values obtained in the presence of AGE alone (Student's *t* test). *B*, typical microphotographs of tube formations of endothelial cells. *a*, control without no additive; *b*, 10 μg/ml BL-2; *c*, 50 μg/ml AGE; *d*, 50 μg/ml AGE plus 10 μg/ml BL-2.

This concentration of AGE was comparable with that of the *in vivo* situation in diabetes; Makita *et al.* reported (13) that human serum AGE levels were elevated more than 2-fold in diabetic patients (about 25 μg/ml) and almost 8-fold in diabetic patients on hemodialysis (about 80 μg/ml) in comparison with that in normal patients.

That it was AGE moieties that elicited the angiogenic activity was evidenced as follows. First, the AGE-BSA employed exhibited the biochemical hallmarks of AGE (Fig. 1 and Table I). Second, control nonglycated BSA made no change (data not shown). Third, a newly developed antiserum against AGE-RNase A could neutralize the growth-promoting effect of AGE-BSA (Fig. 4). Although this antiserum was partially reactive to carboxymethyllysine, it would seem unlikely that the AGE effect could be accounted for by such glycoxidative biproducts of the Maillard reaction, which might be present in trace amounts in the AGE-BSA preparation, because authentic carboxymethylated BSA added to the culture medium at concentrations from 1 to 100 μg/ml failed to stimulate the endothelial cell synthesis of DNA (data not shown). We speculate that the AGE actions on microvascular endothelial cells may require their binding to RAGE, the AGE-specific receptor, as is the case with bovine retinal pericytes (9), human umbilical vein endothelial cells (35), and human pancreatic cancer cells (36).

The present study has also demonstrated that the angiogenic activity of AGE is mainly mediated by autocrine VEGF synthesized by microvascular endothelial cells *per se*. mRNAs for $VEGF_{121}$ and $VEGF_{165}$ are present in microvascular endothelial cells, and their levels are up-regulated by AGE in both dose- and time-dependent manners (Fig. 5, *A* and *B*). AGE did increase *de novo* synthesis of VEGF in endothelial cells (Fig. 5*C*). mRNAs for the two VEGF receptors, *kdr* and *flt 1*, were also detected in human skin microvascular endothelial cells, their relative abundance being *kdr* ≫ *flt 1*. However, their levels were essentially unaltered when exposed to AGE (Fig. 5*B*). This suggests that the ligand expression should be the rate-limiting step in the putative autocrine action of VEGF. In effect, the neutralization experiments established the functional role of VEGF in the AGE-induced endothelial cell growth and tube formation. MoAb against human VEGF could completely inhibit the AGE-induced tube formation as well as the DNA synthesis of microvascular endothelial cells (Figs. 6 and 7). Since the basal growth or tube formation in unexposed cells was not affected by the same concentration of the antibody, the antibody-induced inhibition is not likely the result of its toxic or nonspecific effects. These results thus indicate that autocrine VEGF is the main mediator of the AGE-driven angiogenesis *in vitro*.

In light of the present findings, together with the previous observations, we can now posit an overall scheme concerning the roles of AGE in the development of diabetic microangiopathy (Fig. 8). First, AGE act on pericytes, the microvascular constituent that encircles the endothelium. Through interactions with RAGE, AGE decrease the number of this cell type (9), leading to pericyte dropout, which would in turn relieve the restriction on endothelial cell replication and facilitate angiogenesis. The resultant cessation of pericyte-endothelial cell interactions would impair prostacyclin production (6), which would cause thrombogenesis. Second, AGE act on endothelial cells, which serve as a barrier between circulating blood and parenchyma and produced various vasoactive substances. As shown in this paper, one consequence is angiogenesis that is probably mediated by autocrine VEGF. In addition, the prostacyclin-synthesizing ability of microvascular endothelial cells might be directly inhibited by AGE, as in umbilical endothelial cells (35). Again, the consequence of this would be thrombogenesis. Diminished circulation or microthrombus formation may occur in such lesions, giving rise to hypoxia, the major factor triggering VEGF expression in both endothelial cells and pericytes (20, 37–40). In such circumstances, angiogenesis would further proceed, which may eventually lead to the clinical expression of diabetic microangiopathies, exemplified by proliferative retinopathy. According to this model, procedures that can halt those events, *e.g.* inhibition of AGE formation,[1] AGE absorption by immobilized antibodies, antisense RAGE DNA (35, 36), prostacyclin analogues, or anti-VEGF neutralizing antibodies would then theoretically help circumvent the development and progression of diabetic microangiopathies.

Although this view basically stands on the *in vitro* experiments, in support are several *in vivo* or clinical observations.

[1] Sato *et al.* (51) have recently developed a novel class of inhibitors of AGE formation, which are distinct from aminoguanidine in both structure and mode of action.

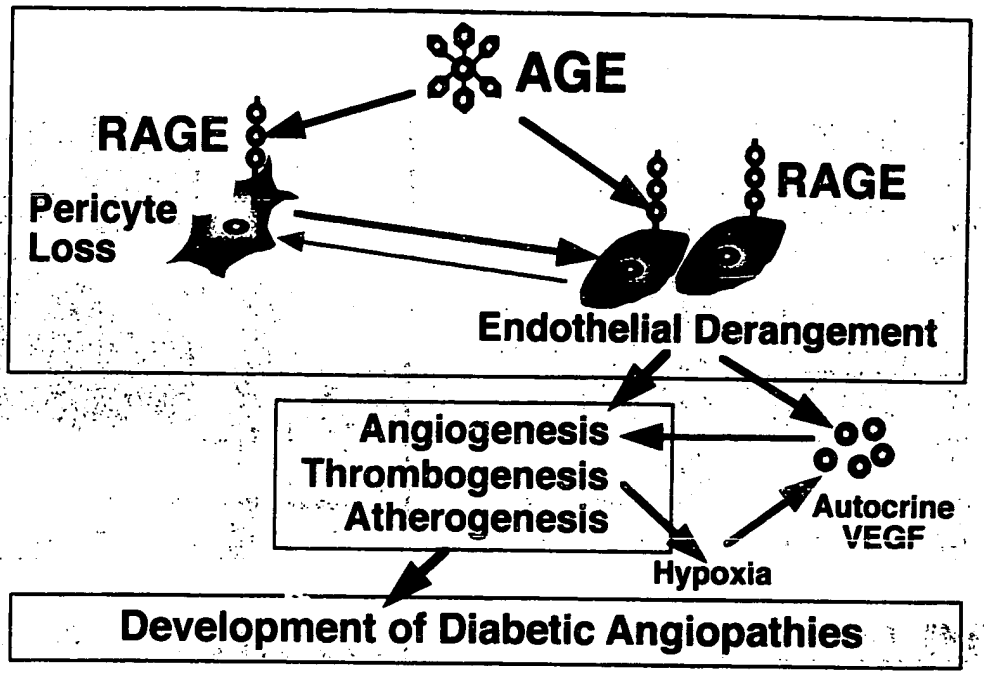

FIG. 8. **Possible mechanism of the development of diabetic microangiopathy.** *AGE*, advanced glycation end products; *RAGE*, a receptor for AGE; *VEGF*, vascular endothelial growth factor. Concerning (1) pericyte-endothelial cell interactions, (2) AGE effect on pericytes, (3) AGE-RAGE interaction in umbilical vein endothelial cells, and (4) hypoxia induction of vascular VEGF, refer to (1) Refs. 6 and 18, (2) Ref. 9, (3) Ref. 35, and (4) Ref. 20, respectively.

Hammes *et al.* (41, 42) reported that aminoguanidine, an inhibitor of AGE formation, prevented AGE accumulation at branching sites of precapillary arterioles and that this inhibitor could diminish pericyte dropout and inhibit abnormal endothelial cell proliferation in streptozotocin-induced diabetic rats. Dolhofer-Bliesener *et al.* (43) have shown that, in human diabetic subjects, the serum level of AGE was associated with the state of late complications, particularly in cases with retinopathy. Wautier *et al.* (44) reported that infusion of diabetic red blood cells into normal rats can induce vascular hyperpermeability, which was completely inhibited by anti-RAGE IgG; they also demonstrated that an antioxidant, probucol, can similarly reverse the red blood cell transfer-induced vascular permeability, suggesting a role of AGE-RAGE interactions and the involvement of an oxidant stress-sensitive pathway in the development of hyperpermeability. Recent clinical studies at different institutions have established that intraocular concentrations of VEGF correlated with active neovascularization (45, 46). Further, the increased permeability of retinal capillaries and the breakdown of the blood-retinal barrier have been shown to be as an early event in both human diabetic subjects and streptozotocin diabetic rats followed by new vessel formation (47, 48). The barrier breakdown would help ensure pericyte access to AGE. Moreover, it is reported that the barrier breakdown could be protected by the treatment of aminoguanidine, suggesting that AGE themselves may be directly involved in the barrier breakdown (48).

Acknowledgments—We thank Professor Kari Alitalo, Helsinki University and Dr. Ulf Eriksson, Ludwig Institute for Cancer Research for kindly providing VEGF-B and VEGF-C, Kurabo Industries, Ltd., Osaka for human capillary endothelial cells, Shin-ichi Matsudaira and Reiko Kitamura for assistance, and Brent Bell for reading the manuscript.

REFERENCES

1. Brownlee, M., Cerami, A., and Vlassara, H. (1988) *N. Engl. J. Med.* **318**, 1315-1321
2. Krolewski, A., Warram, J., Valsania, P., Martin, B., Laffel, L., and Christlieb, A. (1991) *Am. J. Med.* **90**, 56S-61S
3. Feldt-Rasmussen, B. (1986) *Diabetologia* **29**, 282-286
4. Johnson, P. C., Brendel, K., Meezan, E. (1982) *Arch. Pathol. Lab. Med.* **60**, 214-217
5. Kuwabara, T., and Kogan, D. G. (1960) *Arch. Ophthalmol.* **64**, 904-911
6. Yamagishi, S., Kobayashi, K., and Yamamoto, H. (1993) *Biochem. Biophys. Res. Commun.* **190**, 418-425
7. Shepro, D., and Morel, N. M. (1993) *FASEB J.* **7**, 1031-1038
8. Neeper, M., Schmidt, A. M., Brett, J., Yan, S. D., Wang, F., Pan, Y.-C. E., Elliston, K., Stern, D., and Shaw, A. (1992) *J. Biol. Chem.* **267**, 14998-15004
9. Yamagishi, S., Hsu, C.-C., Taniguchi, M., Harada, S., Yamamoto, Y., Ohsawa, K., Kobayashi, K., and Yamamoto, H. (1995) *Biochem. Biophys. Res. Commun.* **213**, 681-687
10. Doi, T., Vlassara, H., Kirstein, M., Yamada, Y., Striker, G. E., and Striker, L. J. (1992) *Proc. Natl. Acad. Sci. U. S. A.* **89**, 2873-2877
11. Esposito, C., Gerlach, H., Brett, J., Stern, D., and Vlassara, H. (1989) *J. Exp. Med.* **170**, 1387-1407
12. Bradford, M. M. (1976) *Anal. Biochem.* **72**, 248-254
13. Makita, Z., Vlassara, H., Cerami, A., and Bucala, R. (1992) *J. Biol. Chem.* **267**, 5133-5138
14. Horiuchi, S., Araki, N., and Morino, Y. (1991) *J. Biol. Chem.* **266**, 7329-7332
15. Micheel, F., and Hagemann, G. (1959) *Chem. Ber.* **90**, 2836-2840
16. Ahmed, M. U., Thorpe, S. R., and Baynes, J. W. (1986) *J. Biol. Chem.* **261**, 4889-4894
17. Reddy, S., Bichlar, J., Wells-Knecht, K. J., Thorpe, S. R., and Baynes, J. W. (1995) *Biochemistry* **34**, 10872-10878
18. Yamagishi, S., Hsu, C.-C., Kobayashi, K., and Yamamoto, H. (1993) *Biochem. Biophys. Res. Commun.* **191**, 840-846
19. Miyazono, K., Okabe, T., Urabe, A., Takaku, F., and Heldin, C.-H. (1987) *J. Biol. Chem.* **262**, 4098-4103
20. Nomura, M., Yamagishi, S., Harada, S., Hayashi, Y., Yamashima, T., Yamashita, J., and Yamamoto, H. (1995) *J. Biol. Chem.* **270**, 28316-28324
21. Aviv, H., and Leder, P. (1972) *Proc. Natl. Acad. Sci. U.S.A.* **69**, 1408-1412
22. Hatakeyama, H., Miyamori, I., Fujita, T., Takeda, Y., Takeda, R., and Yamamoto, H. (1994) *J. Biol. Chem.* **269**, 24316-24320
23. Ooka, H., Chonan, E., Mizutani, K., Fukuda, T., Kuroiwa, Y., Ono, Y., and Shigeta, S. (1992) *Microbiol. Immunol.* **36**, 1305-1316
24. Kubota, Y., Kleinman, H. K., Martin, G. R., and Lawley, T. J. (1989) *J. Cell Biol.* **107**, 1589-1598
25. Grant, D. S., Lelkes, P. I., Fukuda, K., and Kleinman, H. K. (1991) *In Vitro Cell. Dev. Biol.* **27A**, 327-336
26. Hayase, F., Nagaraj, R. H., Miyata, S., Njoroge, F. G., and Monnier, V. M. (1989) *J. Biol. Chem.* **264**, 3758-3764
27. Gugliucci, A., and Bendayan, M. (1996) *Diabetologia* **39**, 149-160
28. Nakayama, H., Taneda, S., Kuwajima, S., Aoki, S., Kuroda, Y., Misawa, K., and Nakagawa, S. (1989) *Biochem. Biophys. Res. Commun.* **162**, 740-745
29. Houck, K. A., Ferrara, N., Winer, J., Cachianes, G., Li, B., and Leung, D. W. (1991) *Mol. Endocrinol.* **5**, 1806-1814
30. Ferrara, N., Houck, K. A., Jakeman, L., and Leung, D. W. (1992) *Endocr. Rev.* **13**, 18-32
31. Termam, B. I., Dougher-Vermazen, M., Carrion, M. E., Dimitrov, D., Armellino, D. C., Gospodarowics, D., and Bohlen, P. (1992) *Biochem. Biophys. Res. Commun.* **187**, 1579-11586
32. Vries, C. D., Escobedo, J. A., Ueno, H., Houck, K. A., Ferrara, N., and Williams, L. T. (1992) *Science* **255**, 989-991

33. Folkman, J., and Haudenschild, C. (1980) *Nature* **288**, 551–556
34. Folkman, J., and Shing, Y. (1992) *J. Biol. Chem.* **267**, 10931–10934
35. Yamagishi, S., Yamamoto, Y., Harada, S., Hsu, C.-C., and Yamamoto, H. (1996) *FEBS Lett.* **384**, 103–106
36. Yamamoto, Y., Yamagishi, S., Hsu, C.-C., and Yamamoto, H. (1996) *Biochem. Biophys. Res. Commun.* **222**, 700–705
37. Namiki, A., Brogi, E., Kearney, M., Kim, E. A., Wu, T., Couffinhal, T., Varticovski, L., and Isner, J. M. (1995) *J. Biol. Chem.* **270**, 31189–31195
38. Simorre-Pinatel, V., Guerrin, M., Chollet, P., Penary, M., Clamens, S. Malecaze, F., and Plouet, J. (1994) *Invest. Ophthalmol. & Visual Sci.* **35**, 3393–3400
39. Shima, D. T., Deutsch, U., and D'Amore, P. A. (1995) *FEBS Lett.* **370**, 203–208
40. Shima, D. T., Adamis, A. P., Ferrara, N., Yeo, K.-T., Yeo, T.-K., Allende, R., Folkman, J., and D'Amore, P. A. (1995) *Mol. Med. (Camb.)* **1**, 182–193
41. Hammes, H. P., Martin, S., Federlin, K., Geisen, K., and Brownlee, M. (1991) *Proc. Natl. Acad. Sci. U. S. A.* **88**, 11555–11558
42. Hammes, H. P., Strödter, D., Weiss, A., Bretzel, R. G., Federlin, K., and Brownlee, M. (1995) *Diabetologia* **38**, 656–660
43. Dolhofer-Bliesener, R., Lechner, B., and Gerbitz, K. D. (1996) *Eur. J. Clin. Chem. Clin. Biochem.* **34**, 355–361
44. Wautier, J. L., Zoukourian, C., Chappey, O., Wautier, M. P., Guillausseau, P. J., Cao, R., Hori, O., Stern, D., and Schmidt, A. M. (1996) *J. Clin. Invest.* **97**, 238–243
45. Aiello, L. P., Avery, R. L., Arrigg, P. G., Keyt, B. A., Jampel, H. D., Shah, S. T., Pasquale, L. R., Thieme, H., Iwamoto, M. A., Park, J. E., Nguyen, H. V., Aiello, L. M., Ferrara, N., and King, G. L. (1994) *N. Engl. J. Med.* **331**, 1480–1487
46. Adamis, A. P., Miller, J. W., Bernal, M.-T., D'Amico, D. J., Folkman, J., Yeo, T.-K., and Yeo, K.-T. (1994) *Am. J. Ophthalmol.* **118**, 445–450
47. Dorchy, H. (1993) *Diabetes Care* **16**, 1212–1214
48. Cho, H. K., Kozu, H., Peyman, G. A., Parry, G. J., and Khoobehi, B. (1990) *Ophthalmic Surg.* **22**, 44–47
49. Olofsson, B., Pajusola, K., Kaipainen, A., von Euler, G., Joukov, V., Saksela, O., Orpana, A., Pettersson, R. F., Alitalo, K., and Eriksson U. (1996) *Proc. Natl. Acad. Sci. U. S. A.* **93**, 2576–2581
50. Joukov, V., Pajusola, K., Kaipainen, A., Chilov, D., Lahtinen, I., Kukk, E., Saksela, O., Kalkkinen, N., and Alitalo, K. (1996) *EMBO J.* **15**, 290–298
51. Sato, F., Katsuno, K., Kobayashi, M., Koizumi, T., Baba, Y., Kusama, H., and Iyobe, A. (1996) *Diabetes* **45**, Suppl. 2, 264 (abstr.)

STIC-ILL QP351.N43

From: Holleran, Anne
Sent: Sunday, March 04, 2001 5:30 PM
To: STIC-ILL
Subject: refs. for 09/266,543

Examiner: Anne Holleran
Art Unit: 1642; Rm 8E03
Phone: 308-8892
Date needed by: ASAP

Please send me copies of the following :

1. Plum, S.M. et al. Vaccine, (2000) 19/9-10, 1294-1303
2. Aonuma, M. et al. Anticancer Res. (1999, Oct) 19(5B): 4039-4044
3. Muller, Y.A. et al. Structure (1998) 6(9): 1153-1167
4. Yamagishi, S. et al. J. Biol. Chem. (1997) 272(13): 8723-8730
5. Koolwijk, P. et al. J. Cell Biology (1996) 132(6): 1177-1188
6. Matsuo, A. et al. Neuroscience (1994) 60(1): 49-66
7. Djakiew, D. et al. Cancer Research (1991) 51(12): 3304-3310
8. Yamanishi, H. et al. Cancer Research (1991) 51(11): 3006-3010
9. Matsuzaki, K. et al. Japanese J. Cancer Research (1990) 81(4): 345-354
10. Kardami, E. et al. Growth Factors (1990) 4(1): 69-80
11. Riss, T.L. et al. J. Cellular Physiology (1989) 138(2): 405-414

regulation of BDNF and
r. molec. Biol. Org. J. 9,

ain-derived neurotrophic
strocytes. *J. Neurosci.* 12,

Pergamon

0306-4522(93)-E0043-P

Neuroscience Vol. 60, No. 1, pp. 49–66, 1994
Elsevier Science Ltd

0306-4522/94 $6.00 + 0.00

IMMUNOHISTOCHEMICAL LOCALIZATION IN THE RAT BRAIN OF AN EPITOPE CORRESPONDING TO THE FIBROBLAST GROWTH FACTOR RECEPTOR-1

A. MATSUO,* I. TOOYAMA,† S. ISOBE,‡ Y. OOMURA,§ I. AKIGUCHI,* K. HANAI,† J. KIMURA* and H. KIMURA†¶

*Department of Neurology, Kyoto University, Kyoto, Japan
†Institute of Molecular Neurobiology, Shiga University of Medical Science, Otsu, Japan
‡Institute of Wakanyaku, Toyama Medical and Pharmaceutical University, Toyama, Japan
§Nipponzoki Institute of Bioactive Science, Hyogo, Japan

Abstract—The localization of fibroblast growth factor receptor-1 was investigated in rat brain by immunohistochemistry using a polyclonal antibody against an acidic peptide sequence of chicken fibroblast growth factor receptor-1. For raising the antisera in rabbits, we synthesized the oligopeptide EDDDDEDDSSSEEKEAD which is a highly acidic region of chicken fibroblast growth factor receptor-1. The oligopeptide was used as a haptenic antigen by conjugating with poly-L-glutamate as a carrier protein. On immunospot assay, the best antiserum was capable of detecting 15.7 pmols of both the chicken and its analogous human oligopeptides but failed to react even with up to 1 nmol of poly-L-glutamate. When rat brain homogenate was examined by Western blots, the antiserum revealed two bands with molecular weights of 145,000 and 75,000 corresponding to known sizes of the membrane-bound and secreted forms of the rat receptor, respectively. Immunohistochemistry in rat brain demonstrated that putative fibroblast growth factor receptor-1 immunoreactivity sites were present mainly in neurons but also in tanycytes and ependymal cells. Positive neurons were distributed widely in various brain regions, but were particularly abundant in such regions as the lateral hypothalamus, substantia nigra, locus coeruleus and raphe nuclei. The present study suggests that fibroblast growth factor receptor-1 is expressed preferentially in certain neuronal systems that appear to be under the influence of fibroblast growth factors in the normal brain. The result should facilitate study of the functional significance of fibroblast growth factors in these brain neurons.

Fibroblast growth factor (FGF) was originally reported as a growth factor which promotes the proliferation of mesodermal tissue.[15] It is now well established, however, that FGFs comprise a family of polypeptides that exhibit mitogenic activity toward a wide variety of not only mesodermal but also neuroectodermal cells.[4] Acidic FGF (aFGF) and basic FGF (bFGF) were the first members of this family that were purified and characterized. Since both FGFs are richly present in the brain,[28,38,41,50] they may have important physiological roles in brain function.

FGFs have been thought to exert their biological activities through interaction with specific cell surface receptors in responsive cells. In order to clarify the roles of FGFs in the brain, therefore, it is essential to comprehend the cellular localization of their receptors in this organ. So far at least four genes of FGF receptors (FGFRs) have been identified.[20] These include; (i) *flg* (FGFR-1) cloned from cDNA libraries of a human brain stem,[7] a human placenta,[18] a human umbilical vein endothelial cell[18] and a chicken embryo[25]; (ii) *bek* (FGFR-2) isolated from a human brain stem cDNA library[7]; (iii) FGFR-3 identified in a human K-562 cDNA library[21] and (iv) FGFR-4 expressed in K562 erythroleukemia cells.[33] Although FGFR-4 has a high and selective affinity for aFGF, the other three react with both aFGF and bFGF. Concerning the expression of FGFR-1 mRNA, some studies in normal mammals (mouse[3] and rat[47]) and developing animals (chicken,[17] mouse[35] and rat[48]) have been reported recently. At the protein level, however, there has been no report dealing with the cellular localization of FGFRs in normal adult mammals.

Therefore, we have tried to prepare antisera specific for one of the FGFRs, aiming to visualize its accurate distribution by immunohistochemistry in the adult rat brain. In the present study, we chose FGFR-1 because its molecular basis has been most extensively studied among the three common receptors for aFGF and bFGF. For raising antisera, a synthetic oligipeptide antigen was selected from the known amino acid sequence for FGFR-1 of chicken,[23] because no report in rat brain was available

¶To whom correspondence should be addressed.
Abbreviations: FGF, fibroblast growth factor; aFGF, acidic FGF; bFGF, basic FGF; FGFR, FGF receptor; EDTA, disodium ethlenediaminetetra-acetate; SDS–PAGE, sodium dodecyl sulfate–polyacrylamide gel electrophoresis; PCR, polymerase chain reaction.

when we started this study. In order to examine whether the obtained antiserum is capable of cross-reacting with rat brain FGFR-1, its partial sequence was analysed by using a polymerase chain reaction (PCR)-cloning method.[29]

EXPERIMENTAL PROCEDURES

Production and characterization of the antiserum to fibroblast growth factor receptor-1

An immunogen was prepared by conjugating 10 mg of the synthetic oligopeptide (EDDDDEDDSSSEEKEAD), the sequence of which is coded in a highly acidic region of FGFR-1 of chicken,[25] to 100 mg of poly-L-glutamate with water soluble carbodiimide. The method of conjugation is essentially identical with that reported previously.[1]

Three Japanese white rabbits (Kiwa Lab., Japan) weighing 2.0–2.5 kg were used for the production of anti-FGFR sera. Prior to immunization, the blood was collected as a control pre-immune serum from each rabbit. The animals were injected every two weeks with the immunogen emulsified with Freund's adjuvant. Blood samples were collected four days after every booster injection. The specificity of the antisera was examined by immunospot assay, western blots and immunoabsorption test.

The immunospot assay was modified from the description of Larsson.[24] In brief, a 1 μl solution of a test compound, in an amount ranging from 1 to 0.0038 nmol, was spotted on a gelatin-coated cellulose acetate membrane. The membrane was then fixed for 1 h with paraformaldehyde vapor at 80°C and washed with 10 mM phosphate-buffered saline (pH 7.4). The membrane was incubated overnight with a primary anti-FGFR serum (1:10000) at room temperature and stained by the immunohistochemical procedure described below.

For western blots, fresh tissues of rat brain were homogenized in five volumes of ice-cold 10 mM Tris–HCl (pH 7.4) containing 1 mM EDTA, phenylmethyl-sulfonyl-fluoride (100 μg/ml), leupeptin (1 μg/ml), pepstatin (1 μg/ml) and aprotinin (1 μg/ml). The homogenate was centrifuged at 15,000 rpm for 20 min at 4°C. The pellet was homogenized at 4°C and the suspension was kept on ice for 1 h in 25 mM Tris–HCl plus 150 mM NaCl (pH 7.4) containing 1% Triton-X 100 and phenylmethyl-sulfonyl-fluoride (100 μg/ml). The suspension was centrifuged at 15,000 rpm for 20 min at 4°C. The supernatant was collected as a crude soluble membrane fraction. About 100 μg of the soluble membrane fraction was electrophoresed, together with a commercial preparation of FGFR fusion protein (110,000 mol. wt; UBI, U.S.A.) in an estimated amount of 100 ng, on 6% sodium dodecyl sulfate–polyacrylamide gel (SDS–PAGE) and then transferred to polyvinyliden difluoride membrane (Immobilon-P, Millipore Japan, Japan). The membrane was incubated for 30 min with 25 mM Tris–HCl containing 150 mM NaCl and 5% skim milk at room temperature and further incubated overnight with a FGFR-1 antiserum (1:10000) in 25 mM Tris–HCl containing 150 mM NaCl and 1% skim milk at room temperature. After washing with 25 mM Tris–HCl containing 150 mM NaCl and 0.1% Tween 20, the membrane was reacted for 2 h with alkaline phosphatase-labeled anti-rabbit IgG (1:2000, GIBCO BRL, U.S.A.) in 25 mM Tris–HCl containing 150 mM NaCl and 1% skim milk at room temperature. The labeling was visualized by incubating with nitroblue tetrazolium (0.33 mg/ml, GIBCO BRL, U.S.A.) and 5-bromo-4-chloro-3-indolyl-phosphate (0.165 mg/ml, GIBCO BRL, U.S.A.) in 100 mM Tris–HCl (pH 9.5) containing 100 mM NaCl and 50 mM $MgCl_2$.

An immunoabsorption test was employed by using another synthetic oligopeptide (EDDDDDDDSSSEEKEAD) which is contained in a highly acidic region of FGFR-1 of the human, instead of the chicken noted above. The oligopeptide (1.5 mg) was conjugated with a 45 μl suspension of Affigel-15 (Bio-Rad, U.S.A.) according to the manufacturer's recommendation. A volume of 0.2 μl FGFR-1 antiserum was diluted with 200 μl of phosphate-buffered saline containing 0.3% Triton X-100 and incubated overnight with a 45 μl suspension of the peptide-bound Affigel-15 at room temperature. The suspension was centrifuged at 1000 rpm for 3 min and the supernatant was collected as an absorbed serum. For a positive control, 200 μl of an antiserum (diluted 1:1000) was incubated overnight at room temperature with 45 μl of unconjugated Affigel-15. After centrifugation, the resulting supernatant was used as a positive control antiserum for the immunoabsorption test.

Tissue preparations for immunohistochemistry

Ten male Wistar rats (Clea Japan Inc., Japan) weighing 200–250 g were used. The animals were housed on a 12 h light/dark schedule (08:00–20:00) and given free access to food and water. Under pentobarbital anesthesia (80 mg/kg), the animals were perfused via the ascending aorta with 10 mM phosphate buffer containing 0.9% NaCl (pH 7.4) followed by a fixative containing 4% paraformaldehyde, 0.2% picrate and 0.35% glutaraldehyde in 100 mM phosphate buffer (pH 7.4). The animals were kept in crushed ice during the perfusion. After perfusion the brain was quickly removed and cut into 5–7-mm coronal blocks. The blocks were immersed for one or two days in a fixative consisting of 4% paraformaldehyde and 0.2% picrate in 100 mM phosphate buffer (pH 7.4). The blocks were then placed in 100 mM phosphate buffer containing 15% sucrose, frozen with dry-ice and cut into 20-μm-thick sections. The sections were collected in phosphate-buffered saline containing 0.3% Triton X-100. All the above procedures were carried out at 4°C.

Immunohistochemical procedures

The sections in a free-floating state were first incubated for three days with FGFR-1 antiserum (diluted 1:10000) at 4°C, for 2 h with biotinylated anti-rabbit IgG (diluted 1:1000, Vector Labs., U.S.A.) at room temperature and for 1 h with the avidin–biotin–peroxidase complex (diluted 1:4000, Vector Labs., U.S.A.) at room temperature. Dilution of antisera and wash of sections were all done with phosphate-buffered saline containing 0.3% Triton X-100. Color was developed by reacting the sections for 20 min with a mixture containing 0.02% 3,3'-diaminobenzidine, 0.0045% H_2O_2 and 0.3% nickel ammonium sulfate in 50 mM Tris–HCl buffer (pH 7.6). The stained sections were mounted on gelatin-coated glass slides, air-dried, dehydrated and cover-slipped. Some sections were counterstained with Neutral Red for histological examination. Image analysis was performed to measure the major axes of immunoreactive cell bodies by using a computer-assisted image analyser (Qube 6000, Nexus Inc., Japan) attached with a light microscope.

Partial sequencing of rat fibroblast growth factor receptor-1

Total RNA was isolated from the whole brain of a rat according to the acid guanidium thiocyanate-phenol method[5] with a slight modification. In brief, approximately 100 mg of fresh brain tissue was homogenized for 45 s at room temperature in 0.6 ml of a denaturing solution consisting of 4 M guanidium thiocyanate, 0.5% sarcosyl, 0.1 M 2-mercaptoethanol in 25 mM sodium citrate (pH 7.0). To the homogenate were added sequentially, 0.12 ml of 2 M sodium acetate (pH 4.0), 0.6 ml of water saturated phenol and 0.12 ml of chloroform, with thorough mixing after the addition of each reagent. The final suspension was vortexed for 15 s, cooled on ice for 15 min and centrifuged at 10,000g for 15 min at 4°C. After centrifugation, the aqueous phase

containing RNA was transferred to a new tube. The remaining pellet was re-extracted two to three times and all the aqueous samples were combined together in the same tube. After the final extraction, RNA in the aqueous solution was precipitated by adding an equal volume of isopropanol and kept at −20°C for 1 h. The solution was then centrifuged at 10,000*g* for 10 min at 4°C and the resulting pellet was washed with 0.5 ml of 4 M lithium chloride to solubilize polysaccharides that were co-precipitated with RNA. The insoluble RNA was collected again by centrifuging at 10,000*g* for 5 min at 4°C, dissolved in 0.3 ml of 4 M guanidium thiocyanate containing 0.5% sarcosyl, 0.1 M 2-mercaptoethanol in 25 mM sodium citrate (pH 7.0) and then re-precipitated with one volume of isopropanol containing 0.2 M sodium acetate (pH 4.0) at −20°C for 1 h. After centrifugation at 3000*g* for 10 min at 4°C, the pellet was washed two times with 70% ethanol, centrifuged and vacuum dried. Finally the pellet was dissolved in 50 μl of distilled water which had been incubated overnight with 0.02% diethyl pyrocarbonate and autoclaved for 20 min at 125 C.

Prior to reverse transcription, 5 μg of the total RNA as prepared above was incubated, to eliminate trace DNA contamination, for 1 h at 37°C with 10 units RNAse free DNAse (Pharmacia, U.S.A.) and 20 units of RNAsin (Pharmacia, U.S.A.). Then the DNAse was inactivated by heating for 5 min at 95°C and the total RNA was reverse-transcribed using 500 pmol of random hexamers (Pharmacia, U.S.A.) with 80 units of Maloney murine leukemia virus reverse transcriptase (Pharmacia, U.S.A.) for 1 h at 37°C. Finally the reverse transcriptase was inactivated by heating for 10 min at 65°C.

About one-tenth of the cDNA obtained was then amplified by PCR with the following primers: primer 1 (sense), 5'-ATACCACCTACTTCTCCGTCAATGT-3' (corresponding to nucleotides 386–410 of mouse bFGF-R mRNA); primer 2 (antisense), 5'-AGTCCGATAGAGT-TACCCGCCAAGC-3' (corresponding to nucleotides 1079–1103 of mouse bFGF-R mRNA).[35] The DNA thermal cycler (Astec, Japan) step program consisted of 30 cycles as follows: 94°C, 30 s; 55°C, 1 min; 72°C, 1 min. The PCR products were electrophoresed in a 1% NuSieve (FMC Products, U.S.A.) /1% Seakem (FMC Products, U.S.A.) agarose gel. The examination by ethidium bromide staining gave a single band of 720 bp, which corresponded well to the size estimated from the sequence of mouse bFGF receptor. The band in the agarose gel was dissected out and the target DNA in the band was eluted by using GeneClean II kit (Bio101, U.S.A.) followed by ethanol precipitation.

For the cloning of the target DNA, pBluescript II (Stratagene, U.S.A.) was first digested with the restriction enzyme EcoRV (Toyobo, Japan) and tailed by using Taq polymerase (Perkin–Elmer/Cetus, U.S.A.) with TTP to both 3'-blunt ends (T-pBS vector).[29] Then the target DNA sequence was inserted into the T-pBS vector by using a DNA ligation kit (Takara, Japan) according to the manufacturer's protocol. The prepared plasmid DNA was transformed into *E. coli* (JM109 cells, Toyobo, Japan) by electroporation. The amplified plasmid DNA was extracted by the alkaline lysis method.[37] The double stranded DNA was purified by using GeneClean II kit and finally applied to a DNA sequencer (A.L.F., Pharmacia, U.S.A.).

RESULTS

Partial nucleotide sequence of rat fibroblast growth factor receptor-1 and its deduced amino acid sequence

The partial nucleotide sequence of rat brain FGFR-1 is shown in Fig. 1. For comparison, previously reported sequences of FGFR-1 in rat prostate tumor cells,[52] mouse embryonic neuroepithelium,[35] and human embryonic lung[9] are also presented. The sequence coding the highly acidic region in rat brain is exactly the same as in all sequences. However, both the rat brain and human lung sequences lack six successive nucleotides downstream from the acidic region. Figure 1b shows the amino acid sequence of the rat brain FGFR-1 deduced from the result in Fig. 1a. Significant homology in deduced sequence can be seen between rat brain and the other sources. In particular, the sequence representing the highly acidic region in rat brain is completely identical with that reported for the three mammals (rat prostate,[52] mouse neuroepithelium[35] and human embryonic lung[9]), but is two amino acids different from that for chicken embryo.[25]

Specificity of antisera against fibroblast growth factor receptor-1

The result of immunospot assay using the highest titer FGFR-1 antiserum is represented in Fig. 2a. This antiserum was capable of detecting 15.7 pmols of both chicken and human oligopeptides coding the highly acidic regions of FGFR-1, but failed to react even with 1 nmol of an oligopeptide coding a corresponding site of human FGFR-4 (NDDEDPKSHRDPSNRHS) and of poly-L-glutamate, the carrier protein of the immunogen. Thus we used this antiserum in various studies as described below.

Although our preliminary experiment indicated a possible impurity of the preparation of FGFR-1 fusion protein, our antiserum detected only one band in this preparation by western blots. The estimated molecular weight was approximately 110,000, corresponding well with predicted molecular weight of the fusion protein (Fig. 2b, lane A). Western blots in rat brain homogenate showed that the antiserum recognized two bands of about 75,000 and 145,000 mol. wt (Fig. 2b, lane B).

In the immunoabsorption test, the absorbed antiserum did not show any positive structures in any sections of rat brain, whereas the positive control antiserum revealed specific staining similar to that observed with the original FGFR-1 antiserum.

Distribution of fibroblast growth factor receptor-1-like immunoreactive structures in rat brain

In rat brain, putative FGFR-1-like immunoreactivity was observed mainly in neurons. Exceptions were a few stained tanycytes and ependymal cells situated in the wall of the cerebral ventricle. As illustrated in Fig. 4, the reaction product in neurons appeared to occur typically on the surface of cells, though there were occasional deposits in the cytoplasm. In some brain regions, dendritic or axonal processes were also visible (Fig. 5). Maps of positive neuronal somata are presented in Fig. 3 with 21 schematic drawings of coronal sections, corresponding to levels in the atlas of Paxinos and Watson.[34]

a

```
HUMAN   451 GGCCTCTATG CTTGCGTAAC CAGCAGCCCC TCGGGCAGTG ACACCACCTA 500
MOUSE   346 GGCCTCTACG CTTGCGTGAC CAGCAGCCCC TCTGGCAGCG ATACCACCTA 395
RAT-P   356 GGCCTCTACG CTTGTGTGAC CAACAGCCCC TCTGGCAGCG ATACCACCTA 405
RAT-B                                                 ATACCACCTA

HUMAN   501 CTTCTCCGTC AATGTTTCAG ATGCTCTCCC CTCCTCGGAG GATGATGATG 550
MOUSE   396 CTTCTCCGTC AATGTCTCAG ATGCACTCCC ATCCTCGGAA GATGATGACG 445
RAT-P   406 CTTCTCCGTC AATGTCTCAG ATGCACTGCC ATCCTCGGAG GACGATGACG 455
RAT-B       CTTCTCCGTC AATGTCTCAG ATGCACTGCC ATCCTCGGAG GACGATGACG

HUMAN   551 ATGATGATGA CTCCTCTTCA GAGGAGAAAG AAACAGATAA CACCAAACCA 600
MOUSE   446 ACGACGATGA CTCCTCCTCG GAGGAGAAAG AGACGGACAA CACCAAACCA 495
RAT-P   456 ATGATGATGA CTCCTCCTCA GAGGAGAAAG AGACAGACAG CACCAAACCA 505
RAT-B       ATGATGATGA CTCCTCCTCA GAGGAGAAAG AGACAGACAA CACCAAACCA

HUMAN   601 AAC------C CCGTAGCTCC ATATTGGACA TCCCCAGAAA AGATGGAAAA 644
MOUSE   496 AACCGTAGGC CTGTAGCTCC CTACTGGACA TCCCCAGAGA AAATGGAGAA 545
RAT-P   506 AACCGTAGGC CTGTGGCGCC ATACTGGACA TCCCCAGAGA AAATGGAGAA 555
RAT-B       AAC------C CTGTGGCGCC ATACTGGACA TCCCCAGAGA AAATGGAGAA

HUMAN   645 GAAATTGCAT GCAGTGCCGG CTGCCAAGAC AGTGAAGTTC AAATGCCCTT 694
MOUSE   546 GAAACTGCAT GCGGTGCCCG CTGCCAAGAC GGTGAAGTTC AAGTGCCCGT 595
RAT-P   556 GAAACTCGAC GCAGTGCCAG CTGCCAAGAC GGTGAAATTC AAATGCCCGT 605
RAT-B       GAAACTGCAC GCAGT
```

b

```
CHICKEN 110 TTYFSVNVSD ALPSAEDDDD EDDSSSEEKE ADNTKPNQA- VAPYWTYPEK 159
HUMAN   165 TTYFSVNVSD ALPSSEDDDD DDDSSSEEKE TDNTKPN--P VAPYWTSPEK 212
MOUSE   130 TTYFSVNVSD ALPSSEDDDD DDDSSSEEKE TDNTKPNRRP VAPYWTSPEK 179
RAT-P   111 TTYFSVNVSD ALPSSEDDDD DDDSSSEEKE TDSTKPNRRP VAPYWTSPEK 160
RAT-B       TTYFSVNVSD ALPSSEDDDD DDDSSSEEKE TDNTKPN--P VAPYWTSPEK

CHICKEN 160 MEKKLHA
HUMAN   213 MEKKLHA
MOUSE   180 MEKKLHA
RAT-P   161 MEKKLDA
RAT-B       MEKKLHA
```

Fig. 1. (a) A partial nucleotide sequence of FGFR-1 for rat brain (RAT-B) in comparison with that reported for rat prostate tumor cell line (RAT-P), mouse embryonic neuroepithelium (MOUSE) and human embryonic lung tissue (HUMAN). (b) The amino acid sequence deduced from the nucleotide sequence of rat brain FGFR-1 (RAT-B). For comparison, similar sequences reported for the RAT-P, MOUSE, HUMAN and chicken embryo (CHICKEN) are shown. Highly acidic regions of FGFR-1 are underlined.

Representative examples of immunohistochemical staining in various regions are shown in the photomicrographs of Figs 4–38. The size of cells was expressed as small (5–10 μm in mean diameter), medium-sized (11–15 μm), large (16–25 μm), or giant (over 25 μm).

Telencephalon

In the main olfactory bulb, putative FGFR-1 positive staining was found in the olfactory nerve layer and in many small cells (6.8 μm in mean diameter) of the periglomerular layer (Fig. 6). The reaction product in the small cells was packed in their cytoplasm, while those in the nerve layer appeared to cover the entire surface of the olfactory nerve bundles. A few positive cells of small size (8.2 μm in diameter) were also seen in the external plexiform layer, whereas no immunoreactive structure was detected in the mitral cell layer or the internal granular layer. In the accessory olfactory bulb, the vomeronasal nerve layer and the adjacent glomerular layer were coated almost uniformly with very tiny positive dots (Fig. 7).

The olfactory tubercle displayed a notable feature of intense staining in the major island of Calleja (Figs 3C–3E, 8, 9). Positively stained tiny dots were densely precipitated in the cytoplasm of the granule cells (Fig. 9) and the mean diameter of such somata was 7.9 μm. Few, if any, positive neurons were seen in either the plexiform, polymorphic or pyramidal layers.

The accumbens nucleus contained a moderate number of positive neurons (Figs 3D–3F, 10 and 11). These cells were small in size (9.2 μm in diameter) and possessed granular reaction products in the cytoplasm (Fig. 11). No positive structure was seen in

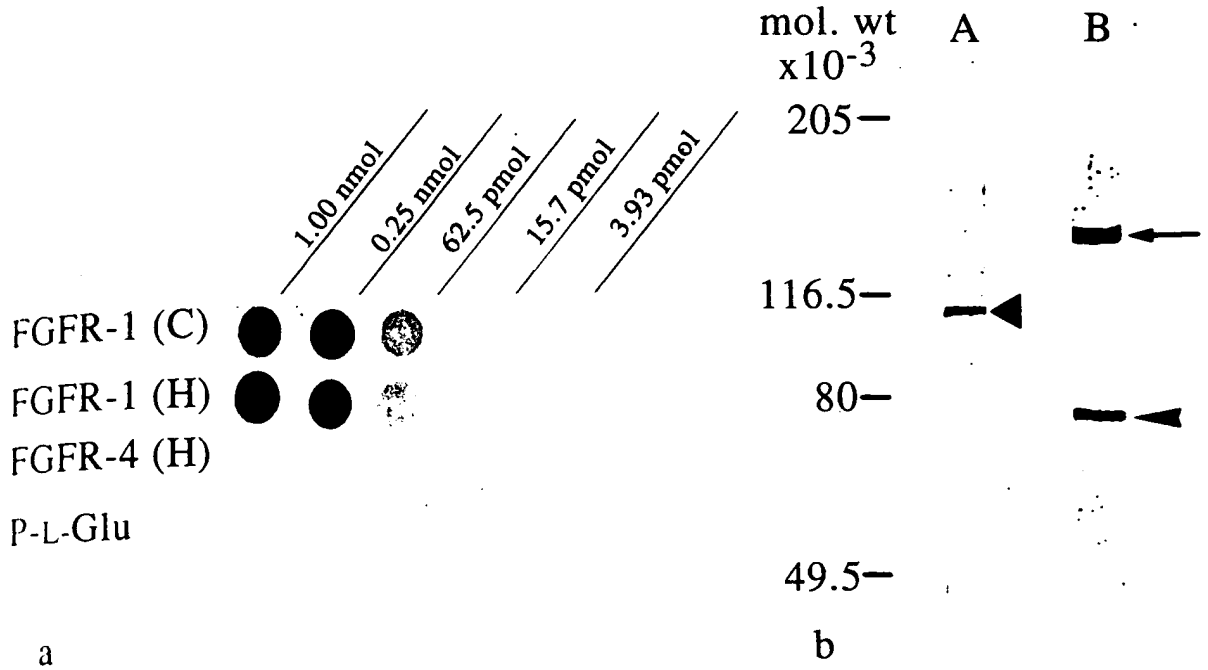

Fig. 2. The specificity of anti-FGFR serum examined by (a) immunospot assay with synthetic peptides or (b) western blots with a fusion protein. (a) Oligopeptides for FGFR-1 of the chicken [FGFR-1(C); lane 1], human [FGFR-1(H); lane 2], human FGFR-4 [FGFR-4(H); lane 3] and Poly-L-glutamate (P-L-Glu; lane 4). The antiserum (diluted 1:10000) detects as small as 15.7 pmols of FGFR-1 of both chicken and human, whereas it fails to recognize as large as 1.0 nmols of FGFR-4 oligopeptide and the carrier protein used for the immunogen to raising the antiserum. (b) The antiserum (diluted 1:10000) recognized 100 ng (as estimated according to the supplier) of FGFR-1 fusion protein with the molecular weight of 110,000 mol. wt (lane A; triangle) and the two bands of 145,000 and 75,000 mol. wt (lane B; arrow and arrowhead, respectively) in the rat brain homogenate.

the caudoputamen (Figs 3C–3I). In the septum (Figs 3C–3E, 12 and 13), medium-sized positive neurons (12.2 μm in diameter) were distributed in the lateral septal nucleus including the dorsal, intermediate and ventral parts, but not in the medial septal nucleus. The intermediate part of the lateral septal nucleus contained a particularly high density of positive cells (Fig. 12). In most cases, these neurons appeared to bear positive reaction products on the surface of somata and their proximal processes (Fig. 13). The diagonal band of Broca contained no positive staining (Fig. 3C, D).

In the cerebral cortex, a moderate density of putative FGFR-1-positive neurons was distributed throughout the entire extent from the frontal to occipital pole (Fig. 3A–3O). These neurons in the neocortex were mainly located in layers III and V (Fig. 14). The positive somata in layer III tended to be generally smaller in size (11.9 μm in diameter) than those in layer V (15.8 μm). They gradually decreased in number in cortices caudal to the retrosplenium. Positive staining was generally confined to the surface regions of perikarya and their proximal processes (Fig. 15). Similarly stained large sized cells (19.2 μm in diameter) were observed in the cingulate cortex (Figs 3A–G, 17, 18), but there was no tendency to locate in definite layers. In the piriform and entorhinal cortices, a few positive neurons were scattered (Fig. 3). These neurons, medium-sized (12.0 μm in diameter) and pyramidal in shape, were often found in layer III.

In the hippocampal formation, conspicuously intense staining was seen in pyramidal cells (20.2 μm in diameter) of the CA2 region (Figs 3I–K, 18), while other CA regions were stained only faintly (Fig. 18). High magnification revealed that the positive reaction product was near to the cell membrane of the CA2 pyramidal cells (Fig. 19). A number of neurons stained with moderate intensity were found in the granule cell layer of the dentate gyrus (6.7 μm in diameter, Fig. 3H–K) and the subiculum (18.2 μm in diameter, Fig. 3J–M).

Medium-sized (12.1 μm in diameter) multipolar neurons with moderate staining intensity were distributed in the amygdaloid complex. These cells were particularly abundant in the central and medial nuclei of the complex (Figs 3G–K, 20–22). Some, but not all, neurons in the bed nucleus of the stria terminalis showed positive staining with moderate intensity (Fig. 3D–F).

Diencephalon

No putative FGFR-1-positive neurons were recognizable in thalamic nuclei, with the exception of the medial habenular nucleus, which contained a few

faintly stained neuronal somata (10.3 μm in diameter, Fig. 3H,I).

In the hypothalamus, the most striking feature was found in the lateral hypothalamic area (Figs 3G–I, 23, 24). Here, intensely stained large neurons (20.8 μm in diameter) were scattered and their processes were also clearly observed to form a meshwork within this area (Fig. 24). A number of positive neurons were located in the dorsomedial (positive cell size: 15.6 μm in diameter, Fig. 3H–I), magnocellular part of the paraventricular (13.3 μm, Figs 3H, 25) and supraoptic nuclei (18.8 μm, Fig. 26) of the hypothalamus. In the suprachiasmatic nucleus, strongly stained small neurons (7.2 μm in diameter) were densely present in its ventromedial part (Fig. 26). The arcuate nucleus contained a moderate number of positive small sized neurons (7.0 μm in diameter). Few, if any, positive cells were observed in the ventromedial hypothalamic nucleus (Fig. 25).The medial forebrain bundle contained positive fiber bundles (Fig. 23).

Mesencephalon

Although no significant staining was present in the superior colliculus, the positive neurons were observed in the external and central nuclei of the inferior colliculus (Figs 3L–N, 31, 32). These cells were large in size (22.0 μm in diameter) and pyramidal in shape with multipolar processes. A small number of positive small sized neurons (9.6 μm in diameter) were also found in the central gray around the cerebral aqueduct (Fig. 3J–O). A few positive neurons with medium-sized somata (12.0 μm in diameter) were

Abbreviations used in figures

2n	optic nerve
3	oculomotor nucleus
3V	third ventricle
4V	fourth ventricle
6	abducens nucleus
A5	A5 noradrenaline cells
ac	anterior commissure
Acb	accumbens nucleus
ACo	anterior cortical amygdaloid nucleus
AOB	accessory olfactory bulb
AP	area postrema
Arc	arcuate hypothalamic nucleus
BIC	nucleus of the brachium of the inferior colliculus
BST	bed nucleus of the stria terminalis
CA1–4	fields CA1–4 of Ammon's horn
Ce	central amygdaloid nucleus
CeM	central amygdaloid nucleus, medial division
CG	central gray
Cg	cingulate cortex
CIC	central nucleus of the inferior colliculus
CLi	caudal linear nucleus of the raphe
CnF	cuneiform nucleus
CPu	caudoputamen
DG	dentate nucleus
DLL	dorsal nucleus of the lateral lemniscus
DM	dorsomedial hypothalamic nucleus
DpMe	deep mesencephalic nucleus
DR	dorsal raphe nucleus
ECIC	external cortex of the inferior colliculus
Ent	entorhinal cortex
EW	Edinger–Westphal nucleus fornix
Fr	frontal cortex
gcc	genu of the corpus callosum
Gl	glomerular layer of the olfactory bulb
ICjM	islands of Calleja, major island
IP	interpeduncular nucleus
IPC	interpeduncular nucleus, caudal subnucleus
IRt	intermediate reticular nucleus
LC	locus coeruleus
LH	lateral hypothalamic area
LPB	lateral parabrachial nucleus
LPGi	lateral paragigantocellular nucleus
LPO	lateral preoptic area
LRt	lateral reticular nucleus
LS	lateral septal nucleus
LSD	lateral septal nucleus, dorsal part
LSI	lateral septal nucleus, intermediate part
LSO	lateral superior olive
LSV	lateral septal nucleus, ventral part
LV	lateral ventricle
Me	medial amygdaloid nucleus
MeA	medial amygdaloid nucleus, anterior part
mfb	medial forebrain bundle
MnR	median raphe nucleus
MP	medial mammillary nucleus, posterior
MPB	medial parabrachial nucleus
MPO	medial preoptic nucleus
MS	medial septal nucleus
MVe	medial vestibular nucleus
Oc	occipital cortex
ON	olfactory nerve layer
Par	parietal cortex
PaV	paraventricular hypothalamic nucleus, ventral part
PCRt	parvocellular reticular nucleus
Pe	periventricular hypothalamic nucleus
Pir	piriform cortex
PMCo	posteromedial cortical amygdaloid nucleus
PnC	pontine reticular nucleus, caudal part
PnO	pontine reticular nucleus, oral part
RLi	rostral linear nucleus of the raphe
RMg	raphe magnus nucleus
ROb	raphe obscurus nucleus
RPa	raphe pallidus nucleus
RPn	raphe pontis nucleus
RRF	retrorubral field
RVL	rostroventrolateral nucleus
S	subiculum
SCh	suprachiasmatic nucleus
SFO	subfornical organ
SHi	septohippocampal nucleus
SHy	septohypothalamic nucleus
SNC	substantia nigra, pars compacta
SNR	substantia nigra, pars reticulata
SO	supraoptic nucleus
Sol	nucleus of the solitary tract
Sp5	spinal trigeminal nucleus
StHy	striohypothalamic nucleus
TS	triangular septal nucleus
TT	tenia tecta
Tu	olfactory tubercle
Tz	nucleus of the trapezoid body
VCA	ventral cochlear nucleus, anterior part
VDB	nucleus of the vertical limb of the diagonal band
VMH	ventromedial hypothalamic nucleus
VTA	ventral tegmental area

er). Few, if any, positive
ntromedial hypothalamic
al forebrain bundle con-
(Fig. 23).

aining was present in the
ve neurons were observed
l nuclei of the inferior
2). These cells were large
and pyramidal in shape
small number of positive
in diameter) were also
/ around the cerebral
v positive neurons with
μm in diameter) were

ventral part

icleus
cleus, anterior part
lle

icleus, posterior
ucleus
is

eus

alamic nucleus, ventral

nucleus
ılamic nucleus

amygdaloid nucleus
is, caudal part
is, oral part
f the raphe

eus

us
eus
ompacta
ticulata

ract
;
is

body
anterior part
ıb of the diagonal band
ıic nucleus

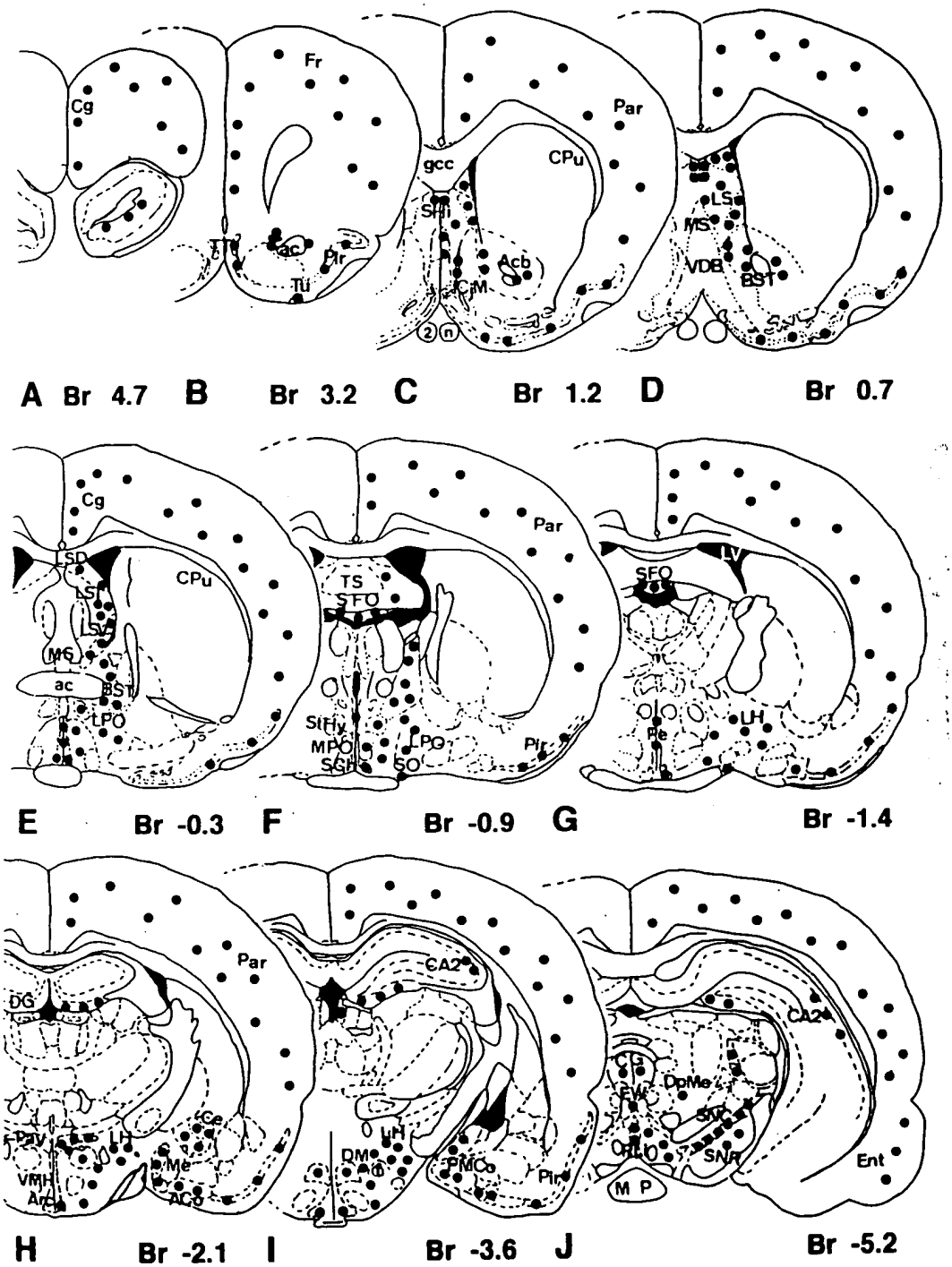

Fig. 3A–J.

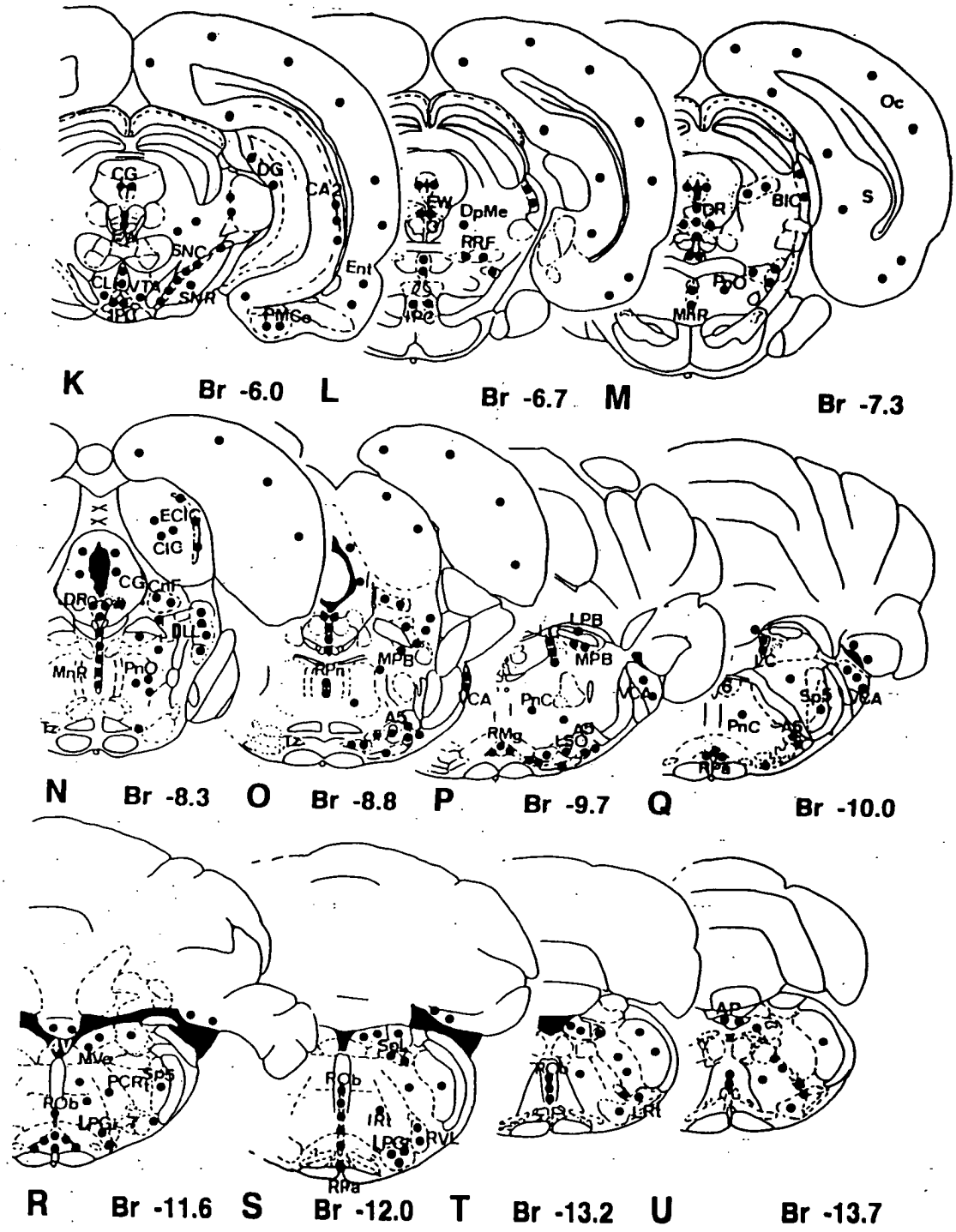

Fig. 3. Mapping of FGFR-1 positive neuron (dots) in coronal sections. Schematic drawings based on the atlas of Paxinos and Watson. Br indicates Bregma. For further details see text.

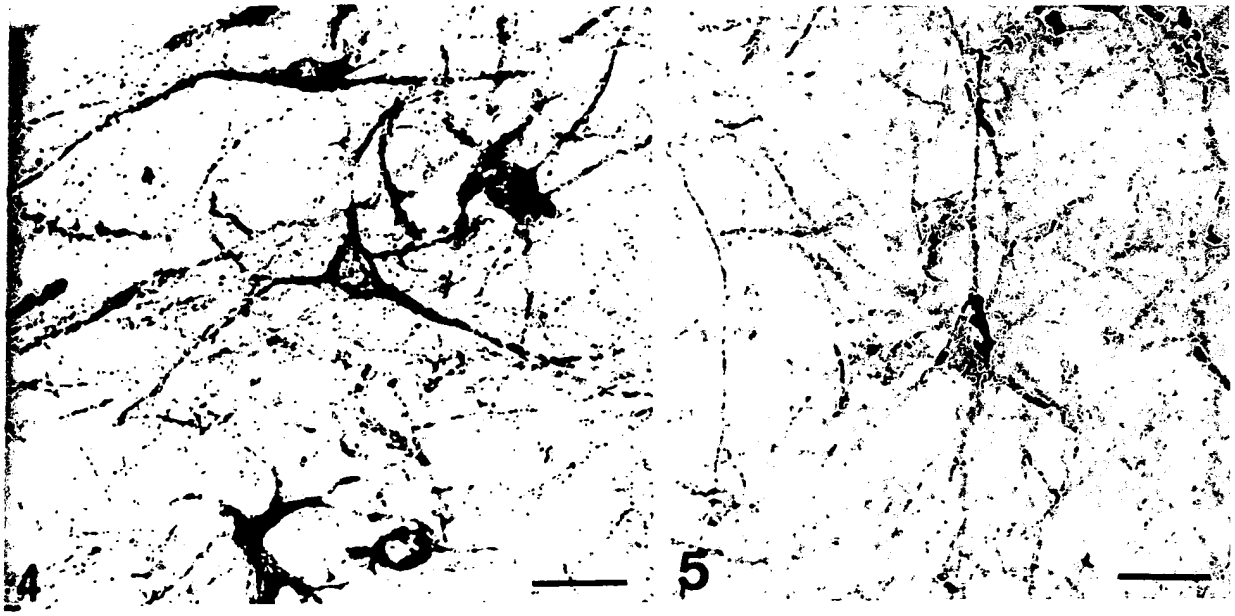

Figs 4–5. Representative FGFR-1-like immunopositive neurons in the pars compacta of the substantia nigra (Fig. 4) and ventral tegmental area (Fig. 5). The reaction products in neurons appeared to occur typically on the surface of cells, though they were occasionally deposited in the cytoplasm. In some brain regions, dendritic or axonal processes were also visible. Scale bars = 25 μm.

scattered in the deep mesencephalic nucleus (Fig. 3J–L).

In the mesencephalon, the pars compacta of the substantia nigra exhibited the most intense staining in the brain (Figs 3J–K, 27, 28). Positive medium-sized neurons (14.8 μm in diameter) were so intensely stained that their morphological shapes could be observed in detail. Stained processes emanating from these cells extended mostly toward the pars reticulata (Fig. 28). The ventral tegmental area also contained many intensely stained neuronal somata (15.4 μm in diameter) and processes (Fig. 3J–K, 29). A moderate number of positive small sized neurons (7.1 μm in diameter) were present in the interpeduncular nucleus (Fig. 29).

The accessory oculomotor nucleus (the Edinger–Westphal nucleus) had intensely stained neurons (16.1 μm in diameter). However, both the main oculomotor and the trochlear nuclei contained no positive structures (Fig. 3J–L).

It was notable that the dorsal raphe nucleus contained many intensely stained neurons (Figs 3M–O, 30). These neurons were medium-sized (14.6 μm in diameter) and multipolar in shape and their processes formed a dense meshwork within the nucleus. A few positive neuronal somata were observed in the rostral

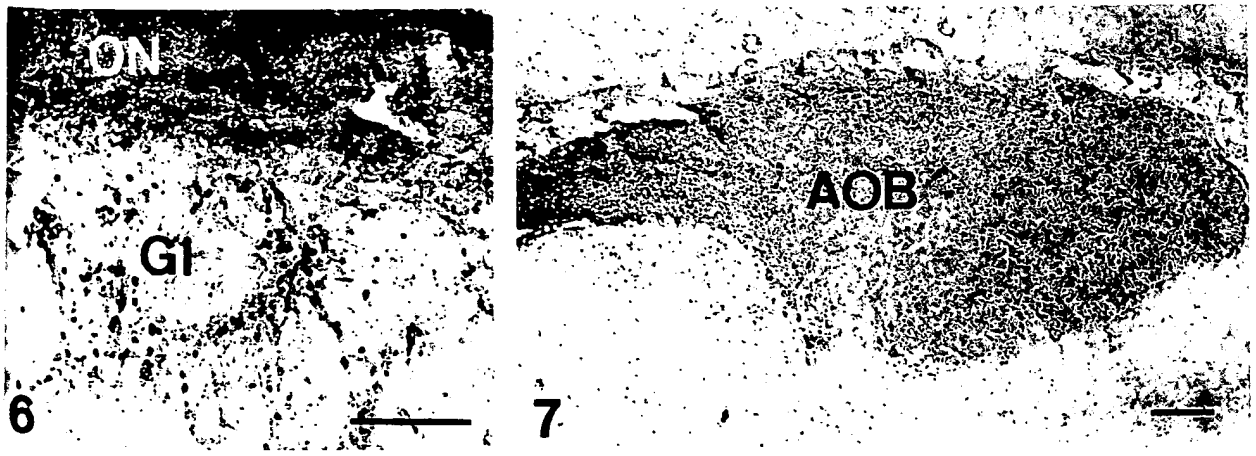

Figs 6–7. FGFR-1-like immunoreactive structures observed in the main olfactory bulb (Fig. 6) and in the accessory olfactory bulb (Fig. 7, AOB). Note the positive periglomerular cells (Gl) and diffuse staining of the olfactory nerve layer (ON). Scale bars = 100 μm.

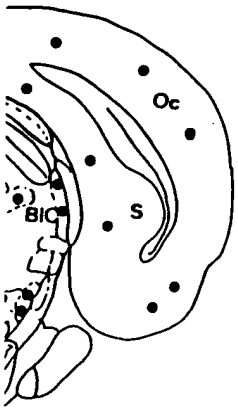

Br -7.3

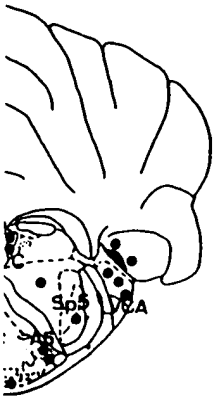

Br -10.0

Br -13.7

gs based on the
ext.

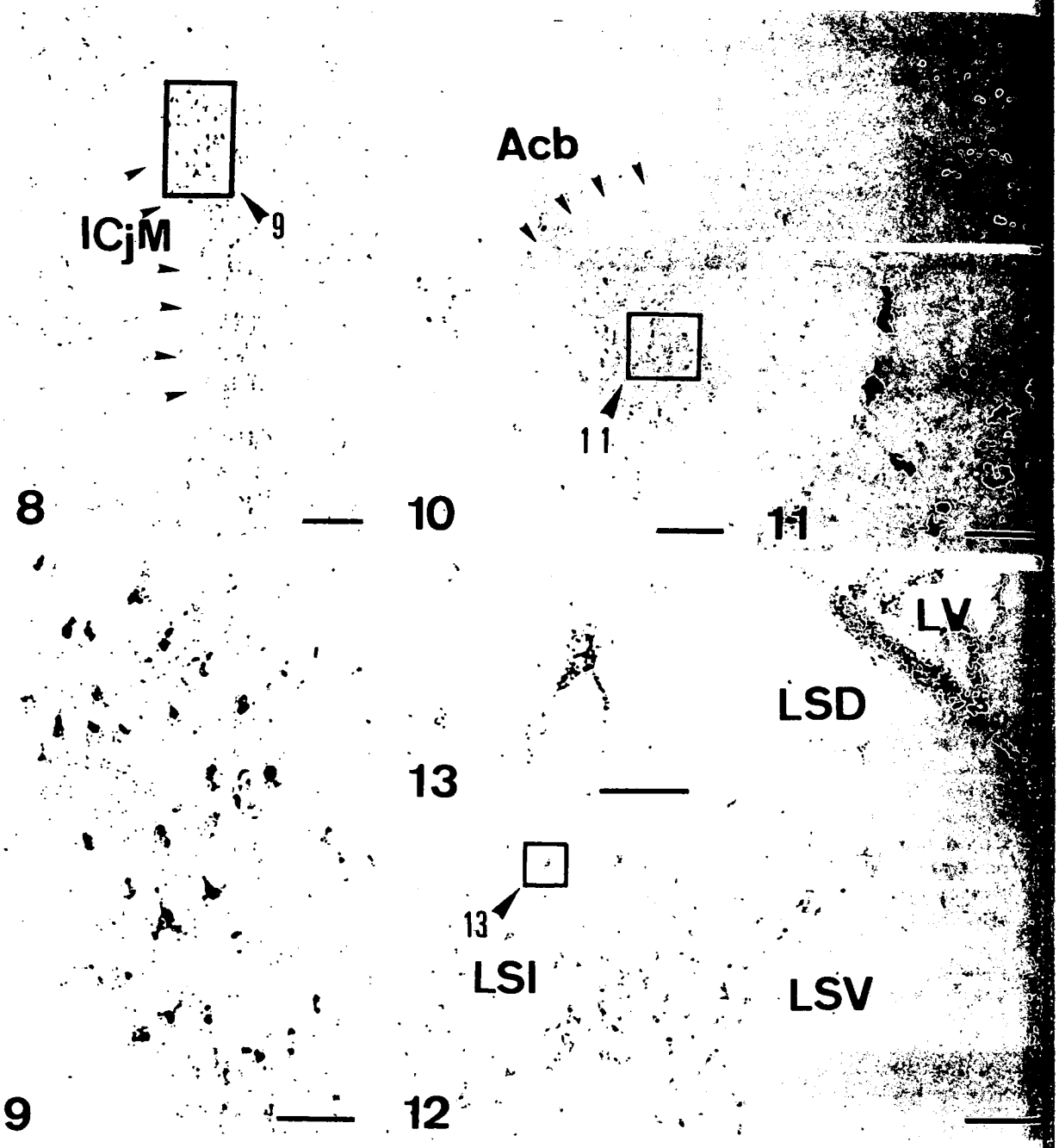

Figs 8–13. FGFR-1 positive neurons in the major island of Calleja (Figs 8, 9), accumbens nucleus (Figs 10, 11) and lateral septal nucleus (Figs 12, 13). Dotty granules are in neuronal somata and their processes. Scale bars = 100 μm,(Figs 8, 12); 200 μm,(Fig. 10); 25 μm, (Figs 9, 11, 13).

(19.8 μm in diameter, Fig. 3J) and caudal linear nuclei (14.2 μm, Fig. 3K–L) and the retrorubral field (10.9 μm, Fig. 3L).

Pons and medulla

The locus coeruleus and the nucleus subcoeruleus displayed an intense immunoreactivity. Medium-sized (14.9 μm in diameter) oval neurons were packed in the locus coeruleus, while relatively large (18.4 μm in diameter) multipolar cells were seen in the nucleus subcoeruleus (Fig. 3P–Q, 35). Moderately stained neurons were observed in the parabrachial nucleus (positive cell size: 11.6 μm in diameter, Fig. 3O–P), the nucleus of the lateral lemniscus (18.0 μm, Fig. 3N), the pontine nucleus (12.9 μm, Fig. 3M–Q) and the trapezoid nucleus (16.3 μm, Fig. 3N–P, 33). In the vestibular nuclei, the medial nucleus possessed a moderate density of positive neurons (25.2 μm in diameter, Fig. 3R–S). A few positive neurons were observed in the other three subnuclei, the superior

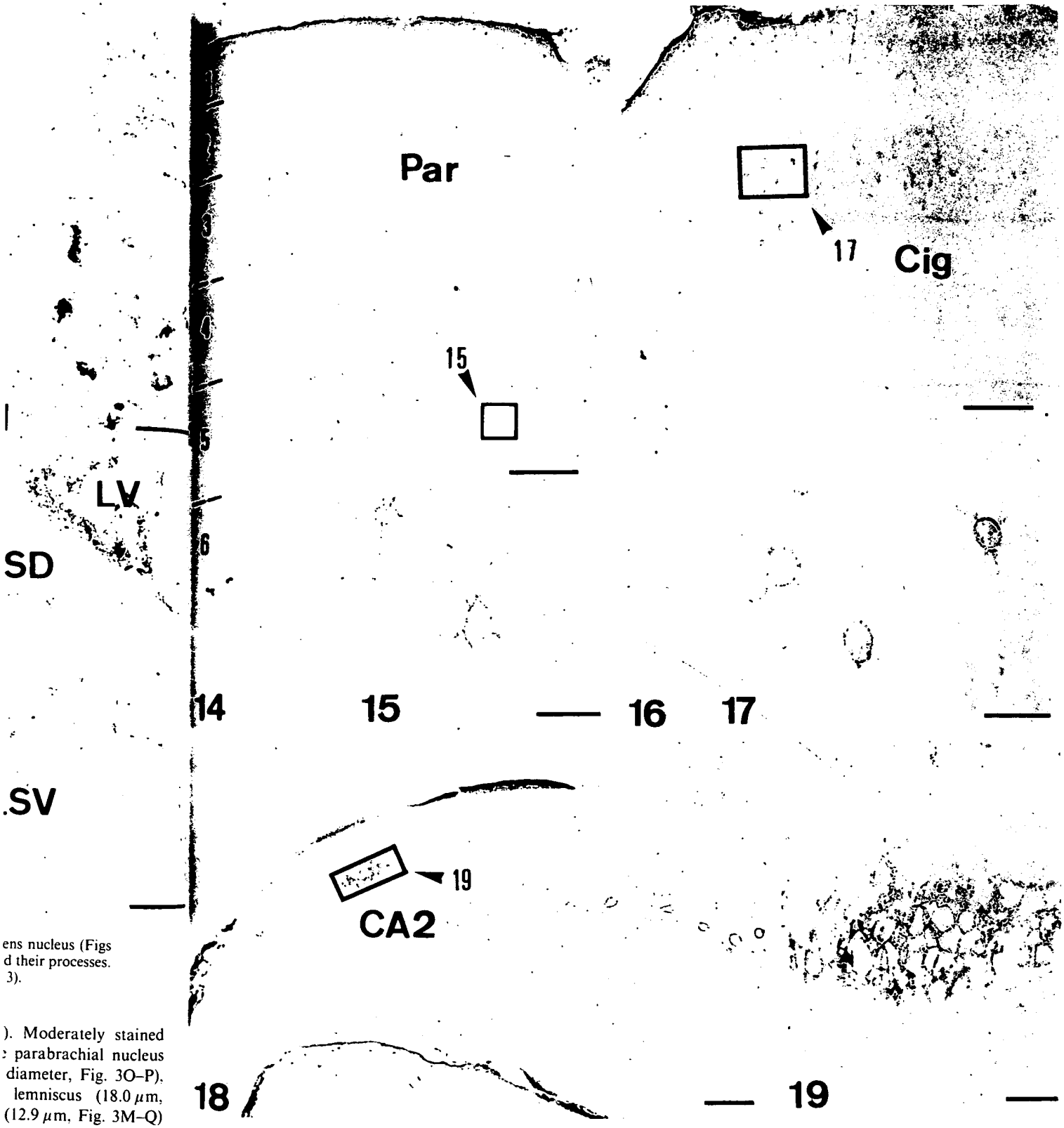

ens nucleus (Figs
d their processes.
3).

). Moderately stained
parabrachial nucleus
diameter, Fig. 3O–P),
lemniscus (18.0 μm,
(12.9 μm, Fig. 3M–Q)
3 μm, Fig. 3N–P, 33).
dial nucleus possessed
neurons (25.2 μm in
positive neurons were
ubnuclei, the superior

Figs 14–19. FGFR-1 positive neurons in the parietal cortex (Figs 14, 15), cingulate cortex (Figs 16, 17) and hippocampus (Figs 18, 19). In the neocortex, the positive neurons are mainly distributed in layers III and V (Fig. 15). Under high magnification (Figs 15, 17), the cell somata and proximal processes were visible by the antiserum. Note that pyramidal neurons in the CA2 region are intensely stained (Figs 18, 19). Scale bars = 200 μm, (Figs 14, 16, 18); 25 μm, (Figs 15, 17, 19).

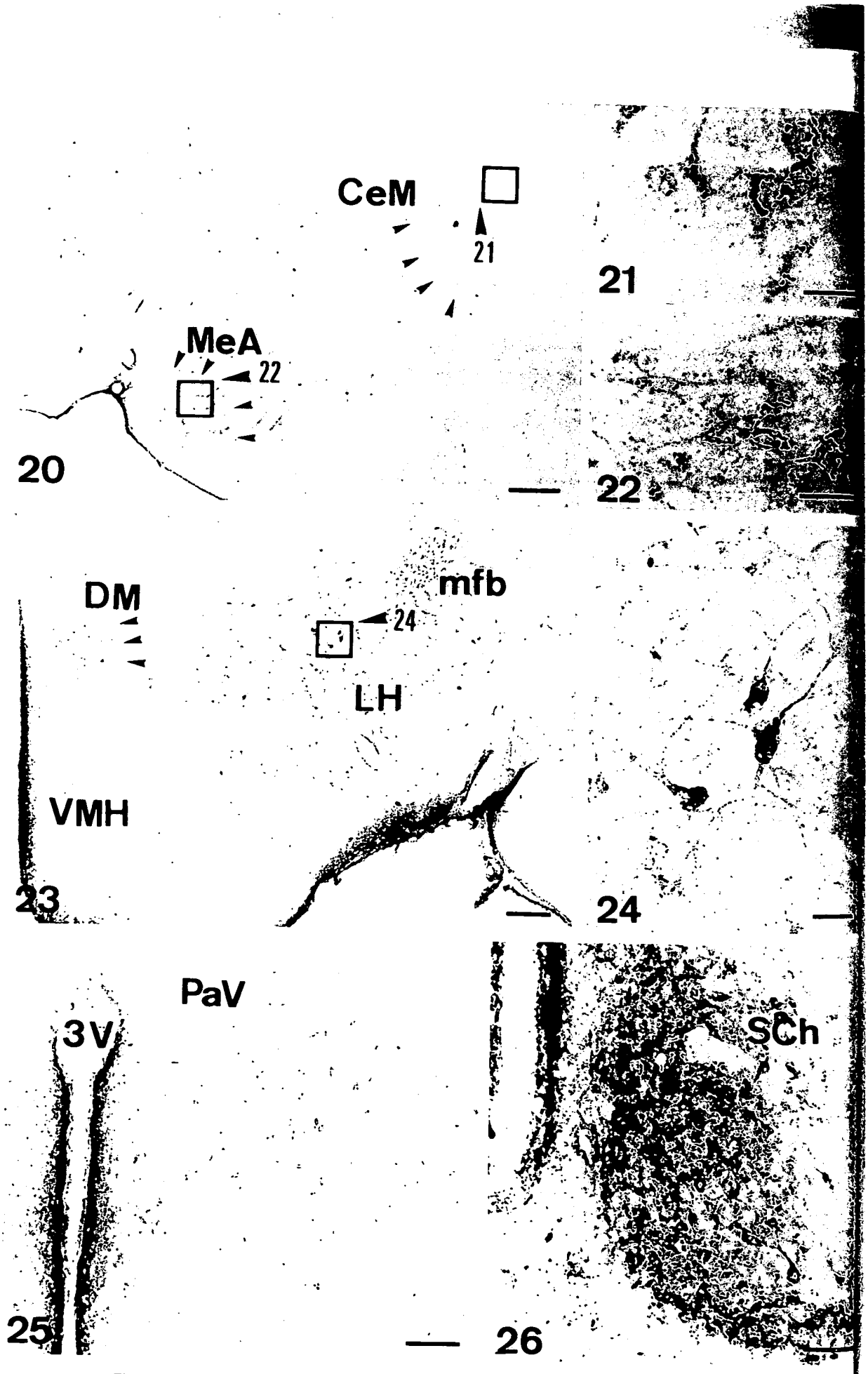

Figs 20–26. FGFR-1 positive neurons observed in the amygdaloid complex (Figs 20–22), lateral hypothalamic area (Figs 23, 24), paraventricular hypothalamic nucleus (Fig. 25) and suprachiasmatic nucleus (Fig. 26). Note intense staining in the lateral hypothalamic area but not in the ventromedial hypothalamic nucleus (Fig. 20). Scale bars = 200 μm, (Fig. 20); 25 μm, (Figs 21, 22, 24); 100 μm, (Figs 23, 25, 26).

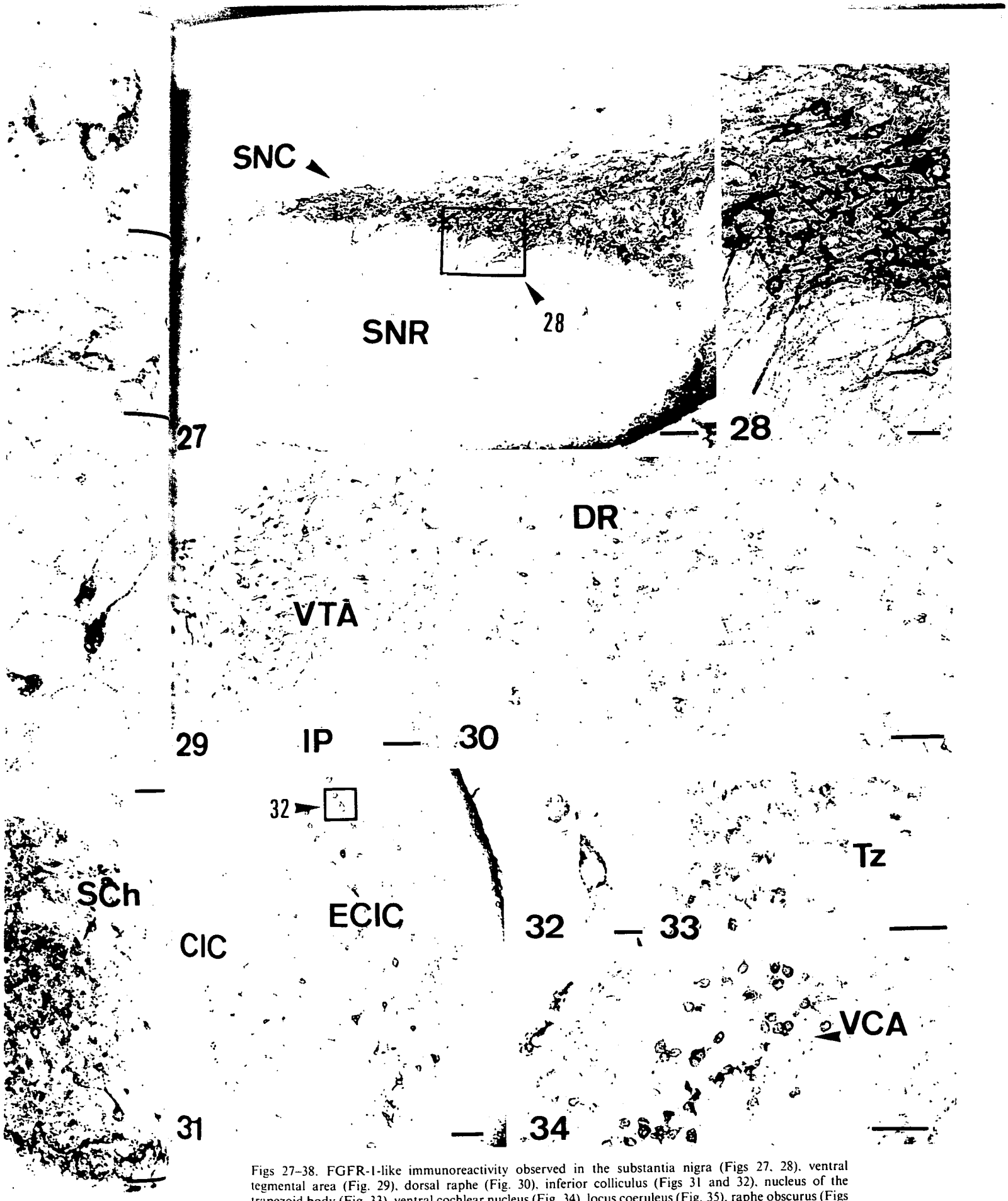

Figs 27–38. FGFR-1-like immunoreactivity observed in the substantia nigra (Figs 27, 28), ventral tegmental area (Fig. 29), dorsal raphe (Fig. 30), inferior colliculus (Figs 31 and 32), nucleus of the trapezoid body (Fig. 33), ventral cochlear nucleus (Fig. 34), locus coeruleus (Fig. 35), raphe obscurus (Figs 36, 37) and cerebellum (Fig. 38). Particularly in the pars compacta of the substantia nigra, neuronal somata and their processes are intensely stained (Fig. 27). The ependyma beneath the crus cerebri are stained nonspecifically. Scale bar = 100 μm. (Figs 27, 29–31, 33–36, 38); 25 μm. (Figs 28, 32, 37).

lateral hypothala-
c nucleus (Fig. 26).
othalamic nucleus
s 23, 25, 26).

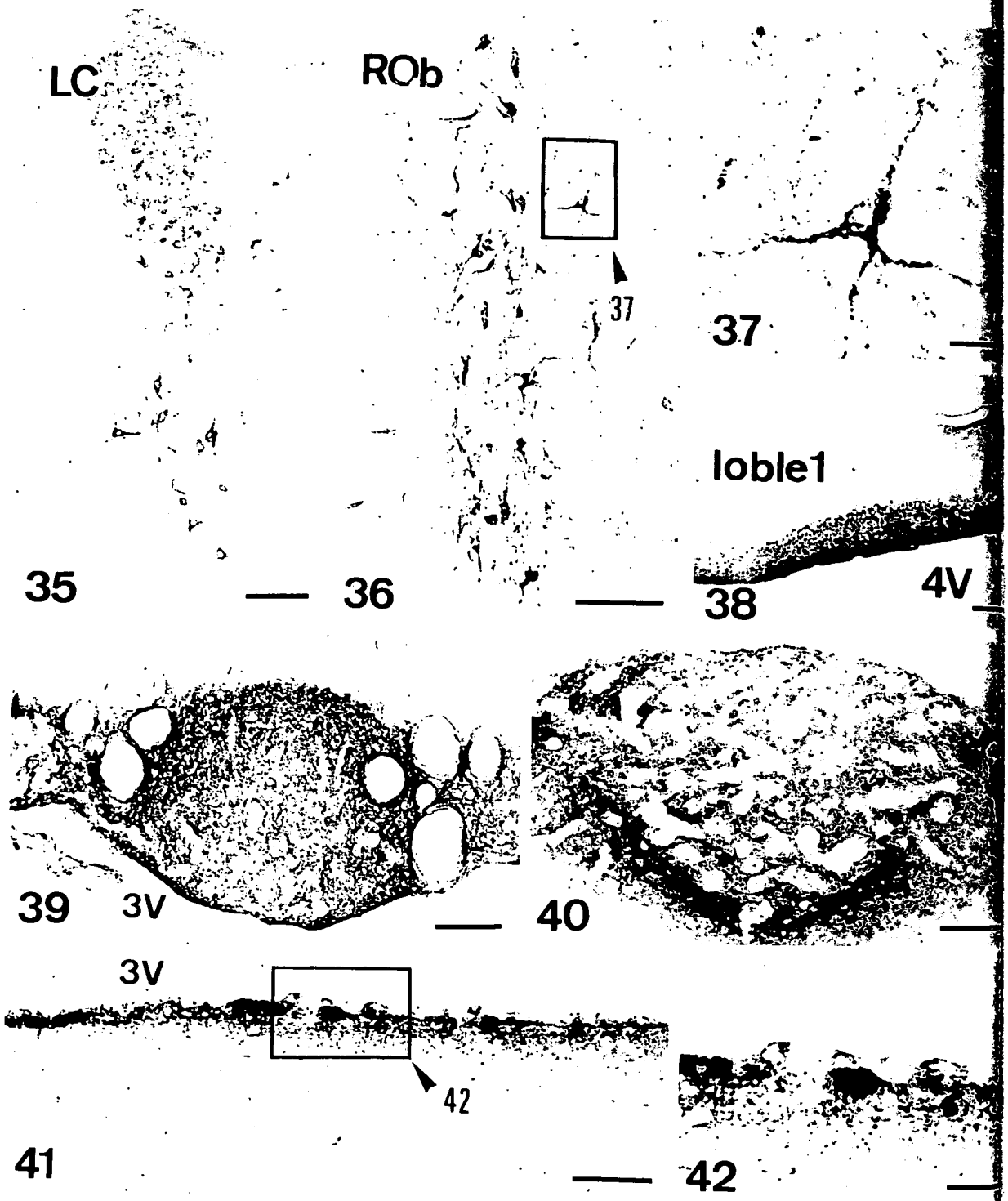

Figs 39–42. FGFR-1-like immunopositive structures in the subfornical organ (Fig. 39), area postrema (Fig. 40) and ependymal cells on the 3rd ventricular wall (Figs 41, 42). Scale bars = 100 μm, (Figs 35–37); 25 μm, (Fig. 38).

(positive cell size: 21.5 μm in diameter), lateral (18.7 μm) and spinal (20.8 μm) vestibular nuclei. In the cochlear nuclei intensely stained large neurons (24.6 μm in diameter) were observed (Figs 3O–Q, 34).

Similarly to the raphe dorsalis described above, clearly stained neurons were distributed in caudal raphe regions (Fig. 3J–V), including the raphe obscurus (positive cell size: 19.3 μm in diameter, Figs 36,

). area postrema
m. (Figs 35–37);

salis described above.
distributed in caudal
ıding the raphe obscu-
in diameter. Figs 36.

37), median raphe (14.9 μm), raphe pontis (13.4 μm), raphe magnus (19.6 μm) and raphe pallidus (14.6 μm) nuclei.

In the medulla oblongata, moderately stained neurons were found in the A5 region (positive cell size: 16.6 μm in diameter, Fig. 3P–Q), intermediate reticular (16.8 μm) and lateral paragigantocellular nuclei (21.6 μm, Fig. 3R–U). A few positive neurons (22.0 μm in diameter) were scattered in the spinal trigeminal nucleus (Fig. 3P–U). Medium-sized (14.9 μm in diameter), moderately stained neurons were observed in the solitary tract nucleus (Fig. 3Q–U).

Cerebellum

In this structure moderately immunoreactive neurons were mainly distributed in the molecular layer. The regions containing a few such positive small cells (8.0 μm in diameter) included the vestibulocerebellum as the lingula (lobule 1), ventral part of flocculonodular (lobule 10) and a ventral half of uvula (lobule 9). Purkinje cells were never stained positively (Figs 3Q–S, 38) and no stained cells were seen in the cerebellar nuclei.

Circumventricular organs

Positive staining was recognized in some structures contacting the cerebrospinal fluid. Among the circumventricular organs, the organum vasculosum laminae terminalis, subfornical organ and area postrema were filled with numerous tiny positive dots throughout their entire entities. In these organs, a few positive cells were irregularly distributed (Figs 3F–G, U, 39, 40). However, no positive staining was present in the subcommissural organ. In the wall of the third ventricle, some ependymal cells and tanycytes occasionally stained positively (Figs 41 and 42), while no such cells were found in other regions of the cerebral ventricle.

DISCUSSION

Characterization of the fibroblast growth factor receptor-1 antisera

The antiserum used here has been raised against a synthetic peptide, of which sequence (EDDDDEDDSSSEEKEAD) is involved in the highly acidic region of chicken FGFR-1.[25] Prior to immunohistochemical study in rat brain, therefore, it is necessary to ascertain that the antiserum has the capability of reacting with rat FGFR-1. Since rat FGFR-1 had not been sequenced completely when the antiserum was obtained, we analysed a partial sequence of a highly acidic region of rat FGFR-1. The sequence determined (EDDDDDDDSSSEEKEAD) was identical with that of human FGFR-1. The immunospot assay clearly indicated that our antiserum cross-reacted equally with the synthetic rat peptide above, but little with the oligopeptide coding a highly acidic region of human FGFR-4 (NDDEDPKSHRDPSNRHS).[33] The failure of the antiserum reacting with the FGFR-4-related peptide not only supports the antibody specificity for FGFR-1, but also denies a possible crossreactivity with corresponding oligopeptides of other FGFR members including FGFR-2 (GDDEDDTDGAEDFVSEN)[7] and FGFR-3 (GDDEDGEDEAEDTGVDT).[21] Because the tetrapeptide "DDED", a common sequence to FGFR-2, -3 and -4, is also contained in our haptenic oligopeptide (EDDDDEDDSSSEEKEAD), the antiserum should be directed toward epitope(s) other than the tetrapeptide. Since there is no other homologous sequence among the four peptides, it is unlikely that the antiserum may crossreact with FGFR-2 or FGFR-3.

A further analysis by western blots confirmed that the antiserum was capable of detecting not only two specific bands (about 75,000 and 145,000 mol. wt) in rat brain homogenate but also a 100 ng fusion protein of human FGFR-1. All these data strongly supported that the antiserum might recognize equipotentially both rat and human FGFR-1. Since, moreover, the antiserum pre-absorbed with the synthetic rat peptide gave no specific staining in immunohistochemistry, the positive structures reported here were regarded as those representing putative FGFR-1-like immunoreactivity.

What forms of fibroblast growth factor receptor-1 are expressed in rat brain?

The FGFR-1 gene has been predicted to generate multiple forms of receptor protein by alternative splicing. These forms are roughly classified into two, the secreted and the membrane-bound forms. The latter forms are further divided into two; the long types containing three immunoglobulin-like domains and the short types containing two such domains.[19] So far, significant homology in the individual forms seems to exist between different species examined, including the rat brain as reported very recently.[53]

As mentioned above, our antiserum recognized two rat brain components of about 75,000 and 145,000 mol. wt. These small and large components, respectively, are similar in size to the secreted forms (70,000–90,000 mol. wt) and the long membrane-bound forms (135,000–160,000 mol. wt) of FGFR-1 in the chicken,[25, 44] human,[7-9, 18, 19, 36] rat[51, 52] or mouse.[27, 35] The antiserum, however, did not detect a protein band corresponding to short membrane-bound forms of FGFR-1 (120,000–135,000 mol. wt).[7,20,36,51] This is consistent with previous studies at the mRNA level in adult mouse brain, indicating that both secreted and long membrane-bound forms are expressed, while short membrane-bound forms are not.[3, 49] Therefore, the present immunohistochemical results in the rat brain appear to represent either the secreted or the long membrane-bound forms of FGFR-1, although it is not possible to differentiate the two forms in our stained structures.

Localization of putative fibroblast growth factor receptor-1- like immunoreactivity

The present study provides the first map of putative FGFR-1-like immunoreactive structures in adult rat brain. Positive staining occurs almost exclusively in neurons of various brain regions. A minor exception is found in cerebrospinal fluid contacting structures such as ependymal cells and tanycytes in the third ventricle and the components of some circumventricular organs. The pattern of distribution is generally consistent with that of FGFR-1 mRNA as revealed by *in situ* hybridization histochemistry.[47] In the telencephalon, for example, immunoreactive neurons are richly distributed in the limbic system such as the olfactory bulb, amygdala and bed nucleus of the stria terminalis. All these limbic regions have been shown to possess many neurons containing FGFR-1 mRNA.[47] Our study further indicates that FGFR-1-like materials are expressed in some pyramidal cells of the cerebral cortex.

It is already known that FGFs are vital to survival of hippocampal neurons in culture.[46] A significant expression of FGFR-1 mRNA in the hippocampus has been reported. Here we show evidence for the existence of FGFR-1-like immunoreactivity in this structure. Although the reported expression of FGFR-1 mRNA[47] was much higher in both CA3 and CA4 than in CA1 or CA2, our study indicates that the immunoreactive expression is far higher in CA2 than any of the remaining three regions. The reason for this discrepancy is at present unclear. Since pyramidal cells in CA2 have been known to be rich in bFGF [50] and its mRNA,[10] it is presumed that, in CA2, bFGFs act through an autocrine or paracrine mechanism.

In the hypothalamus, a conspicuous collection of immunoreactive cells are observed in the lateral hypothalamic area, although the previous study did not describe the presence of FGFR-1 mRNA in this area.[47] Large neurons in the lateral hypothalamic area have been shown to take up aFGF or bFGF following the administration of a respective FGF into the cerebral ventricle.[11] Moreover, both aFGF and bFGF have been proven to suppress the activity of glucose-sensitive neurons in the lateral hypothalamic area but not to affect glucoreceptor neurons in the ventromedial hypothalamic nucleus.[31] The present finding appears to give additional support for the assumption that FGFs play a role in the brain regulation of feeding, because the lateral hypothalamic area is known to be an appetite controlling center while the ventromedial hypothalamic nucleus is known to be a satiety center.

In the mesencephalon and lower brainstem, FGFR-1 immunoreactivity appears to be preferentially localized in monoaminergic cells. These include dopamine neurons in the ventral tegmental area and the pars compacta of the substantia nigra, noradrenaline cells in the locus coeruleus and serotonin neurons in the raphe nuclei. It is suggested, therefore, that FGFs may act selectively on certain transmitter systems or transmitter pathways. Recent studies have in fact revealed that noradrenergic and cholinergic neurons in the hindbrain express specific trophic phenotypes.[45] In this context, it is interesting to note that all the above aminergic neurons project their axons widely throughout the brain. Whether or not definite aminergic pathways utilize FGFs remains to be elucidated.

Among the aminergic systems, the pars compacta of the substantia nigra displayed a noticeable FGFR-1-like immunoreactivity. The neurons in this nucleus have been shown to express a high level of FGFR-1 mRNA. In addition, bFGF has been shown to exert trophic effects on midbrain dopaminergic cells.[12, 23, 32] Furthermore, mesencephalic dopamine neurons have been reported to contain bFGF.[2, 6, 43] Recently, we reported that Parkinson's disease may be accompanied by changes in bFGF content in dopaminergic cells of the substantia nigra.[42] It may be interesting to examine possible alterations of FGFR-1 expression in Parkinson's disease. The antiserum developed in this study and probes for FGFR-1 mRNA should permit such a study in human brain.

We have previously shown that aFGF-like immunoreactivity is richly distributed in structures covering the cerebral ventricle.[41] Abundant bFGF and its mRNA have also been demonstrated in the rat subfornical organ.[13] In this report, we found intense staining for FGFR-1-like immunoreactivity in some of the circumventricular organs. Since significant amounts of both aFGF and bFGF are detectable in the cerebrospinal fluid,[16] both FGFs may be released from these structures contacting the cerebrospinal fluid. However, signal peptides for secretion were lacking in aFGF and bFGF. It is thus possible that secreted forms of FGFR-1 may play a role as a carrier of FGFs secretion.[18, 51] Obviously, further studies will be required to clarify the unique secretory and uptake mechanisms of FGFs.

Under neuropathological conditions the expression of FGFs has recently been shown to be upregulated, particularly in reactive astrocytes after brain injury.[14,22,26,30] Moreover, we and others have reported that astrocytes containing increased levels of either aFGF or bFGF are found in the brains of Alzheimer's disease patients[39,40,54] and patients with amyotrophic lateral sclerosis.[54] Since FGFs act potentially trophically on neurons, glia cells and endothelial cells, the enhanced FGF expressions may have some significance in the maintenance of brain cells suffering from neurological diseases. To test this hypothesis, precise information is required concerning the interaction between cells expressing FGFs and their target cells bearing FGF receptors.

Acknowledgements—This study was supported partly by grants from the Japan Foundation of Aging and Health (H.K.), Uehara Foundation (I.T.), Sasakawa Medical Foundation (I.T.), Shiga International Cooperation for Medical Research (I.T.) and Special Coordination Funds of the Science and Technology Agency of the Japanese Government (Y.O.).

REFERENCES

1. Abe H., Tooyama I., Renda T., Ersparmer V. and Kimura H. (1992) Production of antiserum to [D-Ala2] deltorphin I and its immunohistochemical application to the mouse brain. *Neuroreport* **3**, 669–672.
2. Bean A. J., Elde R., Cao Y. H., Oellig C., Tamminga C., Goldstein M., Pettersson R. F. and Hökfelt T. (1991) Expression of acidic and basic fibroblast growth factors in the substantia of rat, monkey and human. *Proc. natn. Acad. Sci. U.S.A.* **88**, 10,237–10,241.
3. Bernard O., Li M. and Reid H. H. (1991) Expression of two different forms of fibroblast growth factor receptor 1 in different mouse tissues and cell lines. *Proc. natn. Acad. Sci. U.S.A.* **88**, 7625–7629.
4. Burgess W. H. and Maciag T. (1989) The heparin-binding (fibroblast) growth factor family of proteins. *A. Rev. Biochem.* **58**, 575–606.
5. Chomczynski P. and Sacchi N. (1987) Single-step method of RNA isolation by acid guanidium thiocyanate-phenol-chloroform extraction. *Analyt. Biochem.* **162**, 156–159.
6. Cintra A., Cao Y. H., Oellig C., Tinner B., Bortolotti F., Goldstein M., Pettersson R. F. and Fuxe K. (1991) Basic FGF is present in dopaminergic neurons of the ventral midbrain of the rat. *Neuroreport* **2**, 597–600.
7. Dionne C. A., Crumley G., Bellot F., Kaplow J. M., Searfoss G., Ruta M., Burgess W. H., Jaye M. and Schlessinger J. (1990) Cloning and expression of two distinct high-affinity receptors cross-reacting with acidic and basic fibroblast growth factors. *Eur. molec. Biol. Org. J.* **9**, 2685–2692.
8. Duan D. S., Werner S. and Williams L. T. (1992) A naturally occurring secreted form of fibroblast growth factor (FGF) receptor 1 binds basic FGF in preference over acidic FGF. *J. biol. Chem.* **267**, 16,076–16,080.
9. Eisemann A., Ahn J. A., Graziani G., Tronick S. R. and Ron D. (1991) Alternative splicing generates at least five different isoforms of the human basic-FGF receptor. *Oncogene* **6**, 1195–1202.
10. Emoto N., Gonzalez A. M., Walicke P. A., Wada E., Simmons D. M., Shimasaki S. and Baird A. (1989) Basic fibroblast growth factor (FGF) in the central nervous system: identification of specific loci of basic FGF expression in the rat brain. *Growth Factors* **2**, 21–29.
11. Ferguson I. A. and Johnson E. M. J. (1991) Fibroblast growth factor receptor-bearing neurons in the CNS: identification by receptor-mediated retrograde transport. *J. comp. Neurol.* **313**, 693–706.
12. Ferrari G., Minozzi M. C., Toffano G., Leon A. and Skaper S. D. (1989) Basic fibroblast growth factor promotes the survival and development of mesencephalic neurons in culture. *Devl Biol.* **133**, 140–147.
13. Frautschy S. A., Gonzalez A. M., Martinez M. R., Carceller F., Cuevas P. and Baird A. (1991) Expression of basic fibroblast growth factor and its receptor in the rat subfornical organ. *Neuroendocrinology* **54**, 55–61.
14. Frautschy S. A., Waliche P. A. and Baird A. (1991) Localization of basic fibroblast growth factor and its mRNA after CNS injury. *Brain Res.* **553**, 291–299.
15. Gospodarowicz D. (1974) Localization of a fibroblast growth factor and its effect alone with hydrocortisone on 3T3 cell growth. *Nature* **249**, 123–127.
16. Hanai K., Oomura Y., Kai Y., Nishikawa K., Shimizu N., Morita H. and Plata S. C. (1989) Central action of acidic fibroblast growth factor in feeding regulation. *Am. J. Physiol.* **256**, R217–223
17. Heuer J. G., von Bartheld C. S., Kinoshita Y., Evers P. C. and Bothwell M. (1990) Alternating phases of FGF receptor and NGF receptor expression in the developing chicken nervous system. *Neuron* **5**, 283–296.
18. Johnson D. E., Lee P. L., Lu J. and Williams L. T. (1990) Diverse forms of a receptor for acidic and basic fibroblast growth factors. *Molec. Cell. Biol.* **10**, 4728–4736.
19. Johnson D. E., Lu J., Chen H., Werner S. and Williams L. T. (1991) The human fibroblast growth factor receptor genes: a common structural arrangement underlies the mechanisms for generating receptor forms that differ in their third immunoglobulin domain. *Molec. cell. Biol.* **11**, 4627–4634.
20. Johnson D. E. and Williams L. T. (1993) Structural and functional diversity in the FGF receptor multigene family. *Adv. Cancer Res.* **60**, 1–41.
21. Keegan K., Johnson D. E., Williams L. T. and Hayman M. J. (1991) Isolation of an additional member of the fibroblast growth factor receptor family, FGFR-3. *Proc. natn. Acad. Sci. U.S.A.* **88**, 1095–1099.
22. Kiota Y., Takami K., Iwane M., Shino A., Miyamoto M., Tsukuda R. and Nagaoka A. (1991) Increase in basic fibroblast growth factor-like immunoreactivity in rat brain after forebrain ischemia. *Brain Res.* **545**, 322–328.
23. Knusel B., Michel P. P., Schwaber J. S. and Hefti F. (1990) Selective and nonselective stimulation of central cholinergic and dopaminergic development *in vitro* by nerve growth factor, basic fibroblast growth factor, epidermal growth factor, insulin and the insulin-like growth factors I and II. *J. Neurosci.* **10**, 558–570.
24. Larsson L. (1981) A novel immunocytochemical model system for specificity and sensitivity screening of antisera against multiple antigens. *J. Histochem. Cytochem.* **29**, 408–410.
25. Lee P. L., Johnson D. E., Cousens L. S., Fried V. A. and Williams L. T. (1989) Purification and complementary DNA cloning of a receptor for basic fibroblast growth factor. *Science* **245**, 57–60.
26. Logan A. (1988) Elevation of acidic fibroblast growth factor mRNA in lesioned rat brain. *Molec. Cell Endocr.* **58**, 275–278.
27. Mansukhani A., Moscatelli D., Talarico D., Levytska V. and Basilico C. (1990) A murine fibroblast growth factor (FGF) receptor expressed in CHO cells is activated by basic FGF and Kaposi FGF. *Proc. natn. Acad. Sci. U.S.A.* **87**, 4378–4382.
28. Matsuyama A., Iwata H., Okumura N., Yoshida S., Imaizumi K., Lee Y., Shiraishi S. and Shiosaka S. (1992) Localization of basic fibroblast growth factor-like immunoreactivity in the rat brain. *Brain Res.* **587**, 49–65.
29. Marchuk D., Drumm M., Saulino A. and Collins F. S. (1991) Construction of T-vectors, a rapid and general system for direct cloning of unmodified PCR products. *Nucl. Acids Res.* **19**, 1154.
30. Nieto-Sampedro M., Lim R., Hicklin D. J. and Cotman C. W. (1988) Early release of glia maturation factor and acidic fibroblast growth factor after brain injury. *Neurosci. Lett.* **86**, 361–365.
31. Oomura Y. (1988) Chemical and neuronal control of feeding motivation. *Physiol. Behav.* **44**, 555–560.
32. Otto D. and Unsicker K. (1990) Basic FGF reverses chemical and morphological deficits in the nigrostriatal system of MPTP- treated mice. *J. Neurosci.* **10**, 1912–1921.
33. Partanen J., Mäkelä T. P., Eerola E., Korhonen J., Hirvonen H., Claesson W. L. and Alitalo K. (1991) FGFR-4, a novel acidic fibroblast growth factor receptor with a distinct expression pattern. *Eur. molec. Biol. Org. J.* **10**, 1347–1354.
34. Paxinos G. and Watson C. (1986) *The Rat Brain in Stereotaxic Coordinates*. 2nd edn. Academic Press, San Diego, CA.

35. Reid H. H., Wilks A. F. and Bernard O. (1990) Two forms of the basic fibroblast growth factor receptor-like mRNA are expressed in the developing mouse brain. *Proc. natn. Acad. Sci. U.S.A.* **87,** 1596–1600.
36. Ruta M., Burgess W., Givol D., Epstein J., Neiger N., Kaplow J., Crumley G., Dionne C., Jaye M. and Schlessinger J. (1989) Receptor for acidic fibroblast growth factor is related to the tyrosine kinase encoded by the fms-like gene (FLG). *Proc. natn. Acad. Sci. U.S.A.* **86,** 8722–8726.
37. Sambrook J., Fritsch E. F. and Maniatis T. (1989) *Molecular Cloning: A Laboratory Manual,* 2nd edn. Cold Spring Harbor Laboratory Press, New York.
38. Stock A., Kuzis K., Woodward W. R., Nishi R. and Eckenstein F. P. (1992) Localization of acidic fibroblast growth factor in specific subcortical neuronal populations. *J. Neurosci.* **12,** 4688–4700.
39. Stopa E. G., Gonzalez A.-M., Chorsky R., Corona R. J., Alvarez J., Bird E. D. and Baird A. (1990) Basic fibroblast growth factor in Alzheimer's disease. *Biochem. biophys. Res. Commun.* **171,** 690–696.
40. Tooyama I., Akiyama H., McGeer P. L., Hara Y., Yasuhara O. and Kimura H. (1991) Acidic fibroblast growth factor-like immunoreactivity in brain of Alzheimer patients. *Neurosci. Lett.* **121,** 155–158.
41. Tooyama I., Hara Y., Yasuhara Y., Oomura Y., Sasaki K., Muto T., Suzuku K., Hanai K. and Kimura H. (1991) Production of antisera to acidic fibroblast growth factor and their application to immunohistochemical study in rat brain. *Neuroscience* **40,** 769–779.
42. Tooyama I., Kawamata T., Walker D., Yamada T., Hanai K., Kimura H., Igarashi K., McGeer E. G. and McGeer P. L. (1993) Loss of basic fibroblast growth factor in substantia nigra neurons in Parkinson's disease. *Neurology* **43,** 372–376.
43. Tooyama I., Walker D., Yamada T., Hanai K., Kimura H., McGeer E. G. and McGeer P. L. (1992) High molecular weight basic fibroblast growth factor-like protein is localized to a subpopulation of mesencephalic dopaminergic neurons in the rat brain. *Brain Res.* **593,** 274–280.
44. Ueno H., Gunn M., Dell K., Tseng A. J. and Williams L. (1992) A truncated form of fibroblast growth factor receptor 1 inhibits signal transduction by multiple types of fibroblast growth factor receptor. *J. biol. Chem.* **267,** 1470–1476.
45. von Bartheld C. S. and Bothwell M. (1992) Development and distribution of noradrenergic and cholinergic neurons and their trophic phenotypes in the avian ceruleus complex and midbrain tegmentum. *J. comp. Neurol.* **320,** 479–500.
46. Walicke P. A., Cowan W. M., Ueno N., Baird A. and Guillemin R. (1986) Fibroblast growth factor promotes survival of dissociated hippocampal neurons and enhance neurite extension. *Proc. natn. Acad. Sci. U.S.A.* **83,** 3012–3016.
47. Wanaka A., Johnson E. M. J. and Milbrandt J. (1990) Localization of FGF receptor mRNA in the adult rat central nervous system by *in situ* hybridization. *Neuron* **5,** 267–281.
48. Wanaka A., Milbrandt J. and Johnson E. M. J. (1991) Expression of FGF receptor gene in rat development. *Development* **111,** 455–468.
49. Werner S., Duan D. S., de Vries C., Peters K. G., Johnson D. E. and Williams L. T. (1992) Differential splicing in the extracellular region of fibroblast growth factor receptor 1 generates receptor variants with different ligand-binding specificities. *Molec. cell. Biol.* **12,** 82–88.
50. Woodward W. R., Nishi R., Meshul C. K., Williams T. E., Coulombe M. and Eckenstein F. P. (1992) Nuclear and cytoplasmic localization of basic fibroblast growth factor in astrocytes and CA2 hippocampal neurons. *J. Neurosci.* **12,** 142–152.
51. Xu J., Nakahara M., Crabb J. W., Shi E., Matuo Y., Fraser M., Kan M., Hou J. and McKeehan W. L. (1992) Expression and immunochemical analysis of rat and human fibroblast growth factor receptor (flg) isoforms. *J. biol. Chem.* **267,** 17,792–17,803.
52. Yan G., Wang F., Fukabori Y., Sussman D., Hou J. and McKeehan W. L. (1992) Expression and transforming activity of a variant of the heparin-binding fibroblast growth factor receptor (*flg*) gene resulting from splicing of the alpha exon at an alternate 3'- acceptor site. *Biochem. biophys. Res. Commun.* **183,** 423–430.
53. Yasaki N., Fujita H., Ohta M., Kawasaki T. and Itoh, N. (1993) The structure and expression of the FGF receptor-1 mRNA isoforms in rat tissues. *Biochim. biophys. Acta* **1172,** 37–42.
54. Yasuhara O., Tooyama I., Akiyama H., Akiguchi I., Kimura J., McGeer P. L., Hara Y. and Kimura H. (1991) Reactive astrocytes express acidic fibroblast growth factor in Alzheimer's disease brain. *Dementia* **2,** 64–70.

(*Accepted* 10 *November* 1993)

STIC-ILL QH 301. J677

From: Holleran, Anne
Sent: Sunday, March 04, 2001 5:30 PM
T : STIC-ILL
Subject: refs. for 09/266,543

Examiner: Anne Holleran
Art Unit: 1642; Rm 8E03
Phone: 308-8892
Date needed by: ASAP

Please send me copies of the following :

1. Plum, S.M. et al. Vaccine, (2000) 19/9-10, 1294-1303
2. Aonuma, M. et al. Anticancer Res. (1999, Oct) 19(5B): 4039-4044
3. Muller, Y.A. et al. Structure (1998) 6(9): 1153-1167
4. Yamagishi, S. et al. J. Biol. Chem. (1997) 272(13): 8723-8730
5. Koolwijk, P. et al. J. Cell Biology (1996) 132(6): 1177-1188
6. Matsuo, A. et al. Neuroscience (1994) 60(1): 49-66
7. Djakiew, D. et al. Cancer Research (1991) 51(12): 3304-3310
8. Yamanishi, H. et al. Cancer Research (1991) 51(11): 3006-3010
9. Matsuzaki, K. et al. Japanese J. Cancer Research (1990) 81(4): 345-354
10. Kardami, E. et al. Growth Factors (1990) 4(1): 69-80
11. Riss, T.L. et al. J. Cellular Physiology (1989) 138(2): 405-414

Cooperative Effect of TNFα, bFGF, and VEGF on the Formation of Tubular Structures of Human Microvascular Endothelial Cells in a Fibrin Matrix. Role of Urokinase Activity

Pieter Koolwijk, Monique G.M. van Erck, Wil J.A. de Vree, Mario A. Vermeer, Herbert A. Weich,* Roeland Hanemaaijer, and Victor W.M. van Hinsbergh

Gaubius Laboratory TNO-PG, 2333 CK Leiden, The Netherlands; and *Department of Gene Expression, GBF, 38124 Braunschweig, Germany

Abstract. In angiogenesis associated with tissue repair and disease, fibrin and inflammatory mediators are often involved. We have used three-dimensional fibrin matrices to investigate the humoral requirements of human microvascular endothelial cells (hMVEC) to form capillary-like tubular structures. bFGF and $VEGF_{165}$ were unable to induce tubular structures by themselves. Simultaneous addition of one or both of these factors with TNFα induced outgrowth of tubules, the effect being the strongest when bFGF, $VEGF_{165}$, and TNFα were added simultaneously. Exogenously added u-PA, but not its nonproteolytic amino-terminal fragment, could replace TNFα, suggesting that TNFα-induced u-PA synthesis was involved. Soluble u-PA receptor (u-PAR) or antibodies that inhibited u-PA activity prevented the formation of tubular structures by 59–99%. ε-ACA and trasylol which inhibit the formation and activity of plasmin reduced the extent of tube formation by 71–95%. TNFα or u-PA did not induce tubular structures without additional growth factors. bFGF and $VEGF_{165}$ enhanced of the u-PAR by 72 and 46%, but TNFα itself also increased u-PAR in hMVEC by 30%. Induction of mitogenesis was not the major contribution of bFGF and $VEGF_{165}$ because the cell number did not change significantly in the presence of TNFα, and tyrphostin A47, which inhibited mitosis completely, reduced the formation of tubular structures only by 28–36%. These data show that induction of cell-bound u-PA activity by the cytokine TNFα is required in addition to the angiogenic factors $VEGF_{165}$ and/or bFGF to induce in vitro formation of capillary-like structures by hMVEC in fibrin matrices. These data may provide insight in the mechanism of angiogenesis as occurs in pathological conditions.

Angiogenesis, the formation of new blood vessels from existing ones, plays an important role in the development and progression of various pathological processes, such as tumor development and rheumatoid arthritis (Folkman and Klagsbrun, 1987; Liotta et al., 1991; Folkman and Shing, 1992; Montesano, 1992; Colville-Nash and Scott, 1992). Fibrin (Dvorak et al., 1992), inflammatory cells (Polverini, 1989), and angiogenic factors (Broadley et al., 1989; Klagsburn and D'Amore, 1991; Shweiki et al., 1992; Plate et al., 1992; Senger et al., 1993; Koch et al., 1994) are commonly observed in angiogenesis associated with disease in man. A series of sequential events can be distinguished during the formation of new microvessels: (*a*) degradation of the vascular basement membrane and the fibrin or interstitial matrix by endothelial cells; (*b*) endothelial cell migration; (*c*) endothelial proliferation; and (*d*) the formation of new capillary tubes and a new basement membrane (Folkman, 1986).

It is generally assumed that urokinase-type plasminogen activator (u-PA)[1] and its inhibitor, the plasminogen activator inhibitor I (PAI-1), are involved in the regulation of the first steps of angiogenesis, i.e., local proteolytic remodeling of matrix proteins and migration of endothelial cells (Pepper et al., 1987; Bacharach et al., 1992; Niedbala et al., 1992; van Hinsbergh, 1992; Vassalli, 1994). u-PA converts plasminogen into the broadly acting serine protease plas-

Please address all correspondence to P. Koolwijk, Gaubius Laboratory TNO-PG, P.O. Box 2215, 2301 CE Leiden, The Netherlands. Tel.: 31 71 518 1446. Fax: 31 71 518 1904. E-mail: P.KOOLWIJK@PG.TNO.NL

1. *Abbreviations used in this paper*: ATF, amino-terminal fragment of u-PA; bFGF, basic fibroblast growth factor; ε-ACA, ε-aminocaproic acid; hMVEC, human microvascular endothelial cells; HUVEC, human umbilical vein endothelial cells; ^{125}I-DIP-u-PA, ^{125}I-labeled diisopropylfluorophosphate-treated u-PA; MMP, matrix metalloproteinase; NBCS, newborn calf serum; PBS-T, PBS supplemented with 0.02% (vol/vol) Tween 20; PAI-1, plasminogen activator inhibitor I; t-PA, tissue-type plasminogen activator; TNFα, tumor necrosis factor-α; u-PA, urokinase-type plasminogen activator; scu-PA, single-chain urokinase-type plasminogen activator; u-PAR, cellular receptor for u-PA; $VEGF_{165}$, 165-kD vascular endothelial cell growth factor.

min, which in turn is able to both degrade fibrin and other matrix proteins, and to activate several matrix metalloproteinases (MMPs), in particular stromelysin-1 (MMP-3), interstitial collagenase (MMP-1), and gelatinase-B (MMP-9) (Woessner, 1991; Docherty et al., 1992; Matrisian, 1992; Nagase, 1994). In human endothelial cells the synthesis of u-PA and several of these matrix metalloproteinases is enhanced by the inflammatory mediators, tumor necrosis factor-α (TNFα) and interleukin-1 (van Hinsbergh et al., 1990; Hanemaaijer et al., 1993). The activity of u-PA is localized by a specific cellular receptor (u-PAR) to the cell surface (Blasi et al., 1994; Danø et al., 1994). The inactive single chain form of u-PA binds to u-PAR and is converted into its active form. In the cell environment active two-chain u-PA is immediately inhibited by PAI-1 (Loskutoff, 1991). The u-PAR enhances this activation and may temporarily protect u-PA activity (Ellis et al., 1991), and provides the cell with the ability to degrade extracellular matrix proteins in a controlled manner (Quax et al., 1991). In endothelial cells the u-PAR expression is enhanced by the angiogenic factors bFGF (Mignatti et al., 1991) and VEGF (Pepper et al., 1992) and by activation of protein kinase C and elevation of cyclic AMP concentration (Barnathan et al., 1990; Langer et al., 1993; van Hinsbergh, 1992).

The formation of capillary structures in three-dimensional matrices of fibrin and collagen has been studied in vitro with bovine endothelial cells (Pepper et al., 1990; Madri et al., 1991; Montesano, 1992; Goto et al., 1993) and rat aorta explants (Nicosia and Ottinetti, 1990). Pepper et al. (1990) demonstrated that the formation of capillary-like tubular structures in a three-dimensional fibrin or collagen matrix is induced by addition of bFGF and counteracted by TGFβ. In these bovine endothelial cells bFGF induces both u-PA activity and u-PAR expression, whereas TGFβ predominantly enhanced PAI-1. A reproducible model to study the formation of capillary-like structures in fibrin matrices with human endothelial cells has not yet been available. Although bFGF also enhances u-PAR expression in human endothelial cells (Mignatti et al., 1991), it is still unable to increase u-PA expression in these endothelial cells (see below).

We have investigated the minimal requirements for human endothelial cells to form capillary-like tubular structures in three-dimensional fibrin matrices. Our data indicate that in addition to angiogenic growth factor(s), an inflammatory mediator, TNFα, is required and u-PAR–bound u-PA activity is involved in the formation of capillary-like tubular structures of human microvascular endothelial cells in these fibrin matrices.

Materials and Methods

Materials

Medium 199 (M199) supplemented with 20 mM Hepes was obtained from Flow Labs. (Irvine, Scotland); tissue culture plastics and Transwell systems were from Costar (Cambridge, MA). Penicillin/streptomycin and bFGF was purchased from Boehringer Mannheim (Mannheim, FRG). A crude preparation of endothelial cell growth factor was prepared from bovine hypothalamus as described by Maciag et al. (1979). Human serum was obtained from a local bloodbank and was prepared from fresh blood from 10–20 healthy donors, pooled, and stored at 4°C; it was not heat-inactivated before use. Newborn calf serum (NBCS) was obtained from GIBCO BRL (Gaithersburg, MD), heparin and thrombin from Leo Pharmaceutics Products (Weesp, The Netherlands), human fibrinogen from Chromogenix AB (Mölndal, Sweden) and horseradish peroxidase (HRP) from Sigma Chem. Co. (St. Louis, MO). Factor XIII was generously provided by Dr. H. Keuper (Behringwerke, Marburg, Germany), human recombinant $VEGF_{165}$ was prepared as described (Fiebich et al., 1992). Human recombinant TNFα was a gift from Dr. J. Travernier (Biogent, Gent, Belgium) and contained 2.45×10^7 U/mg protein and <40 ng lipopolysaccharide per μg protein. Rabbit polyclonal anti–u-PA antibodies and rabbit polyclonal anti–t-PA antibodies were prepared in our laboratory. Single-chain u-PA (Orsini et al., 1991) was kindly provided by Dr. A. Molinari (Farmitalia, Carlo Erbe, Milan, Italy), the amino terminal fragment of u-PA (ATF: amino acids 1-143) was provided by Abbott (Abbott Park, IL). Tyrphostin A47 was obtained from LC Laboratories (Woburn, MA). Aprotinin was purchased from Pentapharm Ltd. (Basel, Switzerland), ε-aminocaproic acid (ε-ACA) was purchased from Merck (Darmstadt, Germany) and CHO cell supernatant containing soluble u-PA receptor (Wilhelm et al., 1994) was a gift from Dr. U. Weidle (Boehringer-Mannheim, Penzberg, Germany). Purified soluble u-PAR was obtained by affinity chromatography using u-PA–coupled Sepharose (>95% pure as determined using SDS-PAGE analysis).

Cell Culture

Human foreskin microvascular endothelial cells (hMVEC) and human umbilical vein endothelial cells (HUVEC) were isolated, cultured, and characterized as previously described (Van Hinsbergh et al., 1987, 1990; Defilippi et al., 1991*a*). Cells were cultured on fibronectin-coated dishes in M199 supplemented with 20 mM Hepes (pH 7.3), 10% human serum, 10% heat-inactivated NBCS, 150 μg/ml crude endothelial growth factor, 5 U/ml heparin, 100 IU/ml penicillin, and 100 μg/ml streptomycin at 37°C under 5%CO_2/95% air atmosphere.

For the evaluation of the role of TNFα, bFGF, and $VEGF_{165}$ on the production of u-PA, tissue-type plasminogen activator (t-PA) and PAI-1, and on the u-PA receptor expression, hMVEC were cultured on fibronectin-coated culture dishes without growth factor for 2 d. Thereafter, the endothelial cells were stimulated with bFGF, $VEGF_{165}$, or TNFα in M199 supplemented with 10% human serum and penicillin/streptomycin for 24 h. The supernatants were collected for the determination of u-PA antigen, t-PA antigen, and PAI-1 antigen by ELISA; the cells were used to determine the u-PA–binding capacity (see below).

ELISAs

u-PA ELISA. The monoclonals used in this ELISA were produced in our laboratory, and recognized single-chain u-PA, two-chain u-PA, and the u-PA/PAI-1 complex with comparable efficiency. 96-well microtiter plates were coated overnight at room temperature with 100 μl of a mixture of two monoclonal antibodies, UK 2.1 and UK 26.15, recognizing different epitopes on the u-PA antigen (0.5 μg/ml each in phosphate buffered saline, PBS). After washing with PBS-0.02% Tween 20 (PBS-T), the plates were incubated for 1 h with 150 μl of 0.1% (wt/vol) casein in PBS-T to block nonspecific protein binding to the plates. The plates were then washed three times with PBS-T and 100 μl of serial dilutions of standard u-PA (UKIDAN®, Serono, Aubonne, Switzerland, assuming that one unit, as determined by the manufacturer, is 10 ng protein) or culture supernatant were added. After 2 h at 37°C, the plates were washed three times and incubated with 100 μl of a biotinylated anti–u-PA antibody (LMW 11.1, 0.4 μg/ml in PBS-T containing 0.1% casein) for 1.5 h at 37°C, followed by a 1-h incubation with 100 μl of HRP conjugated to avidin (1:5.000; Pierce Chem. Co., Rockford, IL). Finally, the plates were washed four times with PBS-T, and 100 μl of tetramethylbenzidine substrate was added to react and the reaction was stopped with 50 μl 2 M H_2SO_4 after 15 min incubation at room temperature. The extinction at 450 nm was measured with a multichannel spectrophotometer (Titertek multiscan, Flow Labs.).

PAI-1 ELISA. Levels of PAI-1 antigen in endothelial cell conditioned media were assayed by ELISA (IMULYSE™PAI-1) obtained from Biopool (Umea, Sweden), according to the manufacturer's description.

t-PA ELISA. Assay of t-PA antigen was performed with the ELISA Thrombonostika t-PA (Organon-Teknika, Turnhout, Belgium) as described by Bos et al. (1992). In this assay, free t-PA and t-PA:PAI-1 complexes are detected with equal efficiency.

Determination of Specific u-PA Binding

Diisopropylfluorophosphate-treated u-PA (Ukidan®) (DIP-u-PA) was radiolabeled using $Na^{125}I$ according to the Iodogen procedure (Pierce

Chem. Co.). Binding of ^{125}I-DIP-u-PA to hMVEC was determined at 0°C. The cells were placed on melting ice and incubated for 10 min with 50 mM glycine-HCl buffer (pH 3.0) to remove receptor-bound endogenous u-PA. Subsequently, the cells were washed twice with ice-cold M199 medium and incubated with 8 nM or the indicated amount of ^{125}I-DIP-u-PA in endothelial cell–conditioned medium (M199 medium supplemented with 1% human serum albumin, conditioned for 24 h) for 3 h. Incubation was performed in endothelial cell–conditioned medium to exclude residual binding of u-PA to cell-associated PAI-1. In parallel incubations, a 50-fold excess of DIP-u-PA was included to assess nonspecific binding. After the incubation period, unbound ligand was removed by extensive washing with ice-cold PBS. Cell-bound ligand was solubilized with 0.3 M NaOH, and the radioactivity was determined in a γ-counter (Cobra Auto gamma, Packard). Specific binding was calculated by subtraction of nonspecific binding from the total binding.

Incorporation of [^{3}H]Thymidine

Incorporation of [^{3}H]thymidine in DNA was determined as previously described (Van Hinsbergh et al., 1983). Confluent cultures of endothelial cells were detached by trypsin/EDTA solution, and seeded at a density of 10^4 cells per cm^2 on fibronectin-coated dishes in M199-Hepes medium supplemented with 10% heat-inactivated newborn calf serum and penicillin/streptomycin with or without 20 ng/ml bFGF. After a preincubation period of 18 h, a tracer amount of [^{3}H]thymidine (0.5 μCi per 2 cm^2 well, added in a 10-μl vol) was added and the cells were incubated for a 6-h period. Subsequently, the cells were washed with PBS, and ^{3}H-labeled DNA was precipitated in 10% trichloroacetic acid, washed twice in 96% ethanol, dissolved in 0.3 ml 0.3 M NaOH and counted in a liquid scintillation counter.

In Vitro Angiogenesis Model

Human fibrin matrices were prepared by addition of 0.1 U/ml thrombin to a mixture of 5 U/ml factor XIII (final concentrations), 2 mg fibrinogen, 2 mg Na-citrate, 0.8 mg NaCl and 3 μg plasminogen per ml M199 medium. 300 or 600 μl of this mixture was added to the wells of 48 or 24-well plates, respectively. After clotting at 37°C, the fibrin matrices were soaked with M199 supplemented with 10% human serum and 10% NBCS for 2 h at 37°C to inactivate the thrombin. Highly confluent endothelial cells were detached and seeded in a 1:1 split ratio on the fibrin matrices and cultured for 24 h in M199 medium supplemented with 10% human serum, 10% NBCS, and penicillin/streptomycin. Then, the endothelial cells were cultured with either of the mediators indicated for 8–12 d. The culture medium was collected and replaced every 2 or 3 d. Invading cells and the formation of tubular structures of endothelial cells in the three-dimensional fibrin matrix were analyzed by phase contrast microscopy and the total number, the total area and the total length of tubelike structures of six randomly chosen microscopic fields/well (7.3 mm^2/field) were measured using a Nikon FXA microscope equipped with a monochrome CCD camera (MX5) connected to a computer with Optimas image analysis software. All three measured parameters correlated well with each other ($r >$ 0.96). The formation of tubular structures of endothelial cells in the three-dimensional fibrin matrix was also analyzed by histological examination after fixation of the matrices as described below. Inhibition experiments were performed by the addition of either 100 KIU/ml aprotinin, 0.5 μg/ml soluble u-PA receptor, 10 μg/ml tyrphostin A47, rabbit polyclonal anti–u-PA (1:100 serum dilution), rabbit polyclonal anti–t-PA (1:100 serum dilution), nonimmune rabbit serum (1:100 serum dilution), or 5 mM ε-ACA to the culture medium.

Histological Analysis

Electron Microscopy. For electron microscopy, the fibrin matrices were fixed and treated as described by Murray et al. (1991). Briefly, the matrices were fixed with 2% glutaraldehyde in 0.15 M Na-cacodylate buffer (pH 7.4), postfixed in 1% osmium tetroxide in the same buffer, dehydrated by a graded series of ethanol and embedded in Epon (LX resin, Ladd Research Industries Inc., Burlington, VT) as described (Murray et al., 1991). The embedded matrices were cut (0.1 μm) perpendicularly to the surface of the matrix sheet, stained with uranyl acetate and lead citrate, and finally analyzed using a Philips EM 410 electron microscope.

Light Microscopy. After overnight fixation at 4°C with 10% formalin and amidoblack 10B (0.1% wt/vol), the matrices were washed three times in aquadest, dehydrated by a graded series of ethanol, and embedded in glycol methacrylate as described (Gerrits et al., 1991). The embedded matrices were cut (3 μm) perpendicularly to the surface of the matrix sheet, stained with 0.1% haematoxylin, and analyzed.

Statistical Analysis

Statistical significance of differences were tested by one-way Anova analysis followed by Dunnett's Multiple Comparisons Test.

Results

Effects of bFGF, VEGF$_{165}$, and TNFα on the Production of Plasminogen Activators and PAI-1 by Human Microvascular Endothelial Cells

When human foreskin microvascular endothelial cells (hMVEC) were stimulated for 24 h with various concentrations of TNFα, a dose-dependent increase of u-PA antigen production was found (Fig. 1 *A*). However, incubation of hMVEC with VEGF$_{165}$ or bFGF did not change the production of u-PA antigen, or even slightly decreased u-PA accumulation in the conditioned medium (Fig. 1 *A*). A similar pattern was seen in the production of PAI-1 antigen by hMVEC (Fig. 1 *B*).

The production of t-PA by hMVEC was dose dependently stimulated by the addition of VEGF$_{165}$ or TNFα but not by bFGF (Fig. 1 *C*). The VEGF$_{165}$- and TNFα-induced increase in t-PA production was consistently observed in a number of hMVEC cultures derived from different donors and was also found at the mRNA level (data not shown). Whereas VEGF$_{165}$ enhanced t-PA synthesis in HUVEC, TNFα did not increase t-PA mRNA and synthesis in HUVEC, in agreement with previous observations (van Hinsbergh et al., 1990).

Simultaneous incubation of hMVEC with bFGF or VEGF$_{165}$ did not influence the TNFα-induced production of u-PA, t-PA, or PAI-1 by hMVEC after 24 h of incubation significantly (data not shown).

Effects of bFGF, VEGF$_{165}$, and TNFα on the Expression of u-PA Receptors on hMVEC

The number of u-PARs on hMVEC was determined from the binding of ^{125}I-DIP-u-PA to these cells. bFGF increased the specific binding of ^{125}I-DIP-u-PA to hMVEC in a concentration-dependent way (Fig. 1 *D*, Table I). Comparably, VEGF$_{165}$ induced an increase in specific ^{125}I-DIP-u-PA binding to hMVEC (Fig. 1 *D*, Table I). This effect was detectable from a concentration of 1–10 ng/ml VEGF$_{165}$, maximal at 50–100 ng/ml VEGF$_{165}$, and was identical in the presence or absence of heparin (not shown). The effects of bFGF and VEGF$_{165}$ were additive (Fig. 1 *D*). Scatchard analysis of the ^{125}I-DIP-u-PA–binding data revealed one type of binding site on hMVEC (Fig. 2). The number of ^{125}I-DIP-u-PA–binding sites increased from 3.8×10^4 sites per endothelial cell to 5.6×10^4, 6.3×10^4, and 9.1×10^4 per cell after incubation with 20 ng/ml bFGF, 100 ng/ml VEGF$_{165}$, or bFGF and VEGF$_{165}$, respectively. The affinity of the u-PAR was not significantly altered by incubation with bFGF and/or VEGF$_{165}$ and ranged from 2.0 nM to 2.9 nM under the various conditions. Cross-linking of ^{125}I-DIP-u-PA with endothelial cell membrane proteins resulted in the formation of a complex of 100 kD (the molecular mass of the u-PA:u-PA receptor complex) in untreated and VEGF- or bFGF-treated cells (not shown).

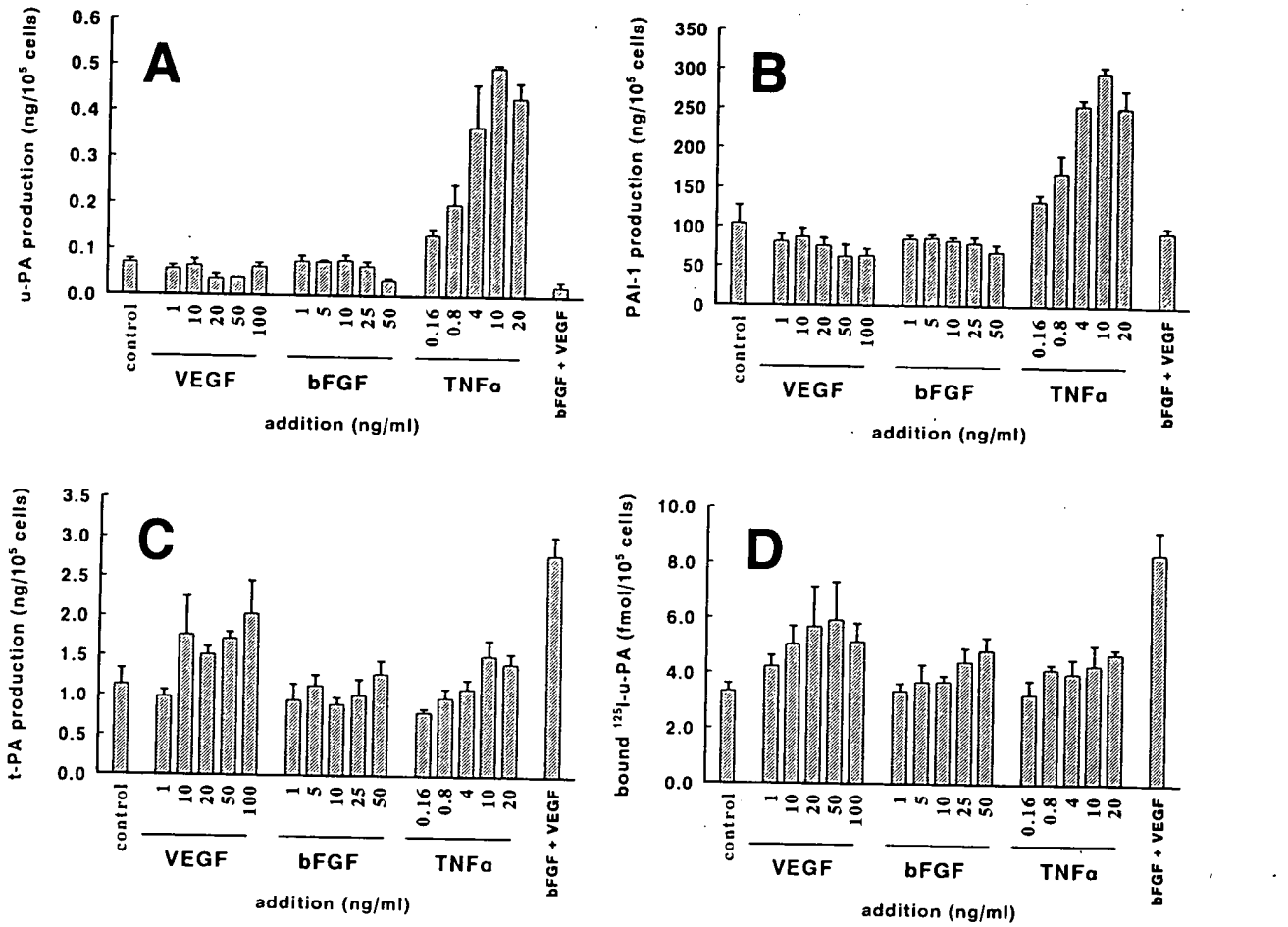

Figure 1. Effect of bFGF, $VEGF_{165}$, and TNFα on ^{125}I-DIP-u-PA binding to and the production of u-PA, t-PA, and PAI-1 by hMVEC. hMVEC were stimulated for 24 h with the indicated amounts of bFGF, $VEGF_{165}$, TNFα, or the combination of 50 ng/ml bFGF and 100 ng/ml $VEGF_{165}$. The amount of (*A*) u-PA antigen, (*B*) PAI-1 antigen, and (*C*) t-PA antigen in the supernatants was determined by ELISA. The number of u-PAR (*D*) was determined by the binding of ^{125}I-DIP-u-PA to the hMVEC as described in Materials and Methods. The data represent mean ±SD of triplicate wells and are representative for three experiments.

An increase in ^{125}I-DIP-u-PA binding was also detected after incubation of hMVEC with TNFα (Fig. 1 *D*; Table I). This was observed in seven independent hMVEC cultures (130 ± 40% increase, mean ± SD), whereas it was not found in four independent cultures of HUVEC (83 ± 4%).

Effect of bFGF, $VEGF_{165}$, and TNFα on Angiogenesis In Vitro

To investigate the ability of bFGF, $VEGF_{165}$, and TNFα to induce human endothelial cell tube formation in vitro, hMVEC were cultured on three-dimensional fibrin matrices in the continuous presence of 50 ng/ml bFGF, 100 ng/ml $VEGF_{165}$, 4 ng/ml TNFα, or combinations of these mediators. After 8–10 d of culture, invading cells and the formation of tubular structures of endothelial cells in the three-dimensional fibrin matrix were analyzed by phase contrast microscopy, and, after fixation of the matrices, by histological examination of cross-sections. In unstimulated cultures and in cultures stimulated with TNFα, confluent monolayers of endothelial cells remained on top of the three-dimensional fibrin matrix, but invading endothelial cells and tubular structures in the fibrin matrix could not be observed (Fig. 3, *a* and *b*, and 4 *a*). Addition of bFGF, $VEGF_{165}$, or the combination of bFGF and $VEGF_{165}$ to the hMVEC induced an increase in the number of endothelial cells on the fibrin matrix (130–155% of control after stimulation with $VEGF_{165}$ or bFGF, respectively).

Table I. Binding of ^{125}I-DIP-u-PA to Human Endothelial Cells

Addition	Binding of ^{125}I-DIP-u-PA (Percent of control)			
	hMVEC		HUVEC	
None	100 (2.6 ± 1.3 fmol/10^5 cells)	(n = 8)	100 (6.4 ± 3.2 fmol/10^5 cells)	(n = 17)
bFGF (20 ng/ml)	172 ± 25*	(n =8)	178 ± 33*	(n = 17)
TNFα (20 ng/ml)	130 ± 40	(n = 7)	83 ± 4	(n = 4)
VEGF (100 ng/ml)	146 ± 40‡	(n = 6)	156 ± 27*	(n = 4)

Binding of ^{125}I-DIP-u-PA to hMVEC was determined at 0°C. Receptor-bound endogenous u-PA was removed by pH treatment as described in Materials and Methods. After washing, the cells were incubated with 7.5 nM ^{125}I-DIP-u-PA for 3 h. In parallel incubations a 50-fold excess of unlabeled DIP-u-PA was included to assess nonspecific binding. Unbound ligand was removed by extensive washing with ice-cold PBS. Cell-bound ligand was solubilized in 0.3 M NaOH, and radioactivity was determined in a γ-counter. Specific binding was calculated by subtraction of nonspecific binding. The data represent the mean ±SD.
*$P < 0.01$.
‡$P < 0.05$.

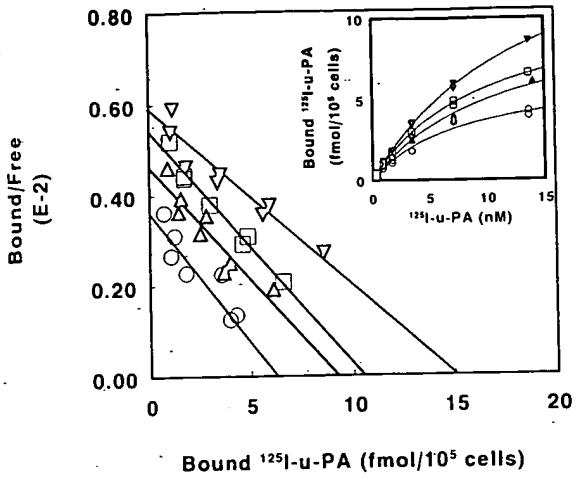

Figure 2. Scatchard analysis of the binding of ^{125}I-DIP-u-PA to hMVEC. hMVEC were preincubated for 24 h in M199 medium, 10% human serum supplemented with 20 ng/ml bFGF (Δ), 100 ng/ml $VEGF_{165}$ (□), 20 ng/ml bFGF plus 100 ng/ml $VEGF_{165}$ (∇), or without growth factor (○). Subsequently, the cells were cooled on ice and binding of ^{125}I-DIP-u-PA was performed as described in the Materials and Methods section. The results of the binding of ^{125}I-DIP-u-PA are shown in the inset.

However, these growth factors failed to induce the formation of tubular structures of endothelial cells in the fibrin matrix (Fig. 3, *c–e*). When TNFα was added simultaneously with bFGF or $VEGF_{165}$ to the hMVEC monolayers, the formation of tubular structures was induced (Fig. 3, *f* and *g*), whereas the number of endothelial cells on top of the fibrin matrix was not significantly changed (95% of control) compared with nonstimulated conditions. Control experiments revealed that the amount of TNFα used in the experiments completely inhibited the bFGF- and $VEGF_{165}$-induced increase in endothelial cell number on top of the fibrin matrix (data not shown). The growth of the tubular structures started after 4–5 d of stimulation and was optimal at day 8–10 after continuous stimulation of the endothelial cell monolayers. However, when hMVEC were stimulated with $VEGF_{165}$, bFGF, and TNFα simultaneously, a more than additive effect of these factors was observed (Fig. 3 *h* and Fig. 4 *b*).

Dose-response experiments using $VEGF_{165}$ and bFGF in the presence of 4 ng/ml TNFα showed that the minimal concentration of $VEGF_{165}$ and bFGF to induce formation of tubular structures of hMVEC was 10 ng/ml and 0.5 ng/ml, respectively, whereas the maximal formation of tubular structures in the presence of 4 ng/ml TNFα required the combination of 100 ng/ml $VEGF_{165}$ and 50 ng/ml bFGF (data not shown).

Histological analysis of the cross-sections perpendicular to the surface of the matrix showed that these capillary-like structures were located in the fibrin matrix underneath the endothelial cell monolayer. The capillary-like structures consist of hMVEC surrounding a lumen (Fig. 4 *d*, *arrows*). Electron microscopy analyses revealed that these hMVEC had cellular polarization, pinocytotic vesicles at the lumenal side, and a basement membrane at the basolateral side of the cell (data not shown). Furthermore these electron microscopy analyses of capillary-like structures of hMVEC revealed remodeling of the fibrin matrix at the basolateral side of the endothelial cells (Fig. 4 *e*, *arrows*).

Similar results were obtained when two other strains of hMVEC from different donors were used. When five different HUVEC isolations were used, heterogenous results were obtained. Three cultures formed tubular structures just like the three hMVEC cultures: only after the addition of TNFα in combination with bFGF and/or $VEGF_{165}$. One HUVEC isolation did not invade the fibrin matrix, even after the addition of bFGF, $VEGF_{165}$ and TNFα, whereas the fifth HUVEC culture formed tubular structures spontaneously (data not shown).

Long-Term Effect of bFGF, $VEGF_{165}$, and TNFα on the Production of u-PA and PAI-1 by Human Microvascular Endothelial Cells

The secretion of u-PA and PAI-1 by the hMVEC cultured on the fibrin matrix was followed during the time period of the formation of tubelike structures of these hMVEC. The u-PA concentration in the supernatants of unstimulated hMVEC did not increase significantly during the culture period of 10 d (Fig. 5 *A*). Incubation of the hMVEC with bFGF, $VEGF_{165}$, or the combination of these two growth factors did not induce an increase in u-PA production. The initial accumulation of u-PA in the endothelial cell conditioned medium during the first 24-h incubation of hMVEC with TNFα (Fig. 1), disappeared during prolonged incubation of hMVEC with TNFα. However, the PAI-1 production rate continued to increase during the 10-d culture period in the presence of TNFα (Fig. 5 *B*). We observed a continued increase in the u-PA production rate by hMVEC when TNFα was added in combination with either bFGF or $VEGF_{165}$, or both growth factors (Fig. 5 *A*). Similarly, PAI-1 antigen production rate by the hMVEC increased during this culture period (Fig. 5 *B*).

Role of Plasminogen Activators, u-PA Receptor, and Plasmin during In Vitro Angiogenesis

The role of u-PA, t-PA, and the role of the expression of u-PAR during the formation of tubular structures of hMVEC in the fibrin matrices was studied by the addition of u-PA or t-PA specific antibodies which inhibit PA activity and by the addition of soluble u-PAR. Both the u-PA specific polyclonal antibodies, the soluble u-PAR containing CHO supernatant, and affinity-purified soluble u-PAR inhibited the formation of tubular structures (Table II). Furthermore, there was also a decrease in the diameter of the tubes after the addition of the u-PA inhibitors (data not shown). In contrast, polyclonal antibodies inhibiting t-PA activity, preimmune serum and control supernatants of CHO cells did not inhibit the formation of tubelike structures significantly. Addition of aprotinin or ε-ACA also inhibited the formation of tubular structures for ~71–95%, respectively, indicating that plasmin activity, which is probably generated by u-PA, is also involved in the formation of tubular structures in the fibrin matrix. When fibrin matrices were made using plasminogen-depleted fibrinogen, no ingrowth of endothelial cells and formation of tubular structures was observed (data not shown).

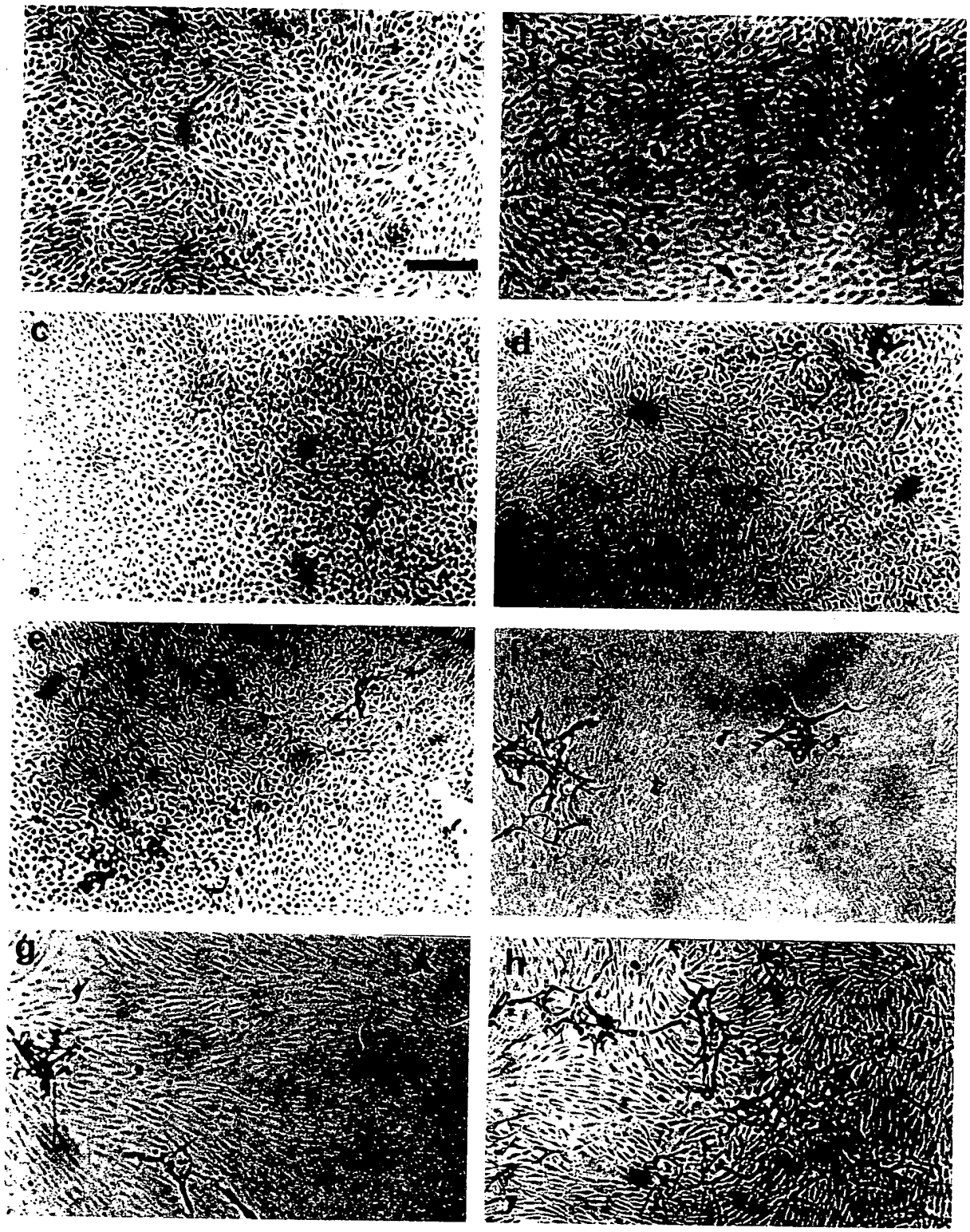

Figure 3. In vitro angiogenesis induced by bFGF, $VEGF_{165}$, and TNFα. hMVEC were cultured on the surface of a three-dimensional fibrin matrix in M199 medium supplemented with 10% human serum and 10% NBCS and stimulated without (*a*) or with 4 ng/ml TNFα (*b*), 50 ng/ml bFGF (*c*), 100 ng/ml $VEGF_{165}$ (*d*), bFGF and $VEGF_{165}$ (*e*), bFGF and TNFα (*f*), $VEGF_{165}$, and TNFα (*g*), or the combination of all three mediators (*h*). After 10 d of culture, nonphase contrast views were taken; the plane of focus is beneath the endothelial surface monolayer. Bar represents 500 μm.

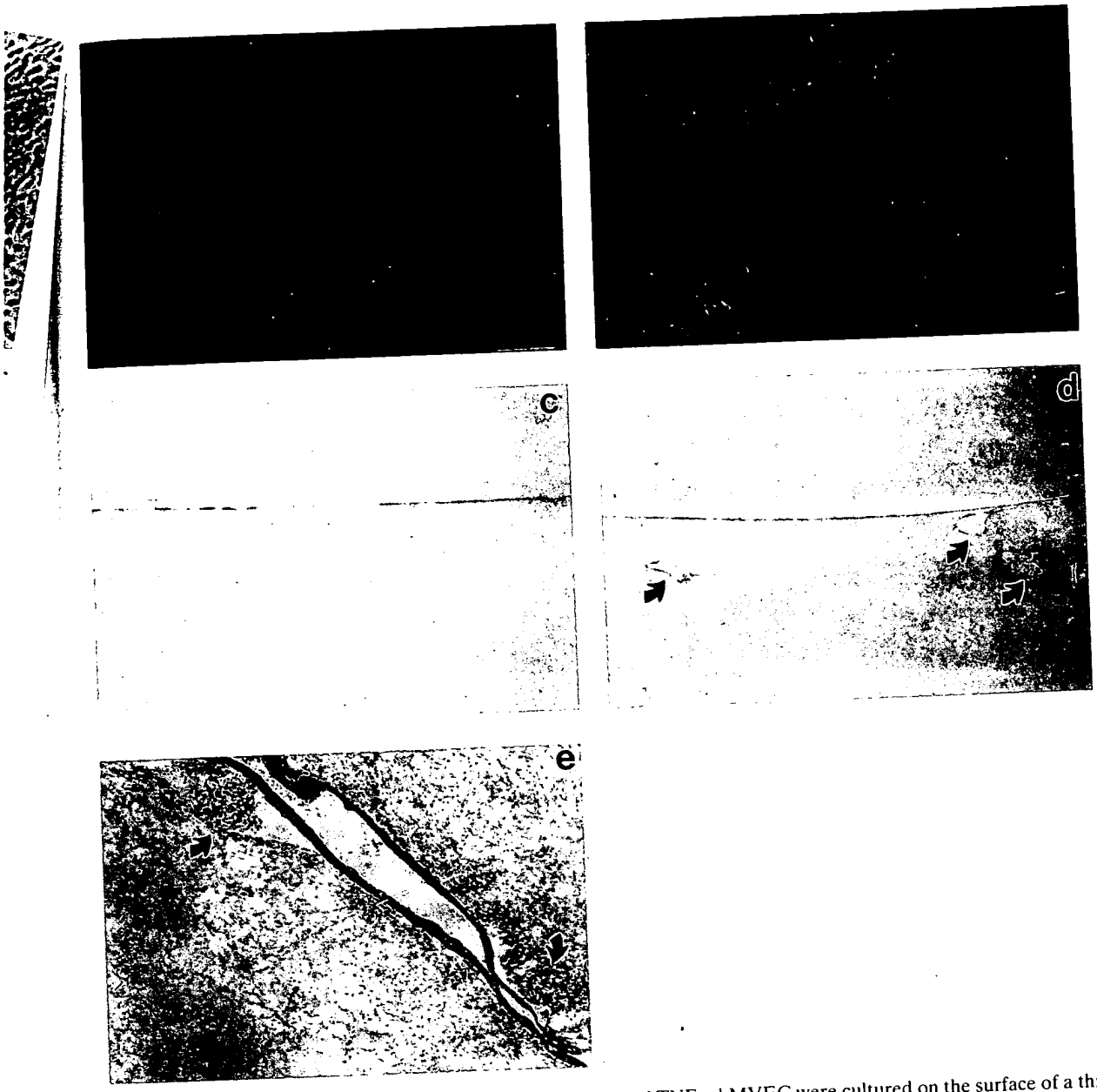

Figure 4. In vitro angiogenesis induced by bFGF, $VEGF_{165}$, and TNFα. hMVEC were cultured on the surface of a three-dimensional fibrin matrix in M199 medium supplemented with 10% human serum and 10% NBCS and stimulated with (*b*, *d*, and *e*) or without (*a* and *c*) the combination of bFGF (50 ng/ml), $VEGF_{165}$ (100 ng/ml), and TNFα (4 ng/ml). (*a* and *c*) After 10 d of culture, phase contrast photomicrographs were taken; the plane of focus is beneath the endothelial surface monolayer. (*c* and *d*) Histological examination of 3 μm cross-sections perpendicular to the matrix surface was performed. Lumens surrounded by endothelial cells are indicated by arrows. Magnification 25. (*e*) Electron microscopy analysis of a tubelike structure of microvascular endothelial cells was performed. Remodeling of the fibrin matrix is observed at the basolateral side of the endothelial cells (*arrows*). Magnification 5,000. Bar, 150 μm.

Formation of Tubelike Structures of hMVEC by Simultaneous Addition of bFGF, $VEGF_{165}$, and Single-Chain u-PA

An increase of u-PA (induced by TNFα in combination with bFGF and $VEGF_{165}$) and the presence of u-PAR (enhanced by bFGF and $VEGF_{165}$) seems to be required for the formation of tubelike structures of hMVEC in the fibrin matrix. To investigate whether the production of u-PA by bFGF- and $VEGF_{165}$-stimulated hMVEC is the limiting step in the formation of the tubelike structures, exogenous single-chain u-PA (scu-PA) was added to the hMVEC cultured on the fibrin matrix. Addition of scu-PA to unstimulated hMVEC or hMVEC stimulated with low doses of bFGF and $VEGF_{165}$, which are sufficient to induce mitogenicity but cause a moderate increase in u-PAR, did not significantly induce the formation of tubelike structures (Fig. 6). However, addition of 10 ng/ml scu-PA to hMVEC stimulated with higher amounts of bFGF and $VEGF_{165}$ resulted in the formation of tubelike structures in the fibrin matrix. The total length of these induced tube-

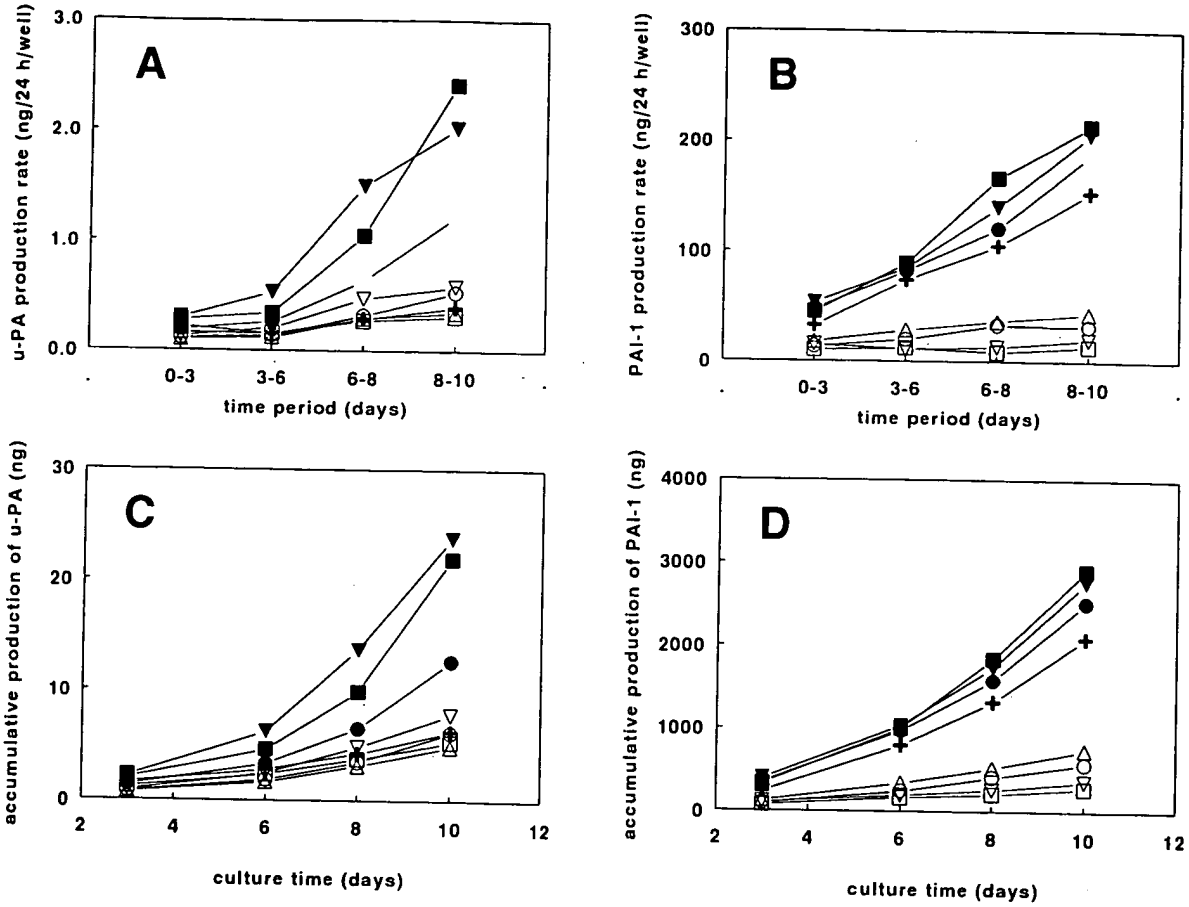

Figure 5. u-PA and PAI-1 production by long-term hMVEC cultures on fibrin matrices. hMVEC were cultured on the surface of a three-dimensional fibrin matrix in M199 medium supplemented with 10% human serum and 10% NBCS (□), and stimulated with bFGF (50 ng/ml, △), $VEGF_{165}$ (100 ng/ml, ○), TNFα (4 ng/ml, +), bFGF and $VEGF_{165}$ (▽), bFGF and TNFα (■), $VEGF_{165}$ and TNFα ( ), or bFGF, $VEGF_{165}$ and TNFα (▼). u-PA and PAI-1 antigen was determined by ELISA as described and the production was expressed as ng/24 h (production rate) or ng/well (cumulative production). Similar results were obtained in four independent experiments.

like structures was higher as compared to that induced by the addition of TNFα. Addition of the amino terminal fragment (ATF) of u-PA did not induce the outgrowth of tubular structures in the fibrin matrix (Fig. 6).

Mitogenesis Stimulates but Is Not Essential for the Formation of Tubular Structures

Both bFGF and $VEGF_{165}$ are mitogenic factors for human endothelial cells. Maximal [^{3}H]thymidine incorporation is reached at 1–4 ng/ml bFGF or $VEGF_{165}$ (data not shown), a much lower concentration needed to increase u-PAR expression. This suggests that different receptors are involved in the mitogenesis and the induction of u-PAR. This suggestion is further strengthened by the observation that [^{3}H]thymidine incorporation and cell proliferation induced by bFGF or $VEGF_{165}$ are inhibited by the tyrosine kinase inhibitor tyrphostin A47 (Fig. 7 *A*), whereas the induction of the u-PAR is not affected by this inhibitor (Fig. 7 *B*).

To investigate whether endothelial cell proliferation is important in our in vitro angiogenesis model, we added the tyrphostin A47 to hMVEC stimulated with a combination of bFGF, $VEGF_{165}$, and TNFα. Addition of 10 μg/ml tyrphostin A47, inhibited the bFGF- and VEGF-induced hMVEC proliferation completely (Fig. 7 *A*) but did not affect the expression of the u-PAR (Fig. 7 *B*), u-PA, or PAI-1 expression (data not shown). This concentration of tyrphostin A47 reduced the formation of tubular structures in the fibrin matrix for 28–36% only (Table II). Control experiments indicated that the amount of tyrphostin A47 in the conditioned media after 48 or 72 h incubation was still sufficient to completely inhibit basal and bFGF-induced [^{3}H]thymidine incorporation in endothelial cells (data not shown). This indicates that proliferation is not essential for the formation of tubular structures of human endothelial cells.

Discussion

Fibrin, angiogenic factors, and inflammatory cells are commonly present in pathological forms of angiogenesis in the adult. In this study we report that, in addition to angiogenic growth factors bFGF and $VEGF_{165}$, the cytokine TNFα is required to induce capillary-like tubular structures of hMVEC in a three-dimensional fibrin matrix.

Furthermore, we demonstrate that the contribution of TNFα, which among many other effects induces u-PA production (van Hinsbergh et al., 1990), is mainly due to its ability to increase receptor-bound u-PA activity because

Table II. Effect of Various Inhibitors on the Formation of Tubular Structures of Human Microvascular Endothelial Cells In Vitro

Addition	Experiment 1		Experiment 2		Experiment 3	
	tube length	inhibition	tube length	inhibition	tube length	inhibition
	μm	%	μm	%	μm	%
None	6333 ± 4033		2667 ± 767		1040 ± 227	
bFGF + $VEGF_{165}$ + TFNα	106833 ± 10000		105167 ± 7887		148073 ± 18007	
bFGF + $VEGF_{165}$ + TFNα						
+ anti–u-PA serum	16667 ± 2500*	90	22667 ± 1153*	80	3107 ± 433*	99
+ anti–t-PA serum	ND		86500 ± 16933	18	153460 ± 16653	4
+ preimmune serum	ND		70667 ± 11167	33	145867 ± 28800	1
+ soluble u-PA receptor	48000 ± 2033‡	59	5167 ± 2180*	96	12440 ± 7753*	92
+ aprotinin	35167 ± 11553*	71	8833 ± 1687*	94	ND	
+ ε-ACA	ND		7553 ± 3087*	95	ND	
+ tyrphostin A47	68833 ± 7320	36	73404 ± 10980	31	106465 ± 5587	28

Human MVEC were cultured on the surface of a three-dimensional fibrin matrix in M199 medium supplemented with 10% human serum and 10% NBCS and stimulated with the combination of bFGF (50 ng/ml), $VEGF_{165}$ (100 ng/ml), and TNFα (4 ng/ml) with or without blocking anti–u-PA antiserum, anti–t-PA antiserum or preimmune serum (1:100 dilution), 0.5 μg/ml soluble u-PA receptor (CHO supernatant [Exps. 1 and 2] and affinity-purified [Exp. 3]), 100 KIU/ml aprotinin, 5 mM ε-ACA, or 10 μg/ml tyrphostin A47. After 10–12 d of culture, phase contrast photomicrographs were taken and the total length of tubelike structures was measured using a microscope equipped with a monochrome CCD camera (MX5) connected to a computer with image analysis software. The data represent the mean length/cm^2 ± SEM of triplicate (Exp. 1) or duplicate (Exps. 2 and 3) wells.
*$P < 0.01$.
‡$P < 0.05$.

u-PA but not its amino terminal fragment (ATF) can replace TNFα, and the formation of tubular structures is inhibited by anti–u-PA antibodies, soluble u-PAR, and plasmin inhibitors.

Our data closely agree with previous studies of Pepper et al. (1990, 1992) who demonstrated with bovine adrenal microvascular endothelial cells that bFGF or $VEGF_{165}$ enhanced endothelial cell migration and formation of capillary-like structures in a fibrin matrix by stimulation of receptor-bound u-PA activity, and that these growth factors acted synergistically to each other. On the other hand, our data seem to contrast with these studies (Pepper et al., 1990, 1992) because bFGF and $VEGF_{165}$ themselves were unable to induce tubelike structures of hMVEC. This difference can be explained by the fact that bFGF and $VEGF_{165}$ are potent inducers of both u-PA and u-PAR in bovine cells (Saksela et al., 1987; Pepper et al., 1991, 1993), but bFGF and $VEGF_{165}$ do not enhance u-PA production in human endothelial cells (Bikfalvi et al., 1991; this study). However, a combination of angiogenic growth factor(s) and TNFα, which is a strong inducer of u-PA in human endothelial cells (van Hinsbergh et al., 1990; Niedbala et al., 1992) provides the requirements needed for the formation of capillary-like structures of hMVEC in vitro.

TNFα has multiple effects on endothelial cells, including the induction of leukocyte adhesion molecules (Bevilac-

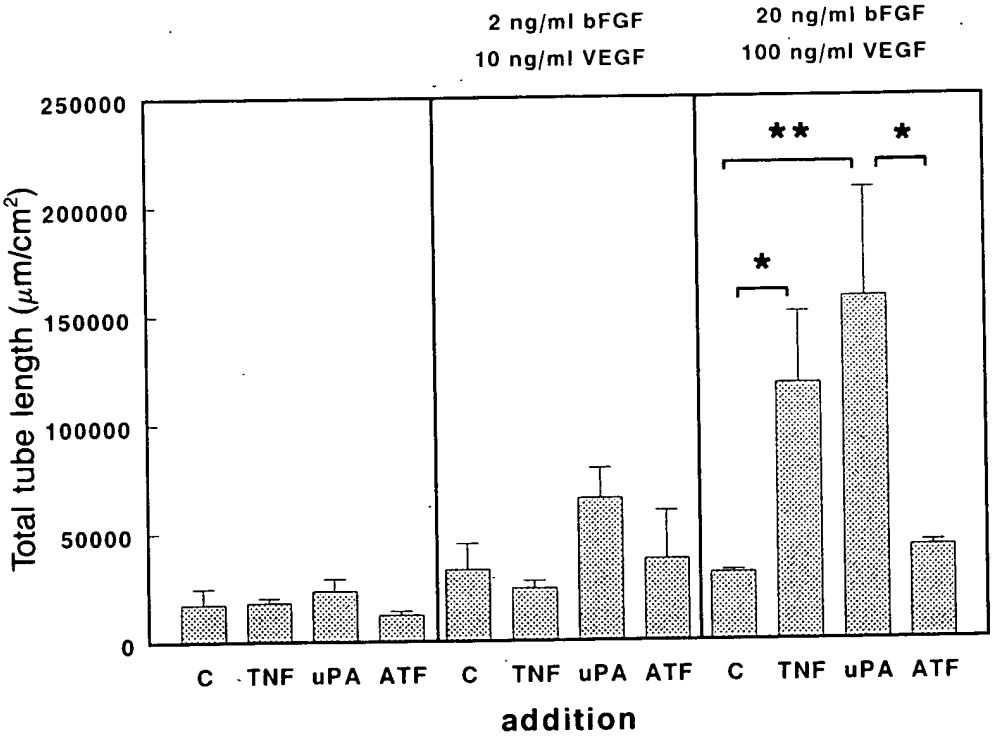

Figure 6. Formation of tubelike structures of hMVEC by simultaneous addition of bFGF, $VEGF_{165}$, and single-chain u-PA. hMVEC were cultured on the surface of a three-dimensional fibrin matrix in M199 medium supplemented with 10% human serum and 10% NBCS and stimulated with the combination of bFGF, $VEGF_{165}$ (as indicated), and either TNFα (4 ng/ml), single-chain u-PA or ATF (10 ng/ml). Total tube-length/cm^2 ± SEM was determined of triplicate wells as described.

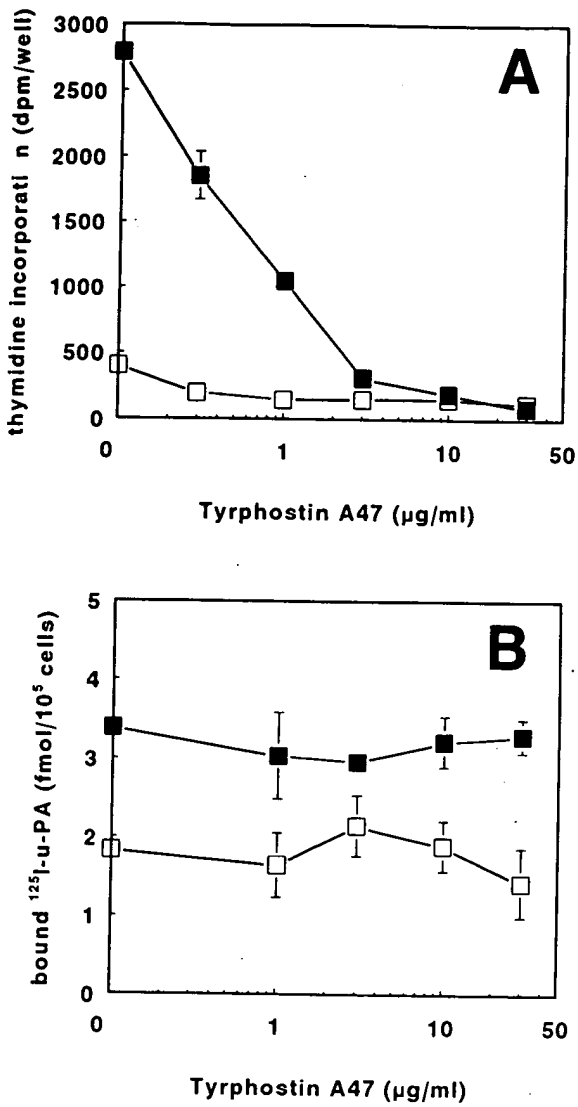

Figure 7. Induction of mitogenesis and u-PAR expression by bFGF and $VEGF_{165}$ proceed by different pathways. Effect of the tyrosine kinase inhibitor tyrphostin A47 on basal and bFGF and/or $VEGF_{165}$ induced proliferation and pericellular u-PA expression of hMVEC. (*A*) Subconfluent hMVEC were cultured in the absence (□) and presence (■) of 20 ng/ml bFGF for 18 h in the presence of increasing amounts of tyrphostin A47. After 18 h, a tracer amount of [^{3}H]thymidine was added to the medium and the incubation continued in the same medium for another 6 h and [^{3}H]thymidine incorporation was determined as described in the Materials and Methods section. (*B*) Confluent hMVEC were cultured for 24 h in M199 medium supplemented with 10% human serum (□) or in M199 supplemented with 10% human serum and 50 ng/ml bFGF and 50 ng/ml $VEGF_{165}$ (■). u-PAR expression was determined by the binding of ^{125}I-DIP-u-PA to the endothelial cells as described in the legend of Fig. 2.

qua et al., 1994), induction of inducible forms of cyclooxygenase and nitric oxide synthase (Hla and Neilson, 1992; Gross et al., 1992), enhanced expression of integrins (Defilippi et al., 1991*a*,*b*), inhibition of mitogenesis (Fratèr-Schröder et al., 1987; Cavender et al., 1989), and induction of u-PA and PAI-1 (van Hinsbergh et al., 1988, 1990; Schleef et al., 1988). Our observation that soluble u-PAR and antibodies, which inhibit u-PA activity, markedly inhibited the formation of capillary-like structures, suggests a role of TNFα-induced u-PA. This suggestion is strengthened by the finding that, similar to TNFα, u-PA can induce the outgrowth of tubular structures but only in the presence of bFGF and/or $VEGF_{165}$. It is likely that the effect of u-PA involves proteolytic activation of plasminogen by receptor-bound u-PA because the ATF of u-PA, which binds similarly to the u-PAR receptor but has no proteolytic activity, was inactive. Furthermore, inhibition of plasminogen activation by ε-ACA, inhibition of plasmin activity by aprotinin or plasminogen withdrawal also reduced the outgrowth of tubular structures.

bFGF and VEGF increased the number of u-PAR in human endothelial cells (Mignatti et al., 1991; this study). Although this may contribute to an increase in u-PA activity on the cell surface, it is unlikely that the effect of the angiogenic growth factors on the stimulation of tubular outgrowth is mainly due to u-PAR enhancement. TNFα, which in hMVEC causes a 30% increase in u-PAR in addition to inducing u-PA synthesis, had no effect when it was added to the cells alone. bFGF and VEGF both are potent mitogens for hMVEC. However, it is unlikely that stimulation of mitogenesis is the predominant effect of these growth factors because little cell proliferation is observed in the presence of TNFα, and a potent inhibitor of both bFGF- and VEGF-induced mitogenesis tyrphostin A47 had only a moderate inhibitory effect on the outgrowth of tubular structures. Furthermore, the optimal concentrations needed to induce mitogenesis and tubular structures differ an order of magnitude both for bFGF and VEGF. Whether this reflects the involvement of different receptors for bFGF and VEGF in mitogenesis and the formation of tubular structures remains to be investigated.

The importance of additional mechanisms by which bFGF and VEGF may act is stressed by our observation that during long-term stimulation of hMVEC with TNFα, the presence of growth factors (bFGF or $VEGF_{165}$) is necessary to give an accelerating u-PA production after several days of incubation. This unexpected observation may suggest that the addition of bFGF and/or $VEGF_{165}$ to hMVEC facilitates hMVEC to respond to TNFα with regard to u-PA production during continuous exposure to TNFα. If that would be the case, addition of u-PA instead of TNFα would not require addition of bFGF and $VEGF_{165}$ for the induction of tubular structures. Our data indicate that at low concentrations of bFGF and $VEGF_{165}$ u-PA has a relatively larger effect than TNFα, but that it does not induce tubular structures in the absence of the growth factors. It should be noted that at present it is not yet known whether the increased u-PA production after prolonged incubation in the simultaneous presence of TNFα, bFGF, and $VEGF_{165}$ is the consequence of an increased number of invading hMVEC or the prerequisite for hMVEC to continue the invasion into the fibrin gel.

The involvement of u-PA activity in the invasion of endothelial cells into the fibrin matrix draws the attention to the proteolytic properties of the u-PA/u-PAR system. However, it should be taken into account that disruption of cell–matrix interaction is only one side of the coin. Simultaneously, the cell has to create new attachment sites by which it "pulls" itself into the fibrin matrix. It is likely

that the mediators used in our model also act on such attachment sites, e.g., by regulation of integrin expression by bFGF (Enenstein et al., 1992) or TNFα (Defilippi et al., 1991*b*). In this context, the recent observation that the u-PAR can act as an adhesion receptor for vitronectin and that u-PA increases the interaction of u-PAR with vitronectin are of interest (Wei et al., 1994; Rao et al., 1995). Enhancement of the number of occupied u-PA receptors not only provides the cell with an enhanced local proteolytic capacity but also provides the cell the capacity to form new attachment sites with the extracellular matrix molecules. This mechanism may provide the endothelial cells with an enhanced capacity to migrate in the fibrin matrix. Vitronectin binds avidly to fibrin and hence may improve the suitability of the fibrin meshwork for cell invasion.

The data presented here, u-PA–dependent formation of capillary-like structures of hMVEC in fibrin matrices, may seem to be contrary to the fact that u-PA–deficient mice develop a normal embryonic and adult vasculature (Carmeliet and Collen, 1994). To our knowledge, the formation of blood vessels during embryonic development is independent of the presence of fibrin and inflammatory mediators, whereas angiogenesis in the adult usually involves fibrin and inflammatory cells. Furthermore, u-PA–deficient mice do have problems with several processes in which u-PA is thought to be involved, such as migration of smooth muscle cells after vascular injury, which are dependent on the presence of a temporary fibrin matrix (Carmeliet and Collen, 1994). Our model is a reflection of "pathological" angiogenesis, and is probably best comparable with angiogenic recanalization of a fibrin clot or the formation of new blood vessels in the temporary fibrin matrix present at sites of chronic inflammation. When angiogenesis proceeds in a fibrous exudate, the matrix to be invaded contains different types of matrix proteins including collagens. It is likely that invading endothelial cells then also attach to other matrix proteins, including collagens and that detachment of the cells needed for migration requires additional proteases, such as stromelysin, collagenases, and gelatinases. It may be of significance that the inflammatory mediator TNFα induces, in addition to u-PA (van Hinsbergh et al., 1990; Niedbala et al., 1992), several of these matrix metalloproteinases in human endothelial cells (Hanemaaijer et al., 1993). The contribution of these matrix-degrading proteinases in the formation of tubular structures in fibrin and more complex matrices has still to be evaluated.

In summary, we found that in addition to endothelial cell growth factors ($VEGF_{165}$ and bFGF), the cytokine TNFα or exogenously addition of u-PA is needed to induce in vitro the formation of capillary-like structures by hMVEC. Inhibition studies demonstrated that this induction requires cell-bound u-PA activity. These data may provide insight in the mechanism of angiogenesis as occurred in pathological conditions in the adult.

The authors thank Bep Blauw, Frits van der Ham, Bea van der Vecht, and Erna Peters for their excellent technical assistance.

Received for publication 7 December 1995 and in revised form 22 December 1995.

References

Bacharach, E., A. Itin, and E. Keshet. 1992. In vivo patterns of expression of urokinase and its inhibitor PAI-1 suggest a concerted role in regulating physiological angiogenesis. *Proc. Natl. Acad. Sci. USA.* 89:10686–10690.

Barnathan, E.S., A. Kuo, K. Kariko, L. Rosenfeld, S.C. Murray, N. Behrendt, E. Ronne, D. Weiner, J. Henkin, and D.B. Cines. 1990. Characterization of human endothelial cell urokinase-type plasminogen activator receptor protein and messenger RNA. *Blood.* 76:1795–1806.

Bevilacqua, M.P., R.M. Nelson, G. Mannori, and O. Cecconi. 1994. Endothelial-leukocyte adhesion molecules in human disease. *Annu. Rev. Med.* 45: 361–378.

Bikfalvi, A., C. Sauzeau, H. Moukadiri, J. Maclouf, N. Busso, M. Bryckaert, J. Plouet, and G. Tobelem. 1991. Interaction of vasculotropin/vascular endothelial cell growth factor with human umbilical vein endothelial cells: binding, internalization, degradation, and biological effects. *J. Cell. Physiol.* 149: 50–59.

Blasi, F., M. Conese, L.B. Møller, N. Pedersen, U. Cavallaro, M.V. Cubellis, F. Fazioli, L. Hernandez-Marrero, P. Limongi, P. Muñoz-Canoves, et al. 1994. The urokinase receptor: structure, regulation and inhibitor-mediated internalization. *Fibrinolysis.* 8:182–188.

Broadley, K.N., A.M. Aquino, S.C. Woodward, A. Buckley-Sturrock, Y. Sato, D.B. Rifkin, and J.M. Davidson. 1989. Monospecific antibodies implicate basic fibroblast growth factor in normal wound repair. *Lab. Invest.* 61:571–575.

Bos, R., K. Siegel, M. Otter, and W. Nieuwenhuizen. 1992. Production and characterization of a set of monoclonal antibodies against tissue-type plasminogen activator (t-PA). *Fibrinolysis.* 6:173–182.

Carmeliet, P., and D. Collen. 1994. Evaluation of the plasminogen/plasmin system in transgenic mice. *Fibrinolysis.* 8:269–276.

Cavender, D.E., D. Edelbaum, and M. Ziff. 1989. Endothelial cell activation induced by tumor necrosis factor and lymphotoxin. *Am. J. Pathol.* 134:551–560.

Colville-Nash, P.R., and D.L. Scott. 1992. Angiogenesis and rheumatoid arthritis - pathogenic and therapeutic implications. *Ann. Rheum. Dis.* 51:919–925.

Danø, K., N. Behrendt, N. Brünner, V. Ellis, M. Ploug, and C. Pyke. 1994. The urokinase receptor. Protein structure and role in plasminogen activation and cancer invasion. *Fibrinolysis.* 8:189–203.

Defilippi, P., V.W.M. van Hinsbergh, A. Bertolotto, P. Rossino, L. Silengo, and G. Tarone. 1991*a*. Differential distribution and modulation of expression of α1/β1 integrin on human endothelial cells. *J. Cell Biol.* 114:855–863.

Defilippi, P., G. Truffa, G. Stefanuto, F. Altruda, L. Silengo, and G. Tarone. 1991*b*. Tumor necrosis factor-α and interferon-γ modulate the expression of the vitronectin receptor (integrin-β3) in human endothelial cells. *J. Biol. Chem.* 266:7638–7645.

Docherty, A.J.P., J. O'Connell, T. Crabbe, S. Angal, and G. Murphy. 1992. The matrix metalloproteinases and their natural inhibitors: Prospects for treating degenerative tissue diseases. *Trends Biotechnol.* 10:200–207.

Dvorak, H.F., J.A. Nagy, B. Berse, L.F. Brown, K.T. Yeo, T.K. Yeo, A.M. Dvorak, L. Vandewater, T.M. Sioussat, and D.R. Senger. 1992. Vascular permeability factor, fibrin, and the pathogenesis of tumor stroma formation. *Ann. NY Acad. Sci.* 667:101–111.

Ellis, V., N. Behrendt, and K. Danø. 1991. Plasminogen activation by receptor-bound urokinase: a kinetic study with both cell-associated and isolated receptor. *J. Biol. Chem.* 266:12752–12758.

Enenstein, J., N.S. Waleh, and R.H. Kramer. 1992. Basic FGF and TGF-β differentially modulate integrin expression of human microvascular endothelial cells. *Exp. Cell Res.* 203:499–503.

Fiebich, B., B. Jäger, C. Schöllmann, K. Weindel, J. Wilting, G. Kochs, D. Marmé, H. Hug, and H.A. Weich. 1993. Synthesis and assembly of functionally active human vascular endothelial growth factor homodimers in insect cells. *Eur. J. Biochem.* 211:19–26.

Folkman, J. 1986. How is blood vessel growth regulated in normal and neoplastic tissue? G.H.A. Clowes memorial award lecture. *Cancer Res.* 46:467–473.

Folkman, J., and M. Klagsburn. 1987. Angiogenic factors. *Science (Wash. DC).* 235:442–447.

Folkman, J., and Y. Shing. 1992. Angiogenesis. *J. Biol. Chem.* 267:10931–10934.

Fràter-Schröder, M., W. Risau, R. Hallmann, P. Gautschi, and P. Böhlen. 1987. Tumor necrosis factor type α, a potent inhibitor of endothelial cell growth *in vitro*, is angiogenic *in vivo*. *Proc. Natl. Acad. Sci. USA.* 84:5277–5281.

Gerrits, P.O., B. Eppinger, H. van Goor, and R.W. Horobin. 1991. A versatile low toxicity glycol methacrylate embedding medium for use in biological research, and for recovered biomaterials prostheses. *Cells & Materials.* 1:189–198.

Goto, F., K. Goto, K. Weindel, and J. Folkman. 1993. Synergistic effect of vascular endothelial growth factor and basic fibroblast growth factor on the proliferation and cord formation of bovine capillary endothelial cells within collagen gels. *Lab. Invest.* 69:508–517.

Gross, S.S., E.A. Jaffe, R. Levi, and R.G. Kilbourn. 1991. Cytokine-activated endothelial cells express an isotype of nitric oxide synthase which is tetrahydrobiopterin-dependent, calmodulin-independent and inhibited by arginine analogs with rank-order of potency characteristic of activated macrophages. *Biochem. Biophys. Res. Commun.* 178:823–829.

Hanemaaijer, R., P. Koolwijk, L. Leclercq, W.J.A. de Vree, and V.W.M. van Hinsbergh. 1993. Regulation of matrix metalloproteinase expression in human vein and microvascular endothelial cells. Effects of tumor necrosis fac-

tor-α, interleukin-1 and phorbol ester. *Biochem. J.* 296:803–809.
Hla, T., and K. Neilson. 1992. Human cyclooxygenase-2 cDNA. *Proc. Natl. Acad. Sci. USA.* 89:7384–7388.
Klagsbrun, M., and P.A. D'Amore. 1991. Regulators of angiogenesis. *Annu. Rev. Physiol.* 53:217–239.
Koch, A.E., L.A. Harlow, G.K. Haines, E.P. Amento, E.M. Unemori, W.L. Wong, R.M. Pope, and N.E. Ferrara. 1994. Vascular endothelial growth factor. A cytokine modulating endothelial function in rheumatoid arthritis. *J. Immunol.* 152:4149–4156.
Langer, D.J., A. Kuo, K. Kariko, M. Ahuja, B.D. Klugherz, K.M. Ivanics, J.A. Hoxie, W.V. Williams, B.T. Liang, D.B. Cines, et al. 1993. Regulation of the endothelial cell urokinase-type plasminogen activator receptor. Evidence for cyclic AMP-dependent and protein kinase-C dependent pathways. *Circ. Res.* 72:330–340.
Liotta, L.A., P.S. Steeg, and W.G. Stetler-Stevenson. 1991. Cancer metastasis and angiogenesis: an imbalance of positive and negative regulation. *Cell.* 64: 327–336.
Loskutoff, D.J. 1991. Regulation of PAI-1 gene expression. *Fibrinolysis.* 5:197–206.
Maciag, T., J. Cerundolo, P.R. Ilsley, and R. Fornad. 1979. An endothelial cell growth factor from bovine hypothalamus: identification and partial characterization. *Proc. Natl. Acad. Sci. USA.* 76:5674–5678.
Madri, J.A., L. Bell, M. Marx, J.R. Merwin, C. Basson, and C. Prinz. 1991. Effects of soluble factors and extracellular matrix components on vascular cell behaviour in vitro and in vivo: models of de-endothelialization and repair. *J. Cell. Biochem.* 45:123–130.
Matrisian, L.M. 1992. The Matrix-degrading metalloproteinases. *BioEssays.* 14: 455–463.
Mignatti, P., R. Mazzieri, and D.B. Rifkin. 1991. Expression of the urokinase receptor in vascular endothelial cells is stimulated by basic fibroblast growth factor. *J. Cell Biol.* 113:1193–1201.
Montesano, R. 1992. Regulation of angiogenesis *in vitro*. *Eur. J. Clin. Invest.* 22: 504–515.
Murray, A.B., H. Schulze, and E. Blauw. 1991. In situ embedding of cell monolayers cultured on plastic surfaces for electron microscopy. *Biotech. & Histochem.* 66:269–272.
Nagase, H. 1994. Matrix metalloproteases. *In* Extracellular Matrix in the Kidney. H. Kiode, and T. Hayashi, editors. Contrib Nephrol. Basel, Karger. Vol. 107. pp. 85–93.
Nicosia, R.F., and A. Ottinetti. 1990. Modulation of microvascular growth and morphogenesis by reconstituted basement membrane gel in 3-dimensional cultures of rat aorta: a comparative study of angiogenesis in matrigel, collagen, fibrin, and plasma clot. *In Vitro Cellular & Developmental Biol.* 26: 119–128.
Niedbala, M.J., and M.S. Picarella. 1992. Tumor necrosis factor induction of endothelial cell urokinase-type plasminogen activator mediated proteolysis of extracellular matrix and its antagonism by γ-interferon. *Blood.* 79:678–687.
Orsini, G., A. Brandazza, P. Sarmientos, A. Molinari, J. Lansen, and G. Cauet. 1991. Efficient renaturation and fibrinolytic properties of prourokinase and a deletion mutant expressed in *Escherichia coli* as inclusion bodies. *Eur. J. Biochem.* 195:691–697.
Pepper, M.S., J.D. Vassalli, R. Montesano, and L. Orci. 1987. Urokinase-type plasminogen activator is induced in migrating capillary endothelial cells. *J. Cell Biol.* 105:2535–2541.
Pepper, M.S., D. Belin, R. Montesano, L. Orci, and J.D. Vassalli. 1990. Transforming growth factor-β-1 modulates basic fibroblast growth factor induced proteolytic and angiogenic properties of endothelial cells in vitro. *J. Cell Biol.* 111:743–755.
Pepper, M.S., N. Ferrara, L. Orci, and R. Montesano. 1991. Vascular endothelial growth factor (VEGF) induces plasminogen activators and plasminogen activator inhibitor-1 in microvascular endothelial cells. *Biochem. Biophys. Res. Commun.* 181:902–906.
Pepper, M.S., N. Ferrara, L. Orci, and R. Montesano. 1992. Potent synergism between vascular endothelial growth factor and basic fibroblast growth factor in the induction of angiogenesis in vitro. *Biochem. Biophys. Res. Commun.* 189:824–831.
Pepper, M.S., A.P. Sappino, R. Stocklin, R. Montesano, L. Orci, and J.D. Vassalli. 1993. Upregulation of urokinase receptor expression on migrating endothelial cells. *J. Cell Biol.* 122:673–684.
Plate, K.H., G. Breier, H.A. Weich, and W. Risau. 1992. Vascular endothelial growth factor is a potential tumor angiogenesis factor in human gliomas in vivo. *Nature (Lond.).* 359:845–848.
Polverini, P.J. 1989. Macrophage-induced angiogenesis: a review. *Macrophage-derived Cell Regulatory Factors.* 1:54–73.
Quax, P.H.A., N. Pedersen, M.T. Masucci, E.J.D. Weening-Verhoeff, K. Dano, J.H. Verheijen, and I.F. Blasi. 1991. Complementation between urokinase-producing and receptor-producing cells in extracellular matrix degradation. *Cell Regulation.* 2:793–803.
Rao, N.K., G.-P. Shi, and H.A. Chapman. 1995. Urokinase receptor is a multifunctional protein: influence of receptor occupancy on macrophage gene expression. *J. Clin. Invest.* 96:465–474.
Saksela, O., D. Moscatelli, and D.B. Rifkin. 1987. The opposing effects of basic fibroblast growth factor and transforming growth factor β on the regulation of plasminogen activator activity in capillary endothelial cells. *J. Cell Biol.* 105:957–963.
Schleef, R.R., M.P. Bevilacqua, M. Sawdey, M.A. Gimbrone, and D.J. Loskutoff. 1988. Cytokine activation of vascular endothelium. Effects on tissue-type plasminogen activator and type 1 plasminogen activator inhibitor. *J. Biol. Chem.* 263:5797–5803.
Senger, D.R., L. Vandewater, L.F. Brown, J.A. Nagy, K.T. Yeo, T.K. Yeo, B. Berse, R.W. Jackman, A.M. Dvorak, and H.F. Dvorak. 1993. Vascular permeability factor (VPF, VEGF) in tumor biology. *Cancer and Metastasis Reviews.* 12:303–324.
Shweiki, D., A. Itin, D. Soffer, and E. Keshet. 1992. Vascular endothelial growth factor induced by hypoxia may mediate hypoxia-initiated angiogenesis. *Nature (Lond.).* 359:843–845.
Van Hinsbergh, V.W.M. 1992. Impact of endothelial activation on fibrinolysis and local proteolysis in tissue repair. *Ann. NY Acad. Sci.* 667:151–162.
Van Hinsbergh, V.W.M., L. Havekes, J.J. Emeis, E. van Corven, and M.A. Scheffer. 1983. Low density lipoprotein metabolism by endothelial cells from umbilical cord arteries and veins. *Arteriosclerosis.* 3:547–559.
Van Hinsbergh, V.W.M., E.D. Sprengers, and T. Kooistra. 1987. Effect of thrombin on the production of plasminogen activators and PA inhibitor-1 by human foreskin microvascular endothelial cells. *Thromb. Haemostas.* 57: 148–153.
Van Hinsbergh, V.W.M., T. Kooistra, E.A. van den Berg, H.M.G. Princen, W. Fiers, and J.J. Emeis. 1988. Tumor necrosis factor increases the production of plasminogen activator inhibitor in human endothelial cells in vitro and in rats in vivo. *Blood.* 72:1467–1473.
Van Hinsbergh, V.W.M., E.A. van den Berg, W. Fiers, and G. Dooijewaard. 1990. Tumor necrosis factor induces the production of urokinase-type plasminogen activator by human endothelial cells. *Blood.* 75:1991–1998.
Vassalli, J.D. 1994. The urokinase receptor. *Fibrinolysis.* 8:172–181.
Wei, Y., D.A. Waltz, N. Rao, R.J. Drummond, S. Rosenberg, and H.A. Chapman. 1994. Identification of the urokinase receptor as an adhesion receptor for vitronectin. *J. Biol. Chem.* 269:32380–32388.
Wilhelm, O., U. Weidle, S. Hohl, P. Rettenberger, M. Schmitt, and H. Graeff. 1994. Recombinant soluble urokinase receptor as a scavenger for urokinase-type plasminogen activator (uPA). Inhibition of proliferation and invasion of human ovarian cancer cells. *FEBS Lett.* 337:131–134.
Woessner, J.F. 1991. Matrix metalloproteinases and their inhibitors in connective tissue remodelling. *FASEB (Fed. Am. Soc. Exp. Biol.) J.* 5:2145–2154.

STIC-ILL Appl. 09/533

From: Holleran, Anne
Sent: Sunday, March 04, 2001 5:30 PM
To: STIC-ILL
Subject: refs. for 09/266,543

Examiner: Anne Holleran
Art Unit: 1642; Rm 8E03
Phone: 308-8892
Date needed by: ASAP

Please send me copies of the following :

1. Plum, S.M. et al. Vaccine, (2000) 19/9-10, 1294-1303
2. Aonuma, M. et al. Anticancer Res. (1999, Oct) 19(5B): 4039-4044
3. Muller, Y.A. et al. Structure (1998) 6(9): 1153-1167
4. Yamagishi, S. et al. J. Biol. Chem. (1997) 272(13): 8723-8730
5. Koolwijk, P. et al. J. Cell Biology (1996) 132(6): 1177-1188
6. Matsuo, A. et al. Neuroscience (1994) 60(1): 49-66
7. Djakiew, D. et al. Cancer Research (1991) 51(12): 3304-3310
8. Yamanishi, H. et al. Cancer Research (1991) 51(11): 3006-3010
9. Matsuzaki, K. et al. Japanese J. Cancer Research (1990) 81(4): 345-354
10. Kardami, E. et al. Growth Factors (1990) 4(1): 69-80
11. Riss, T.L. et al. J. Cellular Physiology (1989) 138(2): 405-414

JOURNAL OF CELLULAR PHYSIOLOGY 138:405–414 (1989)

Characterization of Polyclonal Antibodies That Distinguish Acidic and Basic Fibroblast Growth Factors by Using Western Immunoblotting and Enzyme-Linked Immunosorbent Assays

TERRY L. RISS* AND DAVID A. SIRBASKU
Department of Biochemistry and Molecular Biology, University of Texas Medical School, Houston, Texas 77225

Rabbit polyclonal antibodies were raised against ovalbumin conjugates of purified bovine brain acidic fibroblast growth factor (aFGF) and a synthetic peptide containing the N^{α}-terminal 1–24 amino acid sequence of bovine basic fibroblast growth factor (bFGF). These antibodies were used to specifically detect 1-ng quantities of aFGF and bFGF by using enzyme-linked immunosorbent assay (ELISA) and Western immunoblot procedures. Antibodies raised against aFGF recognized bovine brain aFGF and bovine recombinant aFGF but very poorly recognized recombinant bFGF or purified porcine or bovine pituitary bFGF with ELISA and Western immunoblot procedures. Antibodies raised against bFGF (1–24) recognized purified bovine, porcine, and recombinant human bFGF but only very poorly recognized aFGF with ELISA and Western immunoblot procedures. In vitro addition of anti-bFGF antibodies was able to partially neutralize bFGF-stimulated ^{3}H-thymidine incorporation by COMMA-D mouse mammary epithelial cells while having no effect on aFGF or epidermal growth factor (EGF) stimulation. In vitro addition of anti-aFGF antibodies had no effect on bFGF- or EGF-stimulated ^{3}H-thymidine incorporation, but surprisingly, had a potentiating effect on aFGF stimulation. Antibodies against aFGF immobilized on protein A-Sepharose were able to specifically and completely remove mitogenic activity from solutions containing aFGF but had no effect on removal of mitogenic activity from control solutions containing bFGF or EGF. Similarly, immobilized anti-bFGF antibodies completely removed mitogenic activity from solutions of bFGF, but not aFGF or EGF controls. These antibodies have been useful for the identification and characterization of growth factors from tissue and recombinant sources.

Acidic fibroblast growth factor (aFGF) and basic fibroblast growth factor (bFGF) are two structurally related heparin binding proteins that share a 55% homology of their amino acid sequences (Gimenez-Gallego et al., 1985; Esch et al., 1985a,b; Thomas and Gimenez-Gallego, 1986). Both proteins can bind to the same cell surface receptor (Neufeld and Gospodarowicz, 1986; Olwin and Hauschka, 1986) and have been demonstrated to elicit similar biological responses in vitro (Böhlen et al., 1985; Gospodarowicz et al., 1986b) and in vivo (Esch et al., 1985a). bFGF is widely distributed among different cell types (Thomas et al., 1985; Gospodarowicz et al., 1986a; Lobb et al., 1986) while the distribution of aFGF has been reported to be somewhat more limited (Baird et al., 1985b; Gospodarowicz et al., 1986a; Hauschka et al., 1986). The acidic and basic forms of FGF often have been tentatively identified in tissue or cell extracts by their different ionic strength of elution of mitogenic activity from heparin-Sepharose affinity chromatography (Gospodarowicz et al., 1984; Böhlen et al., 1985; Lobb and Fett, 1984; Esch et al., 1985a,b; Lobb et al., 1986); however, additional means are necessary for the specific identification of trace amounts of these molecules. Because of the structural similarity between aFGF and bFGF, it is likely that they contain similar antigenic epitopes and therefore may be recognized by the same antibodies. Antibodies against intact bFGF isolated from various sources (Moscatelli et al., 1986; Massoglia et al., 1987; Schelling et al., 1987; Bertolini and Hearn, 1987) and various synthetic peptides corresponding to amino acid sequences present in bFGF (Böhlen et al., 1984; Baird et al., 1985a; Wadzinski et al., 1987; Klagsbrun et al., 1986) have been used to characterize the production of this molecule by a variety of cells in vitro. Some of

Received May 20, 1988; accepted September 20, 1988.

*To whom reprint requests/correspondence should be addressed at Schering-Plough Corporation, Biotechnology Cell Culture, 60 Orange Street, Bloomfield, NJ 07003.

these studies have demonstrated that antibodies against bFGF did not recognize aFGF (Moscatelli et al., 1986; Massoglia et al., 1987; Ferrara et al., 1987; Schweigerer et al., 1987b); however, reports characterizing specific antibodies raised against aFGF are lacking.

We report here the demonstration that rabbit polyclonal antibodies raised against ovalbumin conjugates of aFGF and the N^{α}-terminal 24 amino acids of bFGF were able to specifically recognize with minimal cross-reactivity aFGF and bFGF, respectively, using the techniques of 1) ELISA, 2) Western immunoblotting, and 3) specific removal of mitogenic activity from solution by protein A-Sepharose-immobilized antibodies.

MATERIALS AND METHODS

Materials

The following chemicals were purchased from Sigma Chemical Co. (St. Louis, MO): phenylmethylsulfonyl fluoride (PMSF), ethylenediamine tetraacetic acid (EDTA), leupeptin, pepstatin A, Tris[hydroxymethyl]ammoniomethane (Tris), polyoxyethylenesorbitan monolaurate (Tween 20), sodium azide, DEAE-Sepharose, CM-Sephadex C50, protein A-Sepharose CL-4B, ovalbumin, bovine serum albumin (BSA), Dulbecco's phosphate-buffered saline (PBS), and Freund's complete and incomplete adjuvants. Glutaraldehyde 50% solution was purchased from Eastman Kodak Company (Rochester, NY). Trifluoroacetic acid (TFA) and ammonium sulfate were purchased from Fisher Scientific (Fair Lawn, NJ). Acetonitrile was purchased from Mallinckrodt (Paris, KY). Heparin-Sepharose CL-6B was purchased from Pharmacia (Uppsala, Sweden). Prestained low molecular weight protein standards for electrophoresis were purchased from Bethesda Research Labs (Gaithersburg, MD). CM-Affi-Gel Blue, p-nitro blue tetrazolium chloride (NBT), 5-bromo-4-chloro-3-indolyl phosphate-toluidine salt (BCIP), and all other reagents for sodium dodecyl sulfate polyacrylamide gel electrophoresis (SDS-PAGE) were purchased from Bio-Rad Laboratories (Richmond, CA). Dialysis tubing was obtained from Spectrum Medical Industries (Los Angeles, CA). Chemically synthesized peptide containing the N^{α}-terminal 1–24 amino acids of the 146-amino-acid form of bovine-brain-derived bFGF was purchased from Peninsula Laboratories (Belmont, CA). Porcine pituitaries were obtained from Southwestern Biologicals (Pearland, TX). Bovine brains were obtained from Freedman Packing, Inc. (Houston, TX). [Methyl ^{3}H]-thymidine (70 Ci/mmole) was purchased from ICN Radiochemicals (Irvine, CA). Bovine recombinant aFGF was supplied by Dr. Kenneth Thomas (Merck & Co., Inc., Rahway, NJ). Human recombinant bFGF was obtained from AmGen Biologicals (Thousand Oaks, CA). Protein was determined with a Coomassie dye-binding assay kit purchased from Bio-Rad with BSA as the standard.

Purification of aFGF

The purifications of aFGF and bFGF were modified from the procedures of Gospodarowicz (1987). Twenty female bovine brains were packed in ice immediately after removal and transported to the laboratory. The brains were washed in ice-cold PBS and homogenized in 500-g batches in 800 ml 0.15 M $(NH_4)_2SO_4$ containing 1 mM EDTA by using a Waring blendor. The homogenates were combined in a large glass container and proteinase inhibitors were added at the following concentrations: PMSF, 250 μM; pepstatin A, 1 μg/ml; leupeptin, 0.5 μg/ml. The pH of the homogenate was adjusted to 4.5 with 6 N HCl and stirred for 2 hr. The homogenate was centrifuged at 10,000g for 1 hr and the supernatant was filtered through cheesecloth. The pH of the extract was adjusted to 6.0 before addition of 230 g/liter of finely powdered $(NH_4)_2SO_4$. The mixture was stirred for 1 hr and then centrifuged as before. The supernatant was saved, 250 g/liter $(NH_4)_2SO_4$ was added, and the suspension was stirred for 6 hr. The suspension was centrifuged as before; the pellets were suspended in distilled water and dialyzed by using 3,500-molecular-weight-cutoff (MWCO) tubing, first against distilled water and then 0.1 M sodium phosphate (pH 6.0). The dialyzed extract was centrifuged as before, passed through filter paper, and applied to a 5 × 9 cm CM-Sephadex C50 column equilibrated with 0.1 M sodium phosphate (pH 6.0). The column was washed free of unbound material and then eluted with 0.1 M sodium phosphate (pH 6.0) containing 0.15 M NaCl. When the peak of 280-nm absorbing material approached baseline, the column was eluted with 0.1 M sodium phosphate (pH 6.0) containing 0.6 M NaCl. Fractions were assayed by using ^{3}H-thymidine incorporation into COMMA-D mouse mammary epithelial cells as described previously (Riss and Sirbasku, 1987). Those fractions containing mitogenic activity were pooled, the pH was adjusted to 7.0 with dilute NaOH, and the sample was applied to a 1.4 × 7 cm heparin-Sepharose CL-6B column equilibrated with 10 mM Tris (pH 7.0) containing 0.6 M NaCl. The column was washed free of unbound material and then eluted with the same buffer containing 1.0 M NaCl. When the UV 280-nm absorbing material reach a stable baseline, the column was eluted with the same buffer containing 2.0 M NaCl. All fractions were assayed by using COMMA-D cells and those containing mitogenic activity eluted with 1.0 and 2.0 M NaCl were pooled separately. This procedure resulted in the recovery of 2.84 mg of aFGF from the 1.0 M NaCl-eluted peak. A portion of the 1.0 M NaCl-eluted mitogenic activity was applied to a 0.4 × 25 cm Vydac C4 reverse-phase high-pressure liquid chromatography (HPLC) column equilibrated with 0.1% (v/v) TFA. The column was eluted with a linear gradient of 29–50% CH_3CN containing 0.1% (v/v) TFA. Fractions were dried in a Savant Speed Vac concentrator, suspended in water, and assayed for mitogenic activity by using ^{3}H-thymidine incorporation by COMMA-D cells as described previously (Riss et al., 1986; Riss and Sirbasku, 1987). Those fractions containing mitogenic activity were used to raise antibodies.

Purification of bFGF

All procedures were carried out at 4°C. Porcine pituitaries (468 g) were homogenized in 50-g batches in three times volume of PBS containing 20 μg/ml pepstatin A and 13 μM PMSF by using a Tekmar Tissue Mizer (Cincinnati, OH). The total homogenate was centrifuged for 1 hr at 16,000g. The lipid layer was aspirated from the top of each tube and the superna-

tant was poured through several layers of cheesecloth to help retain remaining lipid. The supernatant (1,265 ml) was stirred while 709 g solid $(NH_4)_2SO_4$ was added. After stirring overnight, the suspension was centrifuged at 16,000g for 1 hr and the supernatant was discarded. The pellets were suspended in 600 ml 50 mM Tris (pH 8.0) containing 10 μM PMSF and dialyzed against the same buffer. The dialyzed material was centrifuged at 100,000g and filtered through a 0.2-μm-pore-size membrane. This material, referred to as crude extract, was applied to a 5.0 × 29 cm DEAE-Sepharose column equilibrated with 50 mM Tris (pH 8.0) and 20-ml fractions were collected. After sample application (320 ml), the column was eluted at 2.0 ml/min with 740 ml starting buffer before initiating a linear gradient of NaCl (0–300 mM NaCl in 4.0 liter starting buffer). Fractions containing mitogenic activity which bound to DEAE-Sepharose and were NaCl eluted were separated for use in another study (Riss and Sirbasku, 1989). Fractions containing mitogenic activity which did not bind to DEAE-Sepharose were dialyzed against 0.1 M sodium phosphate and applied to a 2.5 × 28 cm CM-Sephadex C50 column equilibrated with 0.1 M sodium phosphate (pH 6.0). The column was eluted as described for the extract from bovine brain containing aFGF. The mitogenic activity residing in the 0.6 M NaCl-eluted peak was applied to a 0.9 × 14 cm heparin-Sepharose column equilibrated in 10 mM Tris (pH 7.0) containing 0.6 M NaCl. The column was eluted by using the same protocol as for the extract of bovine brain containing aFGF and the mitogenic activity from the 2.0 M NaCl eluted peak was pooled and stored frozen. This procedure resulted in the recovery of 87 μg of bFGF from 468 g of pituitaries.

Preparation of FGF-ovalbumin complexes

Bovine brain aFGF (1.13 mg) purified by using reverse-phase HPLC was speed-vac dried and suspended in 0.8 ml water. A 0.2-ml solution containing 0.45 mg ovalbumin in 0.5 M sodium phosphate (pH 7.4) was combined with the aFGF solution to give a 6:1 molar ratio of aFGF:ovalbumin. A total volume of 135 μl of freshly prepared 13 mM glutaraldehyde in 0.1 M sodium phosphate (pH 7.4) was added in 10-μl aliquots over a period of 30 min. The tube was allowed to stand overnight and then was dialyzed against four 500-ml volumes of PBS by using 2000 MWCO tubing. An equal volume of aFGF-ovalbumin complex solution and Freund's complete adjuvant was emulsified and 1.0 ml/animal was injected into 50 intradermal sites in 2-kg New Zealand white rabbits. During the initial injection period, each of the 2 rabbits (A and B) received approximately 420 μg aFGF. After 5 weeks, animals were boosted with 0.5 ml of a 1:1 emulsion of aFGF-ovalbumin complex solution and Freund's incomplete adjuvant containing 75 μg aFGF. After an additional 4 weeks, antisera were collected from both rabbits and stored at −70°C until use. Antiserum from rabbit B resulted in approximately twice the specific absorbance with ELISA and therefore was used for all experiments described in this report.

The bFGF 1–24 peptide-ovalbumin complex was prepared in a similar manner except 0.5 mg bFGF peptide and 0.84 mg ovalbumin were used to give a 10:1 molar ratio. Each of 2 rabbits (#1 and #2) received the equivalent of 187 μg of bFGF peptide during the initial injections and a boost of 31 μg equivalent of bFGF peptide 4 weeks later. Initial screening of antisera revealed that rabbit #1 yielded a higher specific absorbance with ELISA and therefore was used for all experiments described in this report.

ELISA

Antigen to be tested was diluted in 0.1 M sodium carbonate (pH 9.5) and 100 μl/well was placed in 96-well Immulon 2 plates (Dynatech Laboratories, Inc., Alexandria, VA). The plates were covered with Parafilm and placed at 4°C overnight. The antigen solution was removed by aspiration and nonspecific binding sites were blocked by addition of 150 μl/well of PBS containing 1.0% (w/v) BSA and 0.02% (w/v) sodium azide. The plates were incubated at 37°C for 1 hr; the blocking solution was removed by aspiration; and the wells were washed five times with PBS containing 0.05% (v/v) Tween 20. Each well then received 100 μl of antiserum diluted in PBS containing 1.0% (w/v) BSA and 0.02% (w/v) sodium azide. The plates were covered with Parafilm and incubated at 37°C for 1 hr. The antiserum was removed by aspiration; the wells were washed five times with PBS containing 0.05% (v/v) Tween 20, and 100 μl/well of affinity-isolated goat antirabbit IgG alkaline phosphatase conjugate (Sigma A-8025) diluted 1/1,000 in PBS containing 1.0% (w/v) BSA and 0.02% (w/v) sodium azide were added. The plates were covered with Parafilm and incubated at 37°C for 1 hr. The second antibody was removed by aspiration and the wells were washed five times with PBS containing 0.05% (v/v) Tween 20 and then rinsed twice with distilled water. Each well received 100 μl of 50 mM sodium carbonate (pH 10) containing 1.0 mM $MgCl_2$ and 0.5 g/liter p-nitro-phenyl phosphate (Sigma 104-0). The plates were covered with Parafilm and allowed to stand at ambient temperature until there was adequate color development. Absorbance values at 410 nm were recorded by using a Dynatech MR 600 Microplate Reader and analyzed by the Immunosoft 2.0 software package.

Western immunoblotting

Acidic and bFGF were electrophoresed by using SDS-PAGE and transferred electrophoretically (Trans Blot cell, Bio-Rad) to Immobilon P transfer membrane (Millipore). The transfer was done in 25 mM Tris (pH 8.3), 192 mM glycine, 0.375 g/liter SDS, 20% (v/v) methanol at 25 V, for 15 min and then at 90 V for 90 min. After transfer the membranes were rinsed in Tris-buffered saline (TBS) composed of 20 mM Tris (pH 7.4), 0.15 M NaCl, and 0.02% (w/v) sodium azide and then incubated at ambient temperature on a rotary shaker for 90 min in blocking solution composed of TBS containing 2% (w/v) nonfat dry milk. After blocking, the membranes were transferred to fresh blocking solution containing 1% (v/v) rabbit antiserum against either aFGF or bFGF and incubated for 2 hr on a rocking platform. The membranes were washed four times for 10 min in TBS containing 0.05% (v/v) Tween 20 (TTBS) and then incubated on a rocking platform in blocking solution containing a 1:2,000 dilution of affinity-purified goat antirabbit IgG alkaline phosphatase con-

jugate. The membranes were washed four times for 10 min in 200 ml of TTBS to remove excess secondary antibody. The membranes were rinsed for 5 min in 100 mM Tris (pH 9.5) containing 100 mM NaCl and 5 mM $MgCl_2$ to equilibrate at alkaline pH and then were incubated in the same solution containing 250 μg/ml NBT and 125 μg/ml BCIP to allow for color development. The membranes were rinsed in water to stop color development and were air dried.

Immunoadsorption of FGFs

Protein A-Sepharose CL-4B (Sigma P-3391) was extensively washed by repeated centrifugation in 100 mM phosphate (pH 7.35). The washed protein A-Sepharose was mixed with antiserum in 50-ml conical polypropylene tubes at a ratio of 1.5 ml packed pellet volume of protein A-Sepharose to 10 ml antiserum. The tubes were agitated by using a gyratory shaker at 300 rpm for 24 hr at 4°C. The protein A-Sepharose antiserum suspensions were centrifuged and the pellets were washed five times in PBS. The suspensions were transferred to 1.0-ml polypropylene tubes and centrifuged and the supernatant was removed, leaving approximately a 300-μl pellet volume of protein A-Sepharose in each tube. Growth factor solutions (or vehicle controls) contained in 300 μl of PBS were added and incubated at 4°C for 24 hr. The contents of the tubes were kept in suspension by using a drum roller. At the end of the incubation period, the tubes were centrifuged and the supernatant was assayed for biological activity by using ^{3}H-thymidine incorporation by COMMA-D cells as described by Riss and Sirbasku (1987).

Fractionation of antiserum by using CM Affi-Gel Blue

Ten-milliliter aliquots of antiserum were applied to a 2 × 17 cm CM Affi-Gel Blue column equilibrated with 0.01 M potassium phosphate (pH 7.2) containing 0.15 M NaCl. The UV 280-nm absorbing eluent was collected and brought to 45% saturation with $(NH_4)_2SO_4$ and then stirred for 1 hr. The suspension was centrifuged at 4°C at 5,000g for 20 min and the supernatant was discarded. The pellet was suspended in a 45% saturated solution of $(NH_4)_2SO_4$ and centrifuged as before. The pellets were suspended in 0.01 M potassium phosphate (pH 7.2) containing 0.15 M NaCl and dialyzed against the same buffer with 8000 MWCO tubing. The dialyzed material was 0.2 μm filtered and stored at −70°C.

RESULTS

Characterization of ELISAs specific for aFGF and bFGF

Rabbit antiserum raised against the N^{α}-terminal 24 amino acids of bFGF conjugated to ovalbumin was able to recognize all bFGF samples tested including porcine pituitary bFGF, bovine pituitary bFGF, bovine-brain-derived bFGF, and human recombinant bFGF from two different sources. Figure 1A shows the results of an ELISA using a 1/5,000 dilution of rabbit antiserum raised against brain-derived bFGF (1–24) peptide-ovalbumin complex. Less than 500 pg of porcine pituitary bFGF was detected by using those conditions; however, quantities of bovine brain aFGF as high as 64

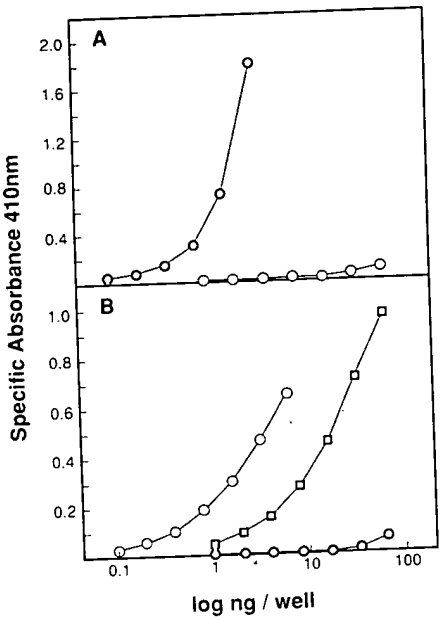

Fig. 1. ELISA of various concentrations of aFGF and bFGF. **A:** Recombinant bFGF (closed circles) was added in duplicate at 0.1–6.4 ng/well and bovine brain aFGF (open circles) was added at 1.0–64 ng/well. A 1/5,000 dilution of antisera raised against brain-derived bFGF 1–24 peptide was used as the primary antibody. **B:** Bovine brain aFGF eluted from heparin-Sepharose with 1.0 M NaCl (open circles; 0.1–6.4 ng/well), bovine brain bFGF eluted from heparin-Sepharose with 2.0 M NaCl (squares; 1.0–64 ng/well), and recombinant bFGF (closed circles; 1.0–64 ng/well) were added to duplicate wells of ELISA plates. A 1/5,000 dilution of antisera raised against bovine brain aFGF was used as the primary antibody. The absorbance at 410 nm was recorded after 6-hr incubation with substrate. The values were plotted as specific absorbance at 410 nm and were calculated by first subtracting a blank (0.047) containing no antiserum from all values; then at each antiserum dilution, the background absorbance of wells with no FGF (ranging between 0.011 and 0.019) was subtracted from absorbance values of FGF-containing wells.

ng/well showed very little specific absorbance, indicating that despite the existence of regions of sequence homology in the peptide used as an immunogen, aFGF was poorly recognized by antiserum raised against bFGF (1–24) peptide-ovalbumin conjugate. Figure 1B illustrates that a 1/5,000 dilution of rabbit antiserum raised against HPLC-purified bovine brain aFGF conjugated to ovalbumin was able to detect less than 500 pg of aFGF with ELISA. With the same conditions, 64 ng of recombinant bFGF showed only minimal specific absorbance, indicating that despite the existence of considerable sequence homology, bFGF was only poorly recognized by the antiserum raised against bovine-brain-derived aFGF. The sample of aFGF used as antigen to coat the ELISA wells was from bovine brain extract that was chromatographed on CM-Sephadex and then eluted from heparin-Sepharose by using 1.0 M NaCl as described in Materials and Methods. Subsequent elution of the bovine brain extract from heparin-Sepharose with 2.0 M NaCl produced a peak of "bFGF" mitogenic activity that was recognized by anti-bFGF as well as by anti-aFGF antiserum with ELISA. With the anti-aFGF antiserum, however, approximately a 6-fold-higher quantity

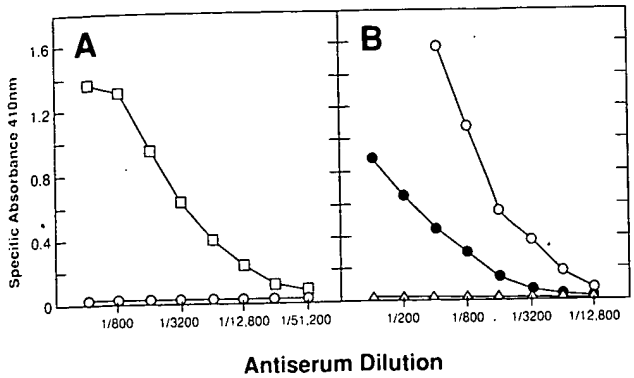

Fig. 2. ELISA of constant quantities of different samples of FGF using varying dilutions of antisera. **A:** Duplicate samples of porcine bFGF were added at 0.84 ng/well and ELISA was done by using various dilutions of antiserum raised against brain-derived bFGF 1–24 peptide (squares) or antiserum raised against bovine brain aFGF (circles). **B:** Duplicate 1 ng/ml samples of bovine pituitary bFGF (triangles), bovine brain aFGF pooled from mitogenic activity eluted from heparin-Sepharose by 1.0 M NaCl (circles), and bovine brain 2.0 M heparin-Sepharose-eluted mitogenic activity (closed circles). Antiserum raised against bovine brain aFGF, added at 1/100–1/12,500 dilutions, was used as the primary antibody. Absorbance at 410 nm was recorded after 4-hr incubation with substrate and specific absorbance was calculated as described in the legend to Figure 1.

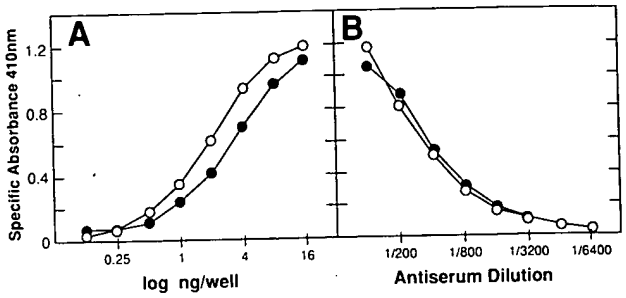

Fig. 3. ELISAs comparing bovine brain aFGF (open circles) eluted from heparin-Sepharose and bovine recombinant aFGF (closed circles). **A:** Duplicate samples of 0.125–16 ng for each protein were added to 96-well plates and ELISA was done as described in Materials and Methods. Antiserum raised against bovine brain aFGF at 1/1,000 dilution was used as the primary antibody. Absorbance 410 nm was recorded after 3-hr incubation with substrate. **B:** Duplicate samples of bovine brain aFGF (open circles) and recombinant bovine aFGF (closed circles) were added at 1.0 ng/well. Antiserum raised against bovine brain aFGF at dilutions of 1/100–1/12,800 were used as the primary antibody. Absorbance at 410 nm was recorded after 3 hr of incubation and specific absorbance was calculated as described in the legend to Figure 1.

of the 2.0 M NaCl-eluted protein was required to give a specific absorbance equal to aFGF eluted from heparin-Sepharose with 1.0 M NaCl, suggesting that most of the immunoreactive material present in the 2.0 M NaCl fraction was bFGF. In light of these results, it is clear that elution of tissue extracts from heparin-Sepharose using different ionic strengths cannot be relied on to give pure bFGF.

The ELISA results shown in Figure 2A demonstrate that 0.84 ng of porcine bFGF could be detected by a wide range of dilutions of antiserum raised against brain-derived bFGF (1–24) peptide-ovalbumin complex. The same range of dilutions of antiserum against bovine brain aFGF showed no reaction against porcine bFGF. The ELISA results shown in Figure 2B demonstrate that a wide range of dilutions of antiserum raised against bovine brain aFGF can easily detect 1 ng of the bovine brain aFGF fraction eluted from heparin-Sepharose with 1.0 M NaCl. The fraction of mitogenic activity from bovine brain that was eluted from heparin-Sepharose with 2.0 M NaCl also was detected with an ELISA using anti-aFGF, although the extent of reaction was far less. It was estimated that the 2.0 M NaCl-eluted fraction contained approximately 12% immunoreactive aFGF. Figure 2B also shows that bovine pituitary bFGF eluted from heparin-Sepharose by using 2.0 M NaCl was not recognized by a wide range of dilutions of antiserum against aFGF. This agrees with the data in Figure 2A for porcine pituitary bFGF.

Although HPLC-purified aFGF was used to prepare the immunogen, it was possible that the antiserum generated recognized an impurity present in the preparation. To ensure that aFGF was being recognized, we tested aFGF samples from two other sources. Purified bovine brain aFGF obtained from the laboratory of Dr. Wallace McKeehan at the Cell Science Center, Lake Placid, NY, also could be detected by using the ELISA procedure described here (not shown). Figure 3 shows a comparison between recombinant aFGF produced in *E. coli* (obtained from Kenneth Thomas, Merck) and bovine brain aFGF eluted from heparin-Sepharose with 1.0 M NaCl. Figure 3A illustrates that when a 1/1,000 dilution of antiserum against bovine brain aFGF was used for ELISA, aFGF purified from bovine brain and recombinant aFGF showed similar specific absorbance for all quantities assayed. The similarity of these two preparations of aFGF was demonstrated further when ELISA of 1 ng/well of each antigen showed a similar reaction for all antiserum dilutions tested. Because the recombinant material was equivalent to purified aFGF using ELISA, this provided evidence that the antiserum raised by using aFGF purified from bovine brain recognized aFGF and not a contaminating protein present in the preparation. The degree of similarity of these two preparations using ELISA was striking considering the inherent error involved in handling such small amounts of protein.

A similar characterization was done by using the antiserum raised against brain-derived bFGF (1–24) peptide-ovalbumin conjugate. A comparison of porcine pituitary bFGF and recombinant bFGF using ELISA is shown in Figure 4. Figure 4A shows that when a 1/1,000 dilution of antiserum raised against bFGF (1–24) was used, recombinant bFGF showed approximately 2-fold more color development than bFGF purified from porcine pituitary. When 1-ng quantities of the 2 preparations of bFGF were assayed by using a wide range of dilutions of the same antiserum (Fig. 4B), the recombinant bFGF sample showed a greater extent of reaction at all dilutions tested. The lesser extent of immunoreactivity of porcine bFGF could be a result of partial proteolytic cleavage, thus removing some of the N^{α}-terminal antigenic determinants, or it could be caused by errors in estimation of protein concentrations.

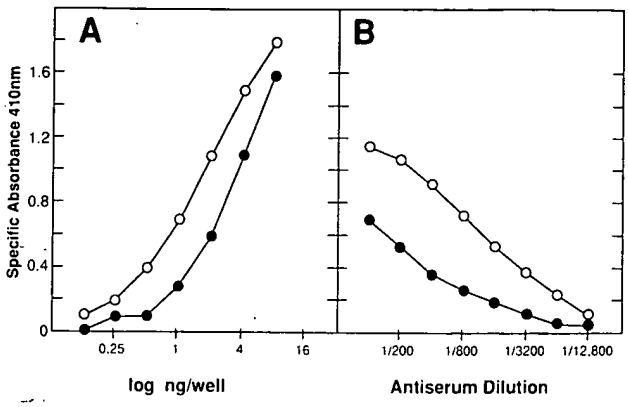

Fig. 4. ELISAs comparing porcine pituitary bFGF (closed circles) and human recombinant bFGF (open circles). **A:** Duplicate samples of 0.125–16 ng for each protein were added to 96-well plates and ELISA was done as described in Materials and Methods. Antiserum raised against brain-derived bFGF 1–24 peptide at 1/1,000 dilution was used as the primary antibody. Absorbance 410 nm was recorded after 30-min incubation with substrate. **B:** Duplicate samples of porcine pituitary bFGF (closed circles) and recombinant human bFGF (open circles) were added at 1.0 ng/well. Antiserum raised against brain-derived bFGF 1–24 peptide at dilutions of 1/100–1/12,800 were used as the primary antibody. Absorbance at 410 nm was recorded after 3 hr of incubation and specific absorbance was calculated as described in the legend to Figure 1.

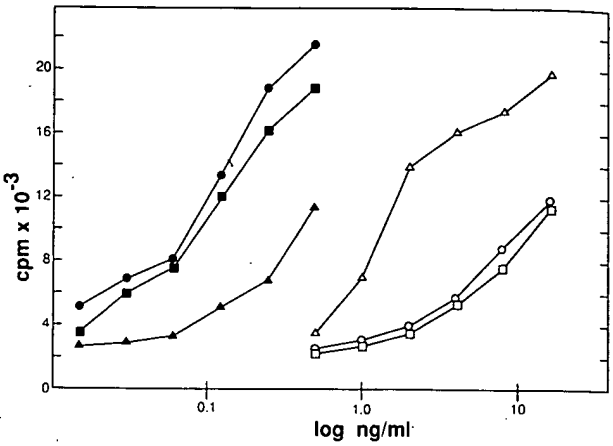

Fig. 5. Effects of addition of CM-Affi-Gel Blue-treated antisera on ^{3}H-thymidine incorporation by COMMA-D cells stimulated by aFGF and bFGF. **A:** Dose response of porcine bFGF alone (closed squares), in the presence of 5 μl CM-Affi-Gel Blue-treated antiserum raised against bovine brain aFGF (closed circles) and in the presence of 5 μl CM-Affi-Gel Blue-treated antiserum raised against brain-derived bFGF 1–24 peptide (closed triangles). **B:** Dose response of bovine brain aFGF alone (open squares) in the presence of 5 μl CM-Affi-Gel Blue-treated antiserum raised against bovine brain aFGF (open triangles) or in the presence of 5 μl CM-Affi-Gel Blue-treated antiserum raised against brain-derived bFGF 1–24 peptide (open circles). Growth factors were diluted in tissue culture medium containing 100 ng/ml heparin in polypropylene tubes and incubated in combination with antibody for 2 hr at ambient temperature before addition to assay plates.

Addition of antisera to cultured cells

Figure 5 shows the effects of addition of CM-Affi-Gel Blue-treated antisera to COMMA-D cells cultured in the presence of bFGF or aFGF. Similar results were obtained by using protein A-Sepharose-purified antiserum (not shown). When anti-bFGF was preincubated with bFGF and then added into the COMMA-D ^{3}H-thymidine incorporation assay, the results were a reduction of the amount of biological activity present compared to bFGF controls incubated without added antibody. The addition of the same quantity anti-bFGF antibodies to samples containing aFGF did not reduce the amount of biological activity present compared aFGF samples which did not receive anti-bFGF. From these results it was concluded that the anti-bFGF preparation could specifically reduce the amount of biological activity present in samples containing bFGF but did not have an effect on biological activity in samples containing aFGF. When the effects of increasing concentrations of anti-bFGF antibodies were tested by using the COMMA-D ^{3}H-thymidine incorporation assay, even the highest doses of anti-bFGF antibodies only partially neutralized the mitogenic effect of bFGF (not shown). The addition of CM-Affi-Gel Blue-treated anti-aFGF antibodies to samples containing bFGF resulted in levels of ^{3}H-thymidine incorporation similar to those measured in samples of bFGF which did not receive anti-aFGF (Fig. 5). Similar effects were obtained by using protein A-Sepharose-purified anti-aFGF (not shown). Addition of either CM-Affi-Gel Blue-treated or protein A-Sepharose-purified anti-aFGF to samples containing aFGF had a stimulative effect resulting in an increased quantity of biological activity compared to the same quantities of aFGF which did not receive anti-aFGF. Addition of various concentrations of CM-Affi-Gel Blue-treated anti-aFGF or anti-bFGF had little effect on the EGF-stimulated and C_o controls used in the COMMA-D cell ^{3}H-thymidine incorporation assay (not shown). The nature of the potentiation of the biological activity of aFGF by addition of partially purified antiserum was not completely understood because the magnitude of stimulation at low levels of aFGF was much greater than the stimulation with no growth factors present (C_o). The data suggest that the presence of antibodies has a stabilizing or potentiating effect on the aFGF molecule similar to the documented effect caused by addition of heparin to tissue culture medium (Gospodarowicz and Cheng, 1986).

Specific removal of mitogenic activity from solution by protein A-Sepharose-immobilized anti-aFGF and anti-bFGF

To reduce complications which may be caused by contaminating mitogens present in antisera prepared by using CM-Affi-Gel Blue, we used protein A-Sepharose to bind and immobilize IgGs from antiserum raised against 1) bovine brain aFGF and 2) brain-derived bFGF (1–24) peptide. The protein A-bound immobilized antibodies then were extensively washed to remove traces of serum and preparations of immobilized anti-aFGF and anti-bFGF were incubated in a series of tubes containing aFGF, bFGF, buffer control (C_o), or EGF control. The supernatants resulting from those incubations were assayed for mitogenic activity by using ^{3}H-thymidine incorporation by COMMA-D cells. This procedure eliminated the addition of trace amounts of serum or growth factor antibodies to the

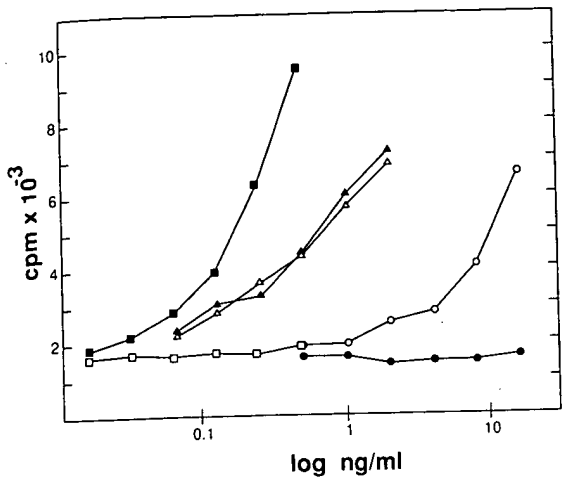

Fig. 6. Removal of mitogenic activity from solutions of growth factors by incubation with antibodies bound to protein A-Sepharose. Solutions containing 1.12 ng porcine bFGF, 37.5 ng bovine brain aFGF, 4.7 ng EGF control, and incubation buffer control (all in 300 μl PBS containing 100 ng/ml heparin) were added to 300 μl packed pellet volume of protein A-Sepharose treated with 1) antiserum raised against bovine brain aFGF or 2) antiserum raised against brain-derived bFGF 1–24 peptide. The protein A-Sepharose treatment with antisera and growth factor incubations with the immobilized antibodies were for 24 hr at 4°C as described in Materials and Methods. After incubation, 2–64-μl volumes of supernatant were assayed for incorporation of ^{3}H-thymidine by COMMA-D cells. bFGF + anti-aFGF (closed squares), bFGF + anti-bFGF (open squares), EGF + anti-aFGF (closed triangles), EGF + anti-bFGF (open triangles), aFGF + anti-aFGF (closed circles), aFGF + anti-bFGF (open circles).

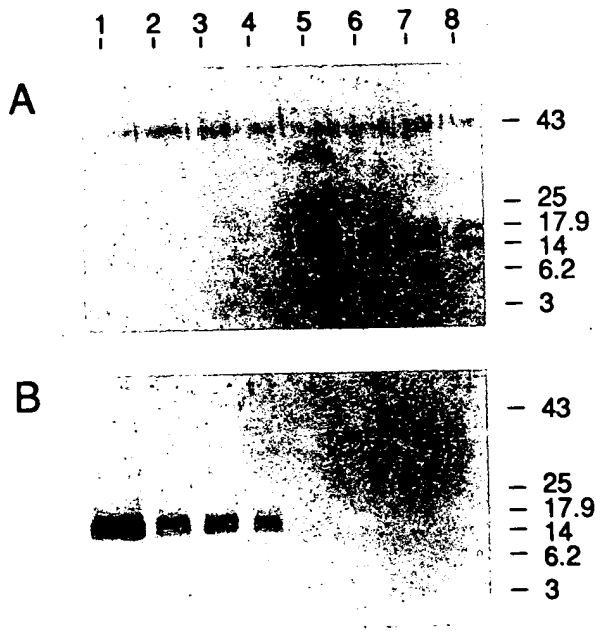

Fig. 7. Western immunoblots of aFGF and bFGF with anti-aFGF antiserum (**A**) and anti-bFGF antiserum (**B**). Samples were subjected to SDS-PAGE and then electrophoretically transferred onto Immobilon P transfer membrane and processed as described in Materials and Methods. **Lanes 1–4** contained 100, 10, 5, and 1 ng, respectively, of bovine pituitary bFGF. **Lanes 5–8** contained 100, 10, 5, and 1 ng, respectively of bovine brain aFGF. Molecular weight standards used were ovalbumin, 43,000; α chymotrypsinogen, 25,000; β-lactoglobulin, 17,900; lysozyme, 14,000; bovine trypsin inhibitor, 6,200; insulin α and β chains, 3,000.

cell culture assay medium, which may have unpredictable effects on the results.

When bFGF was incubated with protein A-Sepharose-immobilized anti-bFGF, the resulting supernatant did not contain detectable biological activity (Fig. 6). The level of ^{3}H-thymidine incorporation was the same as addition of equal volumes of buffer controls incubated with the immobilized antibodies (not shown). When the same preparation of protein A-Sepharose-immobilized anti-bFGF was incubated with either aFGF or EGF, the resulting supernatant contained mitogenic activity. These results suggest that the rabbit polyclonal antibodies raised against brain-derived bFGF (1–24) peptide specifically removed bFGF from solution and did not recognize aFGF or EGF.

When aFGF was incubated with a protein A-Sepharose-immobilized anti-aFGF, the resulting supernatant did not contain detectable mitogenic activity and showed a level of ^{3}H-thymidine incorporation similar to buffer controls incubated with immobilized anti-aFGF. When bFGF or EGF was incubated with the same preparation of immobilized anti-aFGF, the resulting supernatants contained mitogenic activity. These results suggest that the polyclonal antibodies raised against aFGF specifically remove aFGF mitogenic activity from solution and do not recognize bFGF or EGF.

Western immunoblotting of aFGF and bFGF

Western immunoblots of 1–100 ng of aFGF and bFGF are shown using antiserum against aFGF (Fig. 7A) and antiserum against bFGF (Fig. 7B). The anti-aFGF antiserum used in Figure 7A detected a pair of bands of approximately equal intensity in lanes 5–8 containing aFGF. These bands were estimated to be 17 and 14 kDa and probably resulted from proteolytic cleavage during isolation or subsequent sample storage. Because aFGF was linked to ovalbumin as an antigen carrier, the antisera also reacted with the ovalbumin molecular weight standard (not shown). The nonspecific band in all lanes of Figure 7A at 43 kDa was probably immunoreactivity toward ovalbumin contamination. The anti-aFGF antiserum could easily detect 1 ng of bovine brain aFGF (lane 8) eluted from heparin-Sepharose using 1.0 M NaCl. When the anti-aFGF antiserum was used (Fig. 7A), no detectable immunoreactivity was seen in lane 1 containing 100 ng of bFGF. These data clearly demonstrate that bFGF does not cross react with anti-aFGF anti-serum under the conditions in Figure 7. However, in other immunoblots (not shown), 0.2 μg of bFGF did show a faint immunoreactive band when anti-aFGF antiserum was used, confirming the limited degree of cross-reactivity recorded by using ELISA.

The blot incubated with anti-bFGF antiserum (Fig. 7B) shows a pair of immunoreactive bands in lanes 2–4. Additional immunoreactive bands could be seen in lane 1 and when greater quantities of material were applied. In data not shown, a commercial sample of recombinant bFGF also showed numerous immuno-

reactive species. The pair of major bands were estimated to be at 17 and 15 kDa. With this Western immunoblotting protocol, the anti-bFGF antiserum was highly sensitive and could specifically detect 1 ng of bFGF and did not show immunoreactivity with 100 ng of aFGF (lane 5). Similar to the cross-reactivity data obtained for the anti-aFGF antiserum, the anti-bFGF antiserum could detect a faint band of immunoreactive material when higher quantities (0.2 μg) of the heparin-Sepharose 1.0 M NaCl-eluted aFGF were subjected to Western immunoblotting (not shown). The data agree with those obtained by using ELISA, which suggested a slight degree of cross-reactivity for the anti-bFGF antiserum.

As expected, Western immunoblots of bovine brain extract eluted from heparin-Sepharose with 2.0 M NaCl contained a strongly immunoreactive band when anti-bFGF was used and a very faint immunoreactive band when anti-aFGF was used (not shown). These data agree with the ELISA results which suggested a detectable aFGF contamination present in 2.0 M NaCl-eluted bFGF.

DISCUSSION

We report here the production and applications for polyclonal antibodies directed against aFGF and a synthetic peptide corresponding to the N^{α}-terminal 1–24-amino-acid sequence of bFGF. Our report describes an improved sensitivity for the specific detection of aFGF and bFGF by 1) ELISA using a standard solid-phase antigen method, 2) Western immunoblotting using the same electrophoretic transfer conditions for both the cationic bFGF and the anionic aFGF molecules, and 3) specific removal of mitogenic activity from solution using protein A-Sepharose immobilized antibodies.

We believe this to be the first detailed report describing aFGF-specific antiserum. Although there have been numerous reports describing antibodies directed against bFGF, we are not aware of literature reports concerning specific antibodies against aFGF. Because of the structural and functional similarity between aFGF and bFGF (Esch et al., 1985a), most antibodies raised against one molecule often will recognize the other (Wadzinski et al., 1987; Schelling et al., 1987; Pettmann et al., 1986).

There are several previous reports that anti-bFGF antibodies do not recognize aFGF (Moscatelli et al., 1986; Massoglia et al., 1987; Ferrara et al., 1987; Schelling et al., 1987), but no detailed analysis of the extent of cross-reactivity has been presented. We provide the first detailed report characterizing a minimal cross-reactivity of anti-aFGF with bFGF as well as anti-bFGF with aFGF by using three immunological procedures that will be useful in future studies.

We also have demonstrated that antibodies against bFGF added directly to culture medium of COMMA-D cells were able to partially neutralize the mitogenic activity of bFGF. The incomplete neutralization may have been because the antibodies were raised against the N^{α}-24 amino acid sequence of bFGF as the hapten. Mitogenically active N^{α}-terminal truncated microheterogeneous forms of bFGF may have been present which were not recognized with our polyclonal antibodies, although this is unlikely because all bFGF mitogenic activity was removed using immobilized antibodies. A more likely explanation may be that bFGF bound to antibody can still bind to and activate its receptor. Massoglia et al. (1987) have reported that some monoclonal antibodies raised against bFGF do not have the ability to block receptor binding or mitogenic activity of bFGF. In contrast, there are reports describing the use of antibodies against bFGF to completely neutralize mitogenic effects in vitro (Böhlen et al., 1984; Schweigerer et al., 1987a; Ferrara et al., 1987; Neufeld et al., 1987) as well as a report describing reduction of tumor size in vivo (Baird et al., 1986b). The fact that anti-aFGF antiserum was not able to neutralize the mitogenic activity of aFGF in vitro could be due to a variety of reasons including the following: 1) the partially purified antiserum may have contained other mitogens which stimulated COMMA-D cells (although this is unlikely because addition of antiserum to controls did not have a significant effect on thymidine incorporation, 2) the aFGF antibodies must remove a substantially greater amount of aFGF to be able to detect a decreased mitogenic response, because approximately 50-fold-higher concentrations of aFGF were used to elicit a mitogenic response, 3) aFGF bound to antibody could bind to and activate its receptor; and 4) FGFs may exist in association with extracellular matrix components which mask antigenic determinants (Schweigerer et al., 1987b).

We have shown in this report that although heparin-Sepharose has been used for separation and purification of aFGF and bFGF, it is not completely reliable to distinguish between aFGF and bFGF. Previously, Baird et al. (1985a) have reported that some immunoreactive bFGF eluted with 1.1 M NaCl fractions from heparin-Sepharose. Subsequently, Baird et al. (1986b) reported the existence of high-molecular-weight forms of immunoreactive bFGF which occur in flow-through fractions which did not adhere to heparin-Sepharose columns. From the results reported here using ELISA and Western immunoblotting, it is clear that if brain is used as a source of bFGF and if heparin-Sepharose is used to purify and to distinguish between aFGF and bFGF, it is likely that high salt-eluted fractions may contain aFGF. To avoid contamination with aFGF, it would be wise to use a recombinant source of bFGF. However, if a tissue-derived product is used, an organ that does not contain aFGF should be chosen as a source for purification. It is unfortunate that some of the commercially available bFGF is obtained from bovine brain which contains both aFGF and bFGF.

There have been numerous reports of different molecular-weight species of neutral pH extracted bFGF (M_r 150,000–180,000, 70,000, 25,000, 18,000, 16,000, 14,000) as well as elution of multiple forms from reverse-phase HPLC (Gospodarowicz et al., 1984; Mormède et al., 1985; Baird et al., 1986a; Moscatelli et al., 1987; Neufeld et al., 1987; Bertolini and Hearn, 1987). In addition, Klagsbrun et al. (1987) used site-specific antibodies to demonstrate that pH 3.5–4.5 extraction of brain and hepatoma yielded multiple bFGF species resulting from amino terminal cleavages by acid proteinases. They further demonstrated that truncation between the alanine at position +11 and the phenylalanine at position +12 of hepatoma cell

bFGF did not effect its growth factor activity or elution position from heparin-Sepharose.

Our Western immunoblotting results confirmed the presence of microheterogeneous forms and showed more than one immunoreactive band for bovine brain aFGF, porcine pituitary bFGF, bovine pituitary bFGF, and recombinant bFGF. The appearance of multiple forms of purified FGFs is common and may be attributed to natural processing or protease action during isolation or storage (Klagsbrun et al., 1987). One surprising finding was the existence of multiple immunoreactive bands in the commercial sample of recombinant bFGF. The reason for multiple immunoreactive species in recombinant bFGF was not clear although we speculate it could be the result of storage conditions.

From these studies, we conclude that polyclonal antisera can be produced that will specifically recognize subnanogram quantities of either aFGF or bFGF by using standard ELISA or Western immunoblotting procedures. Although the antisera we have characterized do not show complete neutralization of activity by direct addition to the in vitro assay system we employed, immobilized antibodies did specifically remove mitogenic activity from solution.

The highly sensitive and specific immunodetection techniques described here will be useful to identify and discriminate between aFGF and bFGF. These methods can be used to confirm the purity of aFGF and bFGF purified by using heparin-Sepharose affinity chromatography. In addition, the specific antisera characterized in this report may be useful for immunocytochemical techniques to localize FGFs, especially in tissues where both aFGF and bFGF occur.

ACKNOWLEDGMENTS

The authors wish to thank Dr. Kenneth Thomas for supplying us with recombinant aFGF and Dr. Wallace McKeehan for supplying us with a sample of prostatropin (aFGF). We also wish to thank Mr. Beto Zuniga and Ms. Judy Roscoe for their help in preparing illustrations and providing technical assistance. This work was supported by grants from the National Cancer Institute (CA-38024 and CA-26617), American Cancer Society (BC-255), and the Council for Tobacco Research USA, Inc. (2225).

LITERATURE CITED

Baird, A., Böhlen, P., Ling, N., and Guillemin, R. (1985a) Radioimmunoassay for fibroblast growth factor (FGF): Release by the bovine anterior pituitary in vitro. Regul. Pept., *10*:309–317.

Baird, A., Esch, F., Gospodarowicz, D., and Guillemin, R. (1985b) Retina-and eye-derived endothelial cell growth factors: Partial molecular characterization and identity with acidic and basic fibroblast growth factors. Biochemistry, *24*:7855–7860.

Baird, A., Esch, F., Mormède, P., Ueno, N., Ling, L., Böhlen, P., Ying, S.-Y., Wehrenberg, W.B., and Guillemin, R. (1986a) Molecular characterization of fibroblast growth factor: Distribution and biological activities in various tissues. Recent Prog. Horm. Res., *42*:143–205.

Baird, A., Mormède, P., and Böhlen, P. (1986b) Immunoreactive fibroblast growth factor (FGF) in a transplantable chondrosarcoma: Inhibition of tumor growth by antibodies to FGF. J. Cell. Biochem., *30*:79–85.

Bertolini, J., and Hearn, M.J.W. (1987) Isolation characterisation and tissue localisation of an N-terminal-truncated varient of fibroblast growth factor. Mol. Cell. Endocrinol., *51*:187–199.

Böhlen, P., Baird, A., Esch, F., Ling, N., and Gospodarowicz, D. (1984) Isolation and partial molecular characterization of pituitary fibroblast growth factor. Proc. Natl. Acad. Sci. USA, *81*:5364–5368.

Böhlen, P., Esch, F., Baird, A., and Gospodarowicz, D. (1985) Acidic fibroblast growth factor (FGF) from bovine brain: Amino terminal sequence and comparison with basic FGF. EMBO J., *4*: 1951–1956.

Esch, F.A., Baird, A., Ling, N., Ueno, N., Hill, F., Deneroy, L., Klepper, R., Gospodarowicz, D., Böhlen, P., and Guillemin, R. (1985a) Primary structure of bovine pituitary basic fibroblast growth factor (FGF) and comparison with the amino-terminal sequence of bovine brain acidic FGF. Proc. Natl. Acad. Sci. USA, *82*:6507–6511.

Esch, F., Ueno, N., Baird, A., Hill, F., Deneroy, L., Ling, N., Gospodarowicz, D., and Guillemin, R. (1985b) Primary structure of bovine brain fibroblast growth factor (FGF). Biochem. Biophys. Res. Commun., *133*:554–562.

Ferrara, N., Schweigerer, L., Neufeld, G., Mitchel, R., and Gospodarowicz, D. (1987) Pituitary follicular cells produce basic fibroblast growth factor. Proc. Natl. Acad. Sci. USA, *84*:5773–5777.

Gimenez-Gallego, G., Rodkey, J., Bennet, C., Rios-Candelore, M., DiSalvo, J., and Thomas, K. (1985) Brain-derived acidic fibroblast growth factor: Complete amino acid sequence and homologies. Science, *230*:1385–1388.

Gospodarowicz, D. (1987) Isolation and characterization of acidic and basic fibroblast growth factor. In: Methods in Enzymology. D. Barnes and D.A. Sirbasku, eds. Academic Press, Orlando, Vol. 147, pp. 106–119.

Gospodarowicz, D., and Cheng, J. (1986) Heparin protects basic and acidic FGF from inactivation. J. Cell. Physiol., *128*:475–484.

Gospodarowicz, D., Cheng, J., Lue, G.-M., Baird, A., and Böhlent, P. (1984) Isolation of brain fibroblast growth factor by heparin-Sepharose affinity chromatography: Identity with pituitary fibroblast growth factor. Proc. Natl. Acad. Sci. USA, *81*:6963–6967.

Gospodarowicz, D., Massoglia, S.L., Cheng, J., and Fujii, D.K. (1986a) Effect of fibroblast growth factor and lipoproteins on the proliferation of epithelial cells derived from bovine adrenal and brain cortex, bovine corpus luteum, and brain capillaries. J. Cell. Physiol., *127*:121–136.

Gospodarowicz, D., Neufeld, G., and Schweigerer, L. (1986b) Fibroblast growth factor. Mol. Cell. Endocrinol., *46*:187–206.

Hauschka, P.V., Mavrakos, A.E., Iafrati, M.D., Doleman, S.E., and Klagsbrun, M. (1986) Growth factors in bone matrix. Isolation of multiple types by affinity chromatography on heparin-Sepharose. J. Biol. Chem., *261*:12665–12673.

Klagsbrun, M., Sasse, J., Sullivan, R., and Smith, J. (1986) Human tumor cells synthesize an epithelial cell growth factor that is structurally related to basic fibroblast growth factor. Proc. Natl. Acad. Sci. USA, *83*:2448–2452.

Klagsbrun, M., Smith, S., Sullivan, R., Shing, Y., Davidson, S., Smith, J., and Sasse, J. (1987) Multiple forms of basic fibroblast growth factor: Amino terminal cleavages by tumor cell- and brain-cell-derived acid proteases. Proc. Natl. Acad. Sci. USA, *84*:1839–1843.

Lobb, R.R., and Fett, J.W. (1984) Purification of two growth factors from bovine neural tissue by heparin affinity chromatography. Biochemistry, *23*:6295–6299.

Lobb, R.R., Harper, J.W., and Fett, J.W. (1986) Purification of heparin-binding growth factors. Anal. Biochem., *154*:1–14.

Massoglia, S.L., Kenney, J.S., and Gospodarowicz, D.J. (1987) Characterization of murine monoclonal antibodies directed against basic fibroblast growth factor. J. Cell. Physiol., *132*:531–537.

Mormède, P., Baird, A., and Pigeon, P. (1985) Immunoreactive fibroblast growth factor (FGF) in rat tissues: Molecular weight forms and the effects of hypophysectomy. Biochem. Biophys. Res. Commun., *128*:1108–1113.

Moscatelli, D., Joseph-Silverstein, J., Manejias, R., and Rifkin, D.B. (1987) Mr 25,000 heparin-binding protein from guinea pig brain is a high molecular weight form of basic fibroblast growth factor. Proc. Natl. Acad. Sci. USA, *84*:5778–5782.

Moscatelli, D., Presta, M., Joseph-Silverstein, J., and Rifkin, D.B. (1986) Both normal and tumor cells produce basic fibroblast growth factor. J. Cell. Physiol., *129*:273–276.

Neufeld, G., and Gospodarowicz, D. (1986) Basic and acidic fibroblast growth factors interact with the same cell surface receptors. J. Biol. Chem., *261*:5631–5637.

Neufeld, G., Ferrara, N., Schweigerer, L., Mitchell, R., and Gospodarowicz, D. (1987) Bovine granulosa cells produce basic fibroblast growth factor. Endocrinology, *121*:597–603.

Olwin, B.B., and Hauschka, S.D. (1986) Identification of the fibroblast growth factor receptor of Swiss 3T3 cells and mouse skeletal muscle myoblasts. Biochemistry, *25*:3487–3492.

Pettmann, B., Labourdette, G., Weibel, M., and Sensenbrenner, M.

(1986) The brain fibroblast growth factor (FGF) is localized in neurons. Neurosci. Lett., *68*:175–180.

Riss, T.L., Ogasawara, M., Karey, K.P., Danielpour, D., Stewart, B.H., and Sirbasku, D.A. (1986) Use of serum-free hormonally defined media to evaluate the effects of growth factors and inhibitors on proliferation of estrogen-responsive mammary and pituitary tumor cells in culture. J. Tissue Cult. Methods, *10*:133–150.

Riss, T.L., and Sirbasku, D.A. (1987) Growth and continuous passage of COMMA-D mouse mammary epithelial cells in hormonally defined serum-free medium. Cancer Res., *47*:3776–3782.

Riss, T.L., and Sirbasku, D.A. (1989) Identification of a 15,000-molecular-weight form of immunoreactive transforming growth factor α in extracts of porcine pituitary. J. Cell. Physiol., *138*:393–404.

Schelling, M.E., Hawker, J.R., Jr., and Granger, H.J. (1987) Immunochemical comparison of peptide angiogenic factors. Tissue Cell, *19*:463–467.

Schweigerer, L., Malerstein, B., Neufeld, G., and Gospodarowicz, D. (1987a) Basic fibroblast growth factor is synthesized in cultured retinal pigment epithelial cells. Biochem. Biophys. Res. Commun., *143*:934–940.

Schweigerer, L., Neufeld, G., Friedman, J., Abraham, J.A., Fiddes, J.C., and Gospodarowicz, D. (1987b) Capillary epithelial cells express basic fibroblast growth factor, a mitogen that promotes their own growth. Nature (Lond.), *325*:257–259.

Thomas, K.A., and Gimenez-Gallego, G. (1986) Fibroblast growth factors: Broad spectrum mitogens with angiogenic activity. Trends Biochem. Sci., *11*:81–84.

Thomas, K.A., Rios-Candelore, M., Gimenez-Galligo, G., DiSilvo, J., Bennet, C., Rodkey, J., and Fitzpatrick, S. (1985) Pure brain-derived acidic fibroblast growth factor is a potent angiogenic vasicular epithelial cell mitogen with sequence homology to interleukin. Proc. Natl. Acad. Sci. USA, *82*:6409–6413.

Wadzinski, M.G., Folkman, J., Sasse, J., Devey, K., Ingber, D., and Klagsbrun, M. (1987) Heparin-binding angiogenesis factors: Detection by immunochemical methods. Clin. Physiol. Biochem., *5*:200–209.

STIC-ILL

RC261.A1C2
+
mic

From: Holleran, Anne
Sent: Sunday, March 04, 2001 5:30 PM
To: STIC-ILL
Subject: refs. for 09/266,543

Examiner: Anne Holleran
Art Unit: 1642; Rm 8E03
Phone: 308-8892
Date needed by: ASAP

Please send me copies of the following :

1. Plum, S.M. et al. Vaccine, (2000) 19/9-10, 1294-1303
2. Aonuma, M. et al. Anticancer Res. (1999, Oct) 19(5B): 4039-4044
3. Muller, Y.A. et al. Structure (1998) 6(9): 1153-1167
4. Yamagishi, S. et al. J. Biol. Chem. (1997) 272(13): 8723-8730
5. Koolwijk, P. et al. J. Cell Biology (1996) 132(6): 1177-1188
6. Matsuo, A. et al. Neuroscience (1994) 60(1): 49-66
7. Djakiew, D. et al. Cancer Research (1991) 51(12): 3304-3310
8. Yamanishi, H. et al. Cancer Research (1991) 51(11): 3006-3010
9. Matsuzaki, K. et al. Japanese J. Cancer Research (1990) 81(4): 345-354
10. Kardami, E. et al. Growth Factors (1990) 4(1): 69-80
11. Riss, T.L. et al. J. Cellular Physiology (1989) 138(2): 405-414

[CANCER RESEARCH 51, 3304–3310, June 15, 1991]

Regulation of Gr wth by a Nerve Growth Factor-like Protein Which Modulates Paracrine Interacti ns between a Neoplastic Epithelial Cell Line and Stromal Cells of the Human Prostate[1]

Daniel Djakiew,[2] Robert Delsite, Beth Pflug, Jean Wrathall, John H. Lynch, and Makoto Onoda

Department of Anatomy and Cell Biology [D. D., R. D., B. P., J. W., M. O.], Lombardi Cancer Research Center [D. D., J. H. L.], and Department of Surgery, Division of Urology [D. D., J. H. L.], Georgetown University School of Medicine [D. D., R. D., B. P., J. W., M. O.] and Medical Center [J. H. L., D. D.], Washington, DC 20007

ABSTRACT

Nerve growth factor-like substance(s) were identified in both conditioned media of a human prostatic tumor epithelial cell line (TSU-pr1) and a human prostatic stromal cell line (HPS) by Western blot analysis and bioassay of neurite outgrowth of PC12 cells. Nerve growth factor-β (NGF) immunofluorescence was also localized to secretory vesicles in the cytoplasm of both the TSU-pr1 and HPS cells. Western blot of the TSU-pr1 and HPS cell-secreted protein identified an M_r 65,000 major protein which immunoreacted with murine NGF antibody. NGF Western blot of HPS cell-secreted protein also identified an M_r 42,000 minor band under reduced and nonreduced conditions and an M_r 61,000 minor band under reduced conditions. The secreted protein from the TSU-pr1 cells (50 μg/ml) and HPS (50 μg/ml), as well as murine NGF (50 ng/ml) or human recombinant NGF (50 ng/ml), stimulated neurite outgrowth from PC12 cells. This neurite outgrowth activity was partially inhibited by treatment with NGF antibody. Neither the serum containing growth medium nor bovine serum albumin (50 μg/ml) stimulated neurite outgrowth. The NGF-like secretory protein appeared to play a role in the paracrine regulation of prostatic growth between TSU-pr1 cells and HPS cells. The relative growth of TSU-pr1 cells, as indicated by [^{3}H]thymidine incorporation, in response to HPS secretory protein was stimulated 2.8-fold in a dose-dependent manner. In the converse interaction, the relative growth of HPS cells in response to TSU-pr1 secretory protein was stimulated 1.8-fold in a dose-dependent manner. Immunoneutralization of TSU-pr1 and HPS secretory protein was performed with antibody against NGF, acidic fibroblast growth factor, and basic fibroblast growth factor. Removal of the NGF-like protein from the maximal stimulatory dose of TSU-pr1 secretory protein (100 μg/ml) with NGF antibody reduced HPS proliferation to 52% of maximal levels, and immunoneutralization of the NGF-like protein in the maximal stimulatory dose of HPS secretory protein (20 μg/ml) also reduced TSU-pr1 proliferation to 16% of maximal levels. Addition of normal rabbit serum or prior immunoprecipitation of either TSU-pr1 or HPS secretory protein with antibody against acidic fibroblast growth factor and basic fibroblast growth factor did not inhibit the proliferation of either cell type. These results suggest that TSU-pr1 tumor cells and HPS cells secrete NGF-like protein(s) which modulate their paracrine interactive growth *in vitro*.

INTRODUCTION

Prostate cancer has surpassed lung cancer as the leading cause of cancer in men (1). A better understanding of the mechanisms which regulate prostatic growth in the normal and neoplastic prostate may facilitate the clinical manipulation of aberrant prostatic growth. Since the lining epithelium of the prostatic glandular acini are surrounded by a well-developed fibromuscular stroma, cell-to-cell communication has been implicated in mediating aspects of prostatic growth. In this context, paracrine regulation of prostatic growth was first suggested by Franks *et al.* (2) after observing a lack of growth capacity of epithelia which had been separated from their stroma. Subsequently, Cunha (3) and Cunha *et al.* (4) demonstrated that fetal mesenchyme (stroma) recombined with urothelium induced prostatic epithelial morphogenesis and that this morphogenesis occurred in a cell (stroma) density-dependent manner (5). Tissue recombination studies with testicular feminized and wild-type tissues have shown that the target of androgen action is the mesenchyme (4, 6) which in turn mediates the growth of adjacent epithelial cells (7). In adult rat prostatic tissues, androgens mediate the secretion of stromal derived growth factors which stimulate epithelial proliferation (8). Rat stromal secretory proteins also modulate vectorial protein secretion from a neoplastic prostatic epithelial cell line (9). On the other hand, some tumor epithelial cell lines have a reduced requirement for exogenous growth factors (10), consistent with their reduced dependence on androgens and stromal growth factors for their proliferation. Several growth factors have been identified which may function as putative paracrine regulators of prostatic growth. In this context, epidermal growth factor-like (11) and bFGF[3]-like (12, 13) proteins account for a considerable amount of the growth factor activity in the prostate. In addition, aFGF (14), transforming growth factor-β (15, 16), and NGF (17–19) have been identified in the prostate or prostatic tumor cells. Considerable evidence has accumulated demonstrating that NGF secreted by glial cells functions in the paracrine maintenance of neurons (20). Considering the paracrine role of NGF in neurons (20) and its presence in prostatic adenocarcinomas (19), we examined whether NGF may mediate paracrine interactions between a tumor epithelial cell line and stromal cells of the human prostate. In this report we demonstrate the presence of NGF-like proteins in these cells which mediate the paracrine regulation of growth of both the tumor epithelial cell line and the stromal cells *in vitro*.

MATERIALS AND METHODS

Culture of Cell Lines. The human neoplastic epithelial cell line (TSU-pr1) derived from the prostate (21) was a kind gift from Dr. J. Isaacs (Johns Hopkins University, Baltimore, MD). These cells were grown in RPMI-1640 medium (Sigma Chemical Co., St. Louis, MO) supplemented with antibiotics/antimycotic (100 units/ml penicillin, 100 μg/ml streptomycin, 0.25 μg/ml fungizone; Sigma), 10% FCS (Hyclone Co., Logan, UT), and 10^{-7} M T (Sigma). The human prostatic stromal cells were obtained from an adult male following transurethral prostatic resection at Georgetown University Hospital. The tissue was minced into small blocks (1–3 mm^3) and sequentially digested in a collagenase

Received 1/2/91; accepted 4/4/91.

The costs of publication of this article were defrayed in part by the payment of page charges. This article must therefore be hereby marked *advertisement* in accordance with 18 U.S.C. Section 1734 solely to indicate this fact.

[1] This research was funded by NIH Grants CA50229 (to D.D.), N01-NS7-2310 (to J.W.), and P01-NS28130 (to J.W).

[2] To whom requests for reprints should be addressed, at Department of Anatomy and Cell Biology, Georgetown University Medical Center, 3900 Reservoir Road, N. W., Washington, DC 20007.

[3] The abbreviations used are: bFGF, fibroblast growth factor; aFGF, acidic fibroblast growth factor; NGF, nerve growth factor-β; FCS, fetal calf serum; T, testosterone; HPS, human prostatic stroma; DMEM, Dulbecco's modified Eagle's medium; HEPES, 4-(2-hydroxyethyl)-1-piperazineethanesulfonic acid; HS, horse serum; PBS, phosphate-buffered saline; TBS, Tris-buffered saline; BSA, bovine serum albumin; TTBS, TBS containing 0.05% Tween-20 and 0.5% BSA (Sigma); mNGF, murine NGF; hNGF, human recombinant NGF; D.I., DNA index.

enzyme solution as previously described (9). The resulting single-cell suspension and small fragments of tissue were washed in RPMI-1640 medium, resuspended in RPMI-1640 medium containing 10% FCS/T, and plated in 75-mm² flasks (Becton Dickinson Laboratories, Lincoln Park, NJ). After 3 days unattached cells were removed and the remaining cells allowed to proliferate to confluence. These cells were trypsinized and passaged through four successive cycles to obtain a population of HPS free of epithelial contaminants. A seed stock of HPS was subsequently resuspended in RPMI-1640 medium containing 25% FCS/10% dimethyl sulfoxide (Sigma) and frozen at −130°C until use. A rat pheochromocytoma cell line (PC12) was obtained from the American Type Culture Collection (Rockville, MD) and cultured in Ham's F-12/DMEM medium (Irvine Scientific, Santa Ana, CA) supplemented with 15 mM HEPES (Sigma), antibiotics/antimycotic, 10% HS (Gibco BRL, Gaithersberg, MD), and 5% FCS. All cell lines were incubated at 37°C in 5% CO_2/95% air and the media replaced every second day.

Immunofluorescence. The TSU-pr1 cells and HPS cells cultured on glass coverslips were screened for vimentin intermediate filaments, keratin intermediate filaments, and NGF using indirect immunofluorescence as previously described (9). Methanol-fixed cells were blocked with 3% ovalbumin or 5% normal goat serum in PBS at room temperature for 60 min, or at 4°C overnight, and incubated with rabbit anti-murine vimentin antibody (1:100; ICN Immunobiologicals, Lisle, IL), rabbit anti-human keratin antibody (1:25; ICN Immunobiologicals), rabbit anti-murine NGF antibody (1:100; Collaborative Research Inc., Bedford, MA) or normal rabbit serum (1:100; ICN Immunobiologicals) for 60 min. The cells were washed three times in PBS and then incubated with rhodamine-conjugated goat anti-rabbit IgG (1:400–1:1000; ICN Immunobiologicals) at room temperature for 10–30 min. Subsequently, the cells were washed three times in PBS, mounted, and viewed with a Zeiss photomicroscope fitted with an epifluorescence attachment.

Ploidy Analysis of Cell Lines. The ploidy of the TSU-pr1 cells, HPS cells, and murine 3T3 cells were kindly analyzed by Dr. Owen Blair (Lombardi Cancer Research Center, Georgetown University Medical Center, Washington, DC) by the method of Vindelov (22) using propidium iodide as the nuclear stain for the flow cytometry. Chicken erythrocytes and human lymphocytes were used as the internal standard cell types.

Preparation of Secretory Protein. TSU-pr1 cells and HPS cells were grown to confluence in RPMI-1640 medium supplemented with 10% FCS/T and antibiotics/antimycotic. At confluence the cells were washed three times and cultured in Ham's F-12/DMEM medium, with 15 mM HEPES, 2 mM glutamine (Sigma), antibiotics/antimycotic, and T for 24 h. The conditioned media were collected and centrifuged at 1000 ×g to remove particulates, and the supernatant was immediately frozen at −20°C. This procedure was successively alternated with a 24-h incubation in 10% FCS/T with supplements as above. Conditioned media from additional human neoplastic epithelial cell lines (PC-3, DU-145, LNCaP) were similarly prepared with a modification that T was substituted with 10^{-7} M dihydrotestosterone (Sigma) for the LNCaP cells. Conditioned media were concentrated/dialyzed with a hollow-fiber filter cartridge of M_r 10,000 exclusion limit (Cole-Parmer Instruments Co., Chicago, IL) using ice cold distilled water for dialysis. The concentrated dialyzed media were lyophilized and stored at −20°C until use.

Western Blot Analysis of NGF-like Protein. Lyophilized secretory protein from the TSU-pr1 cells and HPS cells, as well as from the PC-3, DU-145 and LNCaP cells, were reconstituted in either reducing or nonreducing sample buffer (23), and 2.5–7.5 μg of these proteins was loaded into each lane of a 12% polyacrylamide minigel and subjected to one-dimensional sodium dodecyl sulfate gel electrophoresis according to the method of Laemmli (23). Subsequently, the separated proteins were electrotransferred to a 0.2-μm nitrocellulose membrane at 0.9 A. The nitrocellulose was blocked with 5% non-fat milk in TBS for 1 h (24), rinsed twice with TTBS, and reacted with NGF antibody (1:1000 in 1% gelatin/TTBS) overnight. The membranes were washed in TTBS twice for 10 min, reacted with horseradish peroxidase-conjugated goat anti-rabbit IgG (1:3000 in 1% gelatin/TTBS; Bio-Rad Labs, Richmond, CA) for 1–3 h, and rinsed in TTBS twice and once with TBS. The immunoreactivity was visualized by the following color development reaction. First, 4-chloro-1-napthol was dissolved to a final concentration of 0.03% in ice cold methanol. Hydrogen peroxide was mixed with TBS at room temperature to a concentration of 0.018%. This solution was added to the 4-chloro-1-napth l solution, and the membranes were incubated in this mixture until color devel ped. The reaction was stopped by replacement of the reaction mixture with distilled water.

Assays of Mitogenic Activities and Immunoneutralization Studies. HPS cells and TSU-pr1 cells were resuspended in RPMI-1640 medium containing 10% FCS/T, seeded at 5×10^4 cells/well in Falcon 24-multiwell tissue culture plates (Becton Dickinson), and incubated in 5% CO_2/95% air. After 24 h the cells were washed three times in Ham's F-12/DMEM medium with 15 mM HEPES and further incubated in various concentrations of either HPS or TSU-pr1 secretory protein, respectively, reconstituted in Ham's F-12/DMEM/T medium with 15 mM HEPES. Additional wells of these cells were cultured in Ham's F-12/DMEM with or without 10% FCS/T, 1% FCS/T, and T. Some of the reconstituted TSU-pr1 and HPS secretory protein (1.5 ml) were mixed with 3–15 μl of polyclonal antibody against murine NGF, bovine aFGF (U.B.I. Inc., Lake Placid, NY), or bovine bFGF (R & D Systems Inc., Minneapolis, MN). A nonimmune normal rabbit serum (ICN Immunobiologicals) and a rabbit IgG (Chemicon International, Inc., Segundo, CA) were used as controls. Subsequently, the secretory protein/antibody mixture was allowed to complex for 1 h at room temperature, followed by centrifugation at 10,000 × g. The supernatant was collected and incubated with the cells as above for the nontreated secretory protein. After a 24-h incubation with the secretory protein or the various control treatments, each well of cells was supplemented with 1 μCi of [³H]thymidine (ICN Radiochemicals, Irvine, CA) and further incubated for 6 h at 37°C in 5% CO_2/95% air. Subsequently, each well was washed three times with 1 ml of ice cold PBS, the cells were fixed in 1 ml of 5% trichloracetic acid (4°C) for 20 min, washed three times with 5% trichloroacetic acid and digested in 0.5 N NaOH (0.3 ml). This solution was neutralized with 0.5 N HCl (0.3 ml) and the incorporated radioactivity was determined by liquid scintillation spectrometry using a Beckmann scintillation counter. Relative growth of cells (25, 26) was calculated from the [³H]thymidine incorporation in the presence of secretory protein or the various culture media preparations divided by [³H]thymidine incorporation in control culture of Ham's F-12/DMEM/T.

Neurite Outgrowth Assay. Neurite outgrowth from PC12 cells was carried out according to the method of Greene and Tischler (27). PC12 cells were suspended in Ham's F-12/DMEM medium with 10% HS/5% FCS and seeded in 24-multiwell tissue culture plates which had been coated with poly-L-lysine (Sigma). Following 24 h incubation at 37°C in 5% CO_2/95% air, the culture medium was replaced with TSU-pr1 and HPS secretory protein (0–100 μg/ml) resuspended in Ham's F-12/DMEM medium with or without 10% HS/5% FCS. In control cultures PC12 cells were incubated with 0–100 μg/ml BSA, 0–100 ng/ml mNGF (Boehringer Mannheim Biochemicals, Indianapolis, MN), and 0–100 ng/ml hNGF (Genentech, South San Francisco, CA), all resuspended in either Ham's F-12/DMEM with or without 10% HS/5% FCS. Additional controls included incubation of PC12 cells in Hank's buffer, Ham's F-12/DMEM alone, or 10% HS/5% FCS in Ham's F-12/DMEM. PC12 cells incubated in each of the above treatments at 37°C in 5% CO_2/95% air were monitored every 24 h for neurite outgrowth during a period of 4 days.

Statistical Analysis. The statistical significance of differences between treatments was tested by Student's t test. The values for the SEM that are given as estimates of the dispersion in the results were calculated for each treatment from estimates of the variance between replicates.

RESULTS

Characterization of TSU-pr1 Cells and HPS Cells by Immunofluorescent Labeling. Fig. 1 shows phase contrast images and corresponding immunofluorescent images of keratin, vimentin,

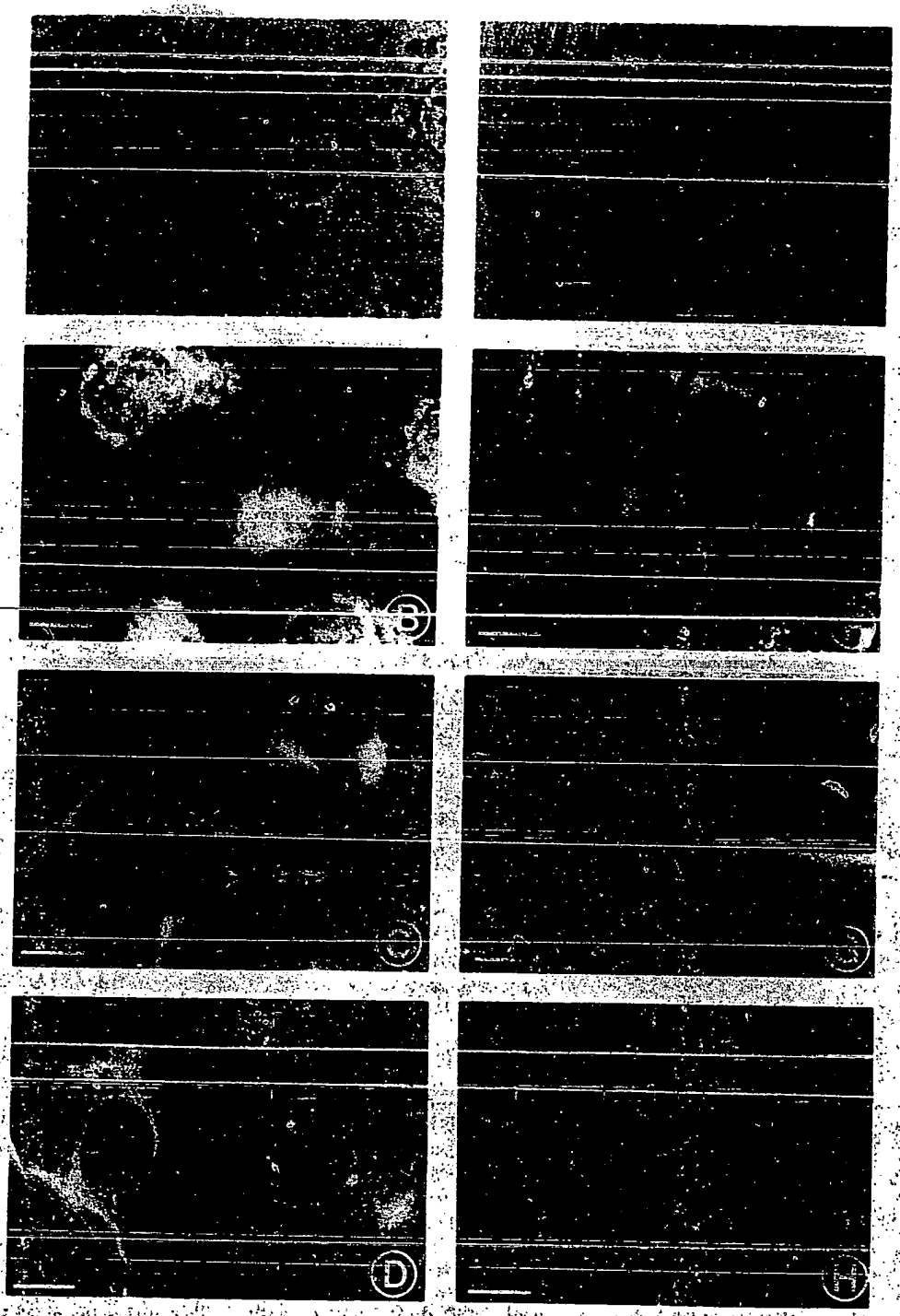

Fig. 1. Human prostatic epithelial tumor cells (TSU-pr1, *A–D*) and stromal cells (HPS *E–H*). *A* and *E*, phase contrast images; *B* and *F*, the corresponding indirect immunofluorescence of NGF; *C* and *G*, the indirect immunofluorescence of vimentin intermediate filaments; *D* and *H*, the indirect immunofluorescence of keratin intermediate filaments immunofluorescence. *Bars*, 13 μm.

and NGF localization in TSU-pr1 cells and HPS cells. The phase contrast image of the TSU-pr1 cells (Fig. 1*A*) shows a centrally located nucleus surrounded by a cytoplasm containing numerous vesicular inclusions. Keratin immunofluorescence of the TSU-pr1 cells (Fig. 1*D*) was localized to filamentous structures throughout the cytoplasm, as was the vimentin immunofluorescence (Fig. 1*C*). The NGF immunofluorescent image of these cells (Fig. 1*B*) shows a diffuse perinuclear staining with distinct vesicular structures in the periphery of the cytoplasm. The phase contrast image of the HPS cells (Fig. 1*E*) sh ws an attenuated cytoplasm containing sparse refractile structures interspersed between an extensive network of stress fibers. HPS cells were slightly immunofluorescent for keratin intermediate filaments (Fig. 1*H*), whereas vimentin immunofluorescence (Fig. 1*G*) was intense and localized to filamentous structures throughout the cytoplasm. Based on the phase contrast images and the vimentin immunofluorescence, the HPS cell line appeared to be 100% pure, lacking epithelial contaminants. NGF immunofluorescence (Fig. 1*F*) of these cells was localized to punctate structures throughout the cytoplasm. At the extremities of the HPS cytoplasm adjacent to the cell borders, large vesicular bodies could be observed as well as in pseudopodia-like extensions of the cytoplasm. In both the HPS and TSU-pr1 cells, the normal rabbit serum controls for the immunofluorescence studies exhibited negligible fluorescence (not shown).

Ploidy of TSU-pr1 and HPS Cells. The ploidy of the various cell lines are expressed as a D.I., where a D.I. of 1.0 (range, 0.9–1.1) is considered diploid and a D.I. <0.9 or >1.1 is considered aneuploid. Hence, the TSU-pr1 cells were recognized as aneuploid with a D.I. of 1.63, the HPS cells with a D.I. of 0.98 are diploid, and in comparison the murine 3T3 cells with a D.I. of 1.69 are aneuploid.

Western Blot f NGF-like Immunoreactivity. Fig. 2 shows the Western blots of NGF-like protein in the TSU-pr1 and HPS secretory protein. Under reduced and nonreduced conditions of the TSU-pr1 (*lanes 1* and *3*) and HPS (*lanes 2* and *4*) secretory proteins a major band of approximately M_r 65,000 was identified. In the HPS secretory protein minor bands of M_r 61,000 and 42,000 were observed under reduced conditions (*lane 2*), whereas under nonreduced conditions (*lane 4*) the only minor band consisted of an M_r 42,000 protein. NGF antibody Western blots of secretory protein from PC-3, DU-145, and LNCaP cells confirmed the presence of NGF-like proteins in these additional neoplastic epithelial cell lines of the human prostate (not shown).

PC12 Neurite Outgrowth. Fig. 3 shows PC12 cells cultured in Ham's F-12/DMEM with 10% HS/5%FCS supplemented with secretory proteins from the TSU-pr1 and HPS cells, as well as BSA, mNGF, and hNGF. PC12 cells cultured with 50 μg/ml TSU-pr1 secretory protein (Fig. 3*A*) or 50 μg/ml HPS secretory protein (Fig. 3*B*) supplemented to Ham's F-12/DMEM with 10% HS/5% FCS exhibited neurite outgrowth in a time- and dose-dependent manner. Generally, neurites were observed after 24 h of culture. These neurites continued to extend for up to 3 days of culture without medium exchange (Fig. 3, *A* and *B*), after which further neurite outgrowth was not observed. Extension of neurites was accompanied by multiple neurite outgrowth from the same cell, branching of the same neurites, and attenuation of the cytoplasm to a squamous phenotype (Fig. 3, *A* and *B*). Negative control cultures of PC12 cells incubated in Ham's F-12/DMEM supplemented with 10% HS/5% FCS (Fig. 3*C*) or supplemented with 50 μg/ml BSA (Fig. 3*D*) did not exhibit characteristics of neurite outgrowth. Additional negative control cultures of PC12 cells incubated in Hank's buffer or Ham's F-12/DMEM alone did not exhibit neurite outgrowth. Positive control cultures of PC12 cells incubated in Ham's F-12/DMEM supplemented with 10% HS/5% FCS supplemented with 50 ng/ml mNGF (Fig. 3*E*) or 50 ng/ml hNGF (Fig. 3*F*) exhibited characteristics of neurite outgrowth comparable to that induced by the TSU-pr1 and HPS secretory protein. NGF antibody immunoneutralization of TSU-pr1 and HPS secretory proteins, as well as the mNGF and hNGF, partially inhibited neurite outgrowth from the PC12 cells (not shown).

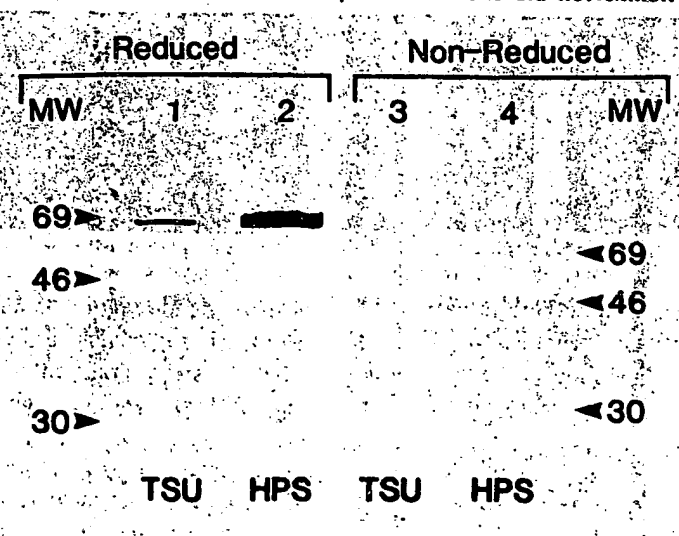

Fig. 2. Western blots of NGF-like proteins in TSU-pr1 cell and HPS cell secretory protein. The location of molecular weight standards (MW; $\times 10^{-3}$), and anti-NGF immunoreacted TSU-pr1 cell protein (*lanes 1* and *3*) and HPS cell protein (*lanes 2* and *4*) under reduced (*lanes 1* and *2*) and nonreduced (*lanes 3* and *4*) conditions are demonstrated. This is a typical Western blot analysis from three independent experiments.

Paracrine Influence of TSU-pr1 and HPS Cell Secretory Protein on Cell Growth. Fig. 4 shows the dose-dependent effect of TSU-pr1 epithelial cell protein on HPS relative proliferation. HPS cells were maximally stimulated 1.8-fold by TSU-pr1 secretory protein at a concentration of 100 μg/ml ($P < 0.05$). HPS relative proliferation was stimulated 10-fold by 10% FCS/T in Ham's F-12/DMEM ($P < 0.01$) and 4-fold by 1% FCS/T in Ham's F-12/DMEM ($P < 0.01$). Prior immunoprecipitation of the maximal stimulatory dose of TSU-pr1 secretory protein (100 μg/ml) with 3 μl NGF antibody/1500 μl secretory protein solution (0.2% antiserum) reduced HPS relative proliferation to 52% of the maximal levels ($P < 0.01$). Addition of NGF antiserum to the maximal stimulatory dose of TSU-pr1 secretory protein equivalent to 1% of the final volume for immunoneutralization resulted in a 4-fold stimulation of HPS cell relative growth. This effect appears to result from unknown components in the NGF antiserum. Hence, immunoneutralization studies were performed with NGF antiserum limited to 0.2% of the total sample volume. Interestingly, prior immunoprecipitation of the TSU-pr1 secretory protein with aFGF or bFGF antibody did not significantly influence the effect of the TSU-pr1 protein on the relative growth of HPS cells. Substitution of the NGF antibody with normal rabbit serum or a rabbit IgG preparation did not significantly inhibit the relative growth of HPS cells in response to TSU-pr1 secretory protein.

Fig. 5 shows the dose-dependent effect of HPS secretory protein on TSU-pr1 relative proliferation. TSU-pr1 proliferation was maximally stimulated 2.8-fold by HPS secretory protein at a concentration of 20 μg/ml ($P < 0.01$). Prior immunoprecipitation of the maximal stimulatory dose of HPS secretory protein (20 μg/ml) with NGF antibody inhibited relative proliferation to 16% of the maximal proliferation of the TSU-pr1 cells ($P < 0.01$). Prior immunoprecipitation of the HPS secretory protein with aFGF or bFGF antibody did not significantly influence the effect of the HPS secretory protein on the relative growth of the TSU-pr1 cells. Replacement of the NGF antibody with normal rabbit serum or a rabbit IgG preparation did not inhibit the relative growth of the TSU-pr1 cells in response to the HPS secretory protein.

DISCUSSION

Vimentin intermediate filaments are generally characteristic of mesenchymal cells, whereas keratin intermediate filaments are generally characteristic of epithelial cells (28). However, some carcinoma cells have been shown to express vimentin and keratin intermediate filaments concurrently (29). Hence, expression of both keratin and vimentin intermediate filaments in the aneuploid TSU-pr1 epithelial tumor cells is consistent with demonstrations of vimentin expression in breast carcinomas (30), breast cancer epithelial cell lines (31), and prostatic epithelial tumor cell lines (14). Expression of vimentin in transformed epithelial cells has been correlated with the more malignant phenotype of hormone-independent cells (31).

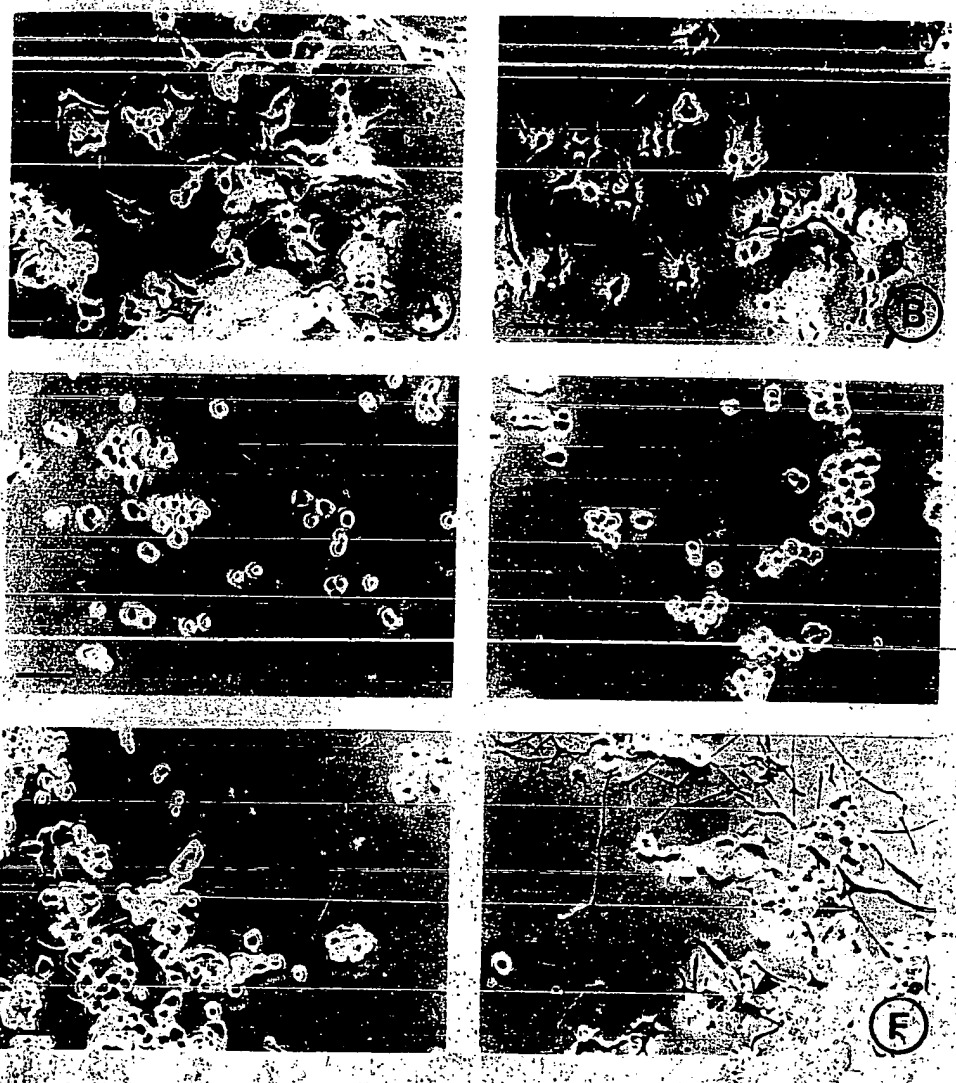

Fig. 3. Neurite outgrowth from PC12 cells. PC12 cells cultured according to process described in "Materials and Methods" for 3 days in the presence of 50 μg/ml TSU-pr1 secretory protein (*A*), 50 μg/ml HPS secretory protein (*B*), 50 μg/ml BSA (*C*), no additional protein (*D*), 50 ng/ml mNGF (*E*), and 50 ng/ml hNGF (*F*). PC12 cells with neurite outgrowth exhibited branching of neurites (*arrows*) and multiple outgrowths of neurites from the same cell (*arrowheads*). The photographs are representative of four independent experiments. *Bars*, 50 μm.

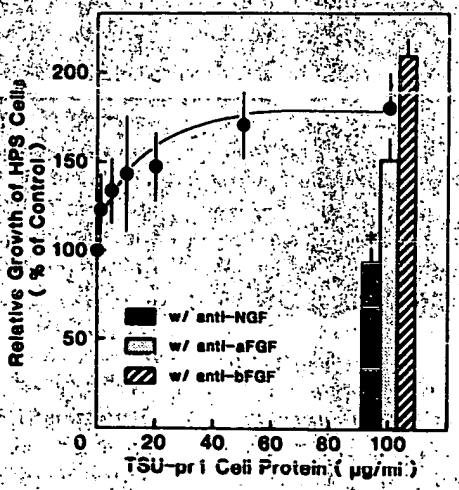

Fig. 4. Dose-dependent relative growth of HPS cells in response to TSU-pr1 secretory protein. Immunoneutralization of the maximal stimulatory dose of TSU-pr1 cell secretory protein (100 μg/ml) with NGF antibody (0.2% antiserum), aFGF antibody, and bFGF antibody. *Point*, mean (*bar*, ±SEM) from four independent experiments. $^*P < 0.01$.

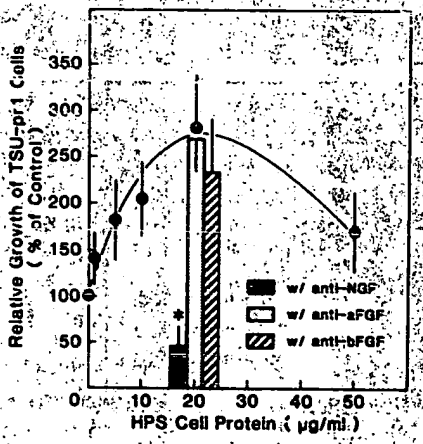

Fig. 5. Dose-dependent relative growth of TSU-pr1 cells in response to HPS cell secretory protein. The maximal stimulatory dose of HPS cell secretory protein (20 μg/ml) was treated with NGF antibody, aFGF antibody, and bFGF antibody. *Point*, mean (*bar*, ±SEM) from seven independent experiments. $^*P < 0.01$.

Therefore, expression of vimentin in immortalized epithelial cells may accompany epithelio-mesenchymal transition to the malignant phenotype. In contrast, the localization of vimentin and relative absence of keratin immunofluorescence in the diploid HPS cell line suggest that these cells have retained an *in vitro* phenotype comparable to their *in vivo* counterparts.

Since the early work of Harper *et al.* (17) demonstrating the presence of NGF-like protein in the prostate gland of the guinea pig, several investigators have found NGF-like proteins throughout the male reproductive system including the seminal

vesicles (20), testis (32, 33), epididymis (33), and spermatozoa (34). Of particular interest is the observation that nonmalignant prostates (35) and prostatic adenocarcinomas (19) are immunoreactive for a NGF-like protein. Our demonstration of the secretion of NGF-like protein(s) by both a human prostatic epithelial tumor cell line (TSU-pr1) and a prostatic stromal cell line (HPS) along with the ability of these proteins to modify the growth of these cells is consistent with a paracrine function for the NGF-like protein(s). Clearly, growth of the epithelial tumor cells appears to be sensitive to the NGF-like protein since immunoneutralization of the HPS secretory protein reduced epithelial tumor cell growth to 16% of that observed with the intact HPS secretory protein. Similarly, growth of the HPS cells appears sensitive to the NGF-like protein since immunoneutralization of the TSU-pr1 secretory protein reduced HPS cell growth to 52% of that observed with the intact TSU-pr1 protein. Hence, it is clear that TSU-pr1 epithelial tumor cells and HPS cells each regulate the growth of the other via a paracrine mechanism mediated by NGF-like protein(s). Interestingly, immunoneutralization of both aFGF and bFGF from the secretory proteins of the TSU-pr1 cells and the HPS cells did not influence the paracrine regulation of growth of these two cell types. The prostate has been shown to be a rich source of aFGF (14) and bFGF (12, 13). However, since aFGF and bFGF lack a hydrophobic leader sequence for their secretion (36), it seems more likely that these FGF proteins may participate in autocrine-regulated growth, as recently suggested by Story *et al.* (13).

Our observations of NGF-like protein(s) in prostatic cell lines are consistent with previous observations of this factor in the prostate gland (17, 18, 20). Whole antiserum and antibodies purified by affinity chromatography against murine submaxillary gland NGF (37) have been shown to completely inhibit the biological activity of prostatic extracts with regard to promotion of nerve fiber outgrowth from dorsal root ganglia *in vitro* (17). The immunofluorescent localization of NGF-like protein to vesicular structures within HPS and TSU-pr1 cells indicates that the protein is present in the secretory pathway, which is a prerequisite for its role as a paracrine growth factor. Furthermore, Western blot analysis and immunoneutralization of the NGF-like protein from conditioned media of both cell types provide additional evidence for its secretion. Western blot of the TSU-pr1 and HPS secretory protein for NGF-like protein identified a major band of approximately M_r 65,000 in both cell types. Since the mature form of murine submaxillary gland NGF is a homodimer (38) consisting of M_r 13,000 subunits (39), which are generated by proteolytic cleavage of a large precursor protein (40), the M_r 65,000 prostatic NGF-like protein recognized in the Western blots either may represent a prostatic precursor form of the NGF protein or may be a distinct protein which belongs to the NGF family of proteins. With regard to the first possibility, precedents for high molecular weight proteins corresponding to putative NGF precursor proteins or partial cleavage products have been reported for the murine submaxillary gland (41, 42) and the rat thyroid (43). The processing of many secretory proteins appears to involve multiple specific proteolytic events (25, 44, 45). Since the Western blots also identified minor bands of slightly lower molecular weight of the NGF-like protein secreted by the HPS cell line, these minor bands may represent partial cleavage products of the M_r 65,000 form. With regard to the NGF family of proteins, two additional genes for neurotrophic proteins have been cloned recently. Brain-derived neurotrophic factor (46) and neurotrophin-3 (47, 48) are polypeptides of similar molecular weights and with isoelectric points to NGF and share nearly 50% homology of amino acid residues. Although these proteins exhibit unique patterns of biological activity for different neurons and distribution patterns of mRNA in the brain (49), it is possible that polyclonal antibodies to NGF may cross-react with these similar molecules. The NGF-like protein(s) that we describe may be the product of one of these neurotrophin genes or of an additional member of this gene family.

In addition to the immunological identity of NGF-like proteins in the TSU-pr1 cells and HPS cells by immunocytochemistry, Western blot, and immunoneutralization, the functional assay of NGF-like activity by PC12 neurite outgrowth in response to secretory proteins from the TSU-pr1 cells and HPS cells provides strong corroborative evidence for the expression of NGF-like protein in these prostatic cells. The PC12 cells can differentiate along the lines of either chromaffin cells or, when grown in the presence of NGF, can differentiate into neuronal like cells (50) as indicated by the phenotypic outgrowth of neurites (27), the development of small vesicles, and the ability to become electrically excitable (51). Hence, the ability of prostatic secretory proteins from TSU-pr1 cells and HPS cells to promote PC12 differentiation to a neuronal phenotype is consistent with the secretion of high molecular weight prostate-specific forms of NGF-like protein.

ACKNOWLEDGMENTS

We are grateful to Dr. S. Brown for technical advice with the Western blots and Genentech Inc. for the gift of the human recombinant NGF.

REFERENCES

1. Reis, L. A., Hankey, B. F., and Edwards, B. K. Cancer Statistics View, 1973–1987. The Surveillance Program-DCPC, National Institutes of Health, United States Department of Health and Human Services, 1990.
2. Franks, L. M., Riddle, P. N., Carbonell, A. W., and Gey, G. O. Comparative study of the ultrastructure and lack of growth capacity of adult human prostate epithelium mechanically separated from its stroma. J. Pathol. *100:* 113–119, 1970.
3. Cunha, G. R. The role of androgens in epithelio-mesenchymal interactions involved in prostatic morphogenesis in embryonic mice. Anat. Rec. *175:* 87–96, 1973.
4. Cunha, G. R., Chung, L. W. K., Shannon, J. M., and Reese, B. A. Stromal-epithelial interactions in sex differentiation. Biol. Reprod. *22:* 19–42, 1980.
5. Chung, L. W. K., and Cunha, G. R. Stromal-epithelial interactions: II. Regulation of prostatic growth by embryonic urogenital sinus mesenchyme. Prostate. *4:* 503–511, 1983.
6. Cunha, G. R., and Lung, B. The possible influences of temporal factors in androgenic responsiveness of urogenital tissue recombinations from wild-type and androgen-insensitive (Tfm) mice. J. Exp. Zool. *205:* 181–194, 1978.
7. Cunha, G. R., Chung, L. W. K., Shannon, J. M., Taguchi, O., and Fujii, H. Hormone-induced morphogenesis and growth: role of mesenchymal-epithelial interactions. Recent Prog. Horm. Res. *39:* 559–595, 1983.
8. Chang, S-M., and Chung, L. W. K. Interaction between prostatic fibroblast and epithelial cells in culture: role of androgen. Endocrinology. *125:* 2719–2727, 1989.
9. Djakiew, D., Tarkington, M. A., and Lynch, J. H. Paracrine stimulation of polarized secretion from monolayers of a neoplastic prostatic epithelial cell line by prostatic stromal cell proteins. Cancer Res. *50:* 1966–1974, 1990.
10. McKeehan, W. L., Adams, P. S., and Fast, D. Different hormonal requirements for androgen-independent growth of normal and tumor epithelial cells from the rat prostate. In Vitro Cell. Dev. Biol. *23:* 147–152, 1987.
11. Jacobs, S. C., Story, M. T., Sasse, J., and Lawson, R. K. Characterization of growth factors derived from the rat ventral prostate. Prostate. *15:* 1106–1110, 1988.
12. Story, M. T., Sasse, J., Jacobs, S. C., and Lawson, R. K. Prostatic growth factor: purification and structural relationship to basic fibroblast growth factor. Biochemistry. *26:* 3843–3849, 1987.
13. Story, M. T., Livingston, B., Baeten, L., Swartz, S. J., Jacobs, S. C., Begun, F. P., and Lawson, R. K. Cultured human prostate-derived fibroblasts produce a factor that stimulates their growth with properties indistinguishable from basic fibroblast growth factor. Prostate. *15:* 355–365, 1989.
14. Mansson, P-E., Adams, P., Kan, M., and McKeehan, W. L. Heparin-binding

growth factor gene expression and receptor characteristics in normal rat prostate and two transplantable rat prostate tumors. Cancer Res., *49:* 2485–2494, 1989.

15. McKeehan, W. L., and Adams, P. Heparin-binding growth factor/prostatropin attenuates inhibition of rat prostate tumor epithelial cell growth by transforming growth factor type beta. In Vitro Cell. Dev. Biol., *24:* 243–246, 1988.
16. Matuo, Y., Nishi, N., Takasuka, H., Masuda, Y., Nishikawa, K., Isaacs., Adams, P., McKeehan, W. L., and Sato, G. H. Production and significance of TGF-beta in AT-3 metastatic cell line established from the Dunning rat prostatic adenocarcinoma. Biochem. Biophys. Res. Commun., *166:* 840–847, 1990.
17. Harper, G. P., Barde, Y. A., Burnstock, Y. A., Carstairs, J. R., Dennison, M. E., Suda, K., and Vernon, C. A. Guinea pig prostate is a rich source of nerve growth factor. Nature (Lond.), *279:* 160–162, 1979.
18. Schwartz, M. A., Fisher, D., Bradshaw, R. A., and Isackson, P. J. Isolation and sequence of a cDNA clone of beta-nerve growth factor from the guinea pig prostate gland. J. Neurochem., *52:* 1203–1209, 1989.
19. DeSchryver-Kecskemeti, K., Balogh, K., and Neet, E. Nerve growth factor and the concept of neural-epithelial interactions. Arch. Pathol. Lab. Med., *111:* 833–835, 1987.
20. Murphy, R. A., Watson, A. Y., and Rhodes, J. A. Biological sources of nerve growth factor. Appl. Neurophysiol., *47:* 33–42, 1983.
21. Iizumi, T., Yazaki, T., Kanoh, S., Kondo, I., and Koiso, K. Establishment of a new prostatic carcinoma cell line (TSU-pr1). J. Urol., *137:* 1304–1306, 1987.
22. Vindelov, L. L. A detergent-trypsin method for the preparation of nuclei for flow cytometric DNA analysis. Cytometry, *3:* 323–327, 1983.
23. Laemmli, U. Cleavage of structural proteins during the assembly of head of bacteriophage T4. Nature (Lond.), *227:* 680–685, 1970.
24. Burnette, W. N. Western blotting: electrophoretic transfer of proteins from sodium dodecyl sulfate-polyacrylamide gels to unmodified nitrocellulose and radioactive detection with antibody and radioiodinated protein A. Anal. Biochem., *112:* 195–203, 1981.
25. Hirata, Y., and Orth, D. N. Conversion of high molecular weight epidermal growth factor (hEGF)/urogastrone (UG) to small molecular weight hEGF-associated arginine esterase. J. Clin. Endocrinol. Metab., *49:* 481–483, 1979.
26. Perkel, V. S., Mohan, S., Herring, S. J., Baylink, D. J., and Linkhart, T. A. Human prostatic cancer cells, PC3, elaborate mitogenic activity which selectively stimulate human bone cells. Cancer Res., *50:* 6902–6907, 1990.
27. Greene, L. A., and Tischler, A. S. Establishment of a noradrenergic clonal line of rat adrenal pheochromocytoma cells which respond to nerve growth factor. Proc. Natl. Acad. Sci. USA, *73:* 2424–2428, 1976.
28. Lazarides, E. Intermediate filaments as mechanical integrators of cellular space. Nature (Lond.), *238:* 249–256, 1980.
29. Ramaekers, F. C. S., Haag, D., Kant, A., Moesker, O., Jap, P. H. K., and Vooijs, G. P. Coexpression of keratin- and vimentin-type intermediate filaments in human metastatic carcinoma cells. Proc. Natl. Acad. Sci. USA, *80:* 2618–2622, 1983.
30. Cattoretti, G., Andreola, S., Clemente, C., D'Amato, L., and Rilke, F. Vimentin and p53 expression on epidermal growth factor receptor-positive, estrogen receptor-negative breast carcinomas. Br. J. Cancer, *57:* 353–357, 1988.
31. Sommers, C. L., Walker-Jones, D., Heckford, S. E., Worland, P., Valverius, E., Clark, R., McCormick, F., Stampfer, M., Abularach, S., and Gelmann, E. P. Vimentin rather than keratin expression in some hormone-independent breast cancer cell lines and in oncogene transformed mammary epithelial cells. Cancer Res., *49:* 4258–4263, 1989.
32. Olson, L., Ayer-LeLievre, C., Ebendal, T., and Seiger, A. Nerve growth factor-like immunoreactivities in rodent salivary glands and testis. Cell Tissue Res., *248:* 275–286, 1987.
33. Ayer-LeLievre, C., Olson, L., Ebendal, T., Hallbook, F., and Persson, H. Nerve growth factor mRNA and protein in the testis and epididymis of mouse and rat. Proc. Natl. Acad. Sci. USA, *85:* 2628–2632, 1988.
34. Schachter, M., Peret, M. W., Moriwaki, C., Wheeler, G. D., Matthews, R. W., Mehta, J. G., and Labedz, T. The varied localization and functional significance of kallikrien-like enzymes in salivary glands, pancreas colon, sex glands and spermatozoa, including evidence for the presence of nerve growth factor (NGF) in bull sperm acrosome. Adv. Exp. Med. Biol., *198* (A): P1–10, 1986.
35. Shikata, H., Utsumi, N., Hiramatsu, M., Minami, N., Nemoto, N., and Shikata, T. Immunohistochemical localization of nerve growth factor and epidermal growth factor in guinea pig prostate gland. Histochemistry, *80:* 411–413, 1984.
36. Thomas, K. A. Fibroblast growth factor. FASEB. J., *1:* 434–440, 1987.
37. Bailey, G. S., Banks, B. E. C., Carstairs, J. R., Edwards, C. D., Pearce, F. L., and Vernon, C. A. Immunological properties of nerve growth factor. Biochim. Biophys. Acta, *437:* 259–263, 1976.
38. Angeletti, R. H., Bradshaw, R. A., and Wade, R. D. Subunit structure and amino acid composition of mouse submaxillary gland nerve growth factor. Biochemistry, *10:* 463–469, 1971.
39. Greene, L. A., Varon, S., Piltch, A., and Shooter, E. M. Subunit structure of the beta subunit of mouse 7S nerve growth factor. Neurobiology, *1:* 37–42, 1971.
40. Scott, J., Selby, M., Urdea, M., Quiroga, M., Bell, G. I., and Rutter, W. Isolation and nucleotide sequence of a cDNA encoding the precursor of mouse nerve growth factor. Nature (Lond.), *302:* 538–540, 1983.
41. Berger, E., and Shooter, E. Evidence for pro-beta-nerve growth factor, biosynthetic precursor to beta-nerve growth factor. Proc. Natl. Acad. Sci. USA, *74:* 3647–3651, 1977.
42. Saboori, A. M., and Young, M. Nerve growth factor: biosynthetic products of the mouse salivary glands. Characterization of stable high molecular weight and 32000 Dalton nerve growth factor. Biochemistry, *25:* 5565–5571, 1986.
43. Dicou, E., Lee, J., and Brachet, P. Synthesis of nerve growth factor mRNA and precursor protein in the thyroid and parathyroid glands of the the rat. Proc. Natl. Acad. Sci. USA, *83:* 7084–7088, 1986.
44. Kemper, B., Habener, J. F., Mulligan, R. C., Potts, J. T., and Rich, A. Preproparathyroid hormones. A direct translation product of parathyroid messenger RNA. Proc. Natl. Acad. Sci. USA, *71:* 3731–3735, 1974.
45. Chan, S. J., Keim, P., and Steiner, D. F. Cell free synthesis of rat preproinsulin: characterization and partial amino acid sequence determination. Proc. Natl. Acad. Sci. USA, *73:* 1964–1968, 1976.
46. Leibrock, J., Lottspeich, F., Honh, A., Hofer, M., Hengerer, B., Masiakowski, P., Thoenen, H., and Barde, Y. A. Molecular cloning and expression of brain-derived neurotrphic factor. Nature (Lond.), *341:* 149–152, 1989.
47. Maisonpierre, P. C., Belluscio, L., Squinto, S., Ip, N. Y., Furth, M. E., Lindsay, R. M., and Yancopoulos, G. D. Neurotrophin-3: a neurotrophic factor related to NGF and BDNF. Science (Washington DC), *247:* 1446–1451, 1990.
48. Rosenthal, A., Goeddel, D. V., Nguyen, T., Lewis, M., Shih, A., Laramee, G. R., Nikolis, K., and Winslow, J. W. Primary structure and biological activity of a novel human neurotrophic factor. Neuron, *4:* 767–773, 1990.
49. Phillips, H. S., Hains, J. M., Laramee, G. R., Rosenthal, A., and Winslow, J. W. Widespread expression of BDNF but not NT3 by target areas of basal forebrain cholinergic neurons. Science (Washington DC), *250:* 290–296, 1990.
50. Landis, S. C., and Patterson, P. H. Neural crest cell lineages. Trends Neurosci., *4:* 172–174, 1981.
51. Dichter, M. A., Tischler, A. S., and Greene, L. A. Nerve growth factor-induced increase in electrical excitability and acetylcholine sensitivity of a rat pheochromocytoma cell line. Nature (Lond.), *268:* 501–504, 1977.

STIC-ILL

RC261.A1 C2
↓
mic

From: Holleran, Anne
Sent: Sunday, March 04, 2001 5:30 PM
To: STIC-ILL
Subject: refs. for 09/266,543

Examiner: Anne Holleran
Art Unit: 1642; Rm 8E03
Phone: 308-8892
Date needed by: ASAP

Please send me copies of the following :

1. Plum, S.M. et al. Vaccine, (2000) 19/9-10, 1294-1303
2. Aonuma, M. et al. Anticancer Res. (1999, Oct) 19(5B): 4039-4044
3. Muller, Y.A. et al. Structure (1998) 6(9): 1153-1167
4. Yamagishi, S. et al. J. Biol. Chem. (1997) 272(13): 8723-8730
5. Koolwijk, P. et al. J. Cell Biology (1996) 132(6): 1177-1188
6. Matsuo, A. et al. Neuroscience (1994) 60(1): 49-66
7. Djakiew, D. et al. Cancer Research (1991) 51(12): 3304-3310
8. Yamanishi, H. et al. Cancer Research (1991) 51(11): 3006-3010
9. Matsuzaki, K. et al. Japanese J. Cancer Research (1990) 81(4): 345-354
10. Kardami, E. et al. Growth Factors (1990) 4(1): 69-80
11. Riss, T.L. et al. J. Cellular Physiology (1989) 138(2): 405-414

[CANCER RESEARCH 51, 3006–3010, June 1, 1991]

Proliferation of Shionogi Carcinoma 115 Cells by Glucocorticoid-induced Autocrine Heparin-binding Growth Factor(s) in Serum-free Medium[1]

Hiroshi Yamanishi, N rio Nonomura, Akira Tanaka, Yasuko Nishizawa, Nobuyuki Terada, Keishi Matsumoto,[2] and Bunzo Sato

Departments of Pathology [H. Y., N. N., A. T., Y. N., N. T., K. M.] and Internal Medicine [B. S.], Osaka University Medical School, Kita-ku, Osaka 530, Japan

ABSTRACT

Shionogi carcinoma 115 (SC115) has been accepted for 20 years as an androgen-responsive mouse mammary tumor. Recently, the growth of the tumor was also found to be stimulated by pharmacological, but not physiological, doses of glucocorticoid. In a serum-free culture system [Ham's F-12:Eagle's minimal essential medium (1:1, v/v) containing 0.1% bovine serum albumin], we have established that 10^{-8} M testosterone, or 10^{-6} M dexamethasone significantly stimulates the growth of SC-3 cells (a cloned cell line from a SC115 tumor) via androgen and glucocorticoid receptors, respectively. Recently, we demonstrated that the testosterone-induced growth of SC-3 cells is mediated through autocrine fibroblast growth factor (FGF)-like peptide(s). In the present study, mechanisms of glucocorticoid-induced growth of SC-3 cells were investigated. Serum-free conditioned medium obtained from 10^{-6} M dexamethasone-stimulated SC-3 cells was fractionated by heparin-Sepharose affinity chromatography; one sharp peak of growth-stimulatory activity for SC-3 cells, eluted at 1.3 M NaCl, was identified. When the peak fraction was added to serum-free medium, the shape of SC-3 cells changed from an epithelial to a fibroblast-like appearance, similar to that induced with testosterone or basic (b)FGF. Furthermore, the growth-stimulatory activity induced with the peak fraction as well as testosterone or bFGF was markedly inhibited by anti-bFGF antibody immunoglobulin G (75 to 90% inhibition was obtained), and the specific binding of ^{125}I-bFGF on SC-3 cells was significantly inhibited by the peak fraction. These results suggest that the glucocorticoid-induced growth of SC-3 cells is also mediated through FGF-like peptide(s) in an autocrine mechanism, which is very similar to that induced by testosterone, if not identical.

INTRODUCTION

Androgen-responsive mouse mammary carcinoma, SC115,[3] which was established in 1964 (1), has maintained androgen responsiveness for growth for more than 20 yr. It has been generally accepted that the growth of SC115 cells is stimulated only by androgen *in vivo* (2–6) and in cell culture (7–10) when physiological levels of hormones are considered and that the growth-stimulatory effect of androgen is mediated through AR (3–10). In addition, some rather conflicting data regarding the effects of glucocorticoids on the growth of SC115 cells, such as stimulatory, biphasic, or no effects of glucocorticoids, were also reported (11–13). However, this issue has become more clear by recent studies; the growth is also stimulated by pharmacological, but not physiological, doses of glucocorticoids via GR *in vitro* (14–17) and *in vivo* (16, 17).

We have established a serum-free culture system using SC115 cells [Ham's F-12:MEM (1:1, v/v) containing 0.1% BSA] in order to demonstrate molecular mechanisms of androgen-induced growth of SC115 cells in relation to growth factors (18). In the serum-free medium, the growth of SC115 cells is stimulated not only by physiological levels of androgen but also by pharmacological, but not physiological, levels of glucocorticoid (16–18). By using the serum-free culture system, we recently demonstrated that the androgen-induced growth of SC-3 cells (a cloned cell line from SC115 cells) is mediated through FGF-like growth factor(s) in an autocrine mechanism (19–23). However, little is known about the mechanism of glucocorticoid-induced growth of SC-3 cells. In the present study, we analyzed the serum-free CM obtained from dexamethasone-stimulated SC-3 cells to examine the possibility that the glucocorticoid-induced growth of SC-3 cells is also mediated through such FGF-like growth factor(s), since only FGF was found to stimulate the proliferation of the cells among the various growth factors examined (24).

MATERIALS AND METHODS

Chemicals. [*methyl*-^{3}H]Thymidine, ^{3}H-steroids, and nonradioactive steroids were obtained as described previously (17). BSA (essential fatty acid free) was purchased from Sigma Chemical Co. (St. Louis, MO). Unlabeled bovine brain bFGF was from R&D System, Inc. (Minneapolis, MN). ^{125}I-bFGF (specific activity, 1000 Ci/mmol) was from Amersham International (Buckinghamshire, England). Antibody IgG against bovine brain bFGF (R&D System) and control IgG were obtained as described previously (22). Heparin-Sepharose was from Pharmacia (Piscataway, NJ). The other chemicals used here were of analytical grade.

Cloning and Cell Culture. The cell line used in the present study was derived from an androgen-dependent mouse mammary SC115 tumor. The method for cloning to obtain SC-3 cells (one of androgen-dependent cloned cell lines) was described previously (18). SC-3 cells were cultured continuously in a maintenance medium composed of MEM added with 2% DCC-treated FCS and 10^{-8} M testosterone. Cells were cultured in a humidified incubator in 95% air-5% CO_2 at 37°C.

DNA Synthesis in Cultured Cells. The method in the serum-free medium was described previously (17). It is also outlined briefly in the legend of Fig. 1.

Preparation of Serum-free CM and Partial Purification of Androgen- or Glucocorticoid-induced Growth Factors. SC-3 cells [2, 5, or 8 × 10^5 cells/100-mm dish for testosterone (+), dexamethasone (+), or none (control), respectively] were plated and cultured as described previously (19). Then, serum-free CMs (2 liters) obtained in the absence or presence of 10^{-8} M testosterone or 10^{-6} M dexamethasone were collected, filtered, and concentrated (up to 20-fold) as described previously (19). Before filtration, 10^{-6} M dexamethasone was added to the control CM. CMs obtained in the absence and presence of testosterone or dexamethasone were used as CM(−), CM(T), and CM(D), respectively. The total cell numbers on dishes were almost the same among the three conditions. Each CM (100 ml) was applied to a column of heparin-Sepharose (gel bed volume, 1.0 ml), preequilibrated with 10 mM Tris-HCl buffer (pH 7.0 at 20°C) containing 0.3 M NaCl and 0.2% (w/v) CHAPS. After a wash with 50 ml of the equilibrated buffer, materials bound to the column were eluted with a linear gradient of 0.3 to 2.3 M NaCl in 10 mM Tris-HCl buffer (pH 7.0 at 20°C) containing 0.2% (w/v) CHAPS (20 ml) at a flow rate of 10 ml/h. Each fraction was dialyzed

Received 9/14/90; accepted 3/13/91.

The costs of publication of this article were defrayed in part by the payment of page charges. This article must therefore be hereby marked *advertisement* in accordance with 18 U.S.C. Section 1734 solely to indicate this fact.

[1] Supported in part by a grant-in-aid for cancer research from the Japanese Ministry of Education, Science, and Culture.

[2] To whom requests for reprints should be addressed.

[3] The abbreviations used are: SC115, Shionogi carcinoma 115; SC-3, androgendependent cloned cell line from SC115; AR, androgen receptor; GR, glucocorticoid receptor; CM, conditioned medium; (b)FGF, (basic) fibroblast growth factor; BSA, bovine serum albumin; DCC, dextran-coated charcoal; FCS, fetal calf serum; MEM, Eagle's minimal essential medium; CHAPS, 3-[(3-cholamidopropyl)dimethylammonio]-1-propanesulfonate; IgG, immunoglobulin G.

against 3 liters of Ham's F-12 medium containing 25 mM *N*-(2-hydroxyethyl)piperazine-*N'*-(2-ethanesulfonic acid), pH 7.5, and 0.2% (w/v) gelatin at 4°C for 24 h. The aliquots (3 μl) of each fraction were added to 0.15 ml of serum-free medium to measure the growth-stimulatory activity, which was estimated by [^{3}H]thymidine incorporation into SC-3 cells.

Effect of Anti-bFGF Antibody IgG on DNA Synthesis in SC-3 Cells. The method was described previously (22). It is also outlined briefly in the legend of Fig. 4.

Binding of ^{125}I-bFGF on SC-3 Cells. Subconfluent SC-3 cells on 24-well tissue culture clusters were incubated in serum-free medium for 48 h. After washing twice with binding buffer [Ham's F-12 medium containing 25 mM *N*-(2-hydroxyethyl)piperazine-*N'*-(2-ethanesulfonic acid), pH 7.5, and 0.2% (w/v) gelatin], 0.475 ml of binding buffer containing ^{125}I-bFGF (20 pM) were added to each well. Then, 25 μl of each fraction eluted from a heparin-Sepharose column following application of CM(D) were added. Nonspecific binding was determined in the presence of an excess (1 μg/ml) of unlabeled bFGF. The binding of ^{125}I-bFGF on the cells was permitted by incubation at 15°C for 4 h. After incubation, the cells were washed twice with ice-cold binding buffer and twice with 1 ml of 2 M NaCl in 20 mM *N*-(2-hydroxyethyl)piperazine-*N'*-(2-ethanesulfonic acid), pH 7.5. The cell-associated radioactivity was solubilized by incubation with 0.5 ml of the solubilization buffer (0.5% Triton X-100 in 0.1 M sodium phosphate, pH 8.1) for 20 min at room temperature. Then, aliquots of the solubilization buffer were counted on a Packard MINAXI gamma counter. All binding assays were performed in triplicate.

Uptake and Metabolism of Dexamethasone by SC-3 Cells. SC-3 cells (1×10^6/tube) were incubated with 10^{-8} M [^{3}H]dexamethasone or 10^{-8} M [^{3}H]testosterone in 0.5 ml of the serum-free medium at 37°C for the indicated periods of time. After incubation, each suspension added with 5 ml of ice-cold Hanks' balanced salt solution was immediately applied to 24-mm-diameter Whatman GF/C glass fiber filters in a vacuum manifold. The filters were washed twice with 5 ml of ice-cold Hanks' balanced salt solution. Then, the radioactivity bound to the filters was measured in a scintillation counter.

SC-3 cells (1×10^6/100-mm dish) were incubated with 10^{-8} M [^{3}H]-dexamethasone in the serum-free medium for 2 days at 37°C in 95% air-5% CO_2. Two ml of the cultured medium were taken, and the reaction was terminated by adding 4 ml of chloroform and vortexing twice for 2 min. The chloroform layer was taken out and evaporated under N_2 gas. After adding the carrier-unlabeled dexamethasone (10 μg), the samples were developed on a thin-layer chromatography plate precoated with Silica Gel 60F254 (Merck, Darmstadt, Germany) using cyclohexane:methyl ethyl ketone (1:1, v/v) as a solvent system. The carrier dexamethasone was visualized with a UV lamp. The radioactivity that comigrated with dexamethasone was then measured by scraping off the silica gel into the counting vials containing the scintillation cocktail.

RESULTS

Growth-stimulatory Effects of Androgen or Glucocorticoid on SC-3 Cells in Serum-free Medium. SC-3 cells were cultured with various concentrations of testosterone or dexamethasone for 3 days in serum-free medium, and the effects on [^{3}H]thymidine uptake in SC-3 cells were examined (Fig. 1). Testosterone stimulated the uptake in a concentration-dependent manner, and the maximum uptake was obtained at 10^{-8} M. Dexamethasone also stimulated the uptake in a concentration-dependent manner. In this case, the maximum uptake was obtained at 10^{-6} M and was about 20% of that induced by testosterone. Similar results were also obtained when the effects of testosterone or dexamethasone on cell number were examined (data not shown).

Glucocorticoid-induced Heparin-binding Growth Factor(s) Secreted from SC-3 Cells. To examine the molecular mechanism of glucocorticoid-induced growth of SC-3 cells, CM obtained from 10^{-6} M dexamethasone-stimulated SC-3 cells [CM(D)] was fractionated by heparin-Sepharose affinity chromatography (Fig. 2). One sharp peak of growth-stimulatory activity for SC-3 cells, eluted at 1.3 M NaCl, was identified. Although the growth-stimulatory activity was lower, the elution pattern was almost identical to that obtained from CM of 10^{-8} M test sterone-stimulated SC-3 cells [CM(T)]. CM(−) obtained with ut addition had no such peak.

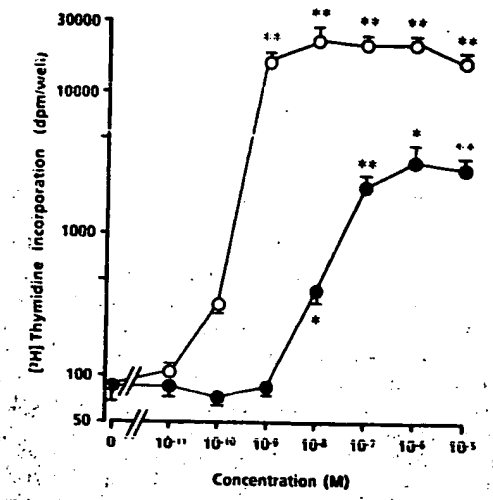

Fig. 1. Stimulatory effects of 10^{-11} to 10^{-5} M testosterone or dexamethasone on [^{3}H]thymidine incorporation in SC-3 cells in serum-free medium. SC-3 cells were plated onto a 96-well plate (3×10^3 cells/well) containing 0.15 ml of MEM added with 2% DCC-treated FCS. On the following day (Day 0), the medium was changed to 0.15 ml of serum-free medium [Ham's F-12:MEM (1:1, v/v) containing 0.1% BSA] in the absence or presence of various concentrations of testosterone (○) or dexamethasone (●). On Day 3, the cells were pulsed with [^{3}H] thymidine (0.15 μCi/0.15 ml per well) for 2 h at 37°C, and the radioactivity incorporated into the cells was measured. *Points*, mean of three determinations; *bars*, SE. *, $P < 0.01$; **, $P < 0.001$, when compared to none (in the absence of testosterone or dexamethasone). The other 2 separate trials also gave similar results.

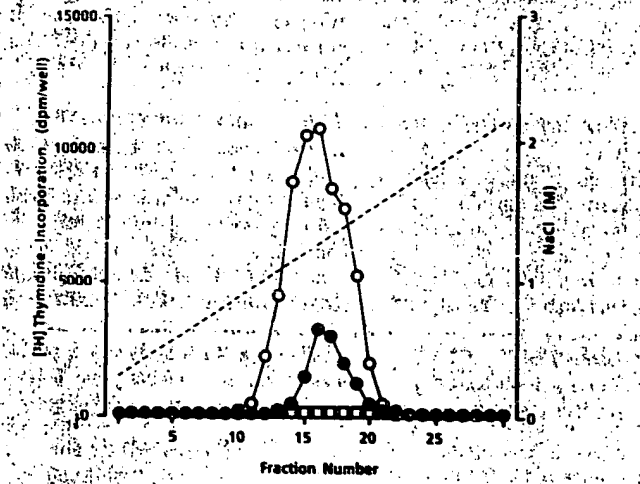

Fig. 2. Heparin-Sepharose affinity chromatography of CMs. Concentrated CMs (20×), obtained from cultured serum-free medium with SC-3 cells in the absence (□) or presence of 10^{-8} M testosterone (○) or 10^{-6} M dexamethasone (●), were prepared (before concentration, 10^{-6} M dexamethasone was added to the CM obtained in the absence of testosterone or dexamethasone), and 100 ml of the concentrated CMs were fractionated by heparin-Sepharose as described in "Materials and Methods." The growth-stimulatory activity in each fraction (2%, v/v) was estimated by [^{3}H]thymidine incorporation in SC-3 cells, as shown in the legend of Fig. 1. *Points*, mean of three determinations. The other 2 separate trials also gave similar results.

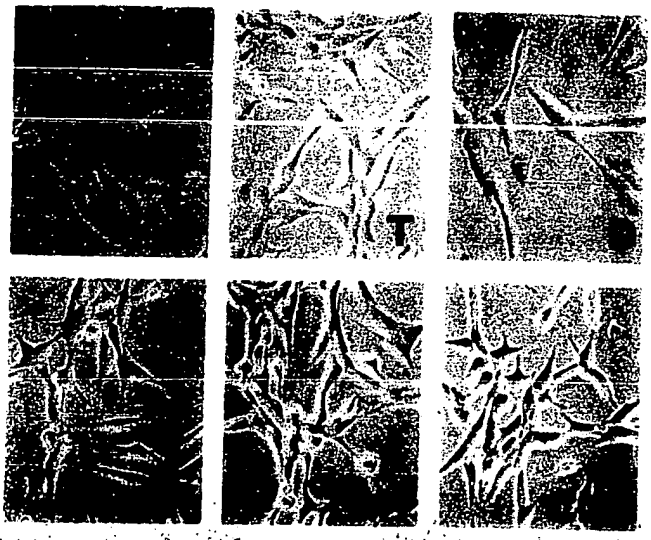

Fig. 3. Epithelial appearance [with no addition (*C*)], fibroblast-like appearance [in the presence of 10^{-8} M testosterone (*T*), 1 ng/ml of bFGF (*FGF*), peak fraction (2%, v/v) from CM(T) (*CMT*), or peak fraction (2%, v/v) from CM(D) (*CMD*)], and intermediate shape of SC-3 cells [in the presence of 10^{-6} M dexamethasone (*D*)] observed on Day 3 of serum-free culture. Cells were photographed through contrast optics. × 100. The other 2 separate trials also gave similar results.

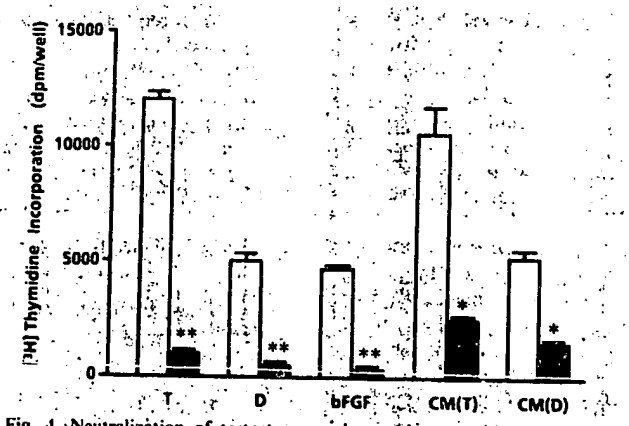

Fig. 4. Neutralization of testosterone-, dexamethasone-, bFGF-, or CMs-induced stimulation of [^{3}H]thymidine uptake in SC-3 cells by anti-bFGF antibody IgG. SC-3 cells were plated as shown in Fig. 1. On the following day, the medium was changed to 0.15 ml of serum-free medium added with 10^{-8} M testosterone (*T*), 10^{-6} M dexamethasone (*D*), 1 ng/ml of bFGF, peak fraction (2%, v/v) from CM(T) [*CM(T)*], or peak fraction (5%, v/v) from CM(D) [*CM(D)*] in the presence of 200 μg/ml of anti-bFGF antibody IgG (■) or control IgG (□). On Day 3, the [^{3}H]thymidine uptake in SC-3 cells was estimated as shown in Fig. 1. *Columns*, mean of three determinations; *bars*, SE. *, $P < 0.01$; **, $P < 0.001$, when compared with control IgG. The other 2 separate trials also gave similar results.

Morphology of SC-3 Cells Stimulated by Androgen, Glucocorticoid, FGF, or Partially Purified Factor(s) from CMs. SC-3 cells cultured in the serum-free medium with no addition showed an epithelial appearance (Fig. 3). The shape was changed to a fibroblast-like appearance by the addition of bFGF (1 ng/ml), testosterone (10^{-8} M), or partially purified growth factor(s) from CM(T) by a heparin-Sepharose column. The shape showed an intermediate morphology in the presence of 10^{-6} M dexamethasone. However, SC-3 cells showed the complete fibroblast-like appearance in the presence of partially purified growth factor(s) from CM(D).

Inhibitory Effects of Anti-bFGF Antibody IgG on the Growth of SC-3 Cells. In previous studies, we demonstrated that anti-bFGF antibody IgG inhibits [^{3}H]thymidine uptake in SC-3 cells induced by testosterone, bFGF, or partially purified androgen-induced growth factor(s) (22, 23). To examine the possibility that the glucocorticoid-induced growth factor(s) is also FGF-like peptide(s), we studied the effect of anti-bFGF antibody IgG on DNA synthesis in SC-3 cells induced by partially purified glucocorticoid-induced growth factor(s). As shown in Fig. 4, [^{3}H]thymidine uptake in SC-3 cells induced with 1 ng/ml of bFGF, 10^{-8} M testosterone, or 10^{-6} M dexamethasone was markedly inhibited (about 90%) by 200 μg/ml of anti-bFGF antibody IgG. The antibody IgG also significantly inhibited [^{3}H]thymidine uptake induced by partially purified androgen- or glucocorticoid-induced growth factor(s). Approximately 75% inhibition was attained.

Interaction of Partially Purified Glucocorticoid-induced Heparin-binding Growth Factor(s) with FGF Receptor on SC-3 Cells. Androgen-induced growth factor(s) secreted from SC-3 cells is shown to bind to the FGF receptor on SC-3 cells (23). In the present study, we examined the possibility that the glucocorticoid-induced growth factor(s) also displaced the binding of bFGF on SC-3 cells. As shown in Fig. 5, the specific binding of ^{125}I-bFGF on SC-3 cells was markedly reduced by the addition of partially purified glucocorticoid-induced growth factor(s) obtained from CM(D), which was present in a peak fraction (Fraction 17 in Fig. 2). On the other hand, the fraction without growth-stimulatory activity (Fraction 28) did not displace the binding of ^{125}I-bFGF on SC-3 cells.

Effects of Dexamethasone on Testosterone-induced DNA Synthesis in SC-3 Cells under Serum-free Conditions. DNA synthesis in SC-3 cells stimulated by testosterone reached a plateau at the concentration of 10^{-8} M (Figs. 1 and 6). When 10^{-6} M dexamethasone was added in various concentrations of testosterone, a marked growth stimulation induced by greater than 10^{-8} M testosterone was significantly inhibited (Fig. 6). On the other hand, a weak stimulation by 10^{-11} to 10^{-10} M testosterone was significantly enhanced by the addition of 10^{-6} M dexamethasone (Fig. 6).

Uptake and Metabolism of Dexamethasone by SC-3 Cells. In order to investigate the reason why the effective concentration of dexamethasone via GR is about 100-fold higher than that of testosterone via AR, the uptake of dexamethasone in SC-3 cells was examined first. As shown in Table 1, the uptake of dexamethasone in SC-3 cells was lower than that of testosterone

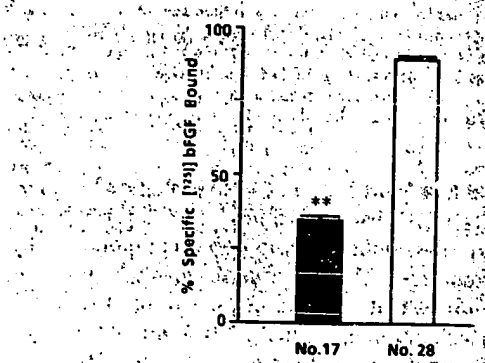

Fig. 5. Inhibition of ^{125}I-bFGF binding on SC-3 cells by partially purified glucocorticoid-induced growth factor(s). SC-3 cells prepared as described in "Materials and Methods" in binding buffer were incubated with ^{125}I-bFGF (20 pM) and 25-μl (5%, v/v) fractions obtained from CM(D) (No. 17, fraction with highest growth-stimulatory activity; No. 28, fraction with no growth-stimulatory activity). The incubation was performed at 15°C for 4 h. The specific binding of ^{125}I-bFGF is expressed as percentage, taking the value without addition of the fractions as 100%. (The absolute cpm of specifically bound bFGF obtained by the addition of No. 28 and No. 17 were 1940 ± 20 and 760 ± 10 cpm/4 × 10^5 cells, respectively.) *Columns*, mean of three determinations; *bars*, SE. **, $P < 0.001$, when compared with control (No. 28). The other 3 separate trials also gave similar results.

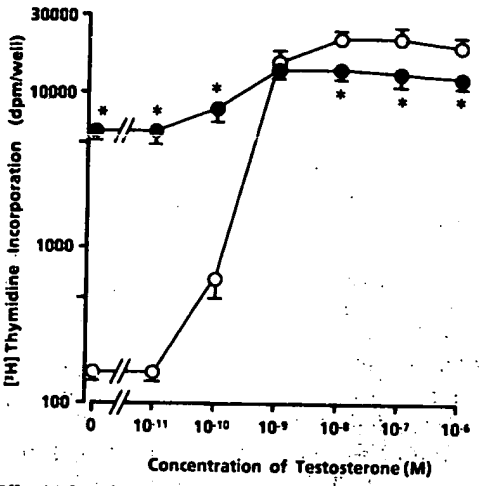

Fig. 6. Effects of 10^{-6} M dexamethasone on DNA synthesis in SC-3 cells induced by 10^{-11} to 10^{-6} M testosterone in serum-free medium. SC-3 cells were plated as shown in Fig. 1. On the following day, the medium was changed to 0.15 ml of the serum-free medium in the absence or presence of various concentrations of testosterone (○) or various concentrations of testosterone plus 10^{-6} M dexamethasone (●). [³H]Thymidine incorporation was measured on Day 3, as shown in Fig. 1. *Points*, mean of three determinations; *bars*, SE. *, $P < 0.01$, when compared with testosterone alone. The other 2 separate trials also gave similar results.

Table 1 *Uptake of dexamethasone or testosterone in SC-3 cells*

SC-3 cells (1×10^6/tube) were incubated with 10^{-8} M [³H]dexamethasone or [³H]testosterone for the indicated periods of time. Uptake of the steroids was measured as described in "Materials and Methods." The other two separate trials also gave similar results.

	Incubation time (min)				
	1	2	5	10	20
Dexamethasone	1.21[a]	1.28	1.75	2.32	3.61
Testosterone	2.17	2.45	4.10	4.71	5.64

[a] Mean of duplicate tubes (fmol/10^5 cells).

(40 to 60%). The uptakes of dexamethasone and testosterone gradually increased during the first 20 min and, thereafter, no more remarkable increases were observed up to 1 h. Metabolism of [³H]dexamethasone by SC-3 cells was examined next. SC-3 cells were cultured in the serum-free medium containing 10^{-8} M [³H]dexamethasone for 2 days. Almost all [³H]dexamethasone (99 ± 1%) in the medium remained unchanged.

DISCUSSION

Recently, we reported that in a serum-free medium containing no growth factors [Ham's F-12:MEM (1:1, v/v) containing 0.1% BSA], only acidic and basic FGFs have stimulatory effects on the growth of SC-3 cells; various concentrations of epidermal growth factor, transforming growth factor α, platelet-derived growth factor, insulin, insulin-like growth factors I and II, or nerve growth factor had no effects (21, 24; Footnote 4). In addition, serum-free conditioned medium obtained from 10^{-8} M testosterone-stimulated SC-3 cells contained autocrine growth factor(s), which was partially purified by heparin-Sepharose affinity chromatography (19–21). In further investigations, we obtained the following findings regarding this partially purified, androgen-induced, heparin-binding growth factor(s). (*a*) SC-3 cells changed their shape from an epithelial to a fibroblast-like appearance by the addition of testosterone, FGFs, or the androgen-induced growth factor(s). (*b*) Growth-stimulatory effects induced by testosterone, FGF, or the androgen-induced growth factor(s) were markedly and similarly neutralized by anti-bFGF antibody IgG (22, 23). (*c*) The androgen-induced growth factor(s) was shown to bind to FGF receptors on SC-3 cells (23). These findings strongly suggest that the androgen-induced growth factor(s) secreted by SC-3 cells is FGF-like peptide(s). The above previous findings on the androgen-induced growth of SC-3 cells through the androgen-induced FGF-like growth factor(s) (19–24) are confirmed by the present results shown in Figs. 1 to 4.

On the one hand, growth-stimulatory effects of high concentrations of glucocorticoids on SC115 cells have been demonstrated by recent (14–17) and the present (Fig. 1) studies. However, the mechanisms of glucocorticoid-induced growth have not been well known. Taking the advantage of our serum-free culture system with no addition of any growth factors, molecular mechanisms of the dexamethasone-induced growth of SC-3 cells were investigated. We found for the first time that serum-free conditioned medium obtained from 10^{-6} M dexamethasone-stimulated SC-3 cells also contains autocrine heparin-binding growth factor(s) (Fig. 2), which was eluted from a heparin-Sepharose column at the same NaCl concentration as that for androgen-induced growth factor(s). However, the amount of this dexamethasone-induced growth factor(s) was much lower than that of testosterone-induced growth factor(s) (Fig. 2). This partially purified dexamethasone-induced factor(s) induced changes of the shape of SC-3 cells to a fibroblast-like appearance (Fig. 3) and inhibited the specific binding of ^{125}I-bFGF on SC-3 cells (Fig. 5), similar to testosterone, FGF, and partially purified testosterone-induced heparin-binding growth factor(s). Furthermore, the growth-stimulatory activity of this partially purified factor(s), FGF, or testosterone-induced factor(s) was markedly and similarly reduced by anti-bFGF antibody IgG (Fig. 4). These data strongly suggest that dexamethasone and testosterone stimulate the growth of SC-3 cells by secreting very similar, if not identical, autocrine FGF-like growth factor(s).

Testosterone exerts its growth-stimulatory effect through AR (3–10). Since dexamethasone does not bind at all to AR in SC-3 cells, its effect is mediated through GR (15, 17, 22). The most acceptable explanation for their growth-stimulatory mechanism is that dexamethasone-GR and testosterone-AR complexes bind to the same or similar region(s) on the DNA and then induce the production of the same autocrine FGF-like growth factor(s) and that the activity of glucocorticoid-GR complexes to induce FGF-like factor(s) is lower than that of androgen-AR complexes. This idea might be supported by our previous observations that dexamethasone weakly stimulates the production and secretion of five secretory proteins in SC-3 cells, which are identical to those induced by testosterone (25). Furthermore, the present findings shown in Figs. 1, 2, and 6 seem to support this idea. Darbre *et al.* (26, 27) also reported using a mouse mammary tumor virus system that dexamethasone and testosterone stimulate via GR and AR, respectively, the same gene in cloned SC115 cells under serum-supplemented conditions. This action could be explained on the basis that the mouse mammary tumor virus long terminal repeat can respond to both androgen-AR and glucocorticoid-GR complexes (26) and that binding sites in DNA for various steroid receptors share, in general, structural similarities (28). However, if this idea is true, a 100-fold difference in effective concentrations between dexamethasone and testosterone is puzzling. Is the marked difference explainable by differential metabolism or

[4] Unpublished results.

uptake of the steroids? These possibilities were examined in this study. Although the uptake of dexamethasone into the cells was slightly lower (40 to 60%) than that of testosterone (Table 1), almost no metabolism of dexamethasone by the cells was demonstrated. In our previous studies (17), the affinity of GR for dexamethasone (K_d 5 nM) was 5-fold lower than that of AR for testosterone (K_d 1 nM) in SC-3 cells. Furtherm re, Nohno *et al.* (29) recently reported that GR in SC115 cells has tw different forms in the DNA-binding domain, compared with the wild-type mouse GR; one has a one-base substitution at 1310 (valine to glycine at 437), and the other (found only in 2 of 17 independent clones) has an additional three-base insertion between 1373 and 1374. When expressed in COS-1 cells, the latter GR from SC115 cells had about half of the activity of the wild-type mouse GR in a chloramphenicol acetyl transferase assay responding to dexamethasone.[5] These previous and the present findings by us and others on GR of SC115 cells, if put together, may explain a portion of the marked difference in the effective concentrations. However, more intensive and detailed investigations on GR of SC-3 cells are required in order to understand the marked difference. Furthermore, in order to know whether FGF-like growth factors produced by androgen and glucocorticoid in SC-3 cells are the same or not, the amino acid sequences of both androgen- and glucocorticoid-induced growth factor(s) should be determined in future studies.

ACKNOWLEDGMENTS

The authors thank Dr. K. Takeda and Dr. T. Komeno, Shionogi Research Laboratories, for supporting these studies.

REFERENCES

1. Minesita, T., and Yamaguchi, K. An androgen-dependent tumor derived from a hormone-independent spontaneous tumor of a female mouse. Steroids, *4:* 815–830, 1964.
2. Minesita, T., and Yamaguchi, K. An androgen-dependent mouse mammary tumor. Cancer Res., *25:* 1168–1175, 1965.
3. Matsumoto, K., Sato, B., and Kitamura, Y. Role of androgen and its receptors in mouse mammary tumor. *In:* B. S. Leung (ed.), Hormonal Regulation of Mammary Tumors, Vol. 1, pp. 216–244. St. Albans, VT: Eden Medical Research, Inc., 1982.
4. Bruchovsky, N., and Meakin, J. W. The metabolism and binding of testosterone in androgen-dependent and autonomous transplantable mouse mammary tumors. Cancer Res., *33:* 1689–1695, 1973.
5. Suzuki, N., Wakisaka, M., Miyauchi, T., Shimazaki, J., and Hosoya, T. Effect of sex hormones on RNA synthesis of androgen-dependent mouse mammary tumor (Shionogi carcinoma). Endocrinol. Jpn., *30:* 15–21, 1983.
6. Bélanger, A., Le Goff, J-M., Proulx, L., Caron, S., and Labrie, F. Presence of C-19 steroids in mammary Shionogi carcinoma (SC115) in castrated mice. Cancer Res., *45:* 6293–6295, 1985.
7. Desmond, W. J., Jr., Wolbers, S. J., and Sato, G. Cloned mouse mammary cell lines requiring androgens for growth in culture. Cell, *8:* 79–86, 1976.
8. King, R. J. B., Cambray, G. J., and Robinson, J. H. The role of receptors in the steroidal regulation of tumor cell proliferation. J. Steroid Biochem., *7:* 869–873, 1976.
9. Jung-Testas, I., Desmond, W., and Baulieu, E. E. Two sex steroid receptors in SC-115 mammary tumor cells. Exp. Cell Res., *97:* 219–232, 1976.
10. Stanley, E. R., Palmer, R. E., and Sohn, U. Development of methods for the quantitative *in vitro* analysis of androgen-dependent and autonomous Shionogi carcinoma 115 cells. Cell, *10:* 35–44, 1977.
11. Watanabe, S., Nohno, T., Omukai, Y., Saito, T., and Senoo, T. Stimulatory effects of dexamethasone and indomethacin on growth of androgen-dependent Shionogi carcinoma 115 in the mouse. Cancer Lett., *16:* 261–266, 1982.
12. Yates, J., and King, R. J. B. Multiple sensitivities of mammary tumor cells in culture. Cancer Res., *38:* 4135–4137, 1978.
13. Nohno, T., Watanabe, S., and Saito, T. Evaluation of effect of host immunity on growth of androgen-dependent Shionogi carcinoma 115 in the mouse. Cancer Lett., *33:* 125–130, 1986.
14. Darbre, P. D., and King, R. J. B. Differential effects of steroid hormones on parameters of cell growth. Cancer Res., *47:* 2937–2944, 1987.
15. Labrie, F., Veilleux, R., and Fournier, A. Glucocorticoids stimulate the growth of mouse mammary carcinoma Shionogi cells in culture. Mol. Cell. Endocrinol., *58:* 207–211, 1988.
16. Omukai, Y., Nakamura, N., Hiraoka, D., Nishizawa, Y., Uchida, N., Noguchi, S., Sato, B., and Matsumoto, K. Growth-stimulating effect of pharmacological doses of glucocorticoid on androgen-responsive Shionogi carcinoma 115 *in vivo* in mice and in cell culture. Cancer Res., *47:* 4329–4334, 1987.
17. Hiraoka, D., Nakamura, N., Nishizawa, Y., Uchida, N., Noguchi, S., Matsumoto, K., and Sato, B. Inhibitory and stimulatory effects of glucocorticoid on androgen-induced growth of murine Shionogi carcinoma 115 *in vivo* and in cell culture. Cancer Res., *47:* 6560–6564, 1987.
18. Noguchi, S., Nishizawa, Y., Nakamura, N., Uchida, N., Yamaguchi, K., Sato, B., Kitamura, Y., and Matsumoto, K. Growth-stimulatory effect of pharmacological doses of estrogen on androgen-dependent Shionogi carcinoma 115 *in vivo* but not in cell culture. Cancer Res., *47:* 263–268, 1987.
19. Nonomura, N., Nakamura, N., Uchida, N., Noguchi, S., Sato, B., Sonoda, T., and Matsumoto, K. Growth-stimulatory effect of androgen-induced autocrine growth factor(s) secreted from Shionogi carcinoma 115 cells on androgen-unresponsive cancer cells in a paracrine mechanism. Cancer Res., *48:* 4904–4908, 1988.
20. Sato, B., Nakamura, N., Noguchi, S., Uchida, N., and Matsumoto, K. Characterization of androgen-dependent autocrine growth factor secreted from mouse mammary carcinoma (Shionogi carcinoma 115). *In:* H. Imura, K. Shizume, and S. Yoshida (eds.), Progress in Endocrinology, 1988, pp. 99–104. Basel: Excerpta Medica, 1988.
21. Nonomura, N., Nakamura, N., Sudo, K., Sato, B., and Matsumoto, K. Proliferation of Shionogi carcinoma cells caused by androgen-induced fibroblast growth factor (FGF)-like peptide in an autocrine mechanism. *In:* M. Serino (ed.), Perspective in Andrology, pp. 431–438. New York: Raven Press, 1989.
22. Lu, J., Nishizawa, Y., Tanaka, A., Nonomura, N., Yamanishi, H., Uchida, N., Sato, B., and Matsumoto, K. Inhibitory effect of antibody against basic fibroblast growth factor on androgen- or glucocorticoid-induced growth of Shionogi carcinoma 115 cells in serum-free culture. Cancer Res., *49:* 4963–4967, 1989.
23. Nonomura, N., Lu, J., Yamanishi, H., Sato, B., Sonoda, T., and Matsumoto, K. Interaction of androgen-induced autocrine heparin-binding growth factor with fibroblast growth factor receptor on androgen-dependent Shionogi carcinoma 115 cells. Cancer Res., *50:* 2316–2321, 1990.
24. Nakamura, N., Yamanishi, H., Lu, J., Uchida, N., Nonomura, N., Matsumoto, K., and Sato, B. Growth-stimulatory effects of androgen, high concentration of glucocorticoid, or fibroblast growth factors on a cloned cell line from Shionogi carcinoma 115 cells in a serum-free medium. J. Steroid Biochem., *33:* 13–18, 1989.
25. Nakamura, N., Nishizawa, Y., Matsumoto, K., Noguchi, S., Terada, N., Uchida, N., and Sato, B. Both androgen and glucocorticoid induce identical secretory proteins in serum-free culture of Shionogi carcinoma 115 cells. Jpn. J. Cancer Res., *78:* 937–945, 1987.
26. Darbre, P. D., Moriarty, A., Curtis, S. A., and King, R. J. B. Androgen regulates MMTV RNA in the short-term in S115 mouse mammary tumor cells. J. Steroid Biochem., *23:* 379–384, 1985.
27. Darbre, P., Page, M. J., and King, R. J. B. Steroid regulation of transfected genes in mouse mammary tumor cells. J. Steroid Biochem., *24:* 125–131, 1986.
28. Beato, M. Gene regulation by steroid hormones: review. Cell, *56:* 335–344, 1989.
29. Nohno, T., Kasai, Y., and Saito, T. Novel cDNA sequence possibly generated by alternative splicing of a mouse glucocorticoid receptor gene transcript from Shionogi carcinoma 115. Nucleic Acids Res., *17:* 445, 1989.

[5] T. Nohno *et al.*, personal communication.

STIC-ILL

adonis
20.00

From: Holleran, Anne
Sent: Sunday, March 04, 2001 5:30 PM
To: STIC-ILL
Subject: refs. for 09/266,543

Examiner: Anne Holleran
Art Unit: 1642; Rm 8E03
Phone: 308-8892
Date needed by: ASAP

Please send me copies of the following :

1. Plum, S.M. et al. Vaccine, (2000) 19/9-10, 1294-1303
2. Aonuma, M. et al. Anticancer Res. (1999, Oct) 19(5B): 4039-4044
3. Muller, Y.A. et al. Structure (1998) 6(9): 1153-1167
4. Yamagishi, S. et al. J. Biol. Chem. (1997) 272(13): 8723-8730
5. Koolwijk, P. et al. J. Cell Biology (1996) 132(6): 1177-1188
6. Matsuo, A. et al. Neuroscience (1994) 60(1): 49-66
7. Djakiew, D. et al. Cancer Research (1991) 51(12): 3304-3310
8. Yamanishi, H. et al. Cancer Research (1991) 51(11): 3006-3010
9. Matsuzaki, K. et al. Japanese J. Cancer Research (1990) 81(4): 345-354
10. Kardami, E. et al. Growth Factors (1990) 4(1): 69-80
11. Riss, T.L. et al. J. Cellular Physiology (1989) 138(2): 405-414

too late

Article title	VEGF and the Fab fragment of a humanized neutralizing antibody: Crystal structure of the complex at 2.4 @9 resolution and mutational analysis of the interface
Article identifier	0969212698004875
Authors	Muller_Y_A Chen_Y Christinger_H_W Li_B Cunningham_B_C Lowman_H_B de_Vos_A_M
Journal title	Structure
ISSN	0969-2126
Publisher	Elsevier Current Trends
Year of publication	1998
Volume	6
Issue	9
Supplement	0
Page range	1153-1167
Number of pages	15
User name	Adonis
Cost centre	
PCC	$20.00
Date and time	Monday, March 05, 2001 11:05:15 PM

VEGF and the Fab fragment of a humanized neutralizing antibody: crystal structure of th compl x at 2.4 Å resolution and mutati nal analysis of th int rfac

Yves A Muller[1,2], Yvonne Chen[1], Hans W Christinger[1], Bing Li[1], Brian C Cunningham[1], Henry B Lowman[1] and Abraham M de Vos[1]*

Background: Vascular endothelial growth factor (VEGF) is a highly specific angiogenic growth factor; anti-angiogenic treatment through inhibition of receptor activation by VEGF might have important therapeutic applications in diseases such as diabetic retinopathy and cancer. A neutralizing anti-VEGF antibody shown to suppress tumor growth in an *in vivo* murine model has been used as the basis for production of a humanized version.

R sults: We present the crystal structure of the complex between VEGF and the Fab fragment of this humanized antibody, as well as a comprehensive alanine-scanning analysis of the contact residues on both sides of the interface. Although the VEGF residues critical for antibody binding are distinct from those important for high-affinity receptor binding, they occupy a common region on VEGF, demonstrating that the neutralizing effect of antibody binding results from steric blocking of VEGF–receptor interactions. Of the residues buried in the VEGF–Fab interface, only a small number are critical for high-affinity binding; the essential VEGF residues interact with those of the Fab fragment, generating a remarkable functional complementarity at the interface.

Conclusions: Our findings suggest that the character of antigen–antibody int rfaces is similar to that of other protein–protein interfaces, such as ligand–r ceptor interactions; in the case of VEGF, the principal difference is that the residues essential for binding to the Fab fragment are concentrated in one continuous segment of polypeptide chain, whereas those essential for binding to the receptor are distributed over four different segments and span across the dimer interface.

Addresses: [1]Department of Protein Engineering, Genentech, Inc., 1 DNA Way, South San Francisco, CA 94080. USA and [2]Forschungsgruppe Kristallographie, Max-Delbrück-Centrum für Molekulare Medizin, Robert-Rössle-Strasse 10, D-13122 Berlin-Buch, Germany.

*Corresponding author.
E-mail: devos@gene.com

Key words: angiogenesis, antibody–antigen recognition, mutagenesis, phage display, X-ray structure

Received: **19 May 1998**
Revisions requested: **29 June 1998**
Revisions received: **13 July 1998**
Accepted: **17 July 1998**

Structure 15 September 1998, 6:1153–1167
http://biomednet.com/elecref/0969212600601153

Introduction

Vascular endothelial growth factor (VEGF) is a highly specific angiogenic factor that has been implicated both in the *de novo* formation of blood vessels during embryogenesis (vasculogensis) and in the sprouting of new blood vessels from pre-existing ones (angiogenesis) [1–3]. The importance of VEGF in normal blood vessel development is emphasized by the observation that deletion of a single VEGF allele is lethal [4,5]. Furthermore, excessive and pathogenic angiogenesis plays a crucial role in a number of diseases, such as diabetic retinopathy and cancer [3]. The high specificity of VEGF for proliferation of vascular endothelial cells makes VEGF antagonists prime candidates for the suppression of pathogenic angiogenesis. This assumption has been substantiated by the suppression of tumor growth *in vivo* following treatment with anti-VEGF antibodies in a murine model [6]. These results prompted the engineering of a humanized version of murine neutralizing anti-VEGF antibody A4.6.1 [7,8], in order to investigate the beneficial effects of anti-angiogenic treatment in humans.

There are two known cellular receptors of VEGF, KDR (kinase domain receptor), which triggers the angiogenic response, and Fms-like tyrosine kinase 1 (Flt-1), the function of which is, as yet, poorly understood [9]. The same 115 N-terminal residues of VEGF are shared by a number of different splicing isoforms that range from 121 to 206 residues in length [10]. Plasmin cleavage of the longer forms shows that the receptor-binding functionality is contained within the first 110 residues [11]. The crystal structure of a truncated construct of VEGF (residues 8–109) [12] demonstrates that VEGF is a member of the cystine knot growth factor family (for a review, see [13]). Extensive mutagenesis data allowed for the mapping of the binding epitopes for KDR and Flt-1 onto the surface of VEGF [14,15] — the binding site was shown to be localized on the two symmetrical poles of the dimer [15]. This general location of the receptor-binding site was confirmed by the crystal structure of VEGF in complex with domain 2 of Flt-1 [16]. This structure also revealed that although the binding determinants for both receptors, as deduced from the mutagenesis studies, overlap

only partially, almost all these residues are in contact with domain 2 of Flt-1, suggesting that VEGF binds to KDR and Flt-1 in a similar fashion.

Neutralizing monoclonal antibody A4.6.1 binds tightly to VEGF, and this binding event prevents receptor activation [6]. In order to gain further insights into the mechanism of action of the antibody, we determined the crystal structure at 2.4 Å resolution of its humanized antigen-binding fragment, Fab-12 [8], in complex with the receptor-binding domain of VEGF. A comparison of this structure with those of free VEGF and of VEGF bound to domain 2 of Flt-1 shows that the neutralization mechanism of the antibody involves steric blocking of the receptor site, and not induced conformational changes in the ligand. We also performed an extensive alanine-scanning mutagenesis analysis [17] of both the combining site of the Fab fragment and the binding epitope of VEGF. Although alanine-scanning mutagenesis of the complementarity-determining regions (CDRs) in order to determine the relative contribution of individual residues to antigen binding has been reported before (for example, [18]), this is the first comprehensive mutational analysis of both the antibody and its antigen in combination with detailed structural information. The results show that only a small proportion of the residues in the interface are important for high-affinity binding, and the important residues of the antibody interact with those of the antigen to generate a remarkable 'functional' complementarity. These findings suggest that antigen–antibody interactions are qualitatively similar to other protein–protein interactions, such as those between receptors and their ligands [19].

Results

Accuracy of the crystallographic model

The crystal structure of the complex between the receptor-binding domain of VEGF (residues 8–109) [20] and the humanized Fab fragment, Fab-12 [8], of monoclonal antibody A4.6.1 was determined at 2.4 Å resolution and refined to a crystallographic R value of 19.6% (free R value 26.6%, Table 1). The crystallographic asymmetric unit contains two Fab molecules bound to the symmetrical poles of the VEGF dimer, and the molecular dyad of the VEGF dimer coincides with the noncrystallographic twofold symmetry of the complex (Figure 1). In both monomers of VEGF, only residues 14–107 are defined by their electron density. In both Fab molecules, the C-terminal residue Cys214 of the light (L) chain is missing and the six C-terminal residues Ser215–Thr220 are disordered in both heavy (H) chains. In addition, loop 128–133 in the constant domain of both heavy chains could not be placed with confidence and was therefore omitted from the model.

The coordinate error of the model as deduced from a σ_A plot [21] is ~0.35 Å; deviations from target-model geometry are 0.012 Å for bond lengths and 1.66° for bond angles.

Table 1

Crystallographic analysis.

Crystallization and data collection	
Space group	$P2_1$
Cell parameters a, b, c (Å)	89.86, 66.98, 140.51
β (°)	94.27
Resolution (Å)	20–2.4 (2.48–2.40)*
Unique reflections	63,147
Average redundancy	3.8
Average I / σ	8.6 (3.5)*
Overall completeness (%)	96.0 (81.3)*
R_{merge}† (%)	7.1 (12.8)*
Model	
Total no. of residues	1050
Contents of asymmetric unit	2 Fab fragments, 1 VEGF dimer
No. of solvent molecules	549
Total non-H atoms	8695
Average B factor (Å²)	42.0
Diffraction agreement	
Resolution (Å)	8.0–2.4
R value (%)	19.6 (31.2)*
No. of reflections	54 493
Free R value (%)	26.6 (34.1)*
No. of reflections	5 908
Anisotropic correction, B_{11}, B_{22}, B_{33}, B_{13} (Å²)	3.7, −8.5, 4.8, −0.31
Stereochemistry	
Rmsd	
in bonds (Å)	0.012
in angles (°)	1.66
in temperature factors of bonded atoms (Å²)	
overall	3.8
mainchain	2.6
sidechain	5.0

*Values for the highest resolution shell given in parenthesis. †R_{merge} is defined as follows: $R_{merge} = 100\ \Sigma|I_1 - I_2|/\Sigma(I_1 + I_2)$

Of all 1050 residues, 89.4% are located in the most favorable regions [22] of the Ramachandran plot. Four residues are located in disallowed regions, namely residues $Ser30_{V_L}$ and $Thr51_{V_L}$ (V_L denotes that the residues are located in the variable region of the light chain) of both Fab molecules in the asymmetric unit. They are part of the CDRs L1 and L2 and will be discussed below. As a result of the noncrystallographic symmetry restraints applied during refinement, the root mean square deviations (rmsds) between equivalent residues are small, namely 0.27 Å for the mainchain atoms (0.45 Å for all atoms) between the VEGF monomers, 0.17 Å (0.40 Å) for the V_L domains, 0.42 Å (0.72 Å) for C_L (light chain, constant, 0.16 Å (0.19 Å) for V_H (heavy chain, variable), and 0.40 Å (0.60 Å) for the C_{H1} (heavy chain, constant) domains.

The average temperature factor of the model is 40.5 Å². Although the average temperature factor of the VEGF dimer at 40.6 Å² is close to this, the average temperature factors of the two Fab fragments are 23.0 Å² and 61.4 Å², respectively (Figure 2). This difference is entirely accounted

for by the differences in mobility between the constant domains, because the variable domains have similar average temperature factors of 23.7 Å^2 and 28.4 Å^2, respectively. It is striking that the lowest temperature factors within both VEGF monomers are found for residues involved in the VEGF–Fab interface (Figure 2a); moreover, these temperature factors are very similar to the average observed for the variable domains. As these residues have higher than average temperature factors in 12 independent copies of free VEGF [12,15], Fab binding appears to have stabilized this region, enabling it to form a well-ordered intermolecular core that extends from VEGF to the variable domain of the Fab fragment.

The constant domain of one Fab fragment has a very high average temperature factor of 100 Å^2. This high thermal mobility is due to the almost complete lack of crystal-packing contacts for this domain; similar differences in mobility between the constant and variable parts of a Fab fragment have been observed before [23]. It should be noted that the presence of the second, crystallographically independent Fab fragment enabled us to model the average position of this domain with accuracy. This approach is not unlike the use of nuclear magnetic resonance (NMR) restraints to introduce additional information in the refinement of ribosomal protein L9 [24], which had similarly high thermal factors.

Figur 1

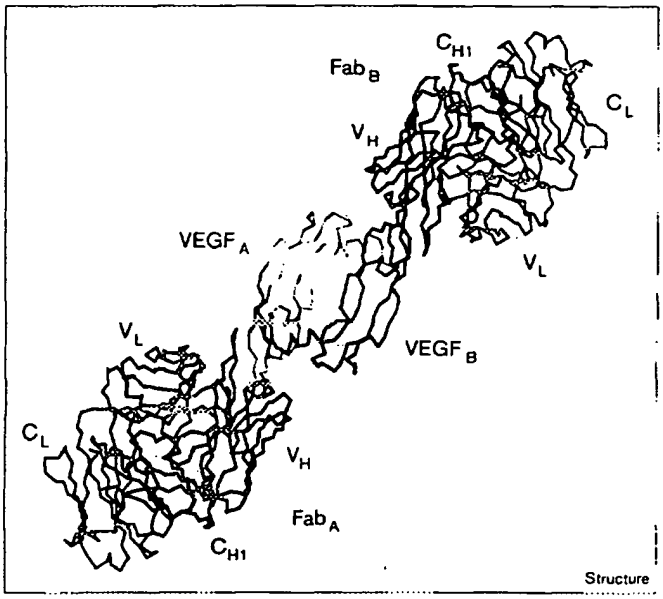

Cα representation of the complex of the VEGF dimer bound to two Fab molecules. The different chains are named as follows: $VEGF_A$ (yellow) and $VEGF_B$ (red), monomers A and B forming the VEGF dimer; Fab_A and Fab_B, Fab molecules A and B; V_L, C_L, V_H, C_{H1}, variable domain and constant domain of the light chain (in green) and of the heavy chain (blue) of the Fab fragment, respectively.

Ov rall structure of VEGF and anti-VEGF Fab

VEGF is a homodimeric protein and belongs to the family of cystine knot growth factors, members of which share a similar monomer fold, but differ in their dimerization mode [13]. The structure of the receptor-binding domain (residues 8–109) of VEGF consists of a central four-stranded β sheet that displays the characteristic cystine knot at one end [13] and possesses a small hydrophobic core at the other end [12,16]. This hydrophobic core is generated by residues from loop regions connecting the strands of the central β sheet, together with residues displayed on the N-terminal α helix of the second subunit, across the dimer interface. The dimerization mode of the VEGF homodimer is similar to that observed for platelet-derived growth factor [25] — a dyad axis oriented perpendicular to the β sheet places the two four-stranded β sheets side by side. No mainchain–mainchain hydrogen bonds are observed between strands across the interface, however.

The overall structure of VEGF in complex with the Fab fragment is very similar to the unbound structure previously reported [12]. The two monomers in the crystallographic asymmetric unit can be superimposed onto the eight monomers observed in the 1.9 Å crystal structure with average rmsds of 0.73 Å (mainchain atoms, residues 15–105). These deviations are of the same magnitude as those among the eight monomers of free VEGF. Nevertheless, although the overall structure is preserved in the complex, small but significant differences are observed for some residues at the binding epitope of the antibody (see below).

The initial framework for the humanization of the anti-VEGF antibody was identical to that used for the anti-HER2 antibody, anti-p185^{HER2} [26], but some adjustments in framework residues were required in order to obtain tight binding [7,8], resulting in an overall sequence identity of 88%. The structures of the variable domains of the anti-VEGF Fab can be superimposed on that of anti-p185^{HER2} [27] with an rmsd of 1.04 Å (900 mainchain atoms used in the superposition); superimposing the constant domains yields a deviation of 0.59 Å (788 mainchain atoms). The two antibodies differ significantly in their elbow angle, despite having complete sequence identity among the residues in the interface between the variable and constant domains. For anti-p185^{HER2}, the elbow angle is about 160° (program CALC-AX; Joachim Meyer, personal communication), in comparison to 140° for both copies of the anti-VEGF Fab. Both these values fall within the range of 127°–225° previously reported for Fab fragments [28].

The CDR loops of the anti-VEGF Fab have the following canonical structures [29]: in the light chain, CDR L1 adopts canonical structure 2, L2 canonical structure 1, and L3 canonical structure 1; for the heavy chain, canonical structure 1 is observed for CDR H1, and canonical structure 2 for

Figure 2

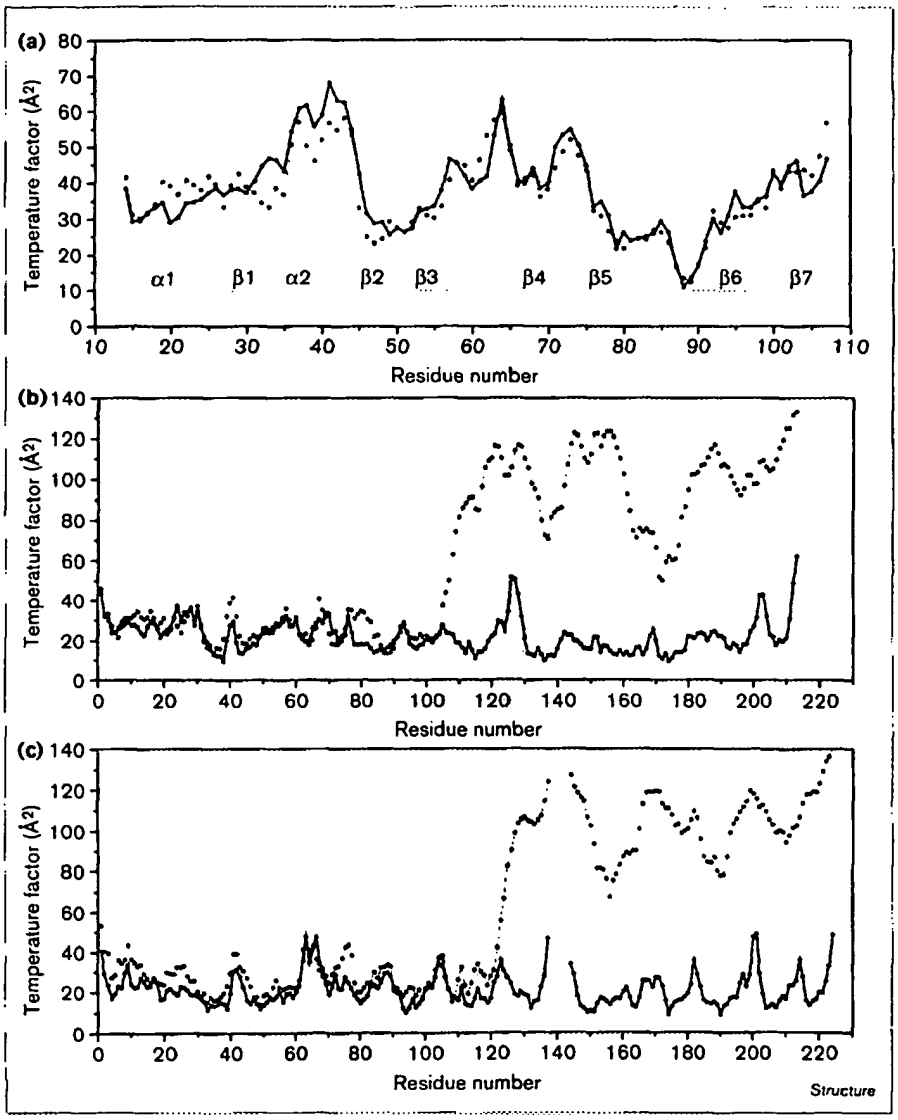

Average mainchain temperature factors per residue for the two copies of each molecule in the asymmetric unit (bold and thin lines). The temperature factors of **(a)** VEGF, **(b)** light chain and **(c)** heavy chain of the anti-VEGF Fab are shown. The lowest temperature factors in VEGF are observed for segment β5–β6, which binds to anti-VEGF. In this segment, the temperature factors are similar to the average temperature factors observed for the variable domains of anti-VEGF. Unusually high temperature factors are observed for the constant domains of the second anti-VEGF Fab molecule (see main text). Secondary structure elements of VEGF are defined as follows: α1 (residues 16–24), β1 (27–34), α2 (35–39), β2 (46–48), β3 (51–58), β4 (67–69), β5 (73–83), β6 (89–99) and β7 (103–105) [12].

H2. To date, only a single type of structure has been reported for CDR L2. In this CDR, the mainchain dihedral angles at Thr51 are close to those expected for left-handed α helices but nonetheless fall into disallowed regions [22] of the Ramachandran plot. Interestingly, the same observation has been made for other Fab fragments whose structures have been determined (e.g. see [27,30,31]). Thus, it appears that the angles observed at position 51 of CDR L2 constitute a real shift from a canonical left-handed helical conformation and that this reflects a general property of L2. A similar observation holds true for position 30 in canonical structure 2 of CDR L1.

Antigen–antibody interface

The anti-VEGF antibody binds VEGF at outer strands β5 and β6 (Figures 1 and 3), in close proximity to the β turn between these strands. The surface area buried in the antigen–antibody interface is 835 Å² for the antibody (Table 2) and 908 Å² for VEGF (Table 3). A total of 19 VEGF residues participate in the interface. Residues from strand β6 contribute 663 Å² (73% of the total buried surface area) and residues from strand β5 contribute 149 Å² (16%). The remaining contacts to the Fab fragment made by VEGF involve two residues displayed from the N-terminal helix α1 (43 Å², or 5%) and two residues from the loop connecting α2 to β2 (53 Å², or 6%; Figure 4).

Of the six CDRs of the antibody, L1 and L2 are not in contact with VEGF. In the remaining CDRs, a total of 25 residues participate in binding, resulting in the following buried surface areas: 68 Å² (8%) for L3, 125 Å² (15%) for H1, 222 Å² (27%) for H2, and 420 Å² (50%) for H3 (Table 2).

Figur 3

Schematic representation of the binding epitope of VEGF for the humanized anti-VEGF antibody. Residues buried in the interface as seen in the crystal structure are colored red; residues marked with yellow display a greater than 20-fold reduction in binding affinity when changed to alanine. For comparison, and to allow discussion of the neutralizing effect of the antibody, residues buried in the interface between VEGF and domain 2 of the Flt-1 receptor [16] are colored blue, and VEGF binding determinants for KDR [15] are in green. The position of the twofold axis of the VEGF dimer is indicated by a black ellipse.

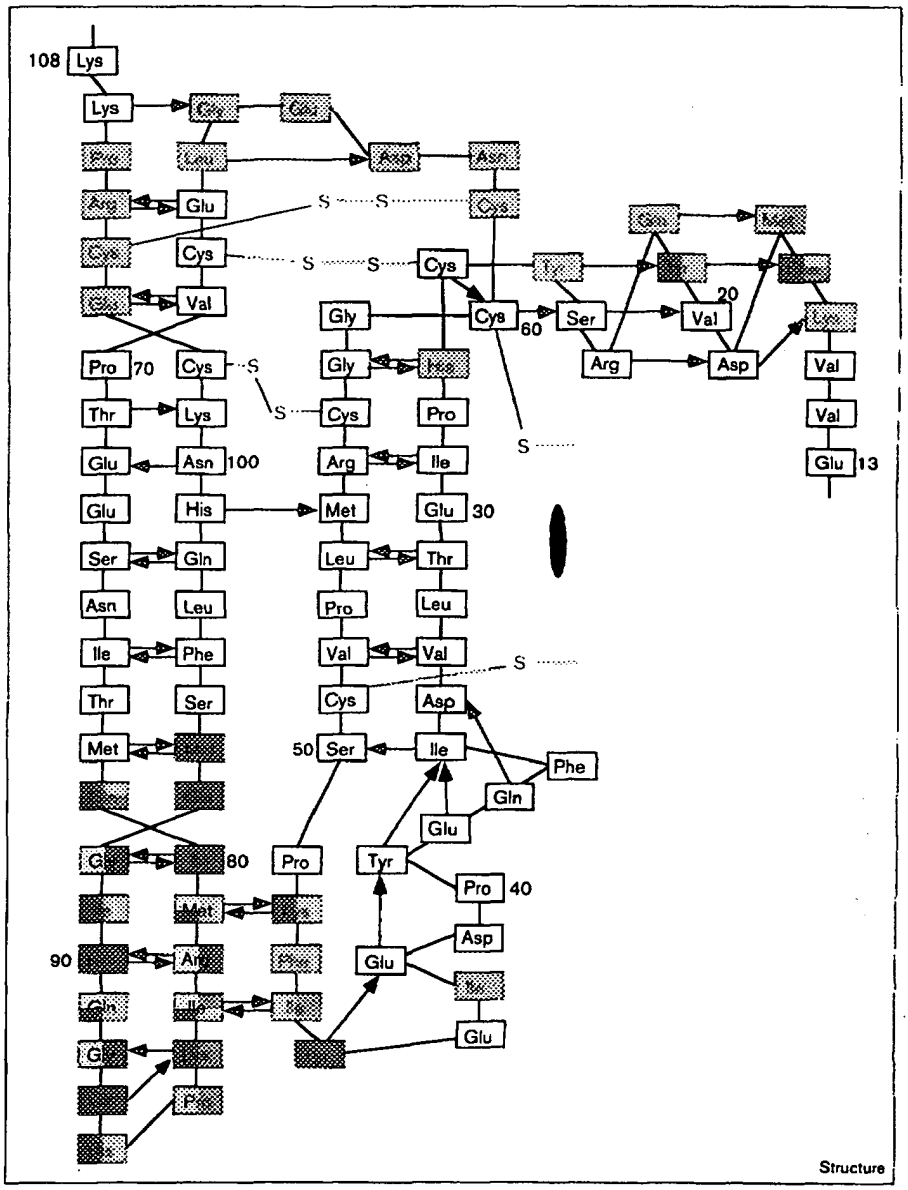

The total buried surface area of 1744 Å^2 is typical of that observed for other Fab fragments bound to protein antigens [32,33]. The CDR usage conforms to the generalization that L2 is often not required for binding, while L3 and H3 are always involved [28,34]. Usually, CDRs of the heavy chain contribute a greater amount of buried surface than those of the light chain [32,34]. The ratio observed for the VEGF–Fab complex, however, with only 8% contributed by the light chain and 92% by the heavy chain, appears extreme.

The CDRs form a shallow cleft on the surface of the antibody. The walls of the cleft are formed by L3 and H3 on one side, and H1 and H2 on the opposite side. With the exception of His86, residues 86–94 of VEGF strand β6 are bound in an almost extended conformation along the floor of the cleft. His86 is at position i+2 of the type II β turn [35] that connects strand β5–β6. Adjacent to this histidine, a β bulge is formed between Gln87 and Gly88 of strand β6 and Lys84 of the adjacent strand, β5 (Figure 3). Residues 89–94 form a total of five main-chain–mainchain hydrogen bonds with the Fab fragment. Residues 89–91 are hydrogen bonded to residues 33–31 of CDR H1, forming a short antiparallel β ladder; a short parallel β ladder is formed between VEGF residues 91–93 and Tyr98–Gly100 of CDR H3. No mainchain–mainchain interactions with the Fab fragment are observed for residues 86–88.

Table 2

Alanine-scanning analysis f th Fab phage.

	V_L-residue number	IC_{50}(mutant)/ IC_{50}(wt)*	Buried area (Å²)		V_H-residue number	IC_{50}(mutant)/ IC_{50}(wt)*	Buried area (Å²)
L1	Arg24	1.3	0	H1	Gly26	2.3	0
	Ala25Ser	1.1	0		Tyr27	34 (44†)	0
	Asn26	1.5	0		Thr28	1.3	0
	Glu27	1.2	0		Phe29	16	0
	Gln28	1.2	0		Thr30	1.3	4
	Leu29	1.4	0		Asn31	>150	86
	Ser30	1.5	0		Tyr32	>150	24
	Asn31	1.7	0		Gly33	6.1	11
	Tyr32	1.9	0		Met34	6.3	0
	Leu33	2.2	0		Asn35	66	0
	Asn34	3.7	0				
				H2	Trp50	>150	53
L2	Phe50	1.4	0		Ile51	3.8	0
	Thr51	0.78	0		Asn52	>150	35
	Ser52	0.75	0		Thr52A	8.6	2
	Ser53	0.76	0		Tyr53	8.7 (9.4†)	96
	Leu54	0.86	0		Thr54	4.4	7
	His55	0.98	0		Gly55	1.1	0
	Ser56	0.85	0		Glu56	1.7	0
					Pro57	1.5	0
L3	Gln89	3.7	0		Thr58	2.6 (4.2†)	29
	Gln90	2.7	0		Tyr59	2.0	0
	Tyr91	14	3		Ala60Ser	1.2	0
	Ser92	0.90	11		Ala61Ser	1.4	0
	Thr93	0.87	2		Asp62	1.4	0
	Val94	1.5	34		Phe63	0.97	0
	Pro95	3.5	0		Phe64	1.2	0
	Trp96	>150	18		Arg65	1.2	0
	Thr97	1.4	0				
				H3	Tyr95	150 (1800†)	13
					Pro96	38	14
					His97	4.1	56
					Tyr98	3.8	122
					Tyr99	4.6	36
					Gly100	1.8	39
					Ser100A	0.7	3
					Ser100B	>150	42
					His100C	2.4 (3.8†)	2
					Trp100D	>150	93
					Tyr100E	19	0
					Phe100F	25	0
					Asp101	1.9	0
					Val102A	1.3	0

*The IC_{50} measurements showed an average error of ~25%. †K_d(mutant)/K_d(wt) by BIAcore; wild type (Y0192) Fab shows an association rate of $4.1 \times 10^4\ M^{-1}\ s^{-1}$ and a dissociation rate of $1.4 \times 10^{-4}\ M^{-1}\ s^{-1}$, yielding a K_d(wt) of 3.4 ± 0.9 nM.

The most prominent structural feature of the interface is the burial of Gly88 of VEGF in a deep pocket on the surface of the antibody-combining site (Figure 5). This pocket is best described as a four-walled box with each wall being made of the sidechain of a single aromatic residue, namely residues Trp96 of CDR L3, Trp50 of H2, and Tyr95 and Trp100D of H3. Gly88 of VEGF is sandwiched between the sidechains of Trp50 of CDR H2 and Trp100D of H3. As a result, its phi and psi angles are ~180°. In addition, hydrogen bonds are formed between Gln87 O of VEGF and Tyr95 Oη of CDR3 H3, as well as between Tyr95 Oη of H3 and Trp96 Nε1 of L3. A similar molecular box contains Gly92 of VEGF, which is sandwiched between His97 and Tyr98 of CDR H3 and nearby residue, Tyr32 of CDR H1. Again, the mainchain torsion angles of Gly92 of VEGF are ~180°.

No salt bridges are found at the interface, but several sidechain-mediated polar interactions are present. The sidechain of Gln89 of VEGF is hydrogen bonded to Thr30 O and Thr52A NH of CDRs H1 and H2, respectively. The sidechain of His90 of VEGF is buried in a small pocket formed by Pro96, Tyr98, Ser100B and Trp100D of CDR H3. His90 Nε2 of VEGF is hydrogen

Tabl 3

Alanine-scanning analysis f VEGF.

VEGF residue	IC_{50}(mutant)/ IC_{50}(wt)*	Buried area (Å²)	Fab residues within 4.5 Å†
Phe17	2.4	26	V_H: Asn31
Tyr21	2.5	17	V_H: Tyr53
Tyr45	4.5	29	V_H: Ser100B, Trp100D
Phe47	1	0	
Lys48	2.2	24	V_H: Tyr53
Gln79	5.6	13	V_H: His97
Ile80	2.6	1	V_H: Tyr98
Met81	74	36	V_H: Thr30, Asn31, Tyr53
Arg82	22	55	V_H: Tyr98, Gly100, Ser100A,Ser100B
Ile83	35	32	V_H: Asn52
Lys84	7.8	12	V_H: Trp100D
His86	2.3	74	V_L: Val94; VH: Trp50, Thr58
Gln87	1.4	115	V_L: Ser92, Val94, Trp96 V_H: Trp50, Tyr95, Trp100D
Gly88	40	37	V_H: Trp50, Tyr95, Trp100D
Gln89	102	131	V_H: Thr30, Asn31, Tyr32, Gly33, Trp50, Ile51, Asn52, Thr52A, Tyr53, Tyr95, Trp100D
His90	1.7	115	V_H: Asn31, Tyr32, Tyr95, Pro96, Tyr98, Ser100B, His100C, Trp100D
Ile91	3.5	75	V_H: Asn31, Tyr32, Pro96, His97, Tyr98
Gly92	107	32	V_H: His97, Tyr98
Glu93	4.9	79	V_H: His97, Tyr98, Tyr99, Gly100
Met94	5.0	5	V_H: Tyr98

*The IC_{50} measurements showed an average error of about 25%. All mutants with fivefold or more decreased affinity for mAb A4.6.1 bound within twofold of wild-type affinity to mAb 32.E.1 (data not shown), which has a separate, dimer-dependent binding epitope [15]. †Fab residues underlined are those with a more than 150-fold decrease in affinity to VEGF, when changed to alanine (see Table 2).

bonded to Ser100B Oγ of H3. In addition, Ser100B Oγ is hydrogen bonded to the guanidinium group of Arg82 of VEGF. The interface does not contain any ordered water molecules, although a number of waters mediating polar interactions between VEGF and the antibody are found at the periphery of the combining site. A sulfate ion was located in close proximity to the combining site. The sulfate is hydrogen bonded to Thr28, Asn31 and Tyr32 of CDR H1 of the Fab fragment, but there are no direct interactions with VEGF (an indirect interaction with the sidechain of Gln79 of VEGF is mediated by a water molecule). We believe that the presence of the sulfate is a crystallization artifact.

Alanin scanning of th interface

In order to assess the relative importance of the contact residues at the interface, a number of mutants, each with a single residue changed to alanine, were generated for both VEGF and the Fab fragment. For the anti-VEGF Fab, the contributions of all 68 sidechains within the six CDRs were assessed by individual mutation of pY0192 Fab-phage (Figure 6) residues to alanine (or to serine for wild-type alanines). Relative binding affinities to VEGF were measured in competitive monovalent phage enzyme-linked immunoabsorbant assays (ELISAs) (see Materials and methods section). The IC_{50} (the concentration of competitor at which 50% inhibition of binding is observed) of the wild-type Fab phage for VEGF was measured at 4.7 ± 1.1 nM, comparing favorably to the measured K_d of 3.4 ± 0.9 nM for the purified wild-type Fab using BIAcore. The use of phage-ELISA techniques for measurement of binding affinities greatly facilitated the scanning of CDR residues. In order to assess the accuracy of this method, five alanine variants representing a wide range of apparent binding affinities by phage-ELISA were tested in a BIAcore assay in addition to the wild type. Within the uncertainties of each technique (±25%) excellent agreements are observed between both methods (Table 2), showing that the phage-ELISA technique can provide accurate measurements of relative binding affinities.

The alanine-scan phage variants displayed a range of affinities, from that of wild type to > 700 nM; all variants showed some VEGF-specific binding (Table 2). In particular, large decreases in affinity (> 150-fold, $-\Delta\Delta G$ > 3 kcal/mol) resulted primarily from substitution of residues located within the heavy-chain CDRs: Asn31 and Tyr32 in H1; Trp50 and Asn52 in H2; and Tyr95, Ser100B, and Trp100D in H3. Among the light-chain CDR residues, only substitution of Trp96 produced so great an effect. Together, these positions define the primary functional sidechain-binding determinants. Less severe reductions in affinity (5–70-fold, $-\Delta\Delta G$ = 1–2.5 kcal/mol) resulted from alanine substitutions at Tyr27, Phe29, Gly33, Met34, and Asn35 of H1, Thr52A and Tyr53 of H2, Pro96, Tyr99, Tyr100E, and Phe100F of H3, and at one light-chain position, Tyr91 of L3. Smaller, but significant, reductions in affinity (2–5-fold, $-\Delta\Delta G$ = 0.4–1 kcal/mol) were also observed at many positions of the heavy-chain CDRs, including those at residues 26, 51, 54, 58–59, 97–98, 100C and 101, as well as at positions 32–34, 89–90, and 95 in the light-chain CDRs. The remaining CDR mutations, including those at the sites of expression-associated mutations Ser24Arg, Ser26Asn, Gln27Glu, Asp28Gln, and Ile29Leu in CDR L1 (see Materials and methods section), showed no significant effect upon VEGF binding affinity. Overall, the results suggest that a large energetic contribution to the Fab–VEGF interaction stems from a subset of CDR residues in H1, H2, and H3, with some contribution from L3.

The mutagenesis analysis of VEGF showed that 12 of the 19 alanine mutants tested displayed at least a fivefold decrease in binding to mAb (murine antibody) A4.6.1

Figure 4

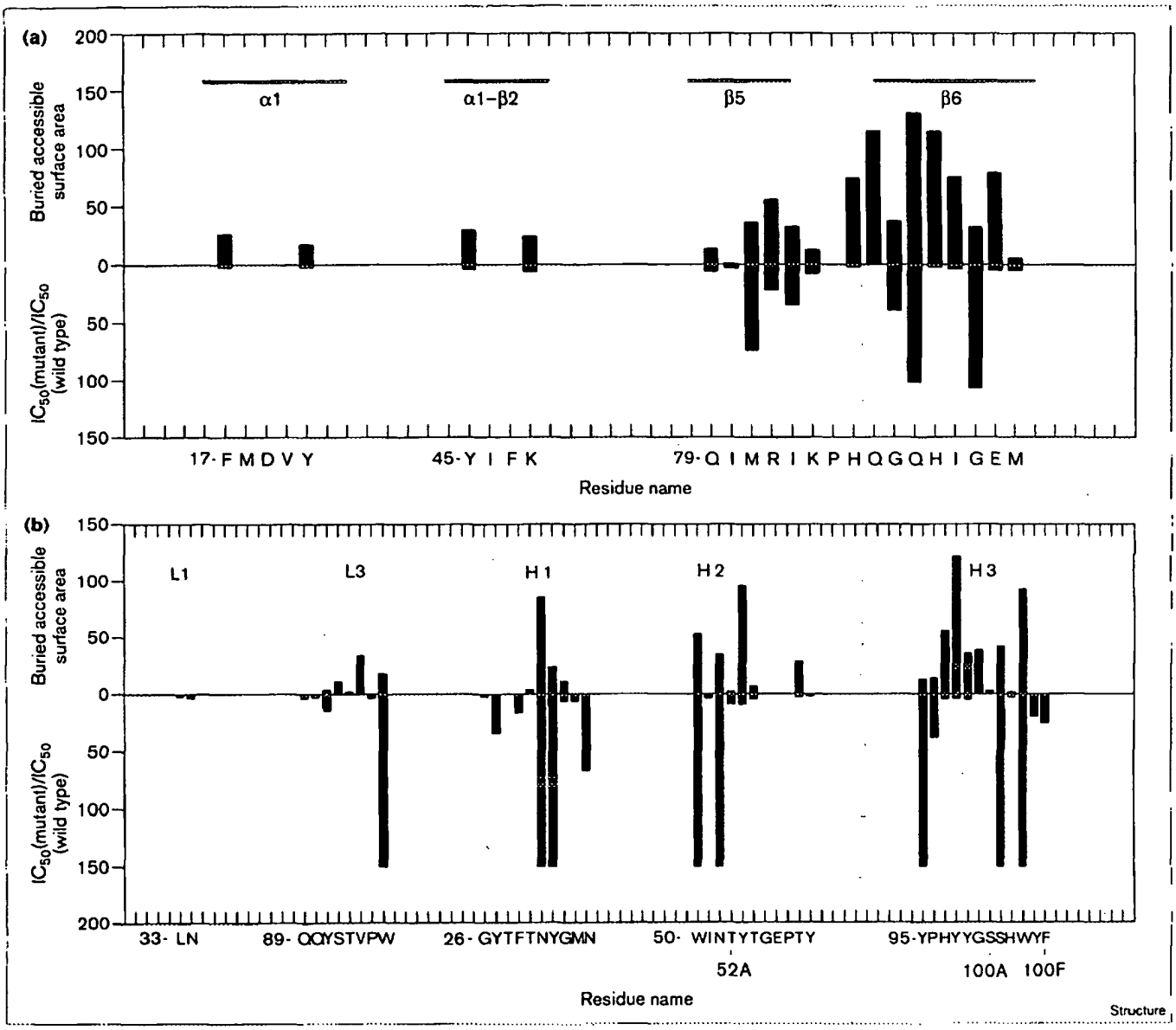

Comparison of accessible surface area buried in the VEGF–Fab interface and contributions of individual residues to the antibody binding as identified by alanine-scanning mutagenesis: **(a)** residues from VEGF, **(b)** residues from the anti-VEGF Fab.

(Table 3). Six of these mutants showed dominant effects, and reduced binding by factors of 22–107 fold (Table 3). These six residues are localized primarily within the 12-residue segment of VEGF that contains strands β5 and β6 along with the intervening β turn. Mutants of Met81, Arg82, Ile83, Gly88, Gln89, and Gly92 showed 74-, 22-, 35-, 40-, 102- and 107-fold ($-\Delta\Delta G$ = 2–3 kcal/mol) decreases in affinity, respectively, relative to the wild type. Smaller, but significant, decreases in binding of about 5–8 fold ($-\Delta\Delta G$ = ~1 kcal/mol) were found for mutations at positions 48, 79, 84, 93 and 94. The overall structural integrity of the alanine mutants with a fivefold or greater effect on mAb A4.6.1 binding was confirmed using a similar ELISA that measured binding affinity of the mutants to mAb 32.E.1, which has a separate, dimer-dependent, binding epitope [15].

Discussion

Antig n–antibody interface

A total of 25 residues of the Fab fragment become buried in the antigen–antibody interface upon binding to VEGF, together constituting the structural epitope. Eight of these residues are critical for binding, as defined by greater than 150-fold decreases in binding upon alanine substitution

Figure 5

Stereoviews of the interface between VEGF and the anti-VEGF Fab. For clarity, the only VEGF residues shown are those in segment β5–β6. **(a)** Surface of the antibody combining site and stick representation of segment β5–β6 of VEGF. The molecular surface of the light chain and heavy chain are shown in grey and blue, respectively. Residues of anti-VEGF critical for binding are shown in magenta. The termini and VEGF residues critical for binding are labeled. **(b)** Atomic detail of the antibody combining site using the same color coding as in (a). For simplicity, the mainchain of the anti-VEGF Fab is shown as a continuous ribbon. Illustrations drawn with the program GRASP [55].

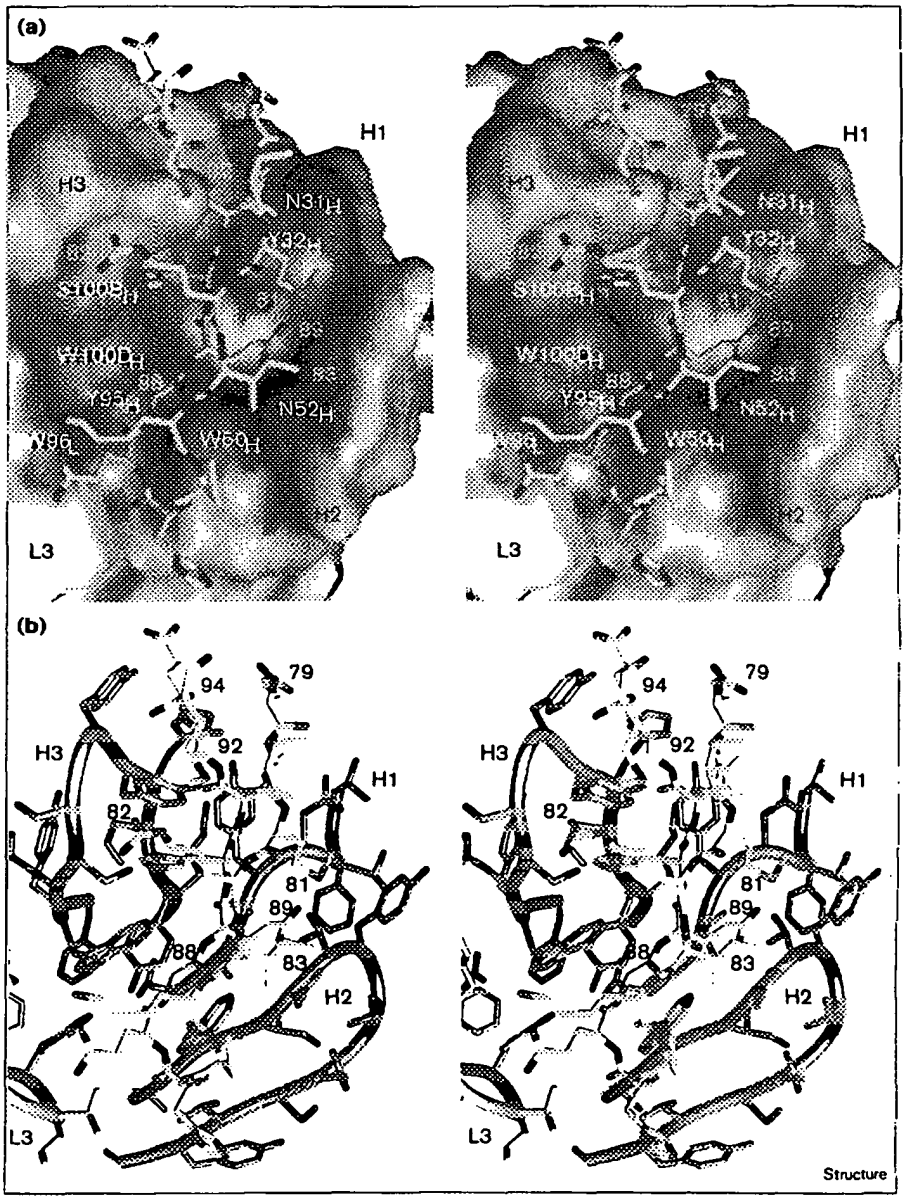

(Table 2), and form the functional epitope of the Fab fragment. Together, these eight residues contribute 360 Å^2 (44%) to the surface area buried in the interface. Five residues are aromatic, the remaining three being two asparagines and a serine. The high proportion of aromatic residues, in particular tyrosine and tryptophan, is a feature of the entire structural epitope, for which 11 residues are aromatic out of total number of 25. This bias has been noted before and reflects a general property of antibody combining sites [23,32,36].

On VEGF, the functional epitope is dominated by six residues; most important are Met81, Gln89 and Gly92, substitution of which reduces affinity by about 70–110 fold. Slightly smaller, but still large, contributions (22–40-fold effects) are made by Arg82, Ile83, and Gly88. In general, alanine-scanning mutagenesis provides a useful method of assessing the relative contributions of individual side-chains to the binding energy [37]. Results at glycine positions are less meaningful, however, because substitution to alanine introduces a stiffening of the protein backbone and requires additional space to accommodate the additional Cβ atom, without providing information on the contribution of the wild-type residue to the free binding energy of the complex. In the case of the VEGF–Fab complex, the structure shows that steric hindrance is likely to be the cause of the decreased affinity of the glycine to alanine mutants at positions 88 and 92.

Figure 6

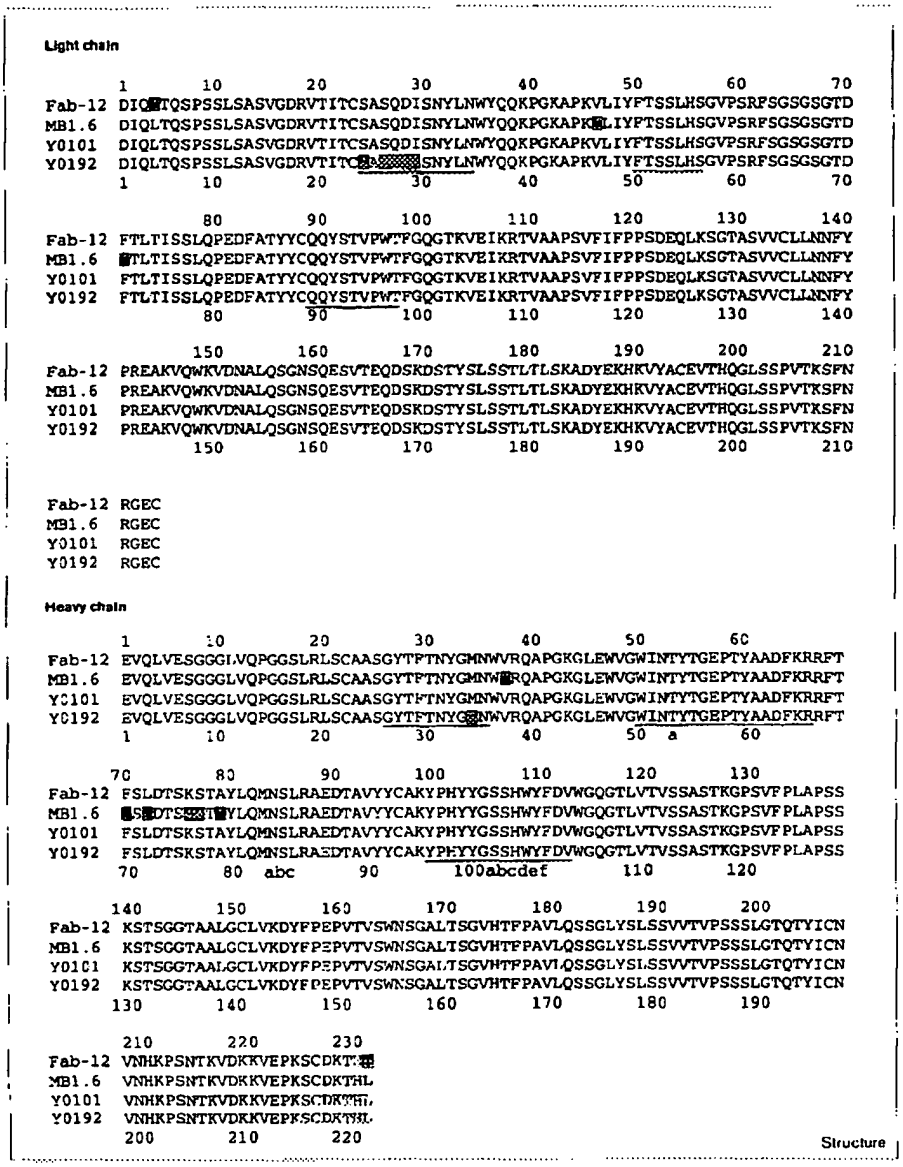

Sequence comparison of anti-VEGF Fab variants. Variant Fab-12 is a previously described humanized version of the murine antibody A4.6.1 [8]. Variant MB1.6 was isolated from an earlier Fab-phagemid library [7] and used to produce a Fab phagemid, called pY0101, similar to Fab-12. Variant Y0192, an expression-optimized derivative of Y0101 (see Materials and methods section for details), was used for the alanine-scanning mutagenesis described here. Residues are numbered sequentially (top) and according to Kabat *et al.* [56] (bottom). CDR regions are underlined. Residues unique to the respective sequences are indicated by shaded boxes.

The direct juxtaposition of important binding determinants from both functional epitopes is striking (Tables 2 and 3). The six dominant binding determinants of VEGF are in intimate contact with the Fab fragment (Figure 4a). The main structural feature is the binding of Gly88 of VEGF through the aromatic box formed by the sidechains of residues Trp96 of CDR L3, Trp50 of CDR H2, and Tyr95 and Trp100D of CDR H3 (Figure 5). In this case, considering the functional importance of both the glycine and the surrounding Fab residues, the direct interactions between the glycine and the box appear to provide significant binding energy. In contrast, for the aromatic box surrounding Gly92 of VEGF, none of the sidechains of the Fab residues is crucial for binding. The structure shows that in this case substitution with alanine is likely to interfere with the formation of the numerous mainchain–mainchain hydrogen bonds observed across the interface at this position. Thus, the steric requirements of this region are likely to be critical for maximum affinity. Additional juxtapositions of important binding determinants are Met81 of VEGF and Tyr53 of H2, Arg82 of VEGF and Ser100B of H3, and Ile83 of VEGF and Asn52 of H2. Although no simple favorable interaction is observed for Ile83 of VEGF, its sidechain is in close contact to a critical CDR H2 residue, Asn52. Finally, the sidechain of VEGF Gln89 is involved in a number of hydrogen bonds with mainchain atoms of CDRs H1 and H2.

From the data presented here, the functional VEGF epitope for Fab binding appears to be rather small. Similar

Figure 7

Stereo representation illustrating the conformational change in strand β6 induced by the antibody upon binding to VEGF. The geometrically averaged Cα backbone calculated from the eight monomers present in the triclinic crystal form of free VEGF is shown in red. At each Cα position, the smallest ellipsoid that fits all Cα atoms of the eight monomers is displayed (calculated with program GEM [57]). The backbone conformation of strands β5–β6 as observed in the VEGF–Fab complex is shown in green. Although for most of the residues involved in binding the observed backbone conformation represents one out of the ensemble of eight structures observed in free VEGF, significant deviations occur for His90 and Gly92, whose Cα positions differ by more than 7.9σ and 10.6σ, respectively, from the positions in the ensemble.

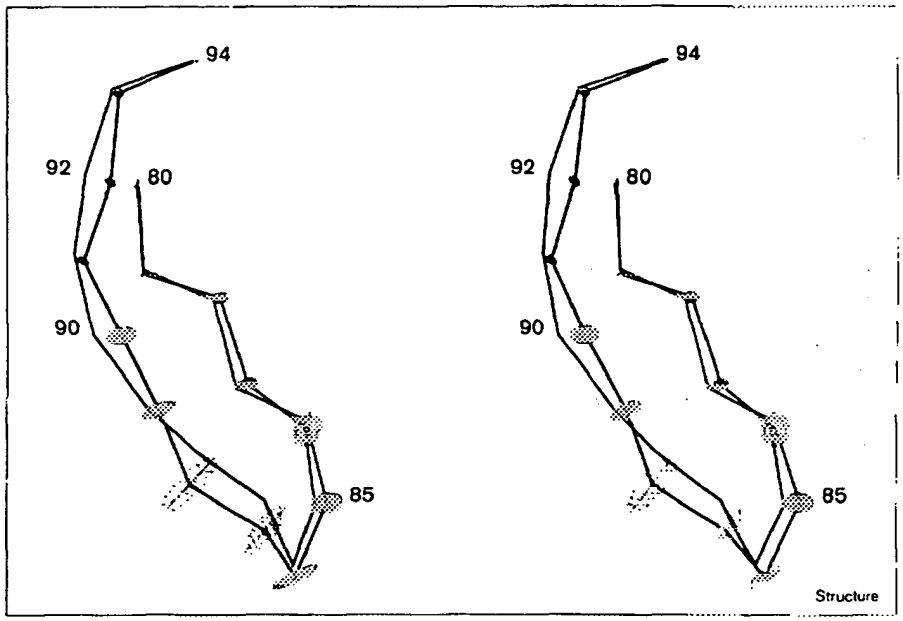

small binding epitopes have been deduced from theoretical considerations for the binding of lysozyme to two different antibodies, D1.3 and HyHEL-5 [38]. These calculations have been corroborated partially by competition studies with homologous avian lysozymes [39]. The size of the functional epitope identified for the anti-VEGF Fab fragment is similar to that identified for the humanized anti-p185^{HER2} antibody [18], using the same method. In this case, however, both the functional epitope of the antigen and the crystal structure of the complex are missing. In the case of anti-p185^{HER2}, a set of only four important binding determinants were identified, namely $His91_{VL}$, $Arg50_{VH}$, $Trp95_{VH}$ and $Tyr100A_{VH}$ [18]. Here, too, aromatic residues prevail and the binding determinants cluster in a shallow pocket on the antibody surface.

General similarities exist between the VEGF–Fab interface and other protein–protein interactions. The interaction between human growth hormone and its receptor has been investigated using the same methods as described here, that is, structure determination of the complex [40,41] and exhaustive alanine-scanning mutagenesis of the binding partners [37,40,42]. In this case, of 32 hormone residues in contact with the receptor, only five contribute most of the binding energy; these are in contact with the five most important residues of the receptor, resulting in a remarkable degree of functional complementarity between the two epitopes [19]. From these studies, it was proposed that only a small subset of the residues buried in a protein–protein interface may be the principal contributor to the binding energy; in the growth hormone example, these residues are clustered together in a small hydrophobic patch surrounded by polar interactions. A similar situation was observed in an analysis of the interaction between tissue factor and coagulation factor VIIa [43,44], where, again, only a small subset of residues contribute most to ligand affinity. In this case, however, these residues form several discontinuous clusters on the protein surface.

In most complexes between protein antigens and antibodies, a number of well-ordered water molecules are found within the combining site [45]. It has been proposed that water molecules are required in order to overcome imperfections in shape complementarity and that such imperfections are characteristic of protein–antibody interactions, possibly because, in contrast to other protein–protein interactions, antigen recognition has not been optimized through evolution, but rather depends on rapid selection pressure [33]. In the case of VEGF, no water molecules are buried in the antigen–Fab interface, and excellent complementarity is observed between segment β6 of VEGF and the combining site. Furthermore, the observation that in the complex the temperature factors of VEGF segment β5–β6 (Figure 2) are very similar to those of the variable domains of the antibody and considerably lower than the rest of VEGF suggests tight packing of the interface. It is worth noting that in the complex of VEGF with domain 2 of its Flt-1 receptor, a channel of water molecules is found in the interface [16]; similar water clusters have also been observed in the growth hormone–receptor interface [40]. Thus, water-mediated contacts are not specific to interfaces between antibody and antigenic protein. With respect to these findings, a remarkable similarity

is observed between the antibody–antigen recognition reported here and protein–protein interactions in general.

Conformational change upon binding

In addition to the crystal structure of the VEGF–Fab complex, the structure of unbound VEGF is also known [12,15]. The triclinic crystal structure contained eight independent copies of the molecule in the asymmetric unit, and superposition of the eight molecules made possible the identification of the conformationally flexible portions of the molecule. The highest deviations were observed within segment β5–β6, and it was shown that the eight conformations represent different 'snapshots' of a concerted 'up and down' loop movement [12]. In the Fab complex, this same segment is intimately involved in antibody binding. Superposition of this segment, as observed in the complex, onto the conformations seen in unbound VEGF shows that, overall, the bound conformation fits well within the range of conformational freedom observed in the unligated structure (Figure 7). Two of its Cα positions do not, however, fall within the range of conformational flexibility of the unbound state. The Cα of VEGF His90 is displaced by 1.3 Å; this corresponds to a 7.9σ movement when considering the standard deviation of the distance deviations among the eight monomers in unligated VEGF. Similarly, a 1.2 Å (10.6σ) displacement is observed for the Cα of VEGF Gly92 (Figure 7). We conclude that the anti-VEGF antibody selects one of the available multiple conformations of this loop upon binding, while inducing small but significant local changes at positions 90 and 92.

The neutralizing effect of anti-VEGF antibody

Binding of VEGF by the anti-VEGF antibody prevents the growth factor from binding to its receptors. The overall structure of residues 8–109 of unbound VEGF is identical to that in the complex with the Fab fragment, demonstrating that the neutralizing effect is not the result of antibody-induced conformational changes in the ligand preventing receptor binding. Recently, we determined the crystal structure of residues 8–109 of VEGF in complex with domain 2 of Flt-1 [16]. A comparison of both structures clearly explains the neutralizing effect of the antibody — of the 19 VEGF residues contributing to the interface in the VEGF–Fab complex, nine are also buried in the interface with domain 2 of Flt-1. It is worth noting that, of these, only a single residue, namely Ile83, is an important binding determinant for both the antibody and the receptor (Figure 3). The neutralizing effect therefore appears to be due to steric hindrance, and not due to competition for the same critical binding determinants.

Biological implications

A comparison of the structure of the VEGF–Fab complex with other antigen–antibody complex structures reveals that the binding mode of VEGF resembles that of linear peptides more closely than that of protein antigens. Whereas peptides are predominantly bound within deep grooves, protein antigens tend to interact at the periphery of the CDRs via a relatively flat surface [46]. Peptides bind predominantly in an almost extended conformation, usually with a β turn next to the terminus [28]. In VEGF, this motif corresponds to strand β6 together with the preceding type II β turn formed by residues Lys84–Gln87. A somewhat similar situation was observed in the recent crystal structure of the N-terminal domain of the interferon-γ receptor α chain in complex with Fab-A6 [23]. Here, too, most of the interactions of the Fab fragment (80%) are with a single continuous loop segment of the receptor, and additional segments make less extensive contributions, generating a discontinuous binding epitope.

Jones and Thornton [33] have shown that interfaces in nonpermanent and nonobligatory complexes, such as antigen–antibody and hormone–receptor interfaces; have smaller interaction surfaces, lower packing densities and involve more polar interactions than seen in permanent complexes that do not exist as independent entities, such as dimeric molecules. Our results on the VEGF–antibody and VEGF–receptor complexes are in agreement with this analysis. The principal difference we observe is the significant extent of fragmentation of the structural binding epitope in the latter, with fewer segments being involved for antigen–antibody interfaces [33]. This difference is even more pronounced when looking at the functional epitope, instead of the structural epitope. In VEGF the important residues all cluster within the continuous segment β5–β6; similar localization of binding determinants is observed for a second neutralizing antibody whose functional epitope resides primarily on helix α1 [15]. In contrast, the binding determinants of VEGF for kinase domain receptor (KDR) are distributed over four different segments [15].

Materials and methods

Complex formation and crystallization

Residues 8–109 of VEGF were expressed, refolded, and purified as previously described [20]. Purified Fab-12 fragment was obtained from Pat McKay (Process Sciences, Genentech, Inc.), mixed with VEGF in a 2.1:1 molar ratio, and purified by size exclusion chromatography (S-200, Pharmacia) in 30 mM Tris-HCl, pH 7.5, 0.4 M sodium chloride. The composition of the resulting complex was verified by SDS PAGE and size exclusion chromatography (data not shown). The protein solution was concentrated to $A_{280} = 7.8$, and used in crystallization trials. Initial hanging-drop experiments using the vapor-diffusion method resulted in isomorphous crystals from two different conditions (15% PEG, 10% isopropanol, 0.2 M ammonium sulfate, 0.1 M MES, pH 6.0; and 2 M ammonium sulfate, 2% MPD, 0.1 M bis-tris-propane, pH 6.5). Crystals used in the structure determination were grown from large sitting drops by equilibrating a mixture of 20 µl protein solution and 20 µl reservoir solution (15% PEG, 10% isopropanol, 0.2 M ammonium sulfate, 0.1 M MES, pH 6.0) against 30 ml reservoir solution. Monoclinic crystals grew to a size of 0.1 mm × 0.2 mm × 0.5 mm in 2–3 weeks. The crystals were

cryoprotected by dipping in 100 µl drops of reservoir solution containing increasing concentrations of glycerol (first 5%, then 10%, then 20%), after which they were flash frozen in liquid nitrogen.

Data collection

A data set to 2.4 Å resolution was collected from two flash-frozen crystals at beamline A1 at the Cornell High Energy Synchrotron Source using a charge-coupled device detector (Area Detector Systems Corp., San Diego) and a wavelength of 0.914 Å. The crystals belonged to space group $P2_1$ with cell parameters a = 89.86 Å, b = 66.98 Å, c = 140.51 Å and β = 94.27°. For each of the two crystals, a low- and a high-resolution pass were recorded and processed independently with the programs DENZO and SCALEPACK [47]. The final data set, obtained after merging 240,859 observations of the individual data sets, contained 63,147 unique reflections (average redundancy = 3.8) and was 96% complete in the resolution range 20–2.4 Å ($R_{Merge}(I) = 7.1\%$).

Structure determination and refinement

The structure of the VEGF–Fab complex was solved by molecular replacement. Taking into consideration the inherent twofold symmetry of the VEGF dimer, we expected that one VEGF dimer would be bound to two Fab molecules. Because of the absence of a crystallographic twofold rotation axis, the molecular dyad had to be noncrystallographic; thus the asymmetric unit would contain one VEGF dimer and two Fab fragments, yielding a Matthews parameter of 3.6 $Å^3$/Da and a solvent content of 66%.

Rotation functions were calculated using a VEGF dimer as a search model ([12]; Brookhaven Protein Data Bank [PDB] accession code 2vpf). The crystal structure of a humanized anti-HER2 Fab fragment, anti-$p185^{HER2}$ ([27]; PDB accession code 1fvd), which had an 88% identical humanization framework [8,26], was used as a model for the Fab portion. In order to avoid bias, the CDRs were removed from the model and a tryptophan residue was substituted by alanine for additional verification purposes. A rotation search and Patterson correlation refinement [48] using the program XPLOR [49] yielded four distinct peaks for the VEGF dimer with correlation coefficients of 5.3–4.9%, while the subsequent highest peaks were below 4.3%. These four peaks correspond to two different candidate rotation solutions, pairs being related by the VEGF molecular dyad. Translation searches did not allow us to identify the correct solution.

With the Fab model, rotation searches calculated with data between 8 and 4 Å resolution, allowing the elbow angle [28] to vary between 110° and 210° in 10° steps yielded one (instead of two) unambiguous solution with a correlation coefficient of 9.8%, with the next peak at 5.6%. The pre-oriented Fab fragment could be readily translated into the unit cell with the program AMORE [50], and translation of the VEGF dimer with the Fab fragment fixed yielded an unambiguous solution for the highest of the two distinct VEGF rotation-solution candidates (R = 48.3% and correlation coefficient = 30.8%). Inspection of this solution with the program O [51] showed that the Fab CDRs would be in contact with VEGF, verifying the correctness of this partial solution, but the absence of any crystal packing contacts in one direction demonstrated that this model was still incomplete.

At this stage, refinement of the partial model was initiated. After rigid-body refinement followed by positional refinement with the program XPLOR [49] using all data between 10 and 3.0 Å resolution (R = 43.8%), clear electron density was observed for the omitted CDRs and tryptophan sidechain in a σ_A-weighted $(2F_o-F_c)\exp(i\alpha_c)$ electron-density map [21]. After several rounds of positional refinement and manual rebuilding with the program O [51], all the CDRs of the Fab fragment could be built with confidence. Clear electron density emerged for the variable part of the second Fab molecule, related to the first Fab fragment via the molecular dyad of the VEGF dimer. After inclusion of this variable fragment, further positional refinement between 10 and 3.0 Å resolution yielded a crystallographic R value of 31.9% (free R value = 38.0%) and maps into which the missing constant domain of the second Fab molecule was positioned, although clear density was only visible for those parts in immediate contact with the variable part of the molecule. Noncrystallographic symmetry restraints were applied in all further refinement, while gradually increasing the resolution to 2.4 Å, refining restrained individual temperature factors, and adding water molecules. At a late stage the structure factors were corrected for observed anisotropy, yielding the final model with a crystallographic R value of 19.6% (free R value = 26.6%) between 8 and 2.4 Å resolution. No bulk solvent correction was applied.

The final model is unusual with respect to the high average temperature factor of 100 $Å^2$ of the constant domain of the second Fab molecule. The use of noncrystallographic symmetry restraints forces this portion to be similar to the well-defined constant domain of the first Fab fragment. Therefore, although this domain contributes only weakly to the overall scattering and is thus poorly defined by the observed data, it could be accurately modeled because of the presence of the second identical and well-defined copy.

Construction of humanized anti-VEGF Fab phage

A monovalent, humanized Fab phagemid for alanine-scanning analysis was constructed by mutation of clone pMB16 (Figure 6), derived from phage humanization of the mAb A4.6.1 [7], to include additional substitutions identified in an optimally humanized variant of Fab-12 [8]. Mutations were made by site-directed mutagenesis [52], and verified by Sequenase (US Biochemical) sequencing. The new variant, pY0101 (Figure 6), contained the Fab-12 sequence, except for mutations Met4Leu in V_L and Thr231Leu in V_H. The former was retained from pMB16 in order to preclude possible methionine oxidation, and the latter was retained in order to retain the original junction (with amber codon for soluble Fab or Fab-g3p expression) sequence to the C-terminal domain of M13 g3p [7]. The Fab phagemid pY0101 was used for initial expression and affinity enhancement experiments in which the V_{L1} CDR residues 24 and 26–29 were randomized. Five codons in V_{L1} of pY0101 were first converted to stop (TAA) codons using the oligonucleotide 5′-GG GTC ACC ATC ACC TGC TAA GCA TAA TAA TAA TAA AGC AAC TAT TTA AAC TGG-3′. After verifying the stop-codon template by sequencing, a library was constructed by mutagenesis with a degenerate oligonucleotide (NNS replacing TAA codons). Fab-phage variants were propagated overnight in XL1-Blue *Escherichia coli* cells (Stratagene), then precipitated and sorted as described in [53]. VEGF binding selections yielded no affinity improvements compared with pY0101; however, one variant, pY0192 (Figure 6), was identified with a marked improvement in expression over pY0101. This clone, containing light chain mutations Ser24Arg, Ser26Asn, Gln27Glu, Asp28Gln, and Ile29Leu, as well as one heavy chain mutation Met34Ile, was used as the background for subsequent alanine-scanning mutagenesis. Each alanine substitution (or serine substitution for wild-type alanine) was constructed by site-directed mutagenesis and verified by DNA sequencing as described above.

VEGF binding assays using Fab-phage ELISA

Phage ELISA assays were performed and used to derive IC_{50} values as described [53]. Immunosorbant plates (Maxisorp plates, Nunc Intermed) were coated overnight at 4°C with 2 µg/ml VEGF in 50 mM carbonate buffer and blocked with 5% instant milk. For normalization of phage concentrations, serial dilutions of Fab phage were made in parallel in ELISA buffer (0.5% bovine serum albumin, 0.05% Tween-20 in phosphate-buffered saline (PBS) and incubated for 1 h at room temperature with immobilized VEGF. Plates were washed, incubated for 1 hour with rabbit anti-phage serum and horse radish peroxidase-conjugated goat anti-rabbit antibody (Pierce), washed again and developed with o-phenylenediamine substrate (Sigma). Normalized, subsaturating concentrations of phage for all Fab variants, as well as wild-type (pY0192), were mixed with serial dilutions (200 nM–0 nM) of VEGF in triplicate. The mixture was then added to VEGF-coated plates and analyzed as described above to determine an IC_{50} for each variant.

BIAcore analysis of Fab binding affinities

Y0192 Fab and several Fab variants were prepared by expression from the Fab-phagemid constructs by transforming the phagemids into a non-suppressor strain of *E. coli* [7]. Following induction of the PhoA promoter, cells were harvested and osmotically shocked, and the Fabs purified by protein G (Pharmacia) affinity chromatography [7]. Protein concentrations were determined using absorbance at 280 nm. Fab binding affinities were measured on a BIAcore-2000 (TM) system (BIAcore, Inc., Piscataway, NJ), essentially as previously described [7]. Carboxymethylated dextran biosensor chips (CM5, BIAcore Inc.) were activated with EDC (N-ethyl-N'-(3-dimethylaminopropyl)-carbodiimide hydrochloride) and NHS (N-hydroxysuccinimide) according to the supplier's instructions. VEGF in 20 mM sodium acetate, pH 4.8, was injected onto the biosensor chip at a concentration of 50 µg/ml to yield approximately 700–1400 resonance-response units (RU) of covalently coupled protein. Unreacted groups were blocked with an injection of 1 M ethanolamine. Kinetics measurements were carried out by injecting twofold serial dilutions of Fab in running buffer (PBS containing 0.05% Tween-20) at 25°C using a flow rate of 20 µl/min. Association rates (k_{on}) and dissociation rates (k_{off}) were calculated using a simple one-to-one Langmuir binding model (BIAcore Evaluation Software v. 2.0; [54]). The equilibrium dissociation constant was calculated as the ratio k_{off}/k_{on}.

Alanine scan of the VEGF-interface residues

Fifty alanine mutants of VEGF had been previously generated and used to elaborate the KDR binding epitope on the hormone [15]. Nineteen of these mutant proteins (Table 3) were used to probe all the sidechain contacts with mAb A4.6.1 as observed in the crystal structure of the complex. For this study, each of these mutants was purified further by anion exchange (Pharmacia HiTrap Q, 1 ml), to remove traces of misfolded monomer, which is known to interact with mAb A4.6.1. Binding affinities were measured with an ELISA that quantitated the binding of mAb A4.6.1 to immobilized VEGF in the presence of a dilution series of competing mutant [15].

Accession numbers

The coordinates and structure factors have been deposited with the Brookhaven Protein Data Bank for immediate release, with accession codes 1bj1 and 1bj1sf.

Acknowledgements

We thank the following colleagues at Genentech, Inc., for generous help: Manuel Baca for providing a Fab-phagemid construct, Han Chen for fermentation runs, David Kahn, Phil Nelson and Marge Winkler for production and purification of the Fab-12 fragment, Tony Kossiakoff, Mike Randal and Mark Ultsch for help with data collection, and Len Presta and Charles Eigenbrot for discussions and comments on the manuscript. We also thank the staff at CHESS for help with beam line A1, and Udo Heinemann at the Max Delbrück Centrum, Berlin, for generous support to YAM.

References

1. Dvorak, H.F., Brown, L.F., Detmar, M. & Dvorak, A.M. (1995). Vascular permeability factor/vascular endothelial growth factor, microvascular hyperpermeability and angiogenesis. *Am. J. Pathol.* **146**, 1029-1039.
2. Ferrara, N. (1995). The role of vascular endothelial growth factor in pathological angiogenesis. *Breast Cancer Res. Treat.* **36**, 127-137.
3. Folkman, J. (1995). Angiogenesis in cancer, vascular, rheumatoid and other disease. *Nat. Med.* **1**, 27-31.
4. Carmeliet, P., *et al.*, & Nagy, A. (1996). Abnormal blood vessel development and lethality in embryos lacking a single VEGF allele. *Nature* **380**, 435-439.
5. Ferrara, N., *et al.*, & Moore, M.W. (1996). Heterozygous embryonic lethality induced by targeted inactivation of the VEGF gene. *Nature* **380**, 439-442.
6. Kim, K.J., *et al.*, & Ferrara, N. (1993). Inhibition of vascular endothelial growth factor-induced angiogenesis suppresses tumour growth *in vivo*. *Nature* **362**, 841-844.
7. Baca, M., Presta, L.G., O'Connor, S.J. & Wells, J.A. (1997). Antibody humanization using monovalent phage display. *J. Biol. Chem.* **272**, 10678-10684.
8. Presta, L.G, *et al.*, & Ferrara, N. (1997). Humanization of an anti-vascular endothelial growth factor monoclonal antibody for the therapy of solid tumors and other disorders. *Cancer Res.* **47**, 4593-4599.
9. Waltenberger, J., Claesson-Welsh, L., Siegbahn, A., Shibuya, M. & Heldin, C.-H. (1994). Different signal transduction properties of KDR and Flt1, two receptors for vascular endothelial growth factor. *J. Biol. Chem.* **269**, 26988-26995.
10. Houck, K.A., Ferrara, N., Winer, J., Cachianes, G., Li, B. & Leung, D.W. (1991). The vascular endothelial growth factor family: identification of a fourth molecular species and characterization of alternative splicing of RNA. *Mol. Endocrinol.* **5**, 1806-1814.
11. Keyt, B.A., *et al.*, & Ferrara, N. (1996). The carboxyl-terminal domain (111-165) of vascular endothelial growth factor is critical for its mitogenic potency. *J. Biol. Chem.* **271**, 7788-7795.
12. Muller, Y.A., Christinger, H.W., Keyt, B.A. & De Vos, A.M. (1997). The crystal structure of vascular endothelial growth factor (VEGF) refined to 1.93 Å resolution: multiple copy flexibility and receptor binding. *Structure* **5**, 1325-1338.
13. Sun, P.D. & Davies, D.R. (1995). The cystine-knot growth-factor superfamily. *Annu. Rev. Biophys. Biomol. Struct.* **24**, 269-291.
14. Keyt, B.A., *et al.*, & Ferrara, N. (1996). Identification of vascular endothelial growth factor determinants for binding KDR and FLT-1 receptors. *J. Biol. Chem.* **271**, 5638-5646.
15. Muller, Y.A., Li, B., Christinger, H.W., Wells, J.A., Cunningham, B.C. & De Vos, A.M. (1997). Vascular endothelial growth factor: crystal structure and functional mapping of the kinase domain receptor binding site. *Proc. Natl Acad. Sci. USA* **94**, 7192-7197.
16. Wiesmann, C., Fuh, G., Christinger, H.W., Eigenbrot, C., Wells, J.A. & De Vos, A.M. (1997). Crystal structure at 1.7 Å resolution of VEGF in complex with domain 2 of the Flt-1 receptor. *Cell* **91**, 695-704.
17. Cunningham, B.C. & Wells, J.A. (1989). High-resolution epitope mapping of hGH-receptor interactions by alanine-scanning mutagenesis. *Science* **244**, 1081-1085.
18. Kelley, R.F. & O'Connell, M.P. (1993). Thermodynamic analysis of an antibody functional epitope. *Biochemistry* **32**, 6828-6835.
19. Wells, J.A. & De Vos, A.M. (1996). Hematopoietic receptor complexes. *Annu. Rev. Biochem.* **65**, 609-634.
20. Christinger, H.W., *et al.*, & De Vos, A.M. (1996). Crystallization of the receptor binding domain of vascular endothelial growth factor. *Proteins* **26**, 353-357.
21. Read, R.J. (1986). Improved Fourier coefficients for maps using partial structures with errors. *Acta Cryst. A* **42**, 140-149.
22. Laskowski, R.A., MacArthur, M.W., Moss, D.S. & Thornton, J.M. (1993). Procheck: a program to check the stereochemical quality of protein structures. *J. Appl. Cryst.* **26**, 283-291.
23. Sogabe, S., *et al.*, & Robinson, J.A. (1997). Neutralizing epitopes on the extracellular interferon γ receptor (IFNγR) α-chain characterized by homolog scanning mutagenesis and x-ray crystal structure of the A6 FAB-IFNγR$^{1-108}$ complex. *J. Mol. Biol.* **273**, 882-897.
24. Hoffman, D.W., Cameron, C.S., Davies, C., White, S.W. & Ramakrishnan, V. (1996). Ribosomal protein L9: a structure determination by the combined use of x-ray crystallography and NMR spectroscopy. *J. Mol. Biol.* **264**, 1058-1071.
25. Oefner, C., D'Arcy, A., Winkler, F.K., Eggimann, B. & Hosang, M. (1992). Crystal structure of human platelet-derived growth factor BB. *EMBO J.* **11**, 3921-3926.
26. Carter, P., *et al.*, & Shepard, H.M. (1992). Humanization of an anti-p185^{HER2} antibody for human cancer therapy. *Proc. Natl Acad. Sci. USA* **89**, 4285-4289.
27. Eigenbrot, C., Randal, M., Presta, L., Carter, P. & Kossiakoff, A.A. (1993). X-ray structures of the antigen-binding domains from three variants of humanized anti-p185^{HER2} antibody 4D5 and comparison with molecular modelling. *J. Mol. Biol.* **229**, 969-995.
28. Wilson, I.A. & Stanfield, R.L. (1994). Antibody-antigen interactions: new structures and new conformational changes. *Curr. Opin. Struct. Biol.* **4**, 857-867.
29. Chothia, C., *et al.*, & Poljak, R.J. (1989). Conformations of immunoglobulin hypervariable regions. *Nature* **342**, 877-883.
30. Bossart-Whitaker, P., Chang, C.Y.Y., Novotny, J., Benjamin, D.C. & Sheriff, S. (1995). The crystal structure of the antibody N10-Staphylococcal nuclease complex at 2.9 Å resolution. *J. Mol. Biol.* **253**, 559-575.
31. Chacko, S., *et al.*, & Sheriff, S. (1996). Refined structures of bobwhite quail lysozyme uncomplexed and complexed with the HyHEL-5 FAB fragment. *Proteins* **26**, 55-65.

32. Davies, D.R. & Cohen, G.H. (1996). Interactions of protein antigens with antibodies. *Proc. Natl Acad. Sci. USA* **93**, 7-12.
33. Jones, S. & Thornton, J.M. (1996). Principles of protein–protein interactions. *Proc. Natl Acad. Sci. USA* **93**, 13-20.
34. Wilson, I.A. & Stanfield, R.L. (1993). Antibody-antigen interactions. *Curr. Opin. Struct. Biol.* **3**, 113-118.
35. Wilmot, C.M. & Thornton, J.M. (1988). Analysis and prediction of the different types of β-turn in proteins. *J. Mol. Biol.* **203**, 221-232.
36. Padlan, E.A. (1990). On the nature of antibody combining sites: unusual structural features that may confer on these sites an enhanced capacity for binding ligands. *Proteins* **7**, 112-124.
37. Cunningham, B.C. & Wells, J.A. (1993). Comparison of a structural and a functional epitope. *J. Mol. Biol.* **234**, 554-563.
38. Novotny, J., Bruccoleri, R.E. & Saul, F.A. (1989). On the attribution of binding energy in antigen-antibody complexes McPC 603, D1-3, and HyHEL-5. *Biochemistry* **28**, 4735-4749.
39. Amit, A.G., Mariuzza, R.A., Phillips, S.E.V. & Poljak, R.J. (1986). Three-dimensional structure of an antigen-antibody complex at 2.8 Å resolution. *Science* **233**, 747-753.
40. Clackson, T., Ultsch, M.H., Wells, J.A. & De Vos, A.M. (1998). Structural and functional analysis of the 1:1 growth hormone:receptor complex reveals the molecular basis for receptor affinity. *J. Mol. Biol.* **277**, 1111-1128.
41. De Vos, A.M., Ultsch, M. & Kossiakoff, A.A. (1992). Human growth hormone and extracellular domain of its receptor: crystal structure of the complex. *Science* **225**, 306-312.
42. Clackson, T. & Wells, J.A. (1995). A hot spot of binding energy in a hormone-receptor interface. *Science* **267**, 383-386.
43. Banner, D.W., *et al.*, & Kirchhofer, D. (1996). The crystal structure of the complex of blood coagulation factor VIIa with soluble tissue factor. *Nature* **380**, 41-46.
44. Kelley, R.F., Costas, K.E., O'Connell, M.P. & Lazarus, R.A. (1995). Analysis of the factor VIIa binding site on human tissue factor: effects of tissue factor mutations on the kinetics and thermodynamics of binding. *Biochemistry* **34**, 10383-10392.
45. Mariuzza, R.A. & Poljak, R.J. (1993). The basics of binding: mechanisms of antigen recognition and mimicry by antibodies. *Curr. Opin. Immunol.* **5**, 50-55.
46. Webster, D.M., Henry, A.H. & Rees, A.R. (1994). Antibody-antigen interactions. *Curr. Opin. Struct. Biol.* **4**, 123-129.
47. Otwinowski, Z. (1993). Oscillation Data Reduction Program. In *Proceedings of the CCP4 Study Weekend: Data Collection and Processing.* (Sawyer, L., Isaacs, N. & Bailey, S. eds). pp. 56-62, SERC Daresbury Laboratory, UK.
48. Brünger, A.T. (1990). Extension of molecular replacement: a new search strategy based on Patterson correlation refinement. *Acta Cryst. A* **46**, 46-57.
49. Brünger, A.T., Kuriyan, J. & Karplus, M. (1987). Crystallographic R factor refinement by molecular dynamics. *Science* **235**, 458-460.
50. CCP4 (1994). The CCP4 suite: Programs for protein crystallography. *Acta Cryst. D* **50**, 760-763.
51. Jones, T.A., Zou, J.-Y., Cowan, S.W. & Kjeldgaard, M. (1991). Improved methods for building protein models in electron density maps and the location of errors in these models. *Acta Cryst. A* **47**, 110-119.
52. Kunkel, T.A., Bebenek, K. & McClary, J. (1991). Efficient site-directed mutagenesis using uracil-containing DNA. *Methods Enzymol.* **204**, 125-139.
53. Lowman, H.B. (1998). Phage display of peptide libraries on protein scaffolds. In *Methods in Molecular Biology, vol. 87: Combinatorial Peptide Library Protocols.* (Cabilly,S., ed.). pp. 249-264, Humana Press, Totowa, NJ, USA.
54. Karlsson, R., Michaelsson, A. & Mattson, A. (1991). Kinetic analysis of monoclonal antibody-antigen interactions with a new biosensor based analytical system *J. Immunol. Methods* **145**, 229-240.
55. Nicholls, A., Bharadwaj, R. & Honig, B. (1993). GRASP: graphical representation and analysis of surface properties. *Biophys. J.* **64**, 166-170.
56. Kabat, E.A., Wu, T.T., Redi-Miller, M., Perry, H.M. & Gottesman, K.S. (1987). *Sequences of Proteins of Immunological Interest, 4th Edition.* National Institute of Health, Bethesda, MD, USA.
57. Browner, M.F., Fauman, E.B. & Fletterick, R.J. (1992). Tracking conformational states in allosteric transitions of phosphorylase. *Biochemistry* **31**, 11297-11304.